

**A Thesis Submitted for the Degree of PhD at the University of Warwick**

**Permanent WRAP URL:**

<http://wrap.warwick.ac.uk/88089>

**Copyright and reuse:**

This thesis is made available online and is protected by original copyright.

Please scroll down to view the document itself.

Please refer to the repository record for this item for information to help you to cite it.

Our policy information is available from the repository home page.

For more information, please contact the WRAP Team at: [wrap@warwick.ac.uk](mailto:wrap@warwick.ac.uk)

# **Non-Kekulé Polyaromatic Hydrocarbons**

**By**

**Anish Mistry**

A thesis submitted in partial fulfilment of the requirements for the

degree of

Doctor of Philosophy in Chemistry

University of Warwick, Department of Chemistry

September 2016

# Contents

Contents .....	i
List of Figures .....	vi
List of Schemes .....	xv
List of Tables.....	xxiii
Acknowledgements .....	xxiv
Declaration .....	xxv
Abbreviations .....	xxvi
Abstract .....	xxviii
1 Chapter 1: Introduction.....	1
1.1 Kekulé conjugated hydrocarbons .....	1
1.2 Larger polycyclic aromatic hydrocarbons.....	5
1.3 Clar sextets .....	6
1.4 Bond lengths.....	11
1.5 Pauling ring bond orders .....	14
1.6 General classifications of different PAHs .....	18
1.6.1 Acenes .....	18
1.6.2 Helicenes .....	23
1.6.3 Phenenes .....	24
1.6.4 Starphenenes .....	27
1.6.5 Rylenes.....	27

1.6.6	Zethrenes .....	29
1.6.7	<i>Peri</i> -condensed polyarenes .....	31
1.6.8	Circulenes.....	35
1.6.9	Alternate and interesting PAHs.....	41
1.7	PAHs; where are they found and what are their uses? .....	46
1.7.1	Health effects .....	48
1.7.2	The uses of PAHs.....	49
1.7.3	Organic light emitting diodes (OLED/PLED) .....	50
1.7.4	Organic field effect transistors (OFET) .....	51
1.7.5	Organic solar cells (OSC) .....	53
1.7.6	Spintronics .....	54
1.7.7	Organic materials .....	56
1.8	PAHs and AFM .....	57
1.8.1	Scanning probe microscopy .....	57
1.8.2	Scanning tunnelling microscopy .....	57
1.8.3	Atomic force microscopy.....	58
1.8.4	Ultra-high resolution AFM .....	59
1.8.5	Uses .....	60
1.8.6	Compound identification and characterisation.....	60
1.8.7	Natural products and stereochemical determination .....	64
1.8.8	Surface reactions .....	65

1.9	Project outline.....	71
2	Chapter 2: Benzo[ <i>cd</i> ]pyrene .....	72
2.1	Introduction .....	72
2.2	The synthesis of 6 <i>H</i> -benzo[ <i>cd</i> ]pyrene.....	75
2.2.1	Optimisation of the synthesis of 6 <i>H</i> -benzo[ <i>cd</i> ]pyrene.....	78
2.3	AFM/STM imaging .....	89
2.4	Summary .....	93
3	Chapter 3: <i>Peri</i> -condensation reactions.....	94
3.1	Introduction .....	94
3.2	Synthesis of 6 <i>H</i> -benzo[ <i>cd</i> ]pyrene using glycerol .....	95
3.3	Anthracene.....	102
3.4	Naphthalene.....	105
3.5	Perylene .....	106
3.6	Multiple ring addition – ‘glycidol units’ .....	107
3.7	Possible mechanism of reaction .....	111
3.8	Carbon-13 labelling experiments. ....	118
3.8.1	Carbon labelled Perinaphthanone (266a).....	119
3.8.2	Carbon labelled 6-oxo-6 <i>H</i> -benzo[ <i>cd</i> ]pyrene.....	126
3.9	The solid black powder product of the annulation reactions.....	133
3.9.1	Infra-red spectroscopy.....	133
3.9.2	Raman spectroscopy.....	134

3.9.3	Solid state NMR (ssNMR) spectroscopy .....	134
3.9.4	Thermogravimetric analysis (TGA).....	134
3.9.5	Energy dispersive X-ray spectroscopy (EDX).....	135
3.9.6	X-ray photoelectron spectroscopy (XPS).....	135
3.9.7	Scanning electron microscopy (SEM) .....	136
3.9.8	Transmission electron microscopy (TEM) .....	136
3.9.9	AFM/STM analysis by IBM Zürich group .....	136
3.9.10	Mass spectrometry .....	140
3.10	Summary .....	144
4	Chapter 4: Synthesis of triangulene .....	145
4.1	Introduction .....	145
4.2	Route 1: Coupling reactions .....	150
4.3	Route 2: Cyclisation method .....	153
4.3.1	Triangulene sample 1 .....	160
4.3.2	Triangulene sample 2 .....	162
4.4	Summary .....	165
5	Chapter 5: Conclusions and future work .....	166
6	Experimental.....	168
6.1	Experimental synthetic chemistry .....	168
6.2	Experimental for Chapter 2 .....	173
6.2.1	Synthesis of 6 <i>H</i> -benzo[ <i>cd</i> ]pyrene: Method 1 .....	173

6.2.2	Synthesis of 6 <i>H</i> -benzo[ <i>cd</i> ]pyrene: Method 2 .....	182
6.3	Experimental for Chapter 3 .....	191
6.3.1	Synthesis of 6 <i>H</i> -benzo[ <i>cd</i> ]pyrene: Method 3 .....	191
6.3.2	Synthesis of intermediates for mechanism determination .....	211
6.3.3	Carbon-13 labelled experiments .....	215
6.3.4	Analysis of the black powder .....	217
6.4	Experimental for Chapter 4 .....	224
6.4.1	Failed triangulene synthesis: Coupling method. ....	224
6.4.2	Synthesis of 3,8-dihydro-3 <i>H</i> ,8 <i>H</i> -dibenzo[ <i>cd,mn</i> ]pyrene .....	229
6.5	Mechanistic scheme with AFM images .....	236
6.6	DFT calculation of the dihydro-triangulene isomers 12 & 12a.....	239
7	References.....	240

## List of Figures

Figure 1: Loschmidt's depictions of compounds (left) with the modern day representations (right). .....	1
Figure 2: Showing that the '4n+2' rule does not consistently apply to polyaromatic hydrocarbons. Where a 'tick' signifies that it obeys Huckel's rule and a 'cross' does not.....	2
Figure 3: Clar's method for determining Kekulé and non-Kekulé structures. <sup>12</sup> .....	3
Figure 4: The Schlenk-Brauns hydrocarbon 11. ....	4
Figure 5: Shows the calculated spin density of triangulene with the large circles indicating greater values as reported by Inoue <i>et al.</i> <sup>29</sup> .....	5
Figure 6: The centric nucleus of benzene species annotated as 'C' in the Armstrong representation, with the later universally represented as a circle shown below them. If the 'C's were replaced with circles it would be exactly like Clar's representations (below). .....	7
Figure 7: Simplest set of linear and bent benzenoid structures. The respective Clar structures of a), b) phenanthrene 6 (isolated olefin), c), d), e), anthracene 5 (migrating) and f), g), triphenylene 14 (fully benzenoid) are shown. <sup>11</sup> .....	8
Figure 8: An addition reaction produces a more stable anthracene intermediate 15, with two Clar sextets. The fully benzenoid triphenylene 14 has extra stability by the contribution of the 2- $\pi$ electrons from each sextet.....	9
Figure 9: Less stable compounds (hexacene 20) have a smaller HOMO-LUMO gap, therefore excitation is easier and coloured compounds can be formed, unlike more stable compounds (dibenzochrysene 21). .....	11
Figure 10: Clar structures and bond lengths (Å) of naphthalene 4, 1,3-butadiene 22 and anthracene 5. <sup>32, 67-70</sup> .....	12



Figure 11: Clar structures and bond lengths (Å) of tetracene 23 and pentacene 24. <sup>32, 72, 73</sup> .....	12
Figure 12: Clar structure and bond lengths (Å) of perylene 25, with the middle bond having a more single bond character. <sup>32, 74</sup> .....	13
Figure 13: Clar structure and bond lengths (Å) of phenanthrene 6, where the central ring has more double bond-like character. <sup>32, 75</sup> .....	13
Figure 14: Shows the Pauling ring bond order of naphthalene 4. <sup>38</sup> .....	15
Figure 15: Pauling ring bond orders of the isomers anthracene 5 and phenanthrene 6. <sup>38</sup> .....	15
Figure 16: Calculated Pauling RBOs of selected PAHs by Randić <i>et al.</i> <sup>38, 81</sup> .....	17
Figure 17: Correlating Clar structures of the selected compounds from Figure 16. <sup>11, 38</sup> .....	17
Figure 18: The first five compounds in the class of acenes. They all have one migrating Clar sextet; both naphthalene 4 and anthracene 5 are white, the rest are coloured compounds. <sup>11</sup> .....	19
Figure 19: Octacene 48 and nonacene 49. ....	22
Figure 20: Chem 3D model of [16]helicene 64. ....	24
Figure 21: The ‘phene’ series (including isomers), the larger they are the more apparent it is that an acene-like migrating sextet is present within each arm of the phene 69. <sup>11, 32, 91</sup> .....	25
Figure 22: The starphene series where each arm of triphenylene 14 is extended in any of the three directions. ....	27
Figure 23: The rylene series, where each is extended by an addition of a naphthalene unit. ....	28

Figure 24: The zethrene series where two Clar sextets lie in the naphthalene units whilst the middle rings have predominantly double bond character.....	30
Figure 25: Movement of one ring on a zethrene 91 turns it from a Kekulé to a non-Kekulé structure. <sup>134</sup> .....	31
Figure 26: <i>Peri</i> -condensed PAHs showing the Clar sextet forms.....	32
Figure 27: Circulene series, with the circumacene subdivision of coronene 115, ovalene 116 and circumanthracene 117. Corannulene 118 and circulene 119 are both bowl shaped. Kekuléne 120 was first synthesised by Staab and Diedrich in 1978 in honour of Kekulé's work on benzene. <sup>36, 145-147</sup> .....	36
Figure 28: Cyclopentenophenanthrene 141, Acepleiadylene 142, Dibenzopentalene 143, Truxene 144 and bisbenzo[3,4] cyclobuta[1,2-a:3,4-b]biphenylene 145, are some structurally interesting PAHs.....	42
Figure 29: 16 of the most common PAH pollutants, (*) are possible carcinogens. <sup>31, 32, 176, 182, 200, 202, 207-209</sup> .....	49
Figure 30: Structure of rubrene 177 and quinacridone 178. ....	51
Figure 31: A simplified depiction of the layers of an OLED.....	51
Figure 32: A simplified depiction of an OFET. ....	52
Figure 33: A simplified depiction of an OSC. ....	53
Figure 34: Structures of polychlorotriphenylmethyl (PTM) 179, nitroxide 180 and galvinoxyl 181 species. ....	55
Figure 35: Diradical example of triangulene 10 and a dibenzo-pentacene 98.....	56
Figure 36: Structures of alizarin 36, xanthene 184 and fluorescein 185 which all incorporate an anthracene moiety. ....	57

Figure 37: a) and b) are images of pentacene by constant current STM by Lagoute <i>et al.</i> c) is a constant current STM image of pentacene by Gross <i>et al.</i> , d) and e) are constant height NC-AFM of pentacene by Gross <i>et al.</i> <sup>258, 261</sup> .....	61
Figure 38: a) and b) are constant height NC-AFM images of HBC 100, by Gross <i>et al.</i> <sup>275</sup> .....	62
Figure 39: The reaction product 188 expected (a) visualised under constant height NC-AFM, while (b) was an unexpected compound 189 found in the mixture formed as a by-product. Image taken from Schuler <i>et al.</i> <sup>277</sup> .....	64
Figure 40: NC-AFM image (a) of natural product Breitfussin 190 with an overlaid structure (b). <sup>274</sup> STM images (c-f) of ( <i>S</i> )-1-(2'-naphthyl)ethyl-(4-phenylbenzoate) (NEP) 191 which can cluster in a triangular form. <sup>278</sup> The molecule consists of a short and long arm which can be identified in the STM image to make characterisation easier. ....	65
Figure 41: Disperse orange 3 on a gold surface with (a) before and (b) after <i>trans</i> to <i>cis</i> STM images. <sup>286</sup> .....	66
Figure 42: STM images before and after cyclodehydrogenation of the precursor molecules of triazafullerene (C <sub>57</sub> H <sub>33</sub> N <sub>3</sub> ) 195 by Otero <i>et al.</i> <sup>289</sup> The precursor 194 can be seen in a triangular shape while the product can be seen as more of a round shape which is smaller in diameter. ....	67
Figure 43: The smallest Olympic ring structure is a non-Kekulé structure 205. ....	72
Figure 44: <sup>1</sup> H NMR spectrum of the crude product of the PPA mediated reaction, conducted at 80 °C for overnight, under N <sub>2</sub> (with adamantane as a standard). ....	80
Figure 45: a) AFM image of benzo[ <i>cd</i> ]pyrene radical 205. <sup>321</sup> .....	90
Figure 46: NC-AFM images of a) 6 <i>H</i> -benzo[ <i>cd</i> ]pyrene 209, b) 6-oxo-6 <i>H</i> -benzo[ <i>cd</i> ]pyrene 210, c) benzo[ <i>cd</i> ]pyrene radical 205, d) 5 <i>H</i> -benzo[ <i>cd</i> ]pyrene 232,	

e) 5-oxo-5 <i>H</i> -benzo[ <i>cd</i> ]pyrene 222, f) 4,5-dihydro-3 <i>H</i> -benzo[ <i>cd</i> ]pyrene 207. The dark areas in images b and c are the C=O regions and the bright areas on images a, d and f are that of the CH <sub>2</sub> regions. <sup>321</sup> .....	91
Figure 47: Corresponding structures to the AFM images from Figure 46.....	91
Figure 48: Isomers of benzo[ <i>cd</i> ]pyrene. <sup>11, 322-324</sup> .....	92
Figure 49: Pauling bond orders of the 6 <i>H</i> -isomer 209, 5 <i>H</i> -isomer 232 and 3 <i>H</i> -isomer 208 of benzo[ <i>cd</i> ]pyrene.....	93
Figure 50: The characterisation data pointed to compounds 244 and 245 having seven-fused ring structures.....	101
Figure 51: a) AFM image of 244, which was prominent in the mixture. <sup>321</sup> .....	101
Figure 52: Compound 259 characterised by AFM (a). <sup>321</sup> .....	105
Figure 53: DFT calculations: a) HOMO of phenalene 182, b) SOMO of the phenalenyl radical 7. ....	114
Figure 54: The three possible additions of a ring onto naphthalene 266b-d, where the squares show the carbons which will never be labelled.....	120
Figure 55: a) Assigned perinaphthanone 266 compound (ppm), b) Expanded section of carbonyl peak, c) <sup>13</sup> C NMR of partially labelled perinaphthanone 266a.....	120
Figure 56: The proportion of labelled to non-labelled signals expected. The top arrows showing the doublet and the bottom non-labelled portion 266.....	122
Figure 57: a) Carbon 2 and its neighbours, b) the <sup>13</sup> C NMR spectrum for C2, c) the observed coupling constants of the labelled perinaphthanone.....	122
Figure 58: The arrows showing the quaternary carbons, which are all singlets and therefore not labelled.....	123

Figure 59: INADEQUATE of perinaphthanone 266a, showing the assignments on the carbonyl ring, where the signals ‘spots’ which are in line with each other are from the same spin system (lines).....	124
Figure 60: INADEQUATE of perinaphthanone 266a showing the rest of the spin systems. ....	125
Figure 61: The analysis of the ADEQUATE results of perinaphthanone 266a, carbons 3, 4 and 8 had overlapping signals.....	125
Figure 62: Mass spectrometry of the <sup>13</sup> C-labelled perinaphthanone 266a where the <sup>13</sup> C <sub>3</sub> mass can be seen. ....	126
Figure 63: The possible additions of rings on the naphthalene starting material (210b-e) to make 6-oxo-6 <i>H</i> -benzo[ <i>cd</i> ]pyrene 210a. The different letters represent the different type of single additions encountered (A-E). In addition, the full assignment of 6-oxo-6 <i>H</i> -benzo[ <i>cd</i> ]pyrene 210 is shown (ppm).....	126
Figure 64: The C6 peak, two types of additions can occur C (double-doublet: 54.5, 4.0 Hz – dashed arrows) and D (triplet: 55.0 Hz – solid arrows) where both can be seen with the non-labelled singlet in the centre. ....	127
Figure 65: C3 (double-doublet: 57.0, 1.5 Hz) coupling to C4 and C5, *peak in the middle is the non-labelled singlet. ....	128
Figure 66: Type A environment of C4 (double-doublet: 57.0, 55.0 Hz – solid arrows), *peak is the non-labelled C4 singlet. In addition, C1 is observed here, with a B type (doublet: 61.5 Hz – dotted line) and an E type environment (double-doublet: 62.5, 53.0 Hz – dashed line), **peak is the non-labelled C1 singlet. ....	129
Figure 67: C2 at 128.7 ppm has both a B (doublet: 62.5 Hz – dotted lines) and E type (double-doublet: 62.0, 53.5 Hz – dashed lines), *peak is the C2 non-labelled singlet.	

C5 at 129.3 ppm, A type environment (double-doublet: 55.0, 1.5 Hz – solid line), **peak is the non-labelled C5 singlet. ....	130
Figure 68: Summary of the quaternary carbons which are labelled with the proposed mechanism, the square represents the C11b which is not labelled. ....	131
Figure 69: <sup>13</sup> C NMR spectrum showing C11a, E type (doublet: 54.0 Hz-dashed line), C2a, B type (doublet: 54.0 Hz-dotted line) and C5a D type spin systems (54.5 Hz- solid line). *peaks are the respective non labelled singlets.....	131
Figure 70: Coupling constant map of <sup>13</sup> C-labelled 6-oxo-6 <i>H</i> -benzo[ <i>cd</i> ]pyrene 210a, all J values are in Hertz. ....	132
Figure 71: Mass spectrum of <sup>13</sup> C-labelled sample of 6-oxo-6 <i>H</i> -benzo[ <i>cd</i> ]pyrene 210a. ....	132
Figure 72: TGA plot of the black powder where the temperature was raised at 10 °C/min from 25 °C - 800 °C. ....	135
Figure 73: Selected AFM images (a-j) of the black powder from the pyrene reaction, with correlating structures. <sup>321</sup> ....	137
Figure 74: a) C <sub>3</sub> -symmetric radical 310 observed by AFM from the black powder. b) STM of the negative ion resonance (NIR) and c) the positive ion resonance (PIR) of 310. <sup>321</sup> d) is the DFT calculated SOMO of 310 by Dr D. Fox.....	138
Figure 75: Selected AFM images (a-f) of compounds found with side chains from the black powder mixture, with the related PAHs shown with addition units (bold). R = unknown side chain. <sup>321</sup> ....	139
Figure 76: The triangular series of graphene fragments which due to their structure, do not have a singlet ground-state. The first structure is the phenalenyl radical 7 and the second is the triangulene diradical 10. ....	146
Figure 77: Tri- <i>tert</i> -butyl triangulene species 350 synthesised by Inoue <i>et al.</i> <sup>29</sup> .....	150

Figure 78: Crystal structure of 9-bromo-10-(2,6- <i>bis</i> (bromomethyl)phenyl)anthracene 355.....	152
Figure 79: All possible dihydro-triangulene isomers 12-12l: 12a is observed whilst 12 was expected. ....	157
Figure 80: <sup>1</sup> H NMR spectrum of dihydro-triangulene 12a, the major isomer (integrated). Other minor peaks can also be seen of what is expected to be other isomers. An expanded version of the aromatic region is also shown where each peak is almost distinguishable. ....	158
Figure 81: <sup>1</sup> H NMR spectrum of dihydro-triangulene 12a where another minor isomer can be seen. This isomer has the same two broad singlets (5.08 & 3.98 ppm) and two doublet of triplets (6.81 & 6.22 ppm) in close proximity to the major isomer 12a.....	159
Figure 82: Pauling Ring Bond Order of two of the main isomers of dihydro-triangulene 12 & 12a.....	160
Figure 83: AFM images on NaCl (100) of oxidised samples a-e, with a possible radical structure shown 367. AFM image of 368 on Cu (111) where the compound shows a bright spot on an inner carbon suggesting an inner hydrogen present. <sup>321</sup> ..	161
Figure 84: STM images on a Cu(111) surface where the dihydride group of 12a can be clearly seen as a very bright spot on the images. <sup>321</sup> ..	162
Figure 85: AFM images of molecules observed on NaCl (100) surface; (a-b) dihydro-triangulene isomers. (c-e) oxidised species including 4,8-dioxo-4 <i>H</i> ,8 <i>H</i> -dibenzo[ <i>cd,mn</i> ]pyrene (f) with its STM image (e). Images on Cu (111) surface of triangulene (g-h) and the corresponding STM (i). Image of triangulene on Xe (111) surface (j). <sup>321</sup> ..	163

Figure 86: a) STM image of the PIR (-1.4 V), b) STM image of the NIR (1.85 V) of triangulene 12a. DFT calculation of c) SOMO 1, d) SOMO 2 and e) SOMO 1 & 2 combined. f) the simulated image of (e) under the STM tip, where the actual images can be seen in (a) & (b). All data and calculations provided by IBM Zürich.<sup>319, 412</sup> 164

Figure 87: IR spectrum of the black powder obtained from pyrene, anthracene and naphthalene, all with very similar readings. ....217

Figure 88: IR of perylene, with similar reading to the other three peri-condensation black products. ....217

Figure 89: Raman spectra of the black powder obtained from the reagents anthracene (1), pyrene (2) and naphthalene (3). ....218

Figure 90: Shows the 500 MHz Carbon-13 solid state MAS NMR spectra of the insoluble product. Two different spin speeds were used to help deduce real peaks from side bands which are denoted as \* .....219

Figure 91: a) XPS survey spectrum of black powder, b) carbon spectrum, c) oxygen spectrum and d) sulfur spectrum, with the different bonds which can be typically expected plotted underneath the peak of each element. ....221

Figure 92: SEM (a, b) of the black powder formed. ....222

Figure 93: a) Electron diffraction pattern of the black powder. (b, c, d) TEM of black solid on a lacy carbon support film. ....223



## List of Schemes

Scheme 1: Illustrates the simplest even-carbon-numbered non-Kekulé benzenoid structure of dihydro-triangulene 12 and the dianion 13.....	5
Scheme 2: The first example of isomeric benzenoid reactivity in 1958, showing that 18 is more reactive than 17. <sup>51</sup> .....	10
Scheme 3: The Haworth synthesis of naphthalene 4. <sup>88-90</sup> .....	19
Scheme 4: Elbs reaction to synthesise anthracene 5 (left) and alizarin 36 to form 5 (right). <sup>98</sup> .....	20
Scheme 5: First synthesis of pentacene 24 by Clar and John, even though in 1911 Phillipi claimed to have synthesised it, many believe he actually made an isomer of dihydro-pentacene 40. <sup>99, 101, 102</sup> .....	20
Scheme 6: Oxidation of 47 to form hexacene 20 by either copper powder or Pd/C. <sup>30, 104, 106</sup> .....	21
Scheme 7: Synthesis of nonacene 49 using an argon matrix at 30 K with UV radiation as reported by Tönshoff and Bettinger. <sup>30, 108</sup> .....	22
Scheme 8: Wood and Mallory cyclised various substituted stilbenes with great success and efficiency; yields of 73 % and 77 % and irradiation for only seven and four hours for phenanthrene 6 and chrysene 27 respectively.....	23
Scheme 9: Synthesis of [8]helicene 63 by Martin <i>et al.</i> represented by the Chem 3D model, utilising the work of Wood and Mallory.....	24
Scheme 10: Pschorr's effective synthesis of phenanthrene 6; nitro group reduction followed by copper catalysis to cyclise the intermediate 73 and finally thermal decarboxylation. <sup>91, 116</sup> .....	26
Scheme 11: Synthesis of heptaphene 77, (*may contain other isomers). <sup>118</sup> .....	26

Scheme 12: The Scholl reaction using aluminium chloride and heat to form 25. <sup>34, 35</sup>	28
Scheme 13: Synthesis of terylene 81 using an intramolecular cyclodehydrogenation in the last step, which is a common reaction in the formation of these type of compound. Further extension upon the rylene axis can provide a synthesis of nanoribbons using similar methods. <sup>30, 122</sup>	28
Scheme 14: Illustrates the inclusion of dicarboxylic imides in enhance their properties.	29
Scheme 15: Staab <i>et al.</i> method (left) and Sondheimer and Mitchell's method (right) both published in 1968. <sup>129, 131</sup>	30
Scheme 16: The synthesis of HBC using the methods of Clar <i>et al.</i> , Halleux <i>et al.</i> and Kübel <i>et al.</i> <sup>36, 56, 135, 136, 138</sup>	33
Scheme 17: The synthesis of bisanthene 101 and a stable derivative 114. <sup>30, 140-143</sup>	34
Scheme 18: Clar's coronene 115 synthesis. <sup>148</sup>	37
Scheme 19: The use of a metal-catalysed reaction to produce coronene 115 in high yields (species 127 reacted immediately) as described by Shen <i>et al.</i> from the previous works of Donovan <i>et al.</i> <sup>151, 152</sup>	38
Scheme 20: Clar's synthesis of ovalene 116 with a two-fold Diels-Alder reaction. <sup>153</sup>	39
Scheme 21: The failed synthesis of circumanthracene 117 by Clar <i>et al.</i> in 1956 where 2, 12-dehydrodinaphthoperopyrene 133 was actually made. <sup>155-157</sup>	40
Scheme 22: The synthesis of circumanthracene 117 by Broene and Diedrich. The conversion from the stilbene like structure 139 to the hindered precursor 140, is like that of Wood and Mallory first used (see Scheme 8) to gain a yield of 93 %. <sup>30, 157</sup>	41

Scheme 23: The synthesis of buckminsterfullerene 155 by Scott <i>et al.</i> , the last step (Flash Vacuum Pyrolysis, FVP) producing a very low yield. <sup>167, 168</sup> .....	43
Scheme 24: A synthetic route to obtain the largest controlled PAH synthesis. <sup>169</sup> .....	45
Scheme 25: A common pollutant dimethylbenz[ <i>a</i> ]anthracene 164 can form dimethylbenz[ <i>a</i> ]anthracene-3,4-diol-1,2 epoxide 167 in the body using metabolic pathways. This compound reacts with DNA to form adducts which are responsible for carcinogenicity such as breast cancer. Benzo[ <i>a</i> ]pyrene 172 is another commonly studied PAH which is known to follow this type of pathway to create carcinogens. <sup>31, 170, 203-206</sup> .....	48
Scheme 26: Illustrates a radical form 7 of the highly studied phenalene 182 after a hydrogen abstraction. 183 is a more stable radical form of the phenalenyl compound 7 with bulky substituents for stability. <sup>244</sup> .....	55
Scheme 27: Synthesis of a cyclotrimer nanographene 188, firstly by a [4+2] cycloaddition followed by a [2+2+2] cycloaddition. <sup>277</sup> .....	63
Scheme 28: The main planar compound 197 can be identified by NC-AFM (b). c) and d) show almost planar side-products which have similar structural arrangement and include a sulfur atom though unclear where and what the structure is exactly. <sup>259</sup> .....	68
Scheme 29: The original Bergman cyclisation, using heat to cyclise the product. The diradical 199 was observed to abstract hydrogens from the solvent 2, 6, 10, 14-tetramethylpentadecane to form benzene. In addition, when CCl <sub>4</sub> was used as a solvent 1,4-dichlorobenzene was observed. <sup>291, 292</sup> .....	69
Scheme 30: NC-AFM images of the (a) dibromo species 201 (b) the diradical 202, (c) enediyene 203. (d) Reversible manipulation formed the opposite enediyene 204. Images taken from Schuler <i>et al.</i> <sup>292</sup> .....	70

Scheme 31: Scholl and Meyers' postulated scheme where later Vollman <i>et al.</i> realised that 206 and 208 were not made in fact 210 and 209 were respectively. <sup>297, 298</sup>	73
Scheme 32: A synthetic route towards 6 <i>H</i> -benzo[ <i>cd</i> ]pyrenium cation 214 by Reid and Bonthron. <sup>302</sup>	74
Scheme 33: Formation of starting material 211, 1-formylpyrene 215 used by Reid and Bonthron to synthesise 6 <i>H</i> -benzo[ <i>cd</i> ]pyrene. <sup>302</sup>	75
Scheme 34: A new route towards the synthesis of 6 <i>H</i> -benzo[ <i>cd</i> ]pyrene 209, where 211 was used immediately to form the major product 212. <sup>304-311</sup>	76
Scheme 35: Pathways to the production of 5-ethoxy-6 <i>H</i> -benzo[ <i>cd</i> ]pyrene 224.	78
Scheme 36: A three-step synthesis of 6 <i>H</i> -benzo[ <i>cd</i> ]pyrene 209, where a number of additional products are formed (8, 207, 210, 222, 227, 228). <sup>312</sup>	79
Scheme 37: Compounds formed from the ring cyclisation using PPA at 80 °C under a dinitrogen atmosphere overnight. Compounds 209, 210 and 222 were the major components isolated.	81
Scheme 38: The independent formation of 4,5-dihydro-3 <i>H</i> -benzo[ <i>cd</i> ]pyrene 207 by the method of Clar and Stewart. <sup>316</sup>	81
Scheme 39: Possible mechanism in which ketone 212 is formed and then reacts further by disproportionation.	83
Scheme 40: Possible mechanism of formation of pyrene 8 from the starting material 211.	83
Scheme 41: The possible mechanism of formation of 4,5-dihydro-3 <i>H</i> -benzo[ <i>cd</i> ]pyrene 207.	84
Scheme 42: Possible mechanism for the formation of 7,8-dihydro-9 <i>H</i> -cyclopenta[ <i>a</i> ]pyrene 227.	85

Scheme 43: Independent PPA reactions; 3,4-dihydro-5 <i>H</i> -benzo[ <i>cd</i> ]pyren-5-one 212, 5-oxo-5 <i>H</i> -benzo[ <i>cd</i> ]pyrene 222, 6 <i>H</i> -benzo[ <i>cd</i> ]pyrene 209 and 6-oxo-6 <i>H</i> -benzo[ <i>cd</i> ]pyrene 210. <sup>302</sup> .....	86
Scheme 44: The isomerisation of 222 to 210, with 209 being the source of the hydride which is regenerated. ....	88
Scheme 45: Disproportionation of alcohol 228 into 209 and 210. <sup>302</sup> .....	89
Scheme 46: An alternative synthesis of 6 <i>H</i> -benzo[ <i>cd</i> ]pyrene 209. <sup>297, 298</sup> .....	94
Scheme 47: The synthesis of benzanthrone 242, with glycerol and sulfuric acid which was used as a common red dye. <sup>325, 326</sup> .....	94
Scheme 48: Formation of the dihydride 209 using glycidol 243 with a balanced equation.....	97
Scheme 49: A possible route to explain why 209 is a major product along with ketone 210 in this reaction. ....	97
Scheme 50: Various compounds isolated from the reaction of pyrene with glycidol in 80 % H <sub>2</sub> SO <sub>4</sub> , approximately 2.0 g of black solid was also obtained. Percentages worked out from the <sup>1</sup> H NMR spectrum and are representative from each pyrene molecule used from the starting material. ....	99
Scheme 51: The independent synthesis of 3-oxo-3 <i>H</i> -benzo[ <i>cd</i> ]pyrene 206 by the method of Didenko <i>et al.</i> <sup>331</sup> .....	100
Scheme 52: Mechanism for the synthesis of 206 using the method of Didenko <i>et al.</i> <sup>331</sup> .....	100
Scheme 53: Various compounds isolated from the reaction of anthracene with glycidol in 80 % H <sub>2</sub> SO <sub>4</sub> , approximately 1.5 g of black solid was also obtained. Percentages worked out from the <sup>1</sup> H NMR spectrum and are representative from each anthracene molecule used from the starting material. ....	103

Scheme 54: Synthesis of 3-oxo-3 <i>H</i> -benz[ <i>de</i> ]anthrone 264, method taken from Cameron <i>et al.</i> <sup>336</sup> .....	104
Scheme 55: Various compounds isolated from the reaction of naphthalene with glycidol in 80 % H <sub>2</sub> SO <sub>4</sub> , approximately 1.7 g of black solid was also obtained. Percentages worked out from the <sup>1</sup> H NMR spectrum and are representative from each naphthalene molecule used from the starting material. ....	106
Scheme 56: Compounds isolated from the reaction of perylene with glycidol in 80 % H <sub>2</sub> SO <sub>4</sub> , approximately 3.1 g of black solid was also obtained. Percentages worked out from the <sup>1</sup> H NMR spectrum and are representative from each perylene molecule used from the starting material.....	107
Scheme 57: The multiple addition at the ' <i>peri</i> ' positions are shown in bold, only one method of addition is shown. ....	108
Scheme 58: The multiple addition at the ' <i>peri</i> ' positions are shown in bold, only one method of addition is shown. ....	109
Scheme 59: The multiple addition at the ' <i>peri</i> ' positions are shown in bold, only one method of addition is shown. ....	110
Scheme 60: The multiple addition at the ' <i>peri</i> ' positions are shown in bold, only one method of addition is shown. ....	110
Scheme 61: The formation of the reactive phenalene 182 intermediate.....	111
Scheme 62: Skraup's quinoline synthesis also uses glycerol as a three-unit addition. <sup>339, 340</sup> .....	111
Scheme 63: Substituted quinolines produced by replacing the glycerol by Doebner and Miller. <sup>342, 343, 348</sup> .....	112
Scheme 64: The acid catalysed formation of acrolein 276 from glycidol 243. <sup>348-354</sup> .....	112

Scheme 65: The possible acid catalysed mechanisms, annulation of naphthalene 4 with acrolein 276.....	113
Scheme 66: Possible acid catalysed radical reaction of the formation of a Kekulé structure pyrene 8.....	115
Scheme 67: If the reaction from a non-Kekulé species proceeded from a polar reaction only a five-membered ring would be made.....	116
Scheme 68: Possible intermediates 300 & 302 in the mechanism of the formation of 6 <i>H</i> -benzo[ <i>cd</i> ]pyrene 209. *Observable in the PPA reaction. ....	117
Scheme 69: Reaction of naphthalene 4 with glycerol doped with <sup>13</sup> C <sub>3</sub> -labelled glycerol (10%), to produce labelled products 8a, 209a, 210a, 266a.....	119
Scheme 70: Abstraction of two hydrogens from dihydro-triangulene 12 to form triangulene 10.....	145
Scheme 71: One of Clar's first synthetic attempts to form triangulene 10. <sup>316, 391</sup> ....	147
Scheme 72: The formation of the dianion 13 by Hara <i>et al.</i> with NMR spectroscopy confirmation.....	148
Scheme 73: Allinson <i>et al.</i> synthetic route to a stable trioxytriangulene derivative 349. <sup>134, 388, 395</sup> .....	149
Scheme 74: Proposed scheme for the synthesis of 4,8-dihydro-4 <i>H</i> ,8 <i>H</i> -dibenzo[ <i>cd,mn</i> ]pyrene 12.....	151
Scheme 75: The different products produced when brominating 9-(2,6-dimethylphenyl)anthracene 353 in the presence of NBS, benzoyl peroxide and light in CCl <sub>4</sub> . <sup>405</sup> .....	153
Scheme 76: An amalgamation of previous synthetic steps in an effort to synthesise dihydro-triangulene 12a. <sup>316, 388</sup> .....	154

Scheme 77: Cyclisation mechanism of 338 where a stable carbocation is produced and the structure tautomerises to make the intermediate 339, this is then reduced by zinc to produce compound 340. ....	156
Scheme 78: Clar's zinc reduction reaction produced 1,2,3,5,6,7-hexahydro-dibenzo[ <i>cd,mn</i> ]pyrene 342, a stable derivative of the triangulene series. ....	160
Scheme 79: Possible explanation into AFM images observed of compounds from the pyrene black powder mixture. Images by IBM Zürich. <sup>321</sup> .....	238



## List of Tables

Table 1: Mass spectrometry results of pyrene derived black powder, where proposed structures are drawn in accordance with the mass observed; pyrene $m/z$ peaks were detected at just over 800.....	141
Table 2: Mass spectrometry results from anthracene derived black powder, where proposed structures are drawn in accordance with the mass observed; anthracene $m/z$ peaks were detected at just over 530.....	142
Table 3: Mass spectrometry results from perylene derived black powder, where proposed structures are drawn in accordance with the mass observed; perylene $m/z$ peaks were detected at just over 510.....	143
Table 4: Optimisation of catalyst and ligand conditions.....	152

## **Acknowledgements**

First and foremost, I would like to thank my supervisor Dr David Fox for his knowledge and guidance throughout this project as well as past and present members of the Fox group and my friends.

Special thanks goes to Dr Ivan Prokes, Edward Tunnah and Robert Perry for their invaluable NMR assistance and Dr Lijiang Song and Philip Aston for their assistance with Mass Spectroscopy. Also my collaborators, IBM Zürich, Leo Gross and Co-workers for their excellent work with the imaging using STM/AFM and Giovanni Costantini and Ben Moreton for their input with STM experiments.

Furthermore, I would like to thank Kasra Razmkhah, Jon Rourke, Helen Thomas, Andrew Clark, Andrew Ross, Andrew Sellars, David Burnett, Guy Clarkson, Stefan Bon, Richard Beanland, Steven Brown, Manjunatha Reddy and Marc Walker for their guidance when using different analytical techniques within this project.

Finally, I would like to give special thanks to my mother, father and brother for their continued support and guidance throughout my studies and I am forever indebted to them.

## Declaration

This thesis is submitted to the University of Warwick in support of my application for the degree of Doctor of Philosophy in Chemistry. It has been composed by myself and has not been submitted in any previous application for any degree.

The work presented (including data generated and data analysis) was carried out by the author except in the cases outlined below:

- All AFM and STS experiments were conducted by IBM Zürich.
- STM was carried out by IBM Zürich and the Giovanni Costantini group at the University of Warwick.
- XPS was conducted by Dr Marc Walker at the University of Warwick.
- DFT calculations were conducted by Dr David Fox at the University of Warwick and in the case of triangulene Dr Niko Pavliček at IBM Zürich.

Parts of this thesis have been published by the author:

- Mistry A. *et al.*, *Chem. Eur. J.*, 2014, 21, 5, 2011-2018.
- Schuler B. *et al.*, *Phys. Rev. Lett.*, 2013, 112, 12, 106103-1-5.

## Abbreviations

AFM	Atomic force microscopy
BDE	Bond dissociation energy
DCM	Dichloromethane
DFT	Density Functional Theory
DMF	Dimethyl formamide
DMS	Dimethyl sulfide
DMSO	Dimethyl sulfoxide
DPAT	Diphenanthro[9, 10- <i>b</i> :9', 10'- <i>d</i> ]thiophene
EDX	Energy dispersive X-ray
Equiv.	Equivalents
ESR	Electron paramagnetic resonance
GC-MS	Gas chromatography mass spectrometry
HBC	Hexabenzocoronene
HOMO	Highest occupied molecular orbital
IBM	International business machines cooperation
IR	Infra-red
LED	Light emitting diode
LOMO	Lowest occupied molecular orbital
<i>m/z</i>	Mass to charge ratio
MALDI	Matrix assisted laser desorption/ionisation
MAS	Magic angle spinning
NC-AFM	Non-contact atomic force microscopy
NIR	Negative ion resonance
NMR	Nuclear magnetic resonance
NOE	Nuclear overhauser effect
OFET	Organic field effect transistor
OLED	Organic light emitting diode
OSC	Organic solar cell
PAH	Polyaromatic Hydrocarbons
PIR	Positive ion resonance

PLEDS	Polymer light emitting diode
PPA	Poly-phosphoric acid
PTM	Polychlorotriphenylmethyl
RBO	Ring bond order
SEM	Scanning electron microscopy
SOMO	Singly occupied molecular orbital
STM	Scanning tunneling microscopy
STS	Scanning tunneling microscopy
TBAF	Tetra-n-butylammonium fluoride
TEM	Transmission electron microscopy
TGA	Thermogravimetric analysis
THF	Tetrahydro furan
TTBP	Tri- <i>tert</i> -butylphosphine
UV	Ultra-Violet
Vis	Visible
XPS	X-ray photoelectron spectroscopy

## Abstract

Non-Kekulé PAHs have been studied for a variety of applications due to the interesting chemistry they possess for such simple organic molecules. PAHs can have both closed and open-shell arrangements which have been of interest recently due to the potential magnetic and electronic properties they can acquire. Due to this, there has recently been a strong interest in graphene which can be viewed as a sheet of PAHs fused together. This thesis describes the formation of particular PAHs including open-shell compounds and how PAHs can be fully characterised using one technique.

Chapter 2 describes the synthesis of 6*H*-benzo[*cd*]pyrene, the starting point of this project. Pentacene and perylene are other five fused ring structures like 6*H*-benzo[*cd*]pyrene which are commonly used due to their fluorescence, thus, this PAH could have interesting properties for material scientists. The production of the benzo[*cd*]pyrene radical by AFM/STM is then described.

Chapter 3 describes *peri*-condensation reactions to form larger PAHs a technique which was commonly used in the 1900s for the addition of an aromatic ring, however, multiple ring additions have been reported to occur. In addition, carbon labelling experiments have been completed to confirm this and the mechanism by which multiple rings add have been discussed. STM/AFM has been used to characterise the compounds formed in the *peri*-condensation reactions as common techniques for characterisation do not provide enough structural data for compound determination.

Chapter 4 discusses the synthesis of 3,8-dihydro-3*H*,8*H*-dibenzo[*cd,mn*]pyrene. Thereafter the use of AFM/STM is then utilised to dehydrogenate 3,8-dihydro-3*H*,8*H*-dibenzo[*cd,mn*]pyrene to form the non-Kekulé structure of triangulene which was simultaneously imaged for the first time.

# 1 Chapter 1: Introduction

## 1.1 Kekulé conjugated hydrocarbons

Hydrocarbons are compounds which contain carbon and hydrogen atoms which can be generalised into acyclic (such as ethane and propylene) and cyclic molecules (such as cyclohexane and benzene). An important group of cyclic hydrocarbons are polyaromatic hydrocarbons (PAHs). These compounds are structurally arranged with two or more fused aromatics, often benzene rings.<sup>1</sup> The Kekulé structure of a PAH is a structural formula based on August Kekulé's 1865 model of benzene, where every  $\pi$  electron pair in a cyclic  $\pi$  system can form a  $\pi$  bond.<sup>2, 3</sup> Archibald Couper and Josef Loschmidt proposed a near-correct model of the structure of benzene in 1861 containing multiple double bonds and a cyclic structure.<sup>4-6</sup> Loschmidt, who suggested the structures of a variety of compounds including triazene, benzidine and benzene, had made a significant step in the true representation of benzene as a large cyclic ring (Figure 1) but did not rationalise his structures.<sup>5-8</sup> Nevertheless, Kekulé had explained aromaticity in relation to the structure and included the alternating double bonds therefore rationalising the support for his theory of benzene fully.<sup>3, 7, 9</sup>

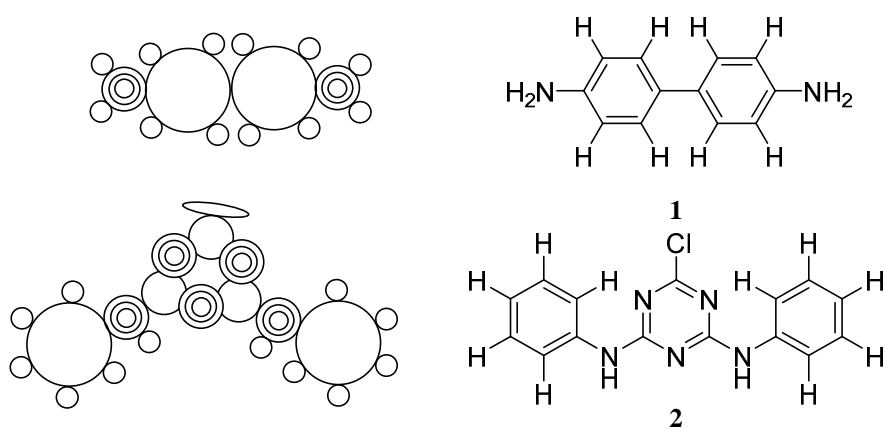


**Figure 1: Loschmidt's depictions of compounds (left) with the modern day representations (right).**





There are a number of ways to analyse compounds to see if it is a Kekulé structure or not; one method is drawing the double bonds into the system one at a time, which can be a laborious process, another similar method shown by Clar *et al.* (Figure 3) is to label each alternate carbon and compare the difference, and if there is a difference then it is a non-Kekulé structure.<sup>11, 12</sup> For example, in Figure 3 anthanthrene **9** has 11 of each marked and non-marked carbons therefore the difference is zero, thus it is a Kekulé structure. However, triangulene **10** has a difference of two, therefore this is a non-Kekulé structure and in this instance a diradical. A non-Kekulé molecule may be defined as one that contains enough atoms but not enough bonds to satisfy the standard rules of valence.<sup>13</sup>

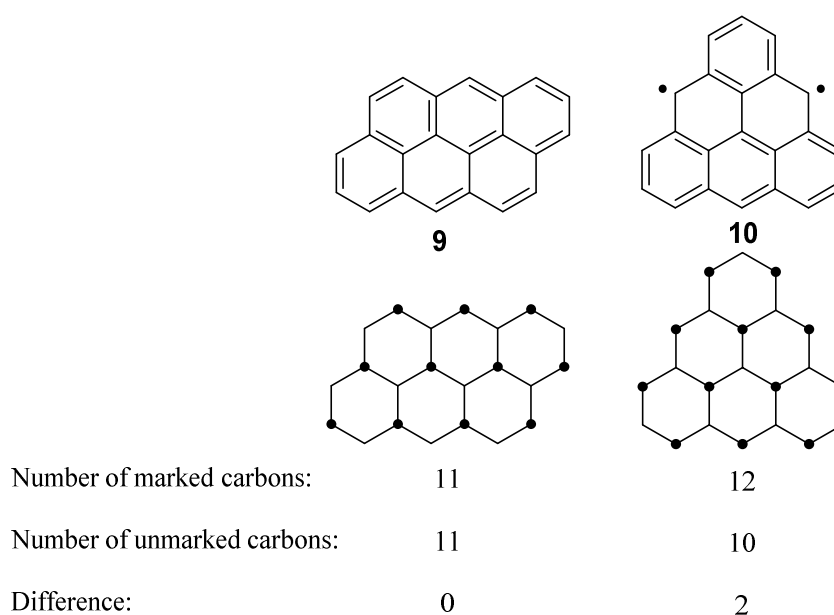


**Figure 3: Clar's method for determining Kekulé and non-Kekulé structures.**<sup>12</sup>

Non-Kekulé molecules are of particular interest due to their unique photochemical excited states and reaction transition states, with the possible incorporation into materials with novel optical, electronic or magnetic properties.<sup>14, 15</sup>

One of the first non-Kekulé triplet ground state structures to be synthesised was in 1915 by Schlenk and Brauns.<sup>16-18</sup> The work of O. Stark *et al.* laid the foundation for the formation of the Schlenk-Braun hydrocarbon **11** as Stark and his co-worker's attempts to form the exocyclic tetraphenyl substituted *m*-xylylene were unsuccessful.<sup>19-23</sup> The two tertiary carbon sites help stabilise the radical but upon exposure to air the compound formed various peroxide products within a day.<sup>19</sup>

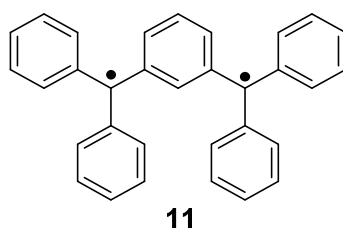
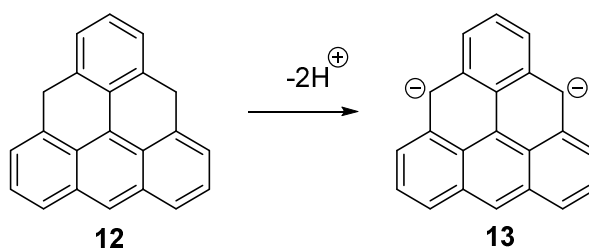


**Figure 4: The Schlenk-Brauns hydrocarbon 11.**

Due to the potential worth of these non-Kekulé molecules, certain polybenzenoids have been of particular interest. Polybenzenoids can be described as fused six-membered rings and there are a number of polyaromatic hydrocarbons which have been identified.<sup>2</sup> In particular, one benzenoid PAH, triangulene **10** (Figure 3), which is the simplest even-carbon-numbered non-Kekulé poly-benzenoid hydrocarbon. This compound has been of interest because the analysis of its instability and observable spin states could be potentially used in electronic devices. However, like most non-Kekulé PAHs it is very reactive and has not been isolated, as reported from the early work of Clar *et al.*<sup>24, 25</sup>

Even though the dihydrides of dihydro-triangulene **12** are readily oxidised, the dianion of triangulene **13** has been synthesised by O. Hara *et al.* (Scheme 1).<sup>26-28</sup> Nevertheless, the diradical form **10** has yet to be isolated. It is suggested that the neutral diradical is more reactive than a single radical and spontaneously dimerises/polymerises.<sup>24, 25</sup>



**Scheme 1: Illustrates the simplest even-carbon-numbered non-Kekulé benzenoid structure of dihydro-triangulene **12** and the dianion **13**.**

Unlike the Schlenk-Brauns hydrocarbon **11**, where the spin density is the highest on the central carbons, the spin density of triangulene **10** is highest around the outside of the molecule (Figure 5).<sup>29</sup> Taking this in to account as well as the proposal that triangulene is flat, a poly-benzenoid and possesses a lower number of isolated benzene rings (see section 1.3: Clar sextets), the radicals are less stable.

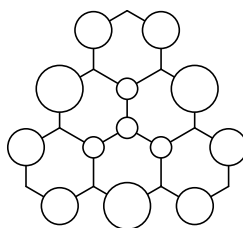


**Figure 5: Shows the calculated spin density of triangulene with the large circles indicating greater values as reported by Inoue *et al.*<sup>29</sup>**

## 1.2 Larger polyaromatic hydrocarbons

Large PAHs are classed as having more than six fused rings. PAHs can be also classed as ‘nanographene’ which can have a diameter up to around 10 nm.<sup>30, 31</sup>

Pioneering work on these ‘nanographenes’ dates back to Roland Scholl (1910) and Erich Clar (1950s) as their work contributed hugely in this area. However, back then harsh conditions were used during synthesis such as strong oxidising agents and high temperatures usually resulting in poor yields. A lack of available analytical techniques makes their work even more remarkable.<sup>30, 32-36</sup> Moreover, it is very

difficult to synthesise large PAHs as their solubility decreases upon increased molecular weight and certain stability issues can restrict those that can be formed. A number of models to explain the bonding and relative stability of PAHs have been proposed and will be discussed herein to help understand this class of compounds further.<sup>11, 32, 33</sup>

### 1.3 Clar sextets

As mentioned previously, the Hückel '4n+2' rule is only applicable to monocyclic aromatic species, and so for multi-ringed species the Clar sextet rule helps provide a qualitative analysis of stability for larger fused poly-benzenoids.

Clar's rule states that the Kekulé resonance structure with the most number of isolated aromatic  $\pi$ -sextets will be the most important and therefore most likely representation of the electronic structure of a polyaromatic hydrocarbon (PAH).<sup>11</sup> An aromatic  $\pi$ -sextet is defined as 'six  $\pi$ -electrons localised in a single benzene-like ring separated from adjacent rings by a formal C-C single bond'.<sup>11, 37</sup>

After the structure of benzene was realised, the idea of the ' $\pi$ -sextet' in aromatic rings can be traced back to Henry Armstrong in 1890, with further major contributions from Sir J. J. Thomson in 1921, Ernest Crocker in 1922 and Henry Armit and Sir Robert Robinson in 1925.<sup>7, 38-41</sup>

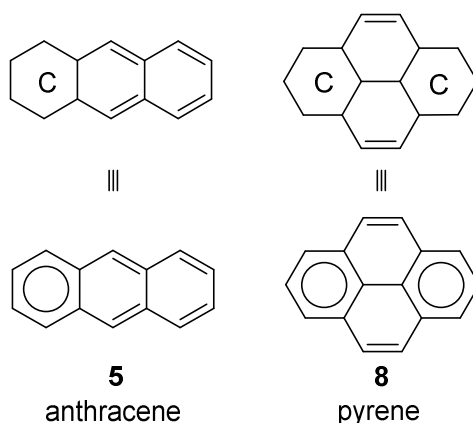


**Figure 6: The centric nucleus of benzene species annotated as 'C' in the Armstrong representation, with the later universally represented as a circle shown below them. If the 'C's were replaced with circles it would be exactly like Clar's representations (below).**

However, it was Clar who applied this to much larger polycyclic benzenoid hydrocarbons and explained the various properties and characterisations observed with this rule. For example, using Clar's rule on phenanthrene **6**, the Clar structures are represented in Figure 7.<sup>11</sup> There are two Clar structures which can be drawn; one with two full isolated sextets (**b**) and the other with one (**a**). Therefore, the one with the greater number of sextets (**b**) is the most likely resonance form in terms of stability. This also suggests that two outer rings of phenanthrene will have more aromatic character than the central ring which can be said to behave more like an olefin. This is supported by various reports as phenanthrene **6** will readily substitute bromines without a catalyst on the middle olefinic ring of (**b**).<sup>11, 42, 43</sup>

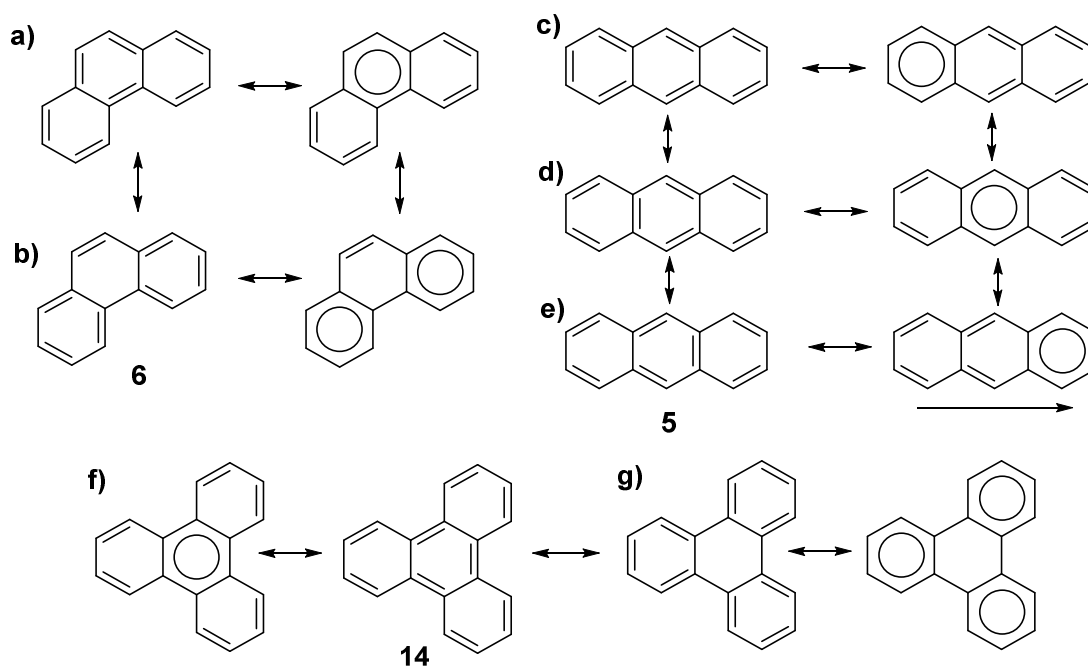


**Figure 7: Simplest set of linear and bent benzenoid structures. The respective Clar structures of a), b) phenanthrene **6** (isolated olefin), c), d), e), anthracene **5** (migrating) and f), g), triphenylene **14** (fully benzenoid) are shown.<sup>11</sup>**

Clar has described that there are three main forms of benzenoid species; 1) those that contain Clar sextets and a double bond, like an ‘isolated olefin’ (phenanthrene **6**), 2) those which contain a Clar sextet and rings which contains two double bonds, which are known as ‘migrating sextets’ as more than one Clar structure can be drawn (anthracene **5**, Figure 7, **c-e**), and 3) those that contain Clar sextets and empty rings which are known as ‘fully benzenoid’ (triphenylene **14**, Figure 7, **f-g**).<sup>11, 37</sup>

As discussed, the structure of phenanthrene with the most Clar sextets is likely to be most representative of the electronics of the compound and this can be used to compare properties of different structures as well. In anthracene, only one Clar sextet (migrating) can be drawn for any one structure (Figure 7, **c-e**), which would suggest that phenanthrene is much more stable than anthracene. This has been proven by experimental and theoretical studies which show that phenanthrene **6** has 4-12 kcal greater aromatic stabilisation energy than that of anthracene **5**.<sup>11, 44-49</sup>

Experimentally, anthracene reacts faster than phenanthrene especially in the central ring. This is due to the resulting intermediate **15** possessing two Clar sextets rather than the one migrating sextet, which provides greater stability, lowering the reaction activation energy (Figure 8).<sup>37, 45, 50</sup>

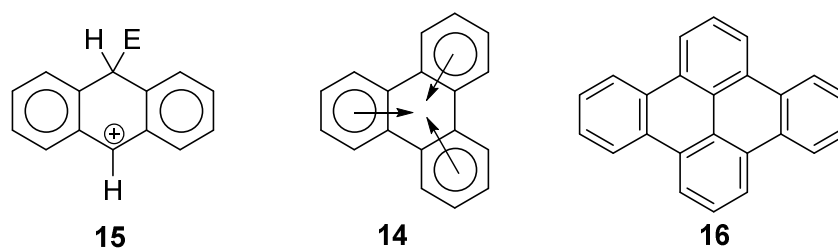
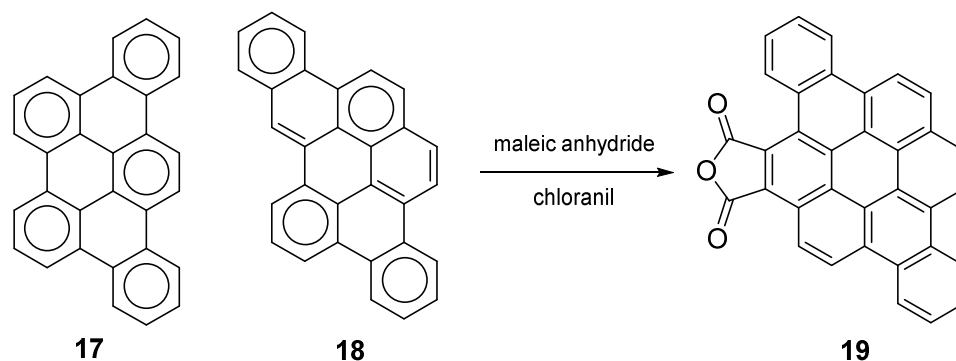


**Figure 8:** An addition reaction produces a more stable anthracene intermediate **15**, with two Clar sextets. The fully benzenoid triphenylene **14** has extra stability by the contribution of the  $2\pi$  electrons from each sextet.

The most stable are the ‘fully benzenoid’ structures which have  $6\pi$  electrons and ‘empty rings’ such as triphenylene **14**, dibenzo[*e,l*]pyrene **16** and tribenzo[*b,n,pqr*]perylene **17** (Scheme 2), which are also known to have extra stability.<sup>11, 51</sup> Clar commented that  $2\pi$  electrons can migrate from one ring to another, when applied to triphenylene **14**, the central ring cannot be empty but has a contribution of  $2\pi$  electrons from each ring shown in Figure 8.<sup>11, 52, 53</sup> Hence, an induced sextet is formed within the middle ring which provides additional stability.<sup>11, 52</sup>

Further support for Clar’s representation of the fully benzenoid series was that triphenylene compared to its isomers ( $C_{18}H_{12}$ , which have two Clar sextets at most) has the largest resonance energy, is chemically less reactive and has the highest ionisation potential and the largest highest occupied molecular orbital to lowest unoccupied molecular orbital (HOMO-LUMO) gap.<sup>11, 37, 45, 54</sup>



**Scheme 2: The first example of isomeric benzenoid reactivity in 1958, showing that **18** is more reactive than **17**.<sup>51</sup>**

In 1958 Clar and Zander found that **18** (benzo[*qr*]naphtho[2,1,8,7-*fghi*]pentacene) is more reactive than **17** (tribenzo[*b,n,pqr*]perylene) as **18** reacts to give **19** but **17** does not (Scheme 2). They realised that when drawing the Clar sextets that **17** was fully benzenoid, therefore very stable unlike its isomer **18**.<sup>51</sup>

The sextet rule also correlates to the ultra-violet/visible (UV/Vis) spectral data. In general, absorption for structures which are more stable (increased number of Clar sextets) will be of shorter wavelength than those that are less.<sup>11, 38, 45, 52, 55-58</sup> This effect is due to structures with more Clar sextets possessing more isolated  $\pi$  systems, which therefore have less inter-ring overlap and thus a larger molecular HOMO-LUMO gap.<sup>37, 45, 55, 59</sup> Another example is that the unstable hexacene **20** (one sextet) is green whereas its isomer dibenzochrysene **21** (four sextets) is colourless (Figure 9).<sup>38, 45, 55, 60</sup>



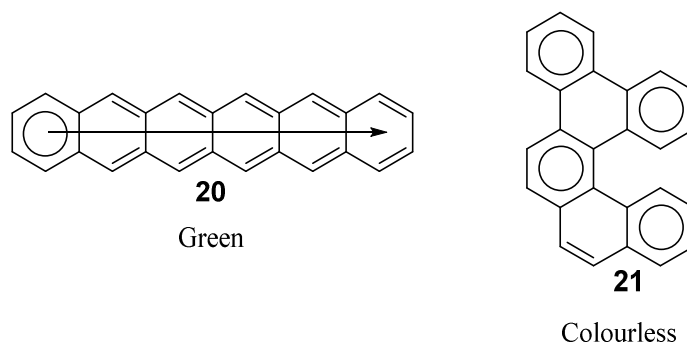


**Figure 9: Less stable compounds (hexacene 20) have a smaller HOMO-LUMO gap, therefore excitation is easier and coloured compounds can be formed, unlike more stable compounds (dibenzochrysenes 21).**

## 1.4 Bond lengths

Another key correlation is the carbon-carbon bond lengths in PAHs as determined by X-ray crystallography data. Typically, single carbon bonds are around 1.54 Å and double bonds are around 1.34 Å in length and if considering benzene, one would assume that a value mid-way at around 1.44 Å would be correct. However, the actual value is 1.39 Å due to the delocalisation of the  $\pi$ -electrons compressing the ring further.<sup>32, 61-65</sup>

It has been proposed that in polyaromatics such as acenes (linearly cata-fused benzenes), there cannot be a double bond between two adjoining rings, therefore if any bonds are short this must be caused by the migration of delocalised electrons in the acene.<sup>24, 32, 52, 66</sup>

For example, drawing the different resonance forms (all the different ways to draw the double bonds in the structure) of the smallest acene naphthalene **4**, and treating them equally, an overall illustration can be formed. This is a Clar sextet in one ring and two double bonds in the other ring (Figure 10).<sup>32</sup> One would probably assume that the electrons are delocalised evenly across the structure forming bond lengths similar to each other. However, the x-ray crystallography results of the actual bond

lengths show some which are significantly different (Figure 10). The ‘**B**’ bonds are much shorter (1.361 Å) than the rest which suggests that they have more double bond character.<sup>32, 67</sup> The bond lengths are consistent with the Clar structure including a ‘butadiene’-like second ring (Figure 10).<sup>32, 63, 68</sup>

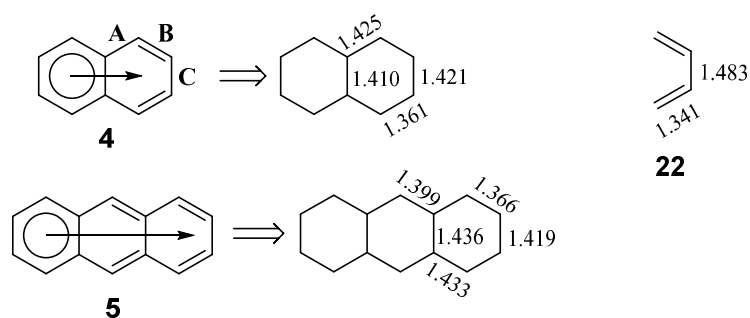


**Figure 10: Clar structures and bond lengths (Å) of naphthalene 4, 1,3-butadiene 22 and anthracene 5.**<sup>32, 67-70</sup>

The ‘butadiene’-like character continues with anthracene **5** (Figure 10) as the compound behaves more like an olefin.<sup>32, 69-71</sup> In continuation along the acene series, the aromatic sextet becomes more dispersed when increasing the number of rings that are being shared along the whole structure. This is illustrated by the bond lengths of tetracene **23** and pentacene **24**, as they become much more similar to each other when increasing the number of rings in the series (Figure 11).<sup>32, 72, 73</sup>

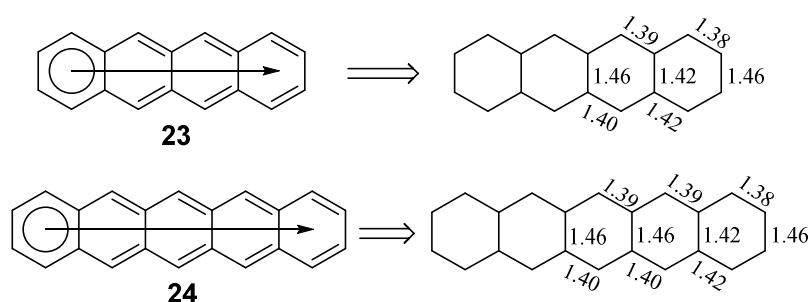


**Figure 11: Clar structures and bond lengths (Å) of tetracene 23 and pentacene 24.**<sup>32, 72, 73</sup>

Extending this theory to the perylene system (Figure 12), the most notable observation is that the middle connecting bonds have almost single bond bond-length

of 1.50 Å. This suggests that perylene **25** is best described as two joined naphthalenes with the other bond lengths similar to naphthalene, agreeing with the Clar structure model.<sup>32, 74</sup> Most of the middle bonds in these perylene-like structures (rylenes - see section 1.6.5) are single bond-like which suggests that the  $\pi$  electrons spend most of the time in acene-like  $\pi$  systems, but one must consider that bond lengths may be different in other states; such as gas and liquid.<sup>32</sup>

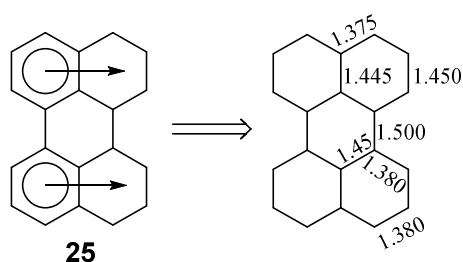


**Figure 12: Clar structure and bond lengths (Å) of perylene **25**, with the middle bond having a more single bond character.**<sup>32, 74</sup>

As mentioned before, the Clar structure of phenanthrene **6** (Figure 7) suggests that the central ring will have more double bond character. The double bond '**D**' has a length of 1.341 Å (Figure 13) which is the shortest in the whole structure and therefore the most alkene-like, agreeing with Clar's theory.<sup>32, 37, 75, 76</sup>

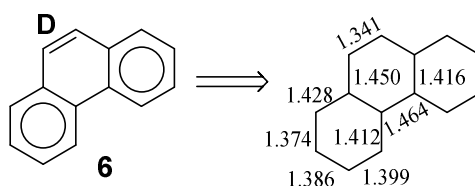


**Figure 13: Clar structure and bond lengths (Å) of phenanthrene **6**, where the central ring has more double bond-like character.**<sup>32, 75</sup>

In summary, the  $\pi$ -sextet concept is important in helping to determine the stability of compounds as electronic delocalisation is considered a stabilising feature.<sup>11, 77</sup> As Zhou and Parr commented; 'the cyclic conjugation forms aromaticity and this sustained induced ring current in compounds shows high stability and low

reactivity'.<sup>78</sup> Thus, coupled with the notion that the most stable Clar structures are those with a closed-shell and with the highest number of Clar sextets (then their isomers), fully benzenoid structures fit these descriptions completely.<sup>11, 51, 79</sup> However, even though this method provides a relatively easy way to qualitatively measure characteristics of PAHs this is not a quantitative method as you cannot determine how much a 'ring' or compound is more aromatic than another in the same structure.<sup>49</sup>

### 1.5 Pauling ring bond orders

Pauling bond orders calculate the number of chemical bonds between two atoms.<sup>38, 48, 80</sup> Recently, Randić and co-workers extended the idea of Pauling bond orders into benzenoid compounds to estimate the aromaticity in each ring, by averaging the C=C content in each ring *via* its Kekulé structure.<sup>38, 81-85</sup> Thus, forming 'Pauling ring bond orders' (RBO) which are defined as 'the sum of Pauling bond orders for the six carbon-carbon bond forming individual rings'.<sup>38</sup> To calculate the value of the Pauling ring bond orders one can simply follow these steps:

- 1) For the given benzenoid draw out every resonance structure.
- 2) Add up the double bonds in each ring (bordering double bonds can count as one for each ring as well).
- 3) Calculate the sum of the number of double bonds in each individual ring and divide by the number of resonance forms. This provides the estimated value for the RBO of each individual ring of the benzenoid (Figure 14 & 15).<sup>38</sup>

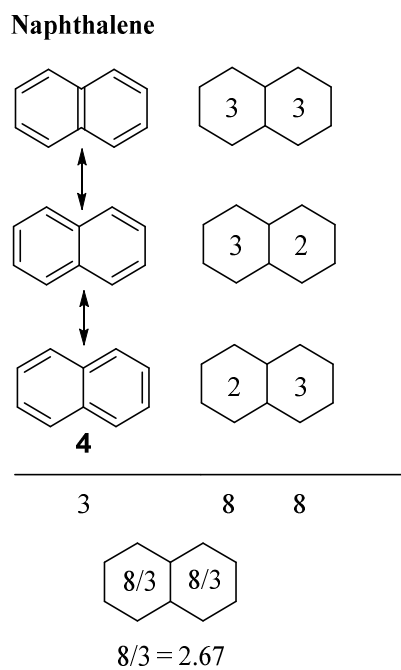


Figure 14: Shows the Pauling ring bond order of naphthalene 4.<sup>38</sup>

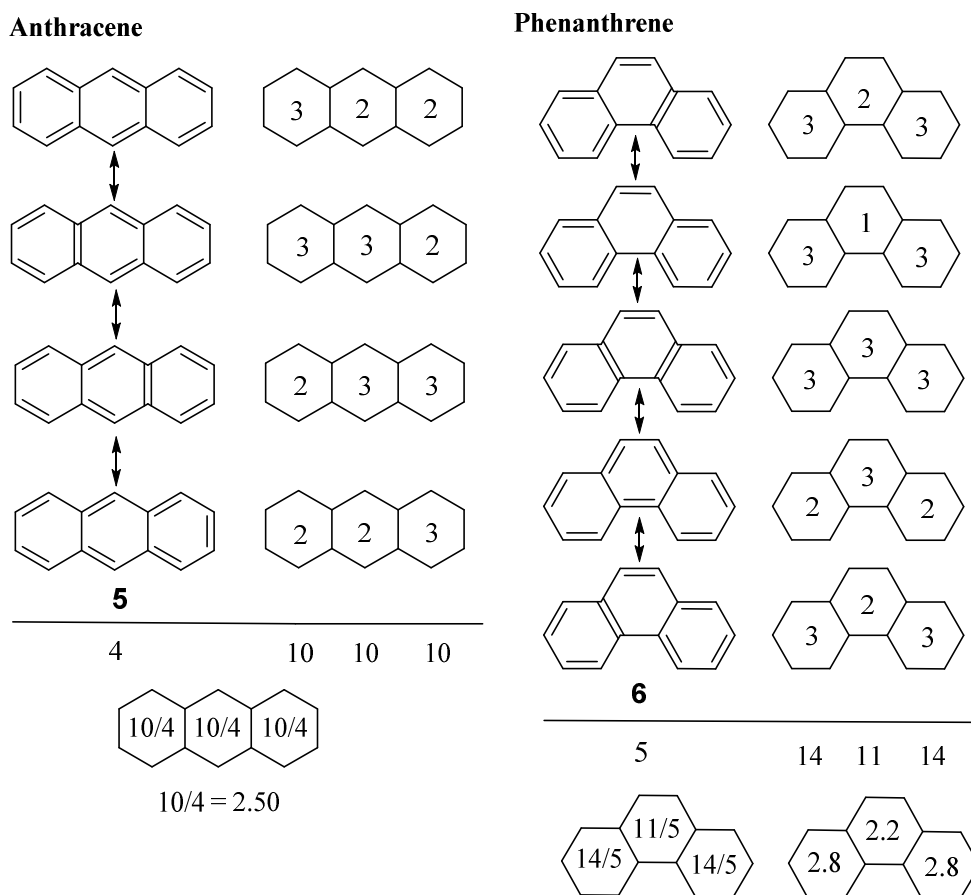


Figure 15: Pauling ring bond orders of the isomers anthracene 5 and phenanthrene 6.<sup>38</sup>

The maximum number of double bonds per ring you may obtain is three, the value obtained for benzene for its Kekulé structure.<sup>38</sup> The linear acenes (Figure 16) show a decrease in value from naphthalene **4** (2.67) to anthracene **5** (2.50) and furthermore tetracene **23** (2.40), pentacene **24** (2.33) and hexacene **20** (2.29).<sup>38</sup> In addition, phenanthrene **6** shows that the central ring has a lower RBO (2.2) than the two outer rings (2.8). As Randić and co-workers pointed out, this information seems to be consistent with Clar's aromatic sextet theory.<sup>38</sup> As discussed in section 1.3, naphthalene and anthracene both contain one migrating sextet; however, increasing the number of rings 'dilutes' the aromaticity of the sextet as it is spread across more rings and therefore the reactivity increases as stability decreases.<sup>11</sup> This correlates to the Pauling RBO values, which decrease along the acenes, and the Pauling RBO values are also the same in each individual ring which supports the 'migrating' sextet theory. In phenanthrene, the Clar structure has two sextets, hence the total RBO value of these outer rings is larger than that of anthracene (which contains one sextet). However, the key factor is that central ring has a lower Pauling RBO which suggests that this ring is less stable, and this is consistent with its increased reactivity.

When an array of PAHs are considered, the correlation is more apparent (Figure 17). For example, the fully benzenoid triphenylene **14** has values close to that of benzene for its 'fixed sextet' (2.89) and the central 'empty' ring has a very low value which is expected when drawing the Clar structure (Figure 17).<sup>38, 81</sup> Perylene **25** is depicted as two sets of naphthalene units fused with a low value central ring. An addition of a ring to one of the naphthalene units on perylene shows an anthracene like structure, again in agreement with Clar (Figure 16).<sup>11, 38, 81</sup>

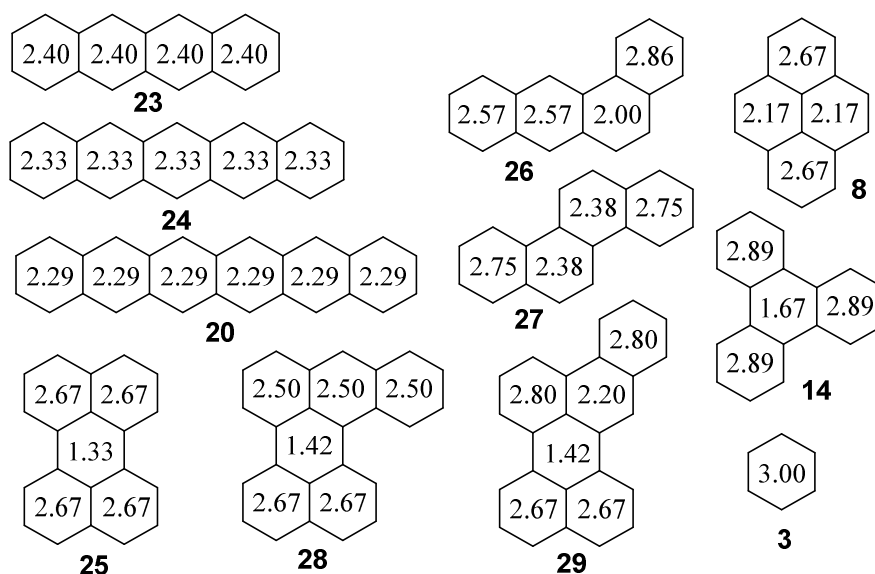


Figure 16: Calculated Pauling RBOs of selected PAHs by Randić *et al.*<sup>38, 81</sup>

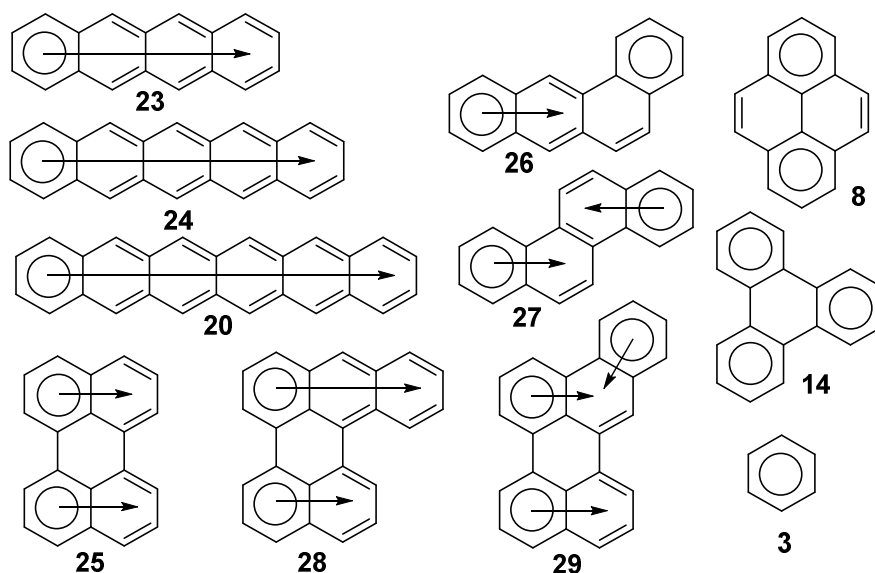


Figure 17: Correlating Clar structures of the selected compounds from Figure 16.<sup>11, 38</sup>

Overall the general correlation with Clar's rule and Pauling RBOs is that the 'fixed sextets' have larger Pauling RBO values than the 'migrating sextets' and the 'isolated olefins', with the fully benzenoid 'empty rings' having the lowest values.<sup>38</sup> Thus the Pauling ring bond order method can now be considered to advance Clar's sextet rule from a qualitative to a quantitative level.<sup>38</sup>

## 1.6 General classifications of different PAHs

The basic building block of PAHs is the benzene ring and these are fused together to form different classes of PAHs, most commonly; acenes, phenes, periacenes, helicenes and circumcenes. Some classes can also fuse four, five and seven membered rings within the structures of the six membered rings to produce arylenes.<sup>11, 30, 32, 33, 36</sup>

### 1.6.1 Acenes

When benzene rings are fused linearly they produce a class of organic compounds known as acenes. Common acenes are naphthalene **4**, anthracene **5**, tetracene **23** and pentacene **24** (Figure 18). As the number of rings on an acene is increased, the energy gap and the stability decreases as there can only be one sextet (Clar's sextet theory) in this group of compounds. For example, anthracene is colourless and as you proceed further in this linear series the HOMO-LUMO gap reduces with increased conjugation, and it takes less energy to promote an electron to an excited state. This in turn increases the wavelength absorbed towards the visible range which results in coloured compounds; tetracene **23** (orange), pentacene **24** (deep blue), hexacene **20** (green). The reactivity also increases as the one aromatic sextet is diluted throughout the structure and therefore they are more olefin-like, as both pentacene and hexacene oxidise readily in air.<sup>11, 38, 45</sup> Pentacene and hexacene have to be handled under inert atmosphere whereas heptacene has not been isolated in pure form due to its instability in air.<sup>32, 36, 86, 87</sup>



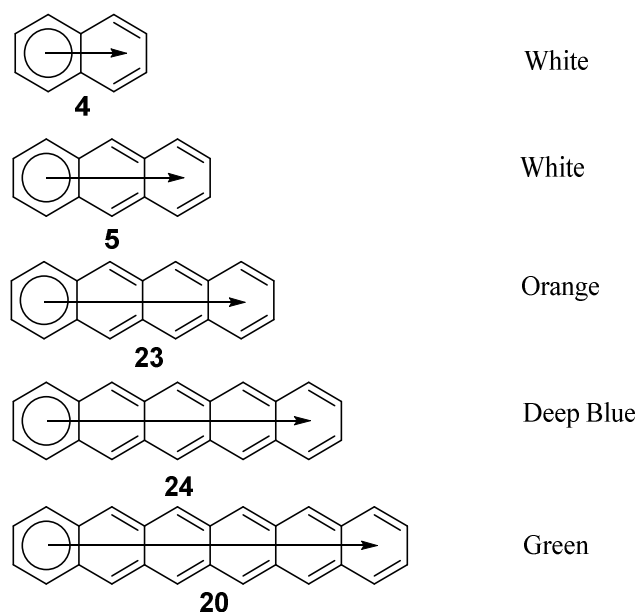
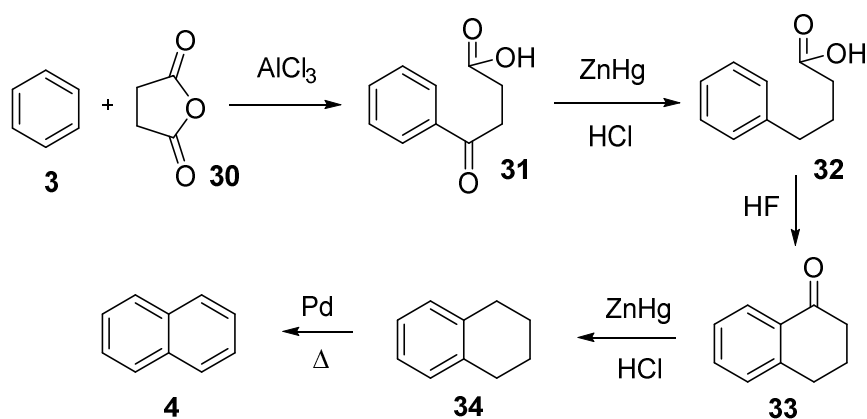


**Figure 18:** The first five compounds in the class of acenes. They all have one migrating Clar sextet; both naphthalene **4** and anthracene **5** are white, the rest are coloured compounds.<sup>11</sup>

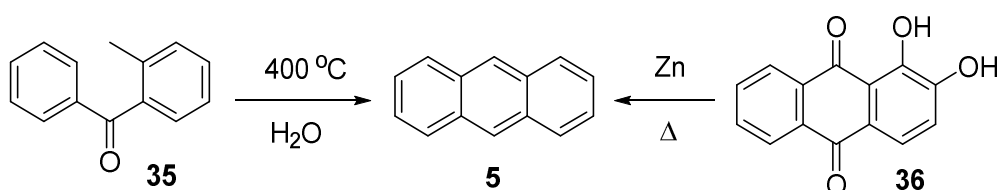
Naphthalene **4** and anthracene **5** are usually obtained from the petroleum industry, whereas the higher acenes have to be made synthetically. Naphthalene can however be made by the Haworth method which was originally used in 1932 to synthesise phenanthrene **6** (Scheme 3).<sup>88-90</sup>



**Scheme 3:** The Haworth synthesis of naphthalene **4**.<sup>88-90</sup>

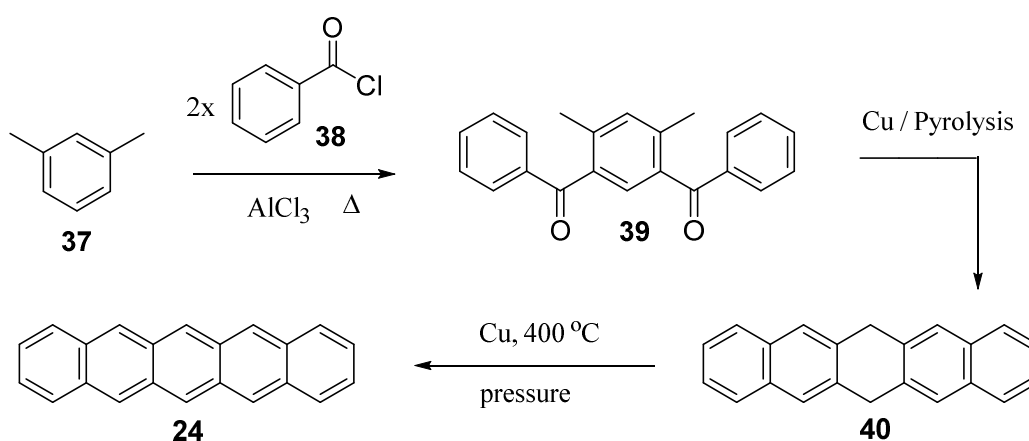
Anthracene was first synthesised by Limpricht in 1866 from benzyl chloride, 34 years after it was discovered in coal-tar by Dumas and Laurent.<sup>32, 91, 92</sup> Anthracene **5** was also synthesised by Liebermann and Graebe in 1868 from the natural product

alizarin **36** (rose madder), by von Baeyer's zinc-dust distillation.<sup>32, 91, 93, 94</sup> Clar later modified von Baeyer's method (with a Zn melt of Zn dust, NaCl and 5 parts ZnCl).<sup>32, 91, 95</sup> Conversely, Liebermann and Graebe have also made alizarin **36** from anthracene **5**, which was an important discovery as this natural product was used as a red dye in industry.<sup>32, 91, 96</sup> William Henry Perkin, renowned for his work in the field of dyes, also discovered the same synthesis of alizarin in that year.<sup>91, 97</sup> Nowadays a common route to synthesise anthracene is to use the Elbs reaction (Scheme 4).<sup>98</sup>



**Scheme 4:** Elbs reaction to synthesise anthracene **5** (left) and alizarin **36** to form **5** (right).<sup>98</sup>

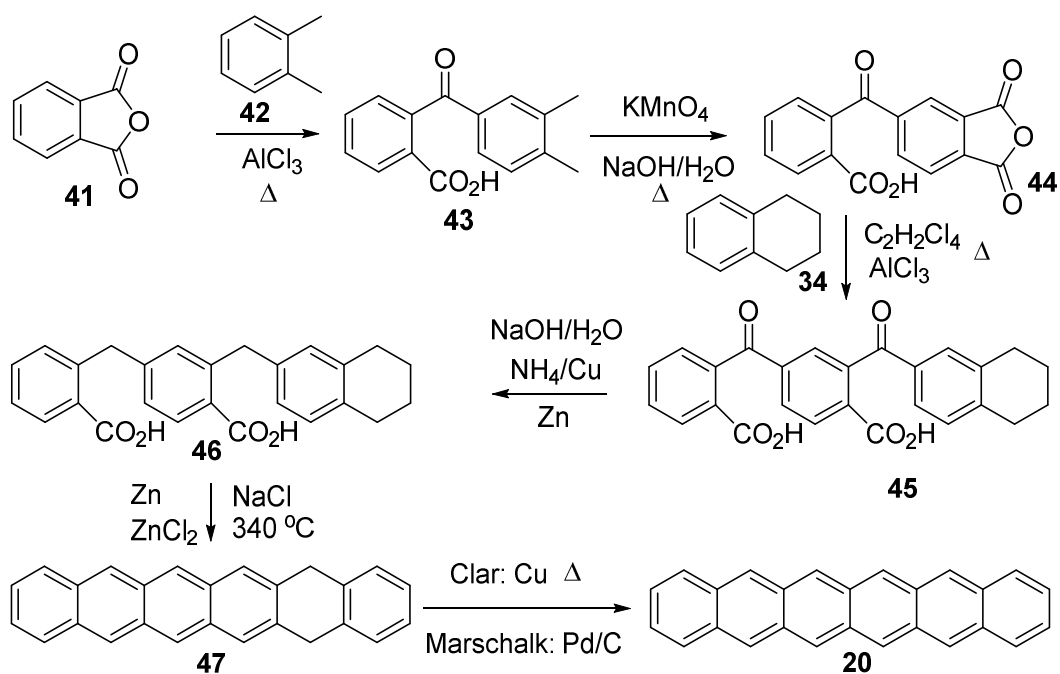
One of the most important acenes in electronics is pentacene **24**. Pentacene was first synthesised by Clar and John starting from a Friedel-Crafts acylation of *m*-xylene **37** with benzoyl chloride **38** (Scheme 5), which includes an Elbs reaction used in the synthesis of anthracene.<sup>91, 98-101</sup>



**Scheme 5:** First synthesis of pentacene **24** by Clar and John, even though in 1911 Phillipi claimed to have synthesised it, many believe he actually made an isomer of dihydro-pentacene **40**.<sup>99, 101, 102</sup>

There have been a number of more efficient synthesis of pentacene reported. Bailey and Madoff in 1953 were able to synthesise it starting from the readily available 1,2-dimethylenecyclohexane and quinone, while Goodings *et al.* were able to reduce a diketo-pentacene precursor with aluminium wire and mercuric chloride.<sup>102, 103</sup>

Hexacene **20** was first synthesised in 1939, independently by both Clar and Marschalk, where they used copper powder and Pd/C catalysts respectively to oxidise dihydro-hexacene **47** (Scheme 6).<sup>104-106</sup>



Scheme 6: Oxidation of **47** to form hexacene **20** by either copper powder or Pd/C.<sup>30, 104, 106</sup>

Due to the unstable nature of larger acenes, bulky substituents have been used to help stabilise these products which in turn makes them more soluble in solution. For example, derivatives of undecacene have been produced by Marschalk but not the unsubstituted analogue as this compound is too unstable.<sup>30, 32, 107</sup>

A notable report by Tönshoff and Bettinger showed that they were able to isolate octacene **48** and nonacene **49** using UV irradiation, by stabilising the compound on an argon matrix at 30 K (Scheme 7).<sup>30, 108</sup>

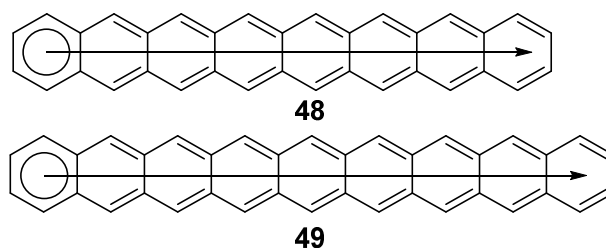
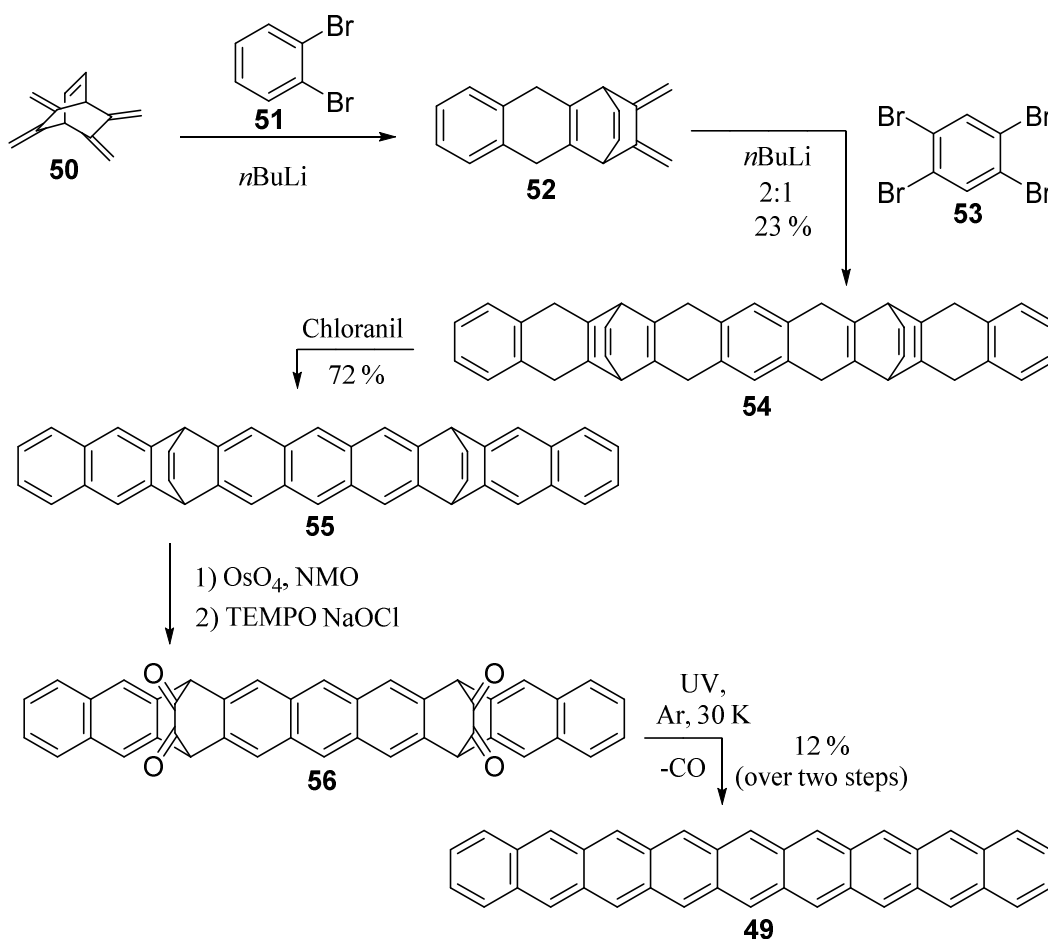


Figure 19: Octacene **48** and nonacene **49**.



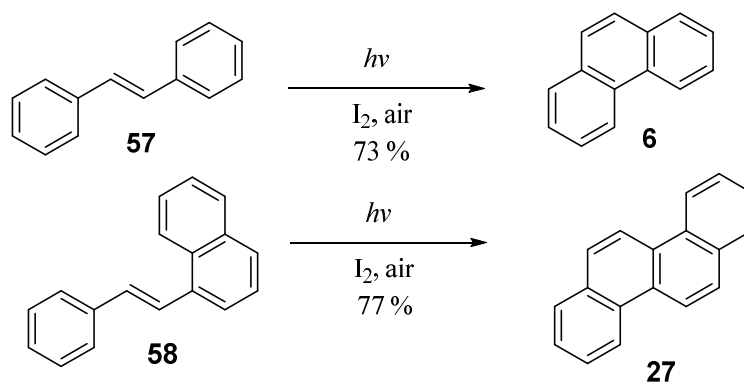
Scheme 7: Synthesis of nonacene **49** using an argon matrix at 30 K with UV radiation as reported by Tönshoff and Bettinger.<sup>30, 108</sup>

This shows that the longer the acene the more polyene character it has and therefore less aromatic stability, as Clar postulated.

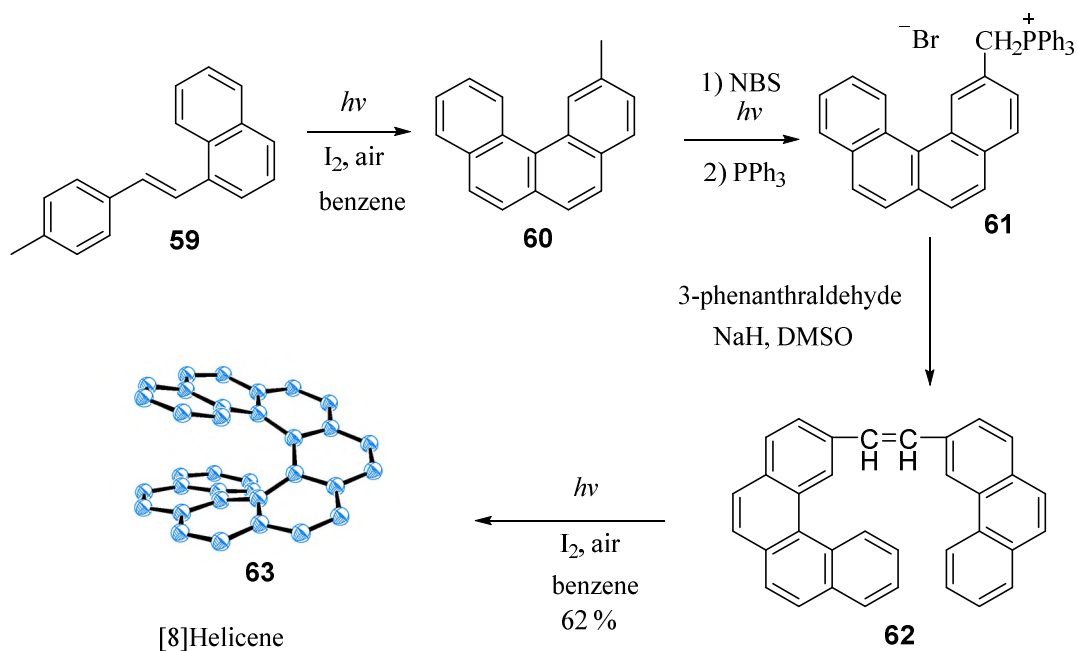
### 1.6.2 Helicenes

When benzenoid rings are annulated in a helical mode, helicenes are formed. These contain one Clar sextet and are interesting due to their unique helical structures introducing chirality into the molecule which is caused by steric overcrowding.<sup>32, 91</sup>

In 1903 the first helicene was produced by Jakob Maisenheimer *via* the reduction of 2-nitronaphthalene.<sup>109</sup> Since then, a key synthesis by Wood and Mallory in 1964 produced phenanthrene **6** using a photochemical induced cyclisation of stilbene **57** (Scheme 8) which is a reaction still used for helicene synthesis today.<sup>91, 110</sup> For example, Martin and Flammang-Barbieux *et al.* made hexa- (60 %) hepta- (20 %), octa- **63** (62 %) and nonahelicene (48 %) using this method as part of the synthesis in the 1960s (Scheme 9).<sup>91, 111, 112</sup>



**Scheme 8: Wood and Mallory cyclised various substituted stilbenes with great success and efficiency; yields of 73 % and 77 % and irradiation for only seven and four hours for phenanthrene **6** and chrysenes **27** respectively.**



**Scheme 9: Synthesis of [8]helicene 63 by Martin *et al.* represented by the Chem 3D model, utilising the work of Wood and Mallory.**

[16]Helicene **64** is the longest helicene produced to date, this was completed by K. Mori *et al.* in 2015 using the same methods as above (Scheme 9).<sup>113</sup>

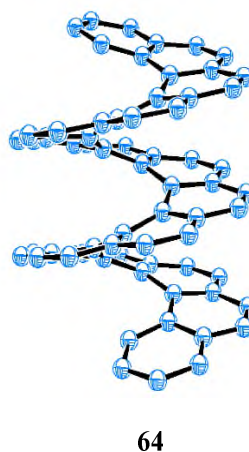


**Figure 20: Chem 3D model of [16]helicene 64.**

### 1.6.3 Phenes

When benzene rings are fused in an angular arrangement, they are called phene-type PAHs. The smallest of which is phenanthrene **6** which can also be regarded as the basis of all phenes as they all have this arrangement incorporated within them.<sup>32, 36</sup>

Examples of the phene series are; phenanthrene **6**, tetraphene **26**, pentaphene **65** & **66** and hexaphene **67** & **68** (Figure 21). This class of PAH are more stable than the acenes as it is possible to draw two Clar sextets within the structures; however, the stability decreases in the same way as with acenes when increasing the number of fused rings in the phene system.<sup>11, 32, 87</sup>

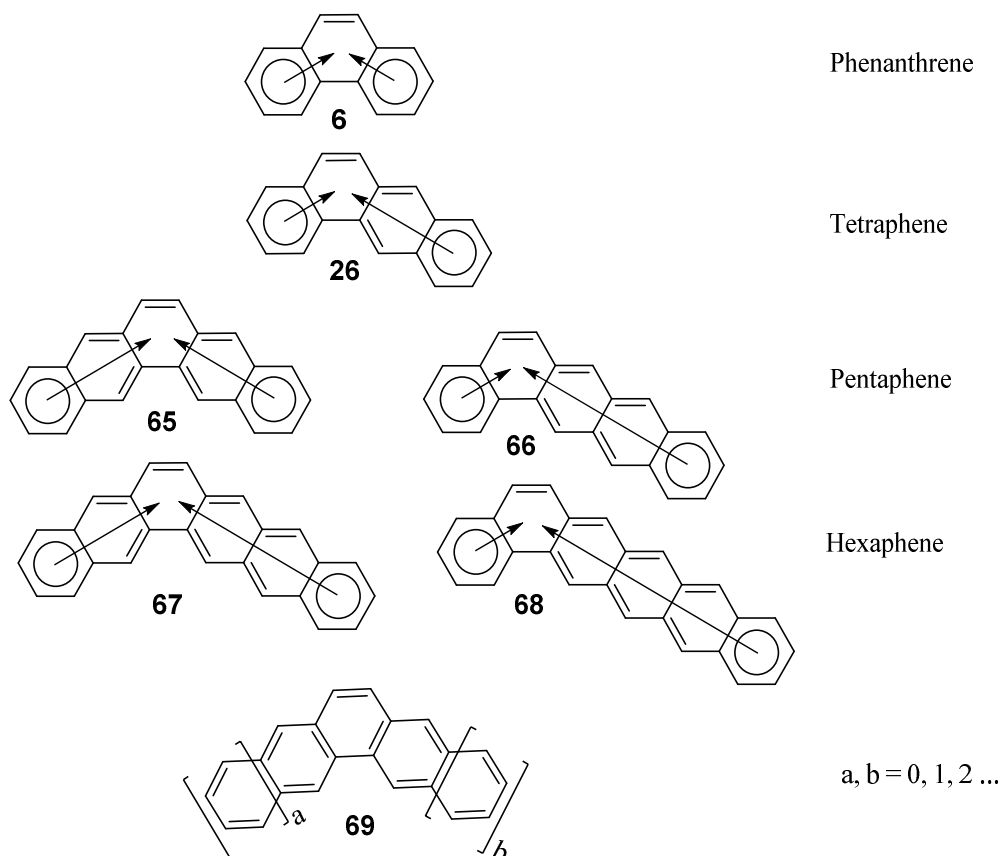
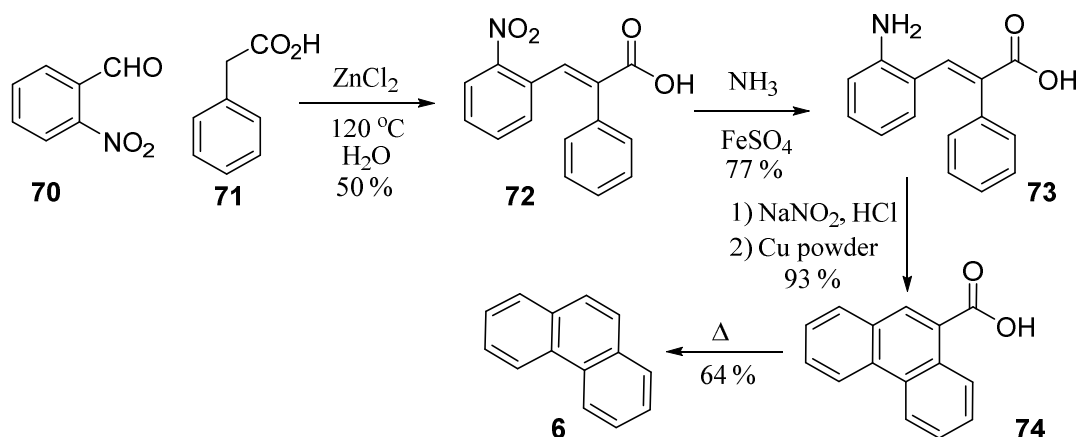


**Figure 21: The ‘phene’ series (including isomers), the larger they are the more apparent it is that an acene-like migrating sextet is present within each arm of the phene **69**.**<sup>11, 32, 91</sup>

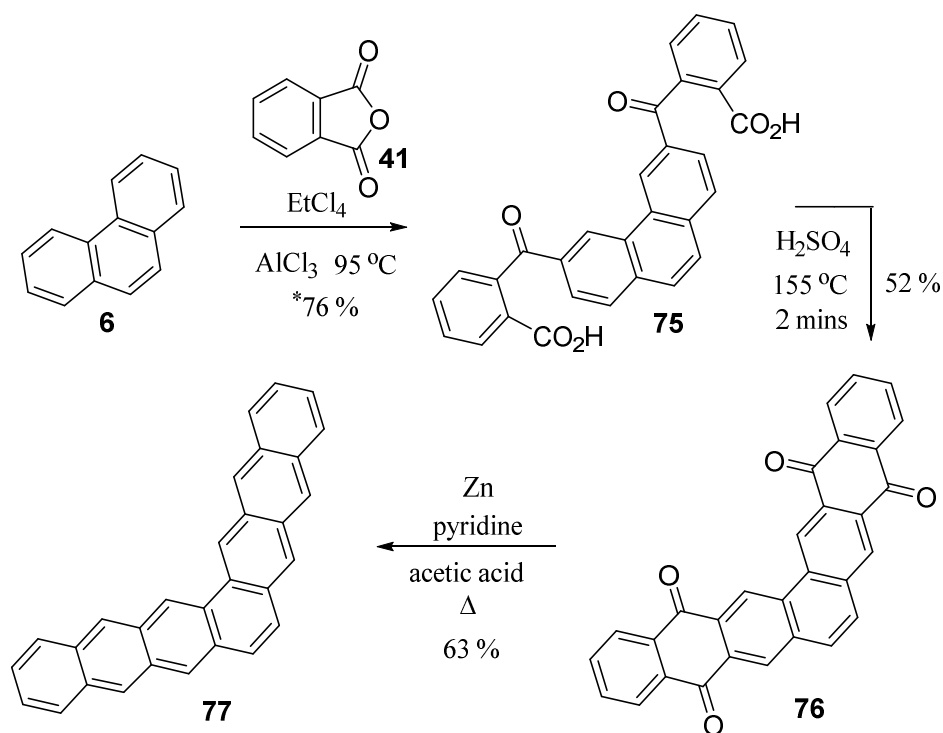
Phenanthrene was first discovered in coal-tar by Ostermayer and Fitting and also by Glaser in 1872. In 1896 Pschorr developed an efficient synthesis by starting with *o*-nitrobenzaldehyde **70** and phenylacetic acid **71** (Scheme 10).<sup>32, 91, 114-116</sup> This condensation reaction was completed under relatively low temperatures (compared to around 300 °C) which was a significant step forward as many other similar

methods such as Graebe's synthesis had used very high temperatures to form PAHs such as pentacene.<sup>32, 91, 117</sup>



**Scheme 10: Pschorr's effective synthesis of phenanthrene 6; nitro group reduction followed by copper catalysis to cyclise the intermediate 73 and finally thermal decarboxylation.**<sup>91, 116</sup>

In 1953 Clar and Kelly published a synthesis of heptaphene **77**, starting from phenanthrene (Scheme 11), where they completed extensive UV studies on this series.<sup>118</sup>



**Scheme 11: Synthesis of heptaphene 77, (\*may contain other isomers).**<sup>118</sup>



### 1.6.4 Starphenes

When three benzenoid branches are added to a central benzene ring and are extended linearly, ‘starphenes’ are produced as they form a ‘star-shaped’ phene with triphenylene **14** being the smallest of them. Starphenes contain three Clar sextets with triphenylene as the only fully benzenoid of this series, showing high stability (Figure 22).<sup>11, 30, 32</sup>

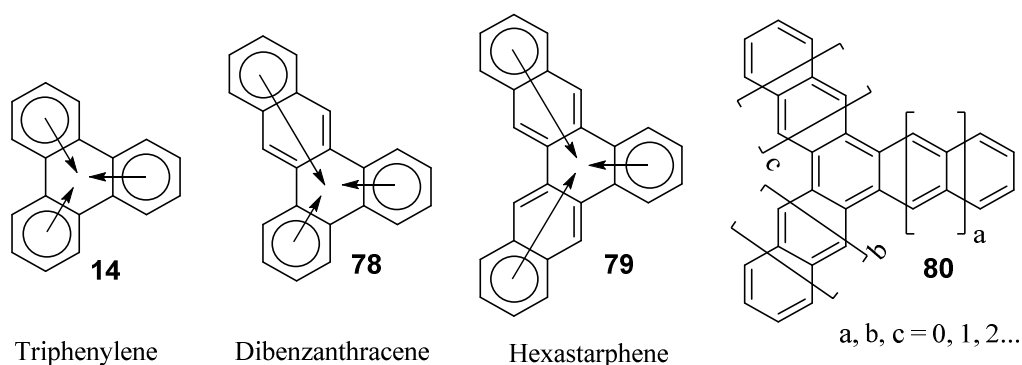


**Figure 22: The starphene series where each arm of triphenylene **14** is extended in any of the three directions.**

Starphenes have been synthesised up to decastarphene by Clar and Mullen.<sup>30, 119, 120</sup>

### 1.6.5 Rylenes

When two or more naphthalene units are *peri*-condensed together the resulting compounds are known as rylenes (Figure 23). The smallest rylene is perylene **25** which was first synthesised by Scholl *et al.* through the dimerisation of naphthalene **4** with  $\text{AlCl}_3$ . (Scheme 12).<sup>121</sup>

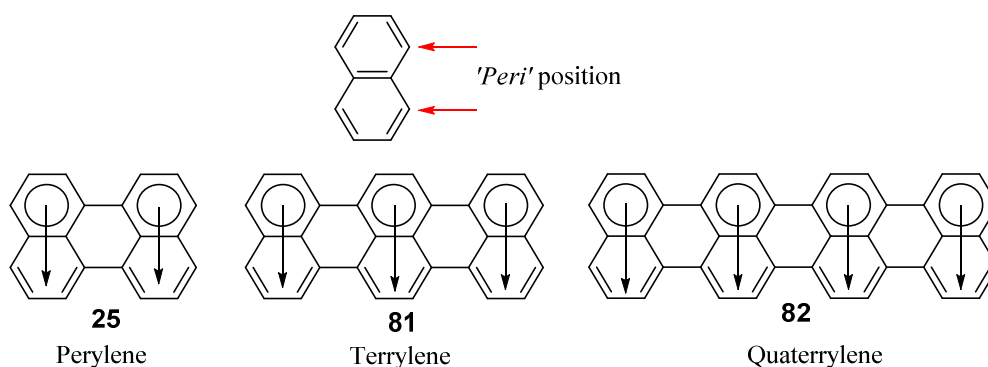
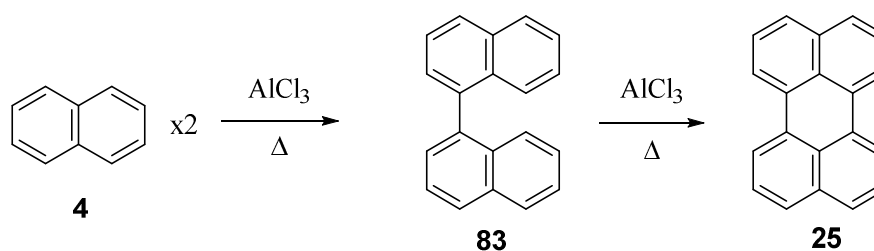
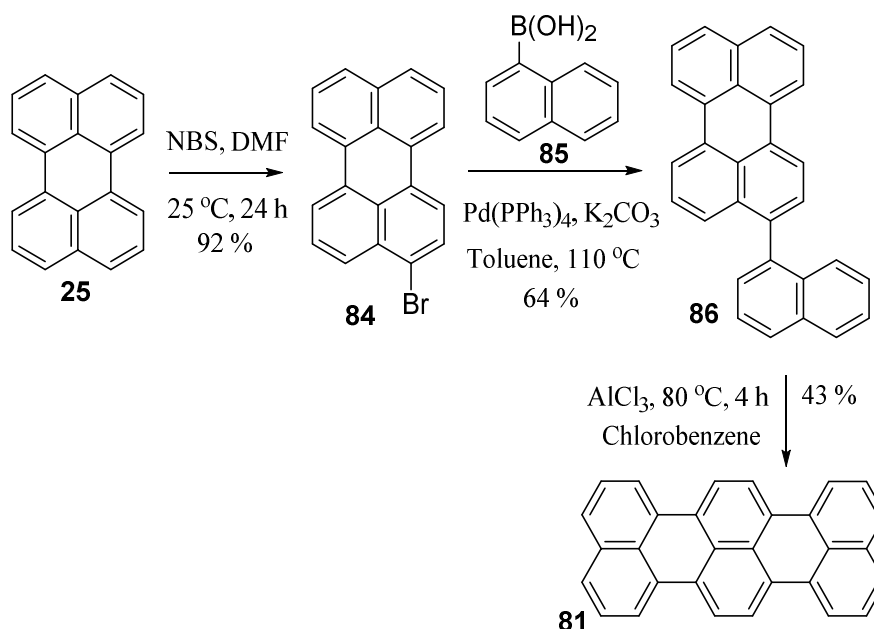


**Figure 23:** The rylene series, where each is extended by an addition of a naphthalene unit.



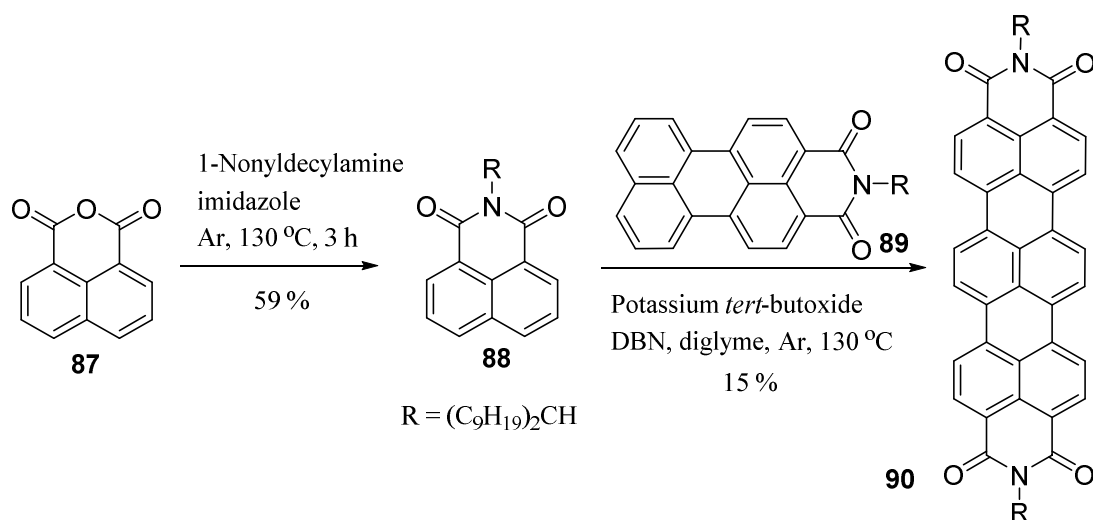
**Scheme 12:** The Scholl reaction using aluminium chloride and heat to form **25**.<sup>34,35</sup>

These sets of PAHs have been extensively studied as they form good dyes, with terrylene **81** and quaterrylene **82** being the two most common.<sup>30, 121, 122</sup>



**Scheme 13:** Synthesis of terrylene **81** using an intramolecular cyclodehydrogenation in the last step, which is a common reaction in the formation of these type of compound. Further extension upon the rylene axis can provide a synthesis of nanoribbons using similar methods.<sup>30, 122</sup>

Recently scientists have incorporated electron withdrawing groups such as dicarboxylic imides at the *peri*-positions to improve their chemical and photostability for the use in electronics and dyes (Scheme 14).<sup>30, 123-125</sup>



**Scheme 14: Illustrates the inclusion of dicarboxylic imides in enhance their properties.**

Octerylene bisamide is the highest rylene reported to date.<sup>30, 126, 127</sup>

### 1.6.6 Zethrenes

When two or more offset benzene rings are sandwiched between two naphthalene units in a 'z' shape, a class of PAHs known as zethrenes are formed (Figure 24). These are not as well-studied as other PAHs due to their low availability and sensitivity to light and air.<sup>11, 30, 33</sup>

According to Clar's rule the two outer naphthalene units are aromatic in character and the middle two ring in zethrene **91** are fixed double bonds with no aromatic character.<sup>11, 30, 33</sup>

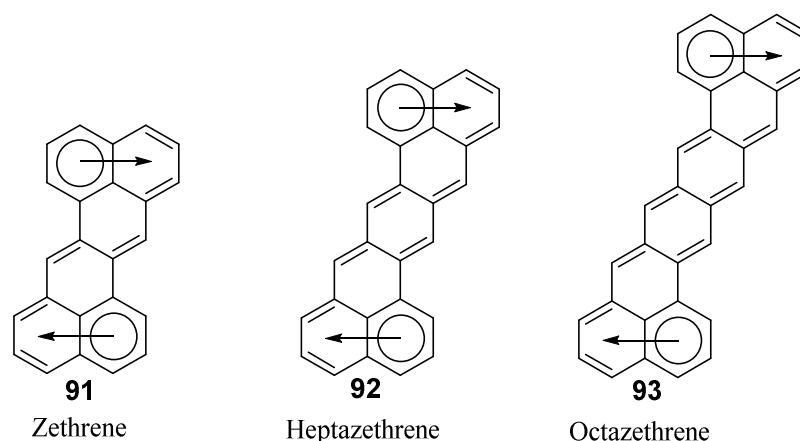
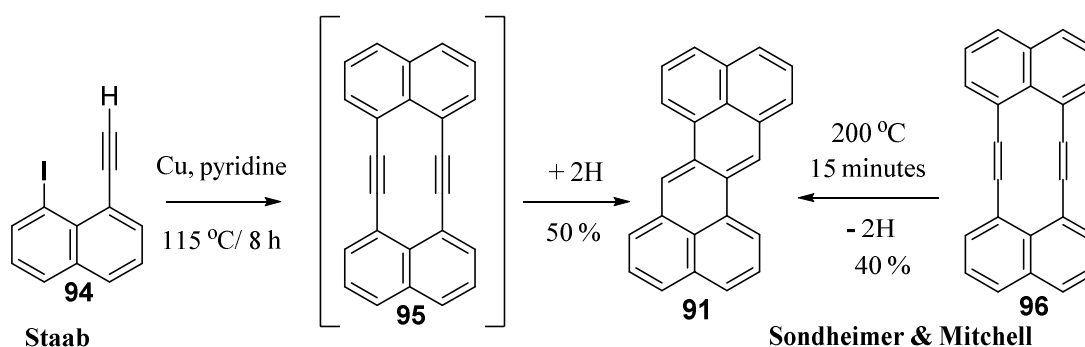


**Figure 24: The zethrene series where two Clar sextets lie in the naphthalene units whilst the middle rings have predominantly double bond character.**

The first zethrene was made by Clar in 1955 starting from di-substituted chrysene **27** in a long and laborious process.<sup>30, 33, 128</sup> However, 13 years later a more convenient synthesis was published by Sondheimer and Mitchell from dinaphth[10]annulene **96**. Staab *et al.* synthesised tetrahydroinaphtho[10]annulene **95** but because of its instability it rapidly cyclised into zethrene **91** under the reaction conditions (Scheme 15).<sup>30, 129-131</sup>



**Scheme 15: Staab *et al.* method (left) and Sondheimer and Mitchell's method (right) both published in 1968.**<sup>129, 131</sup>

As zethrenes become longer they become highly reactive, as Clar and Macpherson found when synthesising heptazethrene **92** and Ernülü did when synthesising octazethrene **93**, with both arenes oxidising very quickly.<sup>30, 33, 132, 133</sup>

The arrangement of these fused benzene rings can contribute to very different properties, even when changing the position of one ring. For example, if a ring is taken from one of the ends of zethrene **91** and placed on the opposing side **97** (top end taken here) the structure turns from a Kekulé to a non-Kekulé form (Figure 25).<sup>134</sup> This in turn forms a whole series of non-singlet ground-state compounds which are even less likely to be isolated.

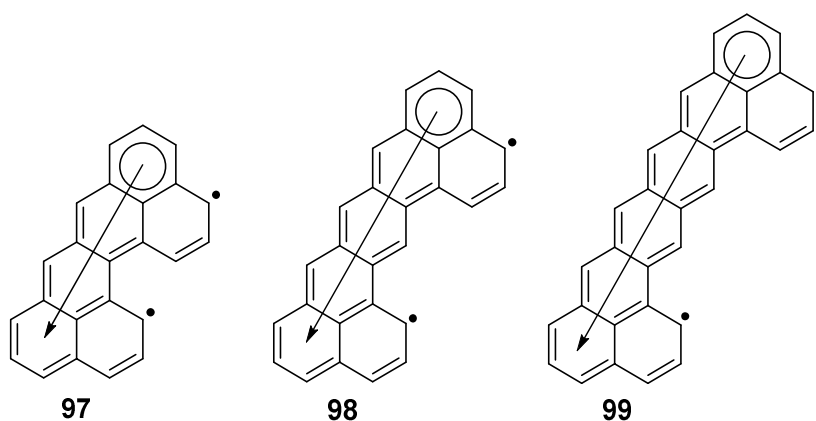


**Figure 25: Movement of one ring on a zethrene **91** turns it from a Kekulé to a non-Kekulé structure.**<sup>134</sup>

### 1.6.7 *Peri*-condensed polyarenes

When benzenoids are fused at their '*peri*' positions a large class of *peri*-condensed PAHs are formed such as pyrene **8** and hexabenzocoronene (HBC) **100**, this class also include the subdivision of '*peri*-acenes'; biasanthene **101**, peritetracene **102** and others such as tetranthene **103**.<sup>11, 32, 33, 36</sup>

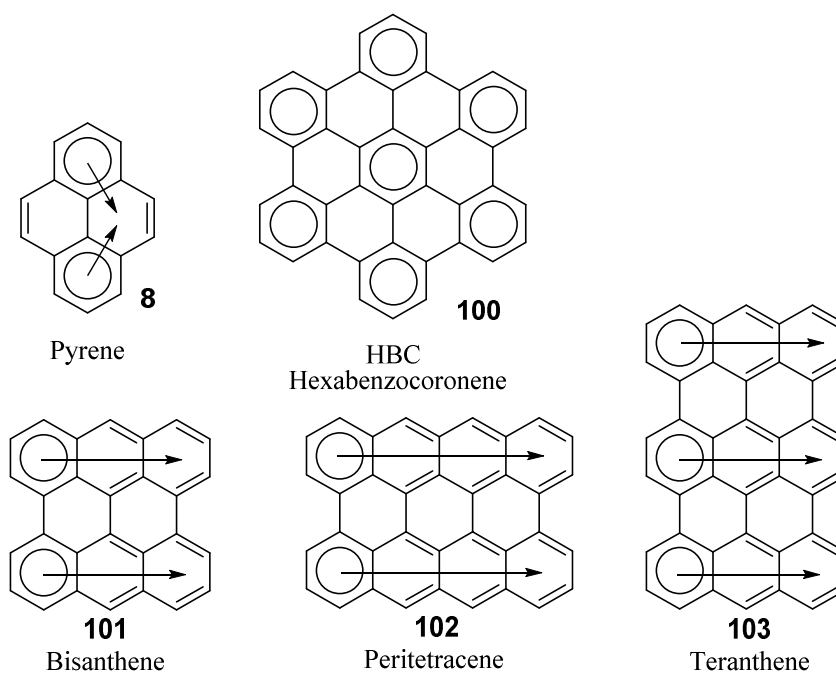


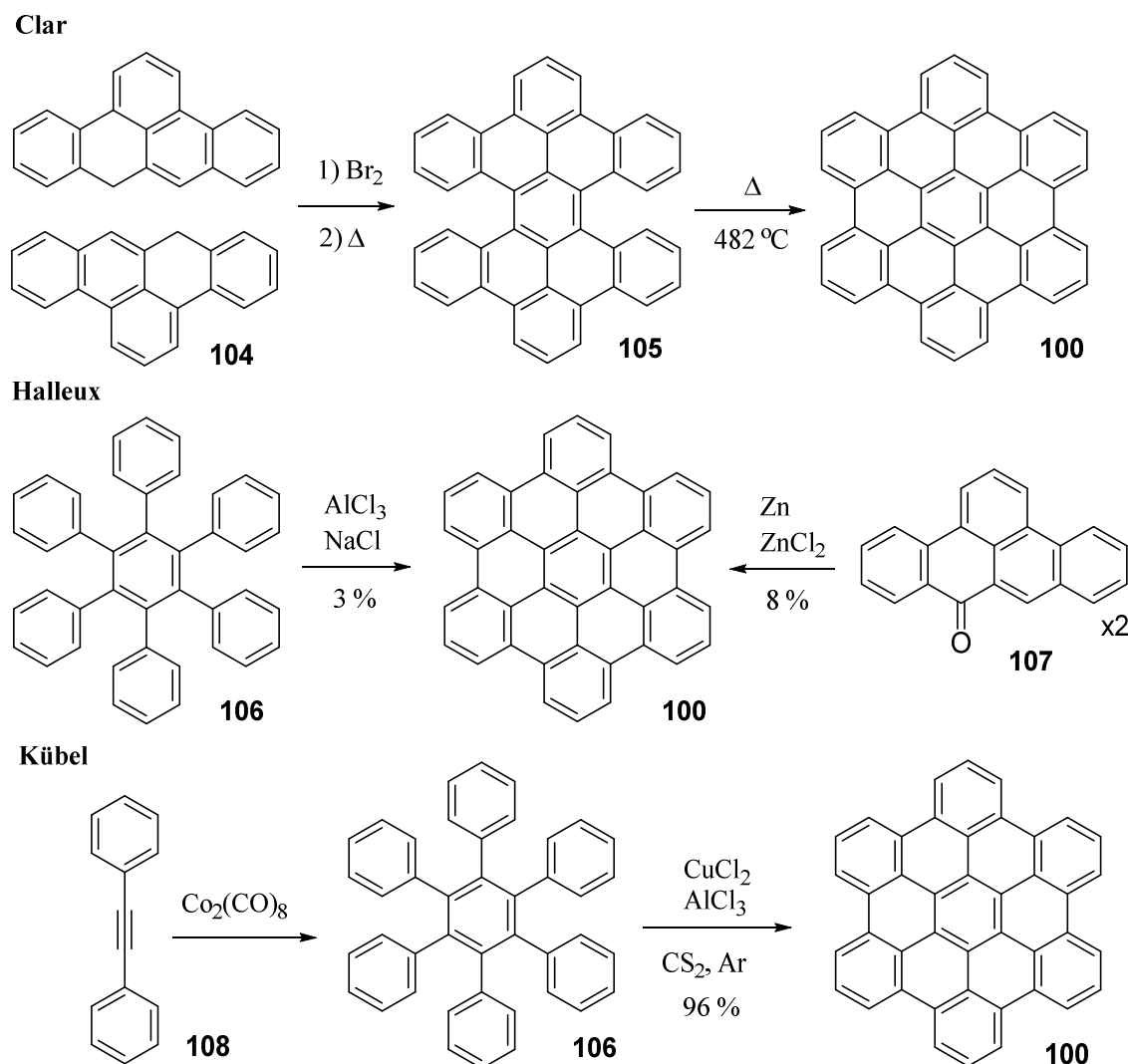
**Figure 26:** *Peri*-condensed PAHs showing the Clar sextet forms.

The number of Clar sextets varies in the *peri*-condensed PAHs as it is a big group of compounds (Figure 26). In each *peri*-acene there are only two Clar sextets which are elongated laterally and therefore have higher chemical activity due to their instability. Those that are elongated longitudinally contain an extra Clar sextet for each additional acene unit (teranthene).<sup>11, 30</sup>

Hexabenzocoronene **100** is a well-studied compound due to its high symmetry, charge carrier mobility, stability and high melting point (>700 °C).<sup>30, 36, 135</sup> HBC is also classed as fully benzenoid because it only contains Clar sextets (and ‘empty’ rings) and no other double bonds. Due to its size and strong molecular  $\pi$ - $\pi$  interactions, HBC has poor solubility in many solvents and so an efficient synthetic strategy is required.<sup>11, 30, 33, 36</sup>

Clar *et al.* first synthesised HBC **100** in 1958 and Halleux *et al.* also reported its synthesis in two different ways in the same year, but the reaction yields were low

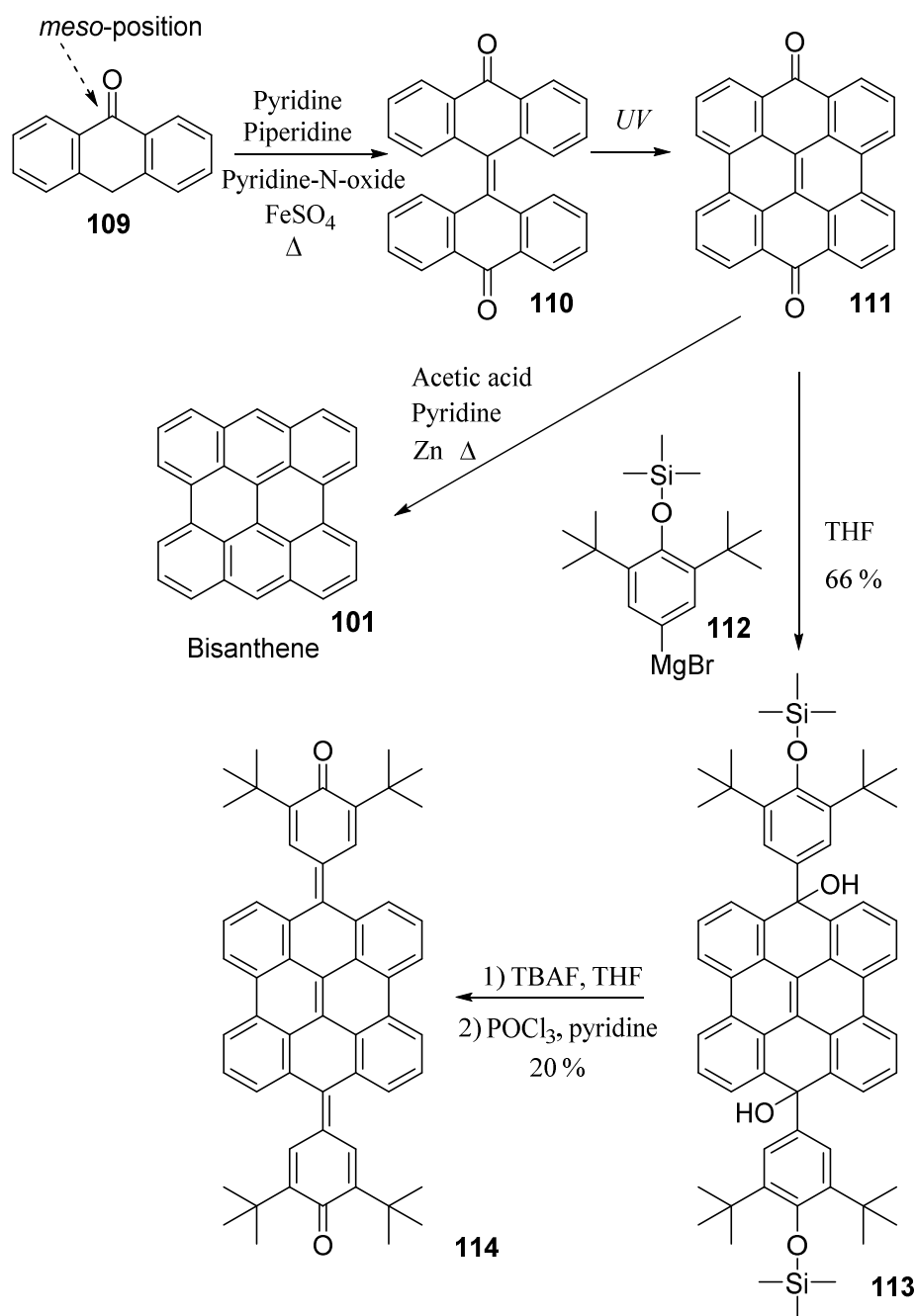
(Scheme 16).<sup>33, 36, 56, 135-137</sup> However, in 2000 Kübel *et al.* produced HBC in 96 % yield by controlling the amount of oxidant and reaction times.<sup>30, 33, 36, 138</sup>



**Scheme 16: The synthesis of HBC using the methods of Clar *et al.*, Halleux *et al.* and Kübel *et al.***<sup>36, 56, 135, 136, 138</sup>

The fusion of two anthracene **5** molecules produces bisanthene **101**, which was first synthesised by Scholl and Meyer in 1934, where the di-keto precursor **111** was reduced with HI and red phosphorus and then heated to 500 °C over copper.<sup>33, 34, 91, 139</sup> This seemed to be an extreme way of reducing the ketones and in 1948 Clar improved this step with a milder zinc-dust reduction, which is still used in a much improved synthesis of bisanthene by Arabei and Pavich.<sup>30, 33, 140-142</sup> Again, the

stability of this compound was an issue as it would readily react with oxygen at the *meso*-position, and so like former compounds, electron withdrawing groups were added within the structure to lower energy levels. Additionally, adding aryl or alkyne substituents at the *meso*-position helps to stabilise the core bisanthrene molecule (Scheme 17).<sup>30, 140, 143</sup>



Scheme 17: The synthesis of bisanthrene 101 and a stable derivative 114.<sup>30, 140-143</sup>



The higher order *peri*-acenes have not yet been synthesised, which is understandable since bisanthene itself is already very reactive; though, there have been derivatives of teranthene **103** produced.<sup>30, 33, 144</sup>

### 1.6.8 Circulenes

Benzenoids which are fused in a macrocyclic arrangement such as corannulene **118**, circulene **119** and Kekuléne **120** are known as circulenes.<sup>30, 36</sup> Furthermore, these forms of PAHs also include circumacenes which are formed when benzenoid rings are added to the bay sides of *peri*-acenes. The name comes from the central acene unit being surrounded in a circle by benzene rings, such as circumbenzene (coronene) **115**, circumnaphthalene (ovalene) **116** and circumanthracene **117**.<sup>30</sup> The number of Clar sextets usually increases with the macrocyclic circulenes where corannulene **118** has two, circulene **119** has three and Kekuléne **120** has six.<sup>36</sup> In the circumacenes, coronene **115** has three and the higher order ones possess four Clar sextets which is more than that can be drawn for the *peri*-acenes therefore circumacenes are known to be more stable.<sup>11, 33</sup>

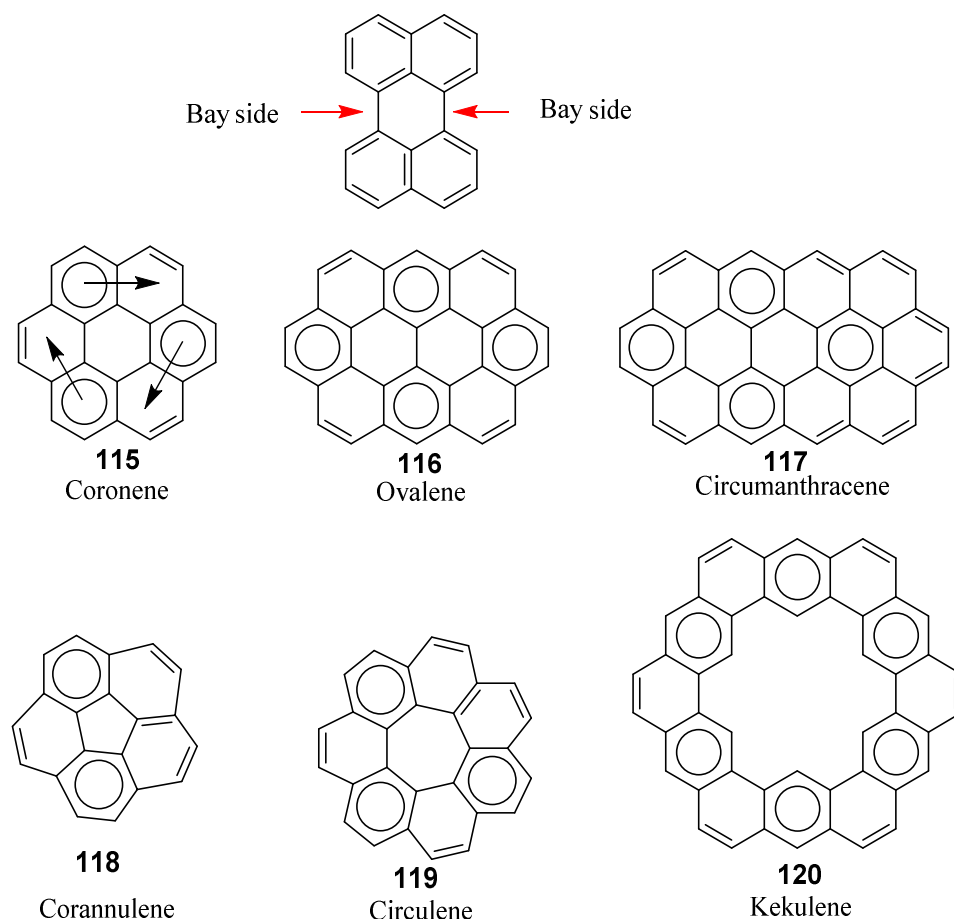
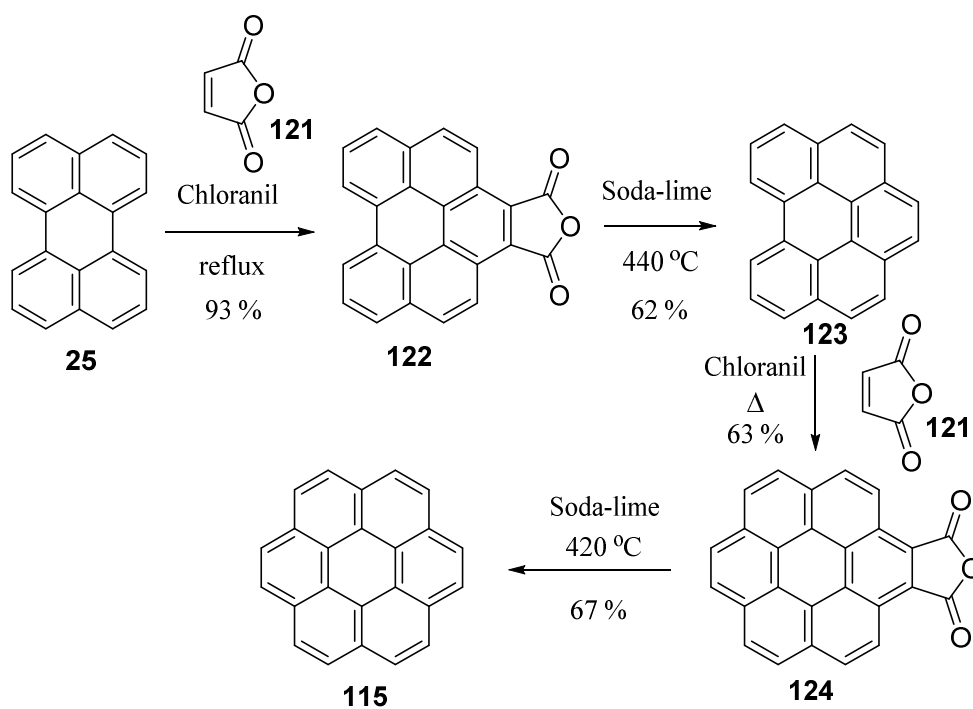


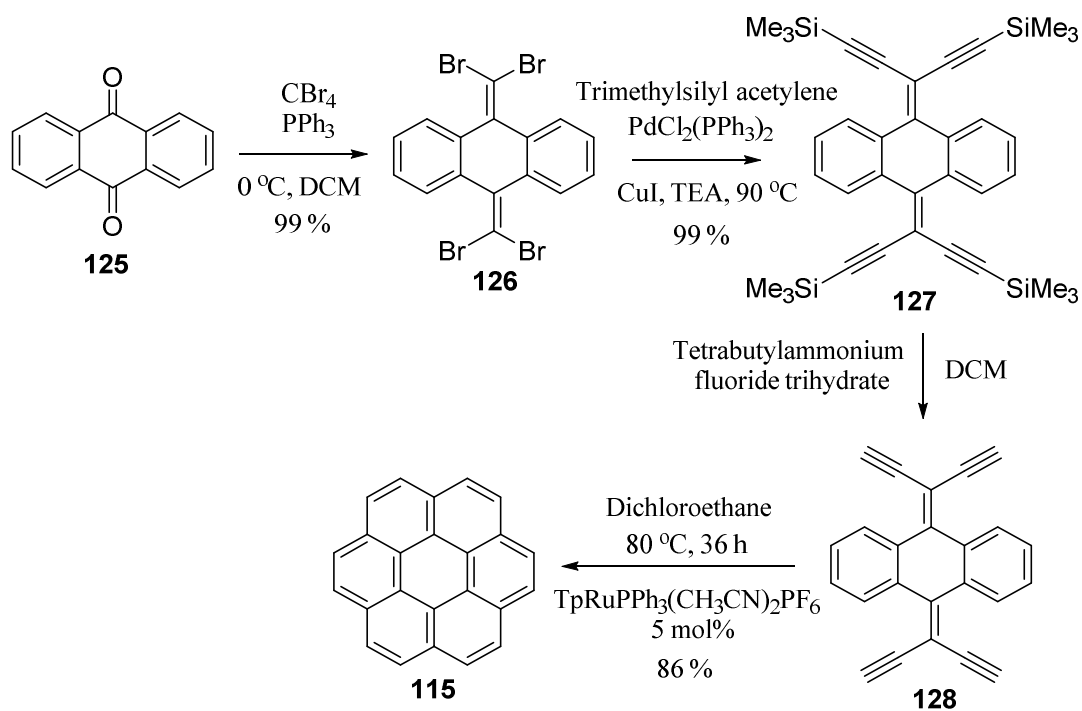
**Figure 27: Circulene series, with the circumacene subdivision of coronene 115, ovalene 116 and circumanthracene 117. Corannulene 118 and circulene 119 are both bowl shaped. Kekuléne 120 was first synthesised by Staab and Diedrich in 1978 in honour of Kekulé's work on benzene.<sup>36, 145-147</sup>**

Scholl first produced coronene **115** in 1932 and in 1957 Clar and Zander published an improved synthesis (Scheme 18).<sup>33, 91, 148, 149</sup> Coronene was of interest due to its unique symmetrical structure which exhibits perfect delocalisation around the ring due to its six-fold symmetry.<sup>30</sup> As demonstrated in Figure 27 above, the three sextets of coronene can migrate to its neighbour forming another ring current. If this was the case the double bonds would react like that of phenanthrene, however it does not. Coronene is 'superaromatic' because of the unique stability produced by its sextet ring current (current produced around the whole structure), is yellow, doesn't dissolve in sulfuric acid, has long phosphorescence and has properties of fully benzenoid compounds.<sup>11, 33, 150</sup>



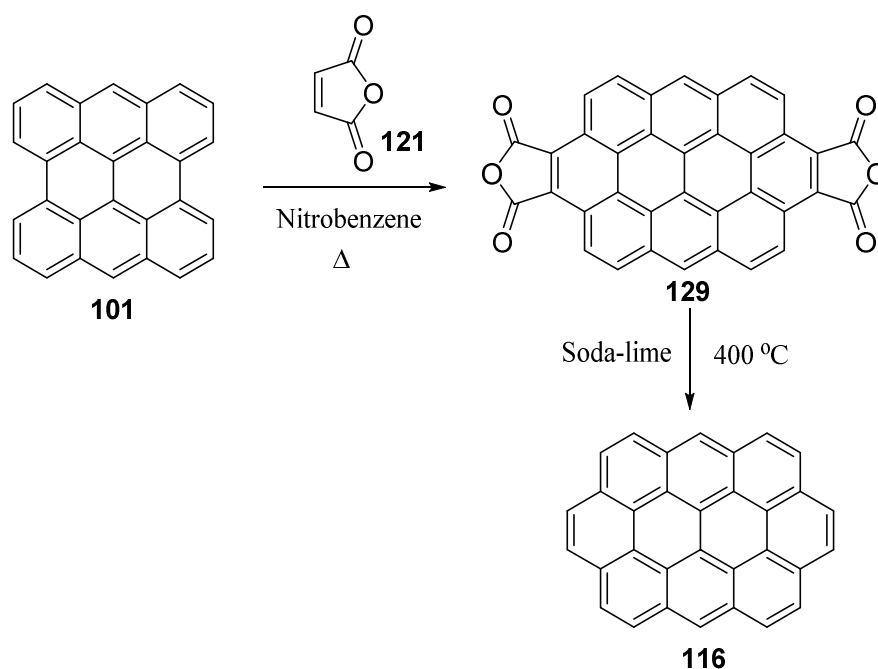
Scheme 18: Clar's coronene 115 synthesis.<sup>148</sup>

Currently with the advances in chemistry much higher yields can now be achieved by using metal catalysts, which is now very common in this field as shown with coronene **115** in Scheme 19.<sup>151, 152</sup>



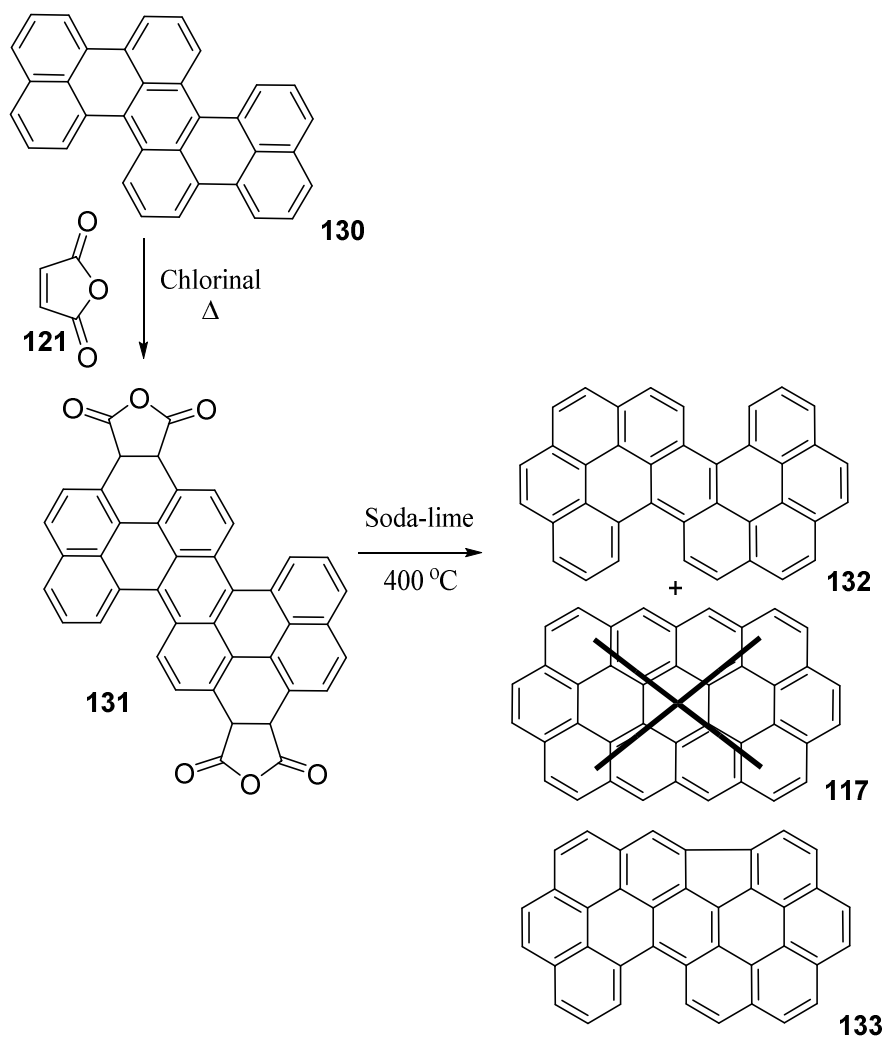
**Scheme 19:** The use of a metal-catalysed reaction to produce coronene **115** in high yields (species **127** reacted immediately) as described by Shen *et al.* from the previous works of Donovan *et al.*<sup>151, 152</sup>

In 1948 Clar synthesised ovalene **116** (Scheme 20) in similar fashion to that of coronene **115** by using maleic anhydride **121** in boiling nitrobenzene and then decarboxylation by heating in soda-lime to produce ovalene.<sup>33, 153, 154</sup> The starting bisanthene **101** was produced directly from its precursor bisanthenequinone **111** as shown in Scheme 17 and used immediately to avoid possible oxidation.<sup>154</sup>



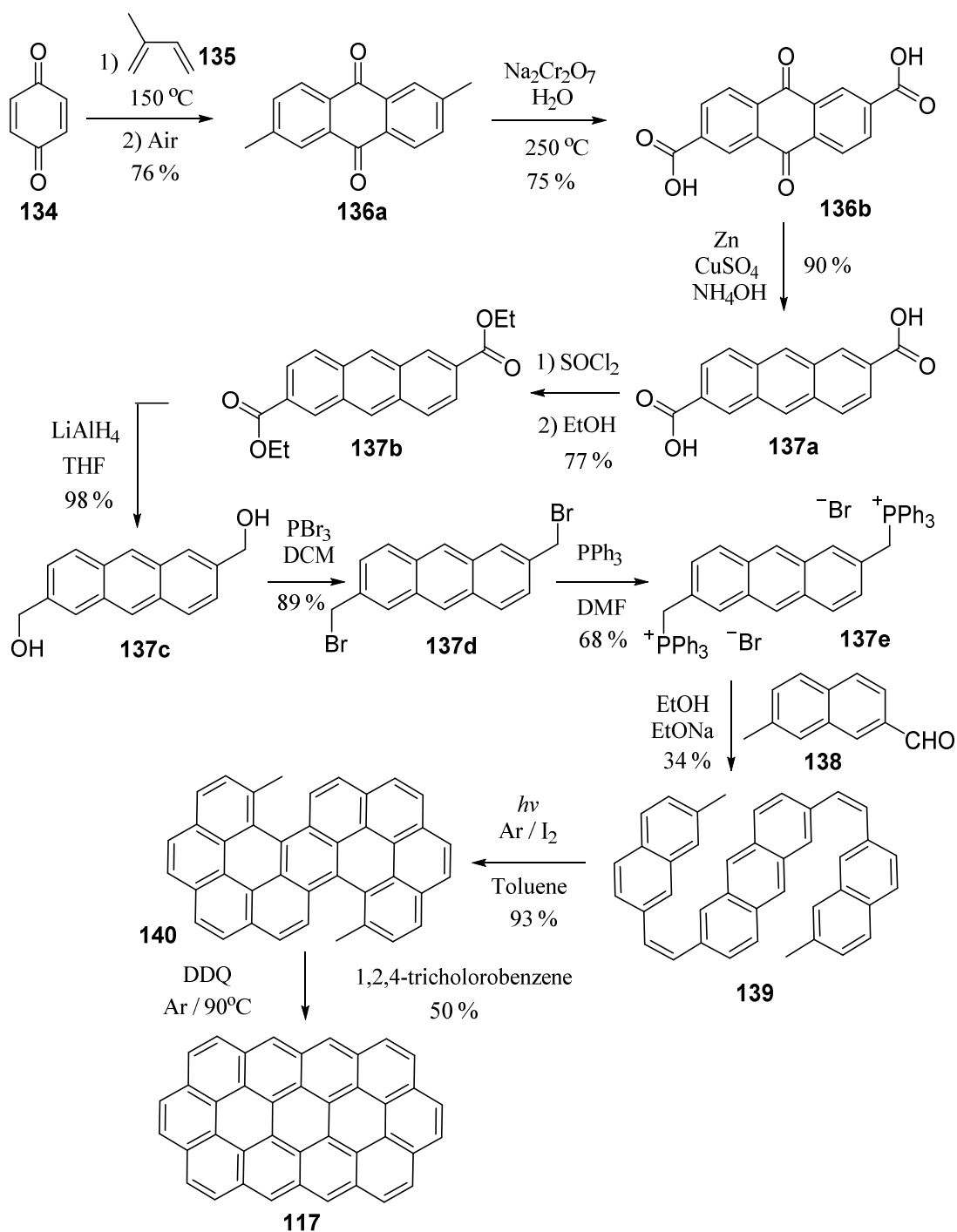
**Scheme 20: Clar's synthesis of ovalene 116 with a two-fold Diels-Alder reaction.**<sup>153</sup>

In 1956, Clar and co-workers thought that they had synthesised circumanthracene **117**. However, in 1981 they reported that the compound which they thought to have been circumanthracene from their synthesis was in fact something else.<sup>30, 155, 156</sup> Diperinaphthyleneanthracene **130** was heated under reflux with maleic anhydride **121** and chlorinal. The dianhydride intermediate **131** was then decarboxylated with soda-lime at 400 °C to produce a mixture of dinaphthoperopyrene **132** and what was thought to be circumanthracene **117** as proven by x-ray crystallography.<sup>155</sup> But in fact it was thought that 2, 12-dehydrodinaphthoperopyrene **133** was made instead by analysing the UV, photoelectron and infra-red (IR) spectra (Scheme 21).<sup>156</sup>



**Scheme 21: The failed synthesis of circumanthracene 117 by Clar *et al.* in 1956 where 2, 12-dehydrodinaphthoperopyrene 133 was actually made.<sup>155-157</sup>**

In 1991 Broene and Diedrich produced circumanthracene in a very long but successful synthesis (Scheme 22) starting from *p*-benzoquinone **134**. The precursor was characterised by nuclear magnetic resonance spectroscopy (NMR), as the product was insoluble in common solvents. However, the UV/Vis spectrum of the product had good agreement with Clar's predicted spectrum.<sup>30, 156, 157</sup>



**Scheme 22:** The synthesis of circumanthracene 117 by Broene and Diedrich. The conversion from the stilbene like structure 139 to the hindered precursor 140, is like that of Wood and Mallory first used (see Scheme 8) to gain a yield of 93%.<sup>30, 157</sup>

### 1.6.9 Alternate and interesting PAHs

This class of PAHs either contain benzenoids fused with other sized rings or those that are not made of benzenoids but fused with other size aromatic rings.

An important example is cyclopentenophenanthrene **141** (Figure 28), which is of significance as it was used to produce several natural products as Cook (1933) stated; they are related to ‘sterols, bile acid and oestrus-producing hormones’.<sup>91, 158</sup>

Acepleiadylene **142** which was first produced by Boekelheide *et al.* (1956) has a unique structure as it incorporates three ring sizes.<sup>91, 159, 160</sup> Dibenzopentalene **143** was one of the first double fused five-membered ring compounds produced by Blood and Linstead and its significance was that it was a stable derivative of a highly reactive pentalene.<sup>91, 161</sup> Truxene **144** and **145** both have unique structures, Truxene is of particular interest due to its use in optoelectronics and appears as fragments of the well-known fullerenes molecules.<sup>91, 162-166</sup> Buckminsterfullerene C<sub>60</sub> **155**, is one of the most recognised ball-structured PAHs, first discovered in 1985 by Kroto *et al.* It was such a ground-breaking discovery that Kroto was awarded the 1996 Nobel Prize in chemistry.<sup>167, 168</sup> Kroto *et al.* used a laser evaporation technique on graphite to create clusters where prominently C<sub>60</sub> fullerenes were formed.<sup>167</sup> Scott *et al.* published a route to synthesise buckminsterfullerene **155** where the very low yielding last step used flash vacuum pyrolysis (FVP) (Scheme 23).<sup>168</sup>

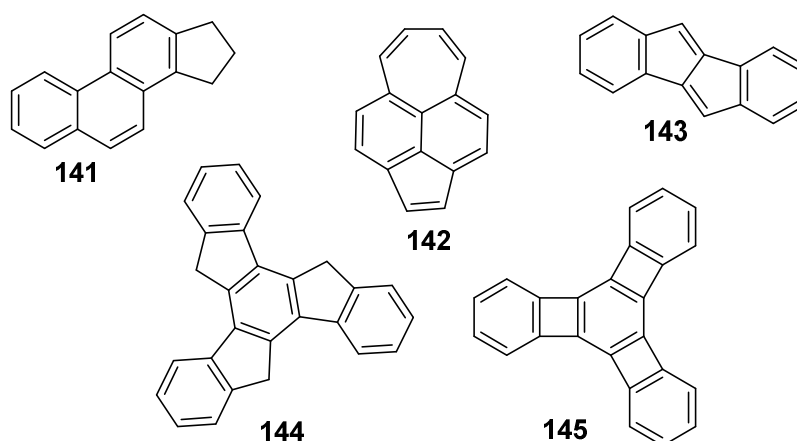
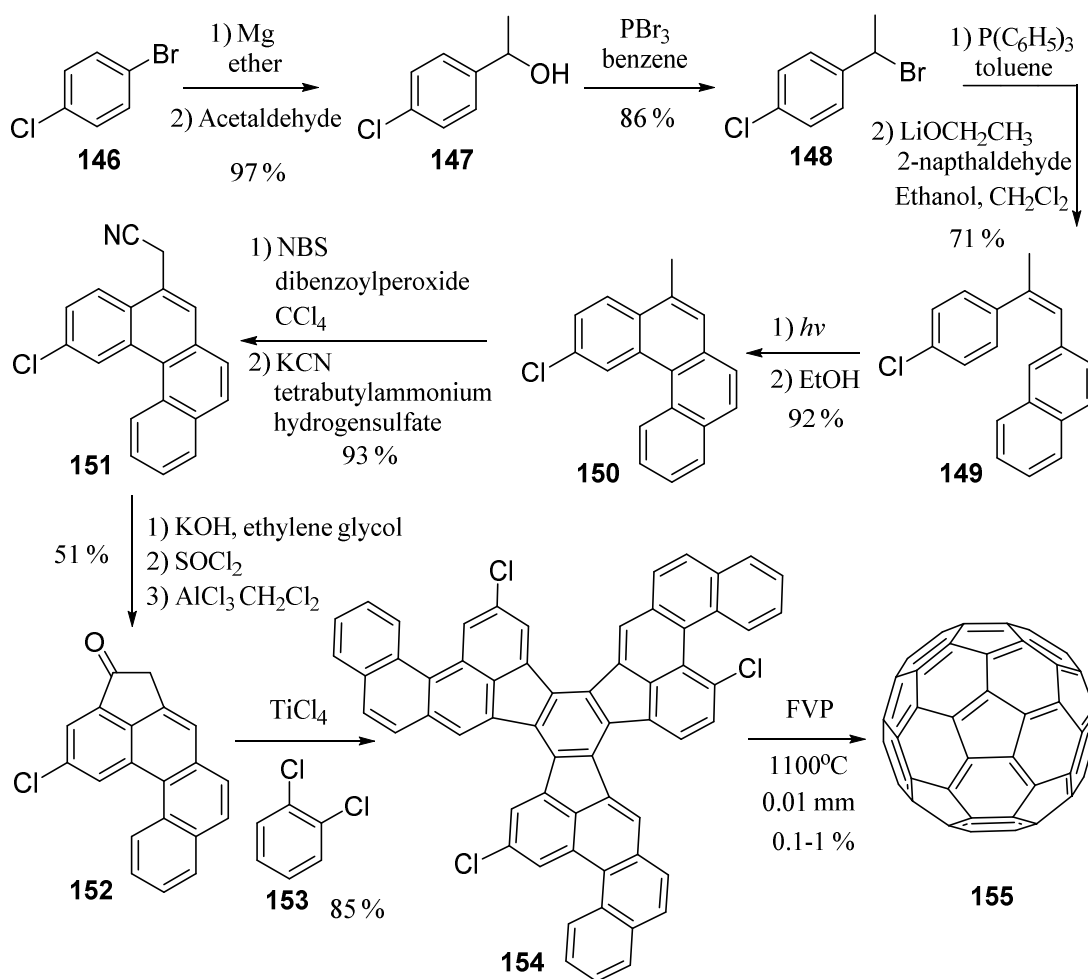


**Figure 28:** Cyclopentenophenanthrene **141**, Acepleiadylene **142**, Dibenzopentalene **143**, Truxene **144** and bisbenzo[3,4]cyclobuta[1,2-a:3,4-b]biphenylene **145**, are some structurally interesting PAHs.

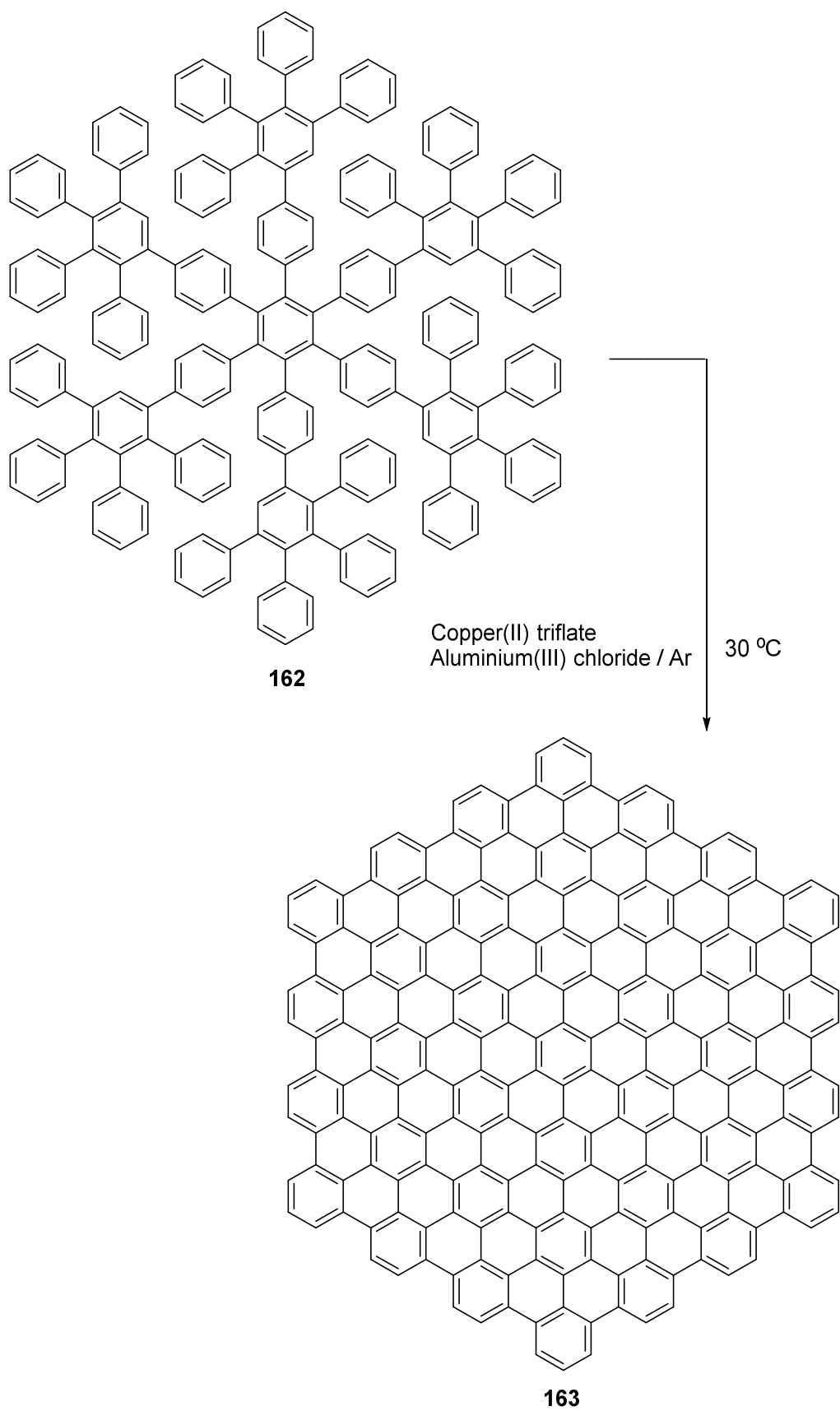




**Scheme 23: The synthesis of buckminsterfullerene 155 by Scott *et al.*, the last step (Flash Vacuum Pyrolysis, FVP) producing a very low yield.<sup>167, 168</sup>**

Obviously not all PAHs can be categorised but are still of interest for their unique structures and properties. This also includes the largest known controlled synthesis of a complete PAH which was produced by Simpson *et al.* in 2002 which contains 222 carbons **163** (Scheme 24).<sup>36, 169</sup> Even though the oligophenylene precursor **162** is very large it was soluble in common solvents which meant full characterisation was possible. The final product was insoluble and could only be characterised by elemental analysis and (matrix assisted laser desorption/ionisation time-of-flight) MALDI-TOF mass spectrometry which also estimated the yield at approximately 99 %.<sup>169</sup>





**Scheme 24: A synthetic route to obtain the largest controlled PAH synthesis.<sup>169</sup>**

## 1.7 PAHs; where are they found and what are their uses?

Commonly, PAHs are formed as unintentional by-products of incomplete combustion. Their hydrophobic nature allows adsorption onto atmospheric particles which are deposited onto sediment and plants, and they are therefore known as a worldwide environmental contaminant.<sup>1, 31, 170-173</sup>

There are many sectors where PAHs are found and formed worldwide and some of these are summarised:

**Oil production:** For example, in the production of fuels and chemicals from fossil fuels.

A large number of PAHs are found in the petroleum industry from crude oil and also from coal-tar which is the by-product of fuel (coke) production from coal. Both coal and crude oil have high carbon content and during processes refining them, temperatures can reach up to 2000 °C which causes chemical pyrolysis that creates a number of different PAHs.<sup>31, 174-178</sup> Some of the most common PAHs are fractionally distilled and recrystallised from these mixtures such as naphthalene, anthracene and phenanthrene.<sup>32</sup> Even benzene was extracted from coal-tar in 1848 by Hofmann and Mansfield twenty-three years after Faraday discovered its presence in compressed oil-gas.<sup>32</sup>

**Agricultural:** Again the burning of organic matter including crops, straw and wood to maintain farm land can form various PAHs by pyrolysis.<sup>31, 179-181</sup>

**Domestic and industrial activity:** The main causes in this area could arguably be fumes from industrial or household chimneys and motor exhausts.<sup>171, 176, 178, 182</sup> Cigarette smoking and domestic combustion in gardens, barbeques and burning plastics are other common factors.<sup>31, 179, 183, 184</sup>

**Soil:** The main source of PAHs in soil is due to air borne fallout, therefore you would expect high levels of PAHs near industrial/ roadside fumes.<sup>31, 177, 178, 185, 186</sup>

**Water:** The PAHs which are trapped in soil can leach into water systems, contaminating the water. In addition, accidental oil spills are another route in which they are introduced into water.<sup>31, 172, 187, 188</sup>

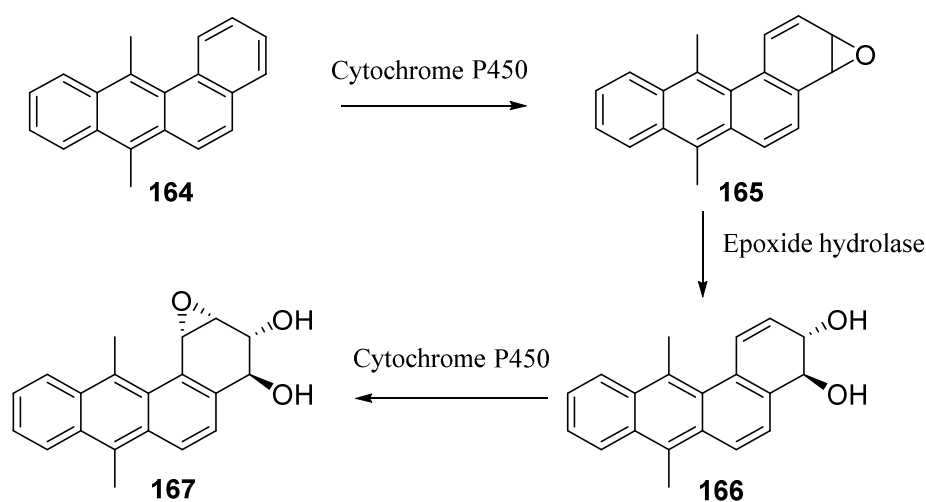
**Food:** PAHs can be introduced through thermal treatments in food preparation, these include smoking, charring and barbequing food as well as introduction through some pesticides.<sup>31, 189, 190</sup>

**Space:** PAHs have been of interest to astronomers and astrophysicists as it has been suggested that they are present in interstellar space. This could provide further understanding of the universe as the IR and UV rich regions of nebulae are suggested to contain forms of polyaromatic hydrocarbons.<sup>191, 192</sup> NASA telescopes have detected these by infra-red signals and a database has been created, more recently fullerenes have been thought to exist in space.<sup>193-198</sup> PAHs can form from chemical reactions starting from the 'big bang' theory through to the formation of new stars where the exertion of high temperatures and pressures on compounds form PAHs through pyrolysis-type reactions.<sup>193-197, 199</sup>

As mentioned previously PAHs can be very difficult to analyse due to their insolubility in common solvents. With this in mind the relative PAH content in the different sectors are calculated using analytical techniques such as (gas chromatography mass spectrometry) GC-MS, chromatography, UV spectroscopy, IR spectroscopy and solid-state NMR.<sup>174, 175, 179, 182, 184, 196, 200-202</sup>

### 1.7.1 Health effects

It is believed PAHs are hazardous and toxic to the health of humans and animals. For example, a number of PAHs are known to be skin irritants and high doses of naphthalene are known to break down red blood cells in the body.<sup>31</sup> There are even more severe implications which have been related to high exposure of PAHs, such as genotoxicity with PAHs associated with damaging DNA and creating birth defects as well as carcinogenicity (Scheme 25).<sup>31, 170, 184, 185, 203-205</sup>



**Scheme 25: A common pollutant dimethylbenz[*a*]anthracene 164 can form dimethylbenz[*a*]anthracene-3,4-diol-1,2 epoxide 167 in the body using metabolic pathways. This compound reacts with DNA to form adducts which are responsible for carcinogenicity such as breast cancer. Benzo[*a*]pyrene 172 is another commonly studied PAH which is known to follow this type of pathway to create carcinogens.**<sup>31, 170, 203-206</sup>

A list of PAHs which are primarily found in air, soil, water and food is given in Figure 29, and these sixteen are thought to be the main priority according to various environmental and health agencies around the world.<sup>31, 176, 182, 200, 202, 207</sup>

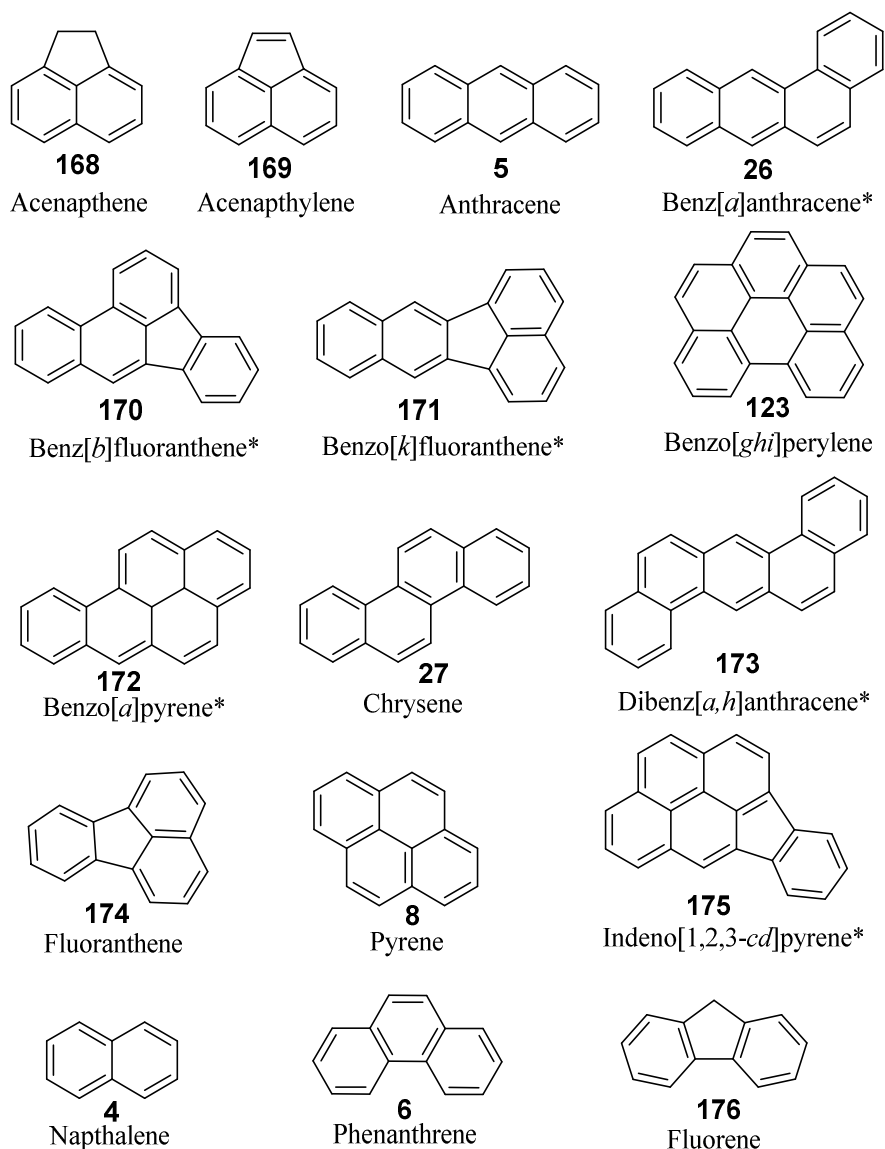


**Figure 29: 16 of the most common PAH pollutants, (\*) are possible carcinogens.** <sup>31, 32, 176, 182, 200, 202, 207-209</sup>

Even though some PAHs are considered to have mutagenic and carcinogenic activity, not all of them do. Consequently, due to the large number of PAHs available and the vast number of which have not been studied, the main population try to avoid significant exposure from these types of compounds as a precaution.

### 1.7.2 The uses of PAHs

Organic electronics is an area which has shown great promise in functionalising organic molecules to exploit their properties for the use in technological devices.

They are seen as being used in low-cost and flexible devices which are easy to dispose of, unlike the more common inorganic species.<sup>210-212</sup> PAHs are used as there are a vast number of them with a variety of properties including size, shape, configuration and stability. Due to the nature of some PAHs it is possible to tune their electronic properties for use in emerging fields, outlined below.

### 1.7.3 Organic light emitting diodes (OLED/PLED)

Electroluminescence was first observed in anthracene **5** based organic materials and in 1986 Tang *et al.* at Eastman Kodak reported the first OLED device using a perylene derivative.<sup>213-216</sup>

An OLED works by the organic compound emitting light when an electrical current is imposed and they are commonly used as a display in mobile phones, TVs, and computer monitors. Furthermore, white OLED devices are being considered for lighting purposes.<sup>215, 217, 218</sup>

The desired features of the organic layer are that it emits the chosen wavelength and has a high charge carrier mobility; the most common compounds that are used are perylene **25**, rubrene **177** and quinacridone **178**.<sup>219-221</sup> Polymeric systems (PLEDS) are also used, for example polyfluorene, where its substituents can be altered to change the wavelength of emission. In particular, for displays the colours blue, green and red are the desired wavelengths to be emitted.<sup>215, 217, 222</sup>



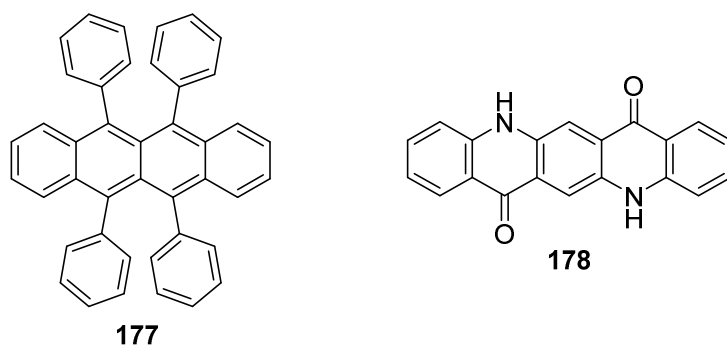


**Figure 30: Structure of rubrene 177 and quinacridone 178.**

An OLED device is usually made up of four layers (Figure 31); a cathode, the organic layer (emissive and conductive layers) and then the anode which is usually made of indium tin oxide due to its transparency and high work function.<sup>215, 219, 223</sup>

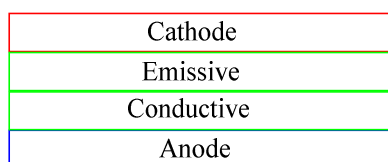


**Figure 31: A simplified depiction of the layers of an OLED.**

The simple mechanics of an OLED are that i) once a voltage is applied the cathode receives electrons while the anode loses them creating holes, ii) the emissive layer is now negatively charged by the influx of electrons and the conductive layer positively charged by holes created by loss of electrons, iii) these holes ‘hop’ across to the emissive layer and meet an electron where a photon is released creating light which continues as long as a voltage is supplied.<sup>215, 219, 223</sup>

The advantages of OLED over normal LED devices are that they are brighter, faster, cheaper and more flexible however they tend not to last as long.

#### **1.7.4 Organic field effect transistors (OFET)**

An OFET is a device which uses the organic molecules as the semiconductor material in the channel by utilising the electric field. The organic channel can be

described as two forms, either p-type (which are hole carriers) that have high HOMO electron donating properties due to  $\pi$ -conjugation, or n-type (which are electron carriers).<sup>211, 224</sup> There are a lot more p-type than n-type as the latter are known to be prone to oxidation, thus, less stable and inefficient in electron trapping.<sup>223, 225</sup>

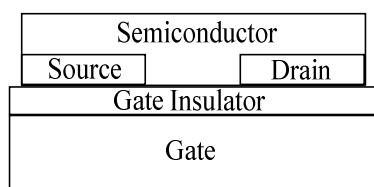


**Figure 32: A simplified depiction of an OFET.**

OFETs have three main components; the source, drain and gate (Figure 32). The organic semiconducting material (p or n-type) forms the charge transporting channel between the source and drain, while the gate controls the charge.<sup>211, 223, 226</sup>

The desired properties of the organic semiconductor are that it has a high-charge carrier mobility, has good stability and gate-insulator capacitance.<sup>223, 227</sup>

The first reported organic OFET was in 1987 by Koezuka *et al.* by using polymeric thiophene.<sup>228</sup> Since then, PAHs have formed the foundation of good OFETs, for example tetracene **23**, pentacene **24**, rubrene **177** (p-type) and perylene **25**. Fullerene derivatives (n-type) such as diindenoperylene and PCBM (phenyl- $C_{61}$ -butyric acid methyl ester) have also been used.<sup>211, 221, 223-226, 229-231</sup>

Pentacene ( $2-3 \text{ cm}^2\text{V}^{-1}\text{s}^{-1}$ ) and rubrene are commonly used as p-type OFETs as they have a high charge mobility. Rubrene **177** has the highest recorded charge mobility with  $35 - 40 \text{ cm}^2\text{V}^{-1}\text{s}^{-1}$  and silicon is only  $1.0 \text{ cm}^2\text{V}^{-1}\text{s}^{-1}$ .<sup>211, 221, 224, 232</sup>

OFETs are potentially, low cost, flexible, light weight and producible on larger scale at low temperatures unlike the high temperatures required for silicon. They can be used for ID cards, smart cards, and display drivers.<sup>211, 225, 226</sup>

### 1.7.5 Organic solar cells (OSC)

An organic solar cell is a photovoltaic device in which the organic molecules absorb light energy and convert it into electrical energy.<sup>215</sup> C<sub>60</sub> fullerenes and perylene derivatives as well as polymeric thiophenes are used as the acceptor and donor materials in organic solar cells.<sup>215, 233, 234</sup> OSCs have a similar construction to OLEDs; there is an anode, an electron donor layer then an electron acceptor layer and finally a cathode (Figure 33).<sup>216, 223, 235</sup>

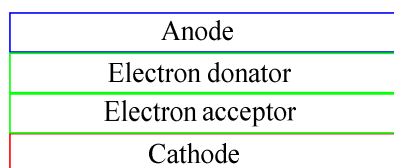


**Figure 33: A simplified depiction of an OSC.**

OSCs work by i) the light, (photon) with energy exceeding the band gap (HOMO-LUMO) is absorbed by the organic material ii) this excites an electron into an unoccupied state above the band gap and creates an electron-hole pair (exciton), iii) the electron-hole pair is separated by the gradient into the acceptor and donor material respectively, iv) the electron and hole are collected at their respective electrodes to a circuit and electrical current is formed.<sup>215, 216, 223, 235, 236</sup>

The attractive nature of OSC is that they are low cost, tuneable, and flexible with very good optical absorption. However, compared to other inorganic and silicon based cells they are known to have low efficiency, stability and strength.<sup>212, 215, 237</sup>

### 1.7.6 Spintronics

Spintronics is the study of spin transport electronics, where the spin of the electron instead of its charge is exploited for information transfer.<sup>238, 239</sup> It is a rapidly growing field of molecular functional materials because of the intrinsic electronic and magnetic properties which may be developed.<sup>240</sup> This can lead to next-generation advances into; increased data processing speed, decreased electrical power consumption, better organic light emitting diodes, solar cells and semiconductors.<sup>241, 242</sup>

Manipulating both electronic and nuclear spin on a sufficiently fast time scale is difficult, but first you need a suitable molecule to investigate.<sup>239</sup> Advantages of organic molecules being employed in this area are that they are low-cost and can make flexible devices which are easy to dispose of.<sup>210</sup> In addition, due to their weak spin orbit coupling and weak interactions, organic molecules are deemed to be suitable for spin transport, where the spin can be maintained over a longer time period and distance than inorganic molecules.<sup>210, 239, 243</sup>

The most interesting of these organic molecules being considered are molecules with an open-shell. These organic radicals have unpaired electrons and thus, a magnetic moment which could favour spin polarisation conservation during the transport process.<sup>210, 243</sup> Molecules such as polychlorotriphenylmethyl (PTM) **179**, nitroxide **180** and galvinoxyl **181** radicals have already been isolated and studied as potential materials in this field (Figure 34).<sup>210, 240</sup>

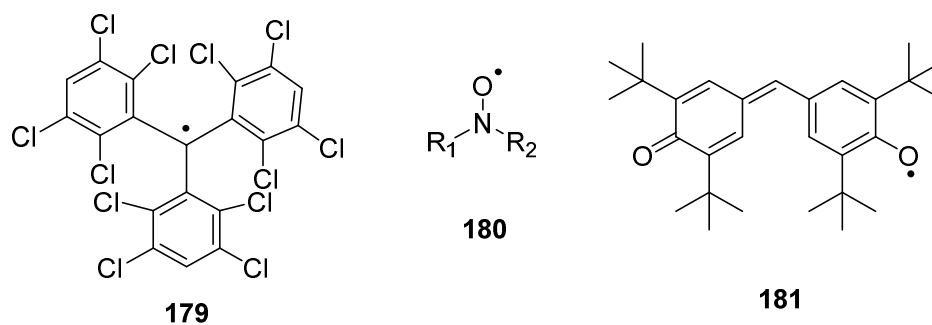
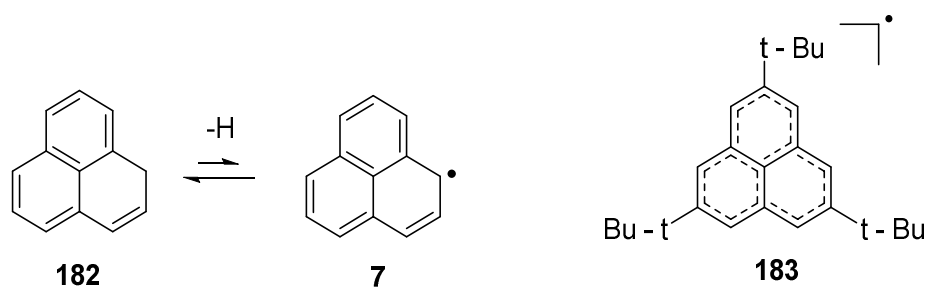


**Figure 34: Structures of polychlorotriphenylmethyl (PTM) 179, nitroxide 180 and galvinoxyl 181 species.**

PAHs have been considered as good targets as there are a number of open-shell frameworks available, which in theory leads to a singly occupied non-bonding molecular orbital (SOMO).<sup>243</sup> Despite this, the stability is an issue as they tend to oxidise and dimerise readily.<sup>25, 33, 243</sup> Furthermore, it is suggested that hydrocarbons with a triangular shape will exhibit non-Kekulé structures with one or more unpaired electron, just like an open-shelled fragment of graphene.<sup>25, 33, 243</sup> Hence, phenalenyl derivatives (Scheme 26) have been studied with bulky substituents as the unsubstituted radical **7** is too reactive to be isolated.<sup>243, 244</sup>



**Scheme 26: Illustrates a radical form 7 of the highly studied phenalene 182 after a hydrogen abstraction. 183 is a more stable radical form of the phenalenyl compound 7 with bulky substituents for stability.<sup>244</sup>**

Triangulene **10** (Figure 35) is another molecule of interest, as previously mentioned alongside other PAHs which tend to have diradical character.<sup>11, 33, 243-245</sup>

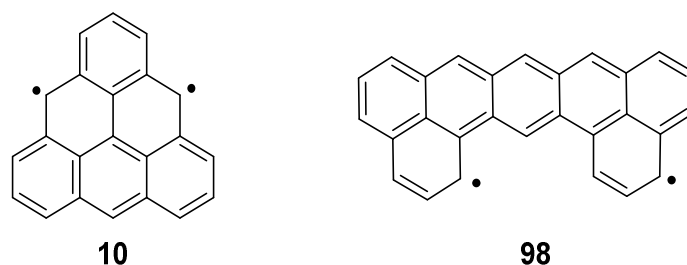


**Figure 35: Diradical example of triangulene 10 and a dibenzo-pentacene 98.**

### 1.7.7 Organic materials

A more recent driving force for the studies into PAHs is in their relation to graphene, which has a number of beneficial properties that scientists hope to exploit. These include materials in next-generation nanoscale electronic devices, machines and quantum information processing systems, more specifically solar cells, batteries and data storage.<sup>30, 36, 246-248</sup>

Graphene can be described as a two-dimensional layer of  $sp^2$ -hybridised carbon atoms and can be viewed as a sheet of benzene rings fused together, hence the consideration of large PAHs as nanographenes.<sup>30, 36, 249</sup> One of the most interesting properties of graphene is the delocalisation of its  $\pi$ -electrons across its whole surface. Usually metal ions use unpaired electrons to relay information as spin carriers, but they can be limited with additional costs and are environmentally inefficient.<sup>244, 249</sup> Scientists have been looking at using radicals within the structure to construct materials with electron spin information carriers for spintronics.<sup>244, 249, 250</sup>

Throughout history PAHs have been used as dyes from naturally found molecules for example alizarin **36**, through to synthetic dyes such as xanthene **184** derivatives and fluoresceins **185** (Figure 36).<sup>96, 251</sup> Most common organic dyes incorporate an anthracene or perylene building block and recently rylenes have been used to create

synthetic dyes of desired colours.<sup>123, 251-253</sup> PAHs are also found as a building block in pharmaceuticals and can be used as biosensors, where perylene is commonly used as a lipid probe and also in asphalt for roads.<sup>254-256</sup>

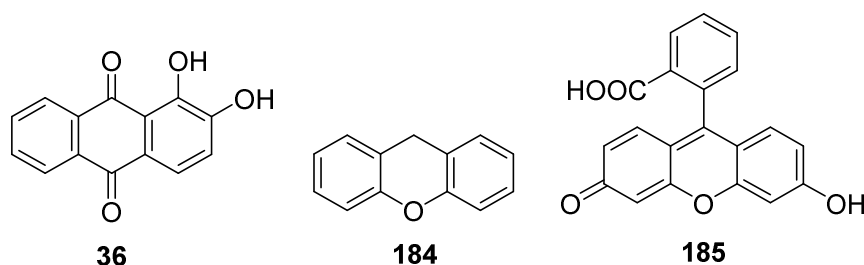


**Figure 36: Structures of alizarin 36, xanthene 184 and fluorescein 185 which all incorporate an anthracene moiety.**

## 1.8 PAHs and AFM

### 1.8.1 Scanning probe microscopy

A number of analytical techniques are used in organic chemistry including NMR spectroscopy, IR spectroscopy and mass spectrometry. Recently, however, different techniques are being used in cross-field applications as their development leads to additional versatility. Scanning Tunneling Microscopy (STM) and Atomic Force Microscopy (AFM) are two techniques which are currently being developed in different fields including imaging in organic chemistry.

### 1.8.2 Scanning tunnelling microscopy

STM was first invented by Binnig and Rohrer in 1981 at IBM Zürich Switzerland and they went on to win the Nobel Prize in physics for this discovery. STM works by bringing a tip close to a surface where a voltage is then applied, allowing the electrons to tunnel through the vacuum to the surface. As the tip moves across the surface the electron tunnelling current is monitored and this information is turned into an image of the area being scanned. As well as maintaining a constant height

you can also maintain a constant current and the tip can be raised and lowered depending on the surface topography. The tip end is about the size of the width of an atom and so high resolution images can be obtained. The resolution of the image is usually dependent on the curvature of the end of the tip, which is typically made from tungsten or carbon nanotubes.

STM is a very sensitive technique and it requires a lot of maintenance in terms of the mechanical parts. The key areas which need to be maintained for it to function properly are maintaining a sharp tip, excellent vibration control, clean surface and a good electrical connection.

### **1.8.3 Atomic force microscopy**

AFM was invented by the same scientists as the STM, Binnig and Rohrer in 1982 which also contributed to their Nobel Prize award. This technique uses a tip on the end of a cantilever to scan across the desired surface and the forces between the tip and surface deflect the cantilever, these forces are measured and can be turned into an image of the surface.

There are 3 main modes of imaging in AFM:

- i) Contact mode: where the cantilever is dragged across the surface of the sample and the force it takes to keep it at the constant position is measured.
- ii) Tapping mode: where the cantilever is oscillated at a constant frequency as it is moved over the surface it taps it then moves off again, when it taps the surface the oscillation frequency changes and this is used to measure the surface features.



- iii) Non-contact mode: when the cantilever is moved over the surface at a nm-pm distance away, usually at a constant height, and the tip senses van der Waals forces on the surface. These forces are then turned into images.

The cantilever tip is usually made of silicon and the apex of the tip is usually a width of a single atom, again the resolution depends on the sharpness of the tip and similar to STM it is a very sensitive technique which is heavily dependent on its parameters.

One of the key differences between these two modalities is that STM can cover a larger surface area and in a shorter timescale than AFM, additionally it can provide a good representation of just about any surface.

#### **1.8.4 Ultra-high resolution AFM**

There have been numerous advances in these techniques since its recent conception and one of these is the production of high-resolution images. The cantilever in basic AFM machines has been upgraded to possess a quartz tuning fork which is typically found in wristwatches. These have one prong which oscillates where a tungsten tip is mounted on the end so it can function as an AFM cantilever. These are much stiffer therefore provide less oscillation and require more force than a silicon cantilever before it breaks. In addition, due to the tungsten metal possessing desired conductivity the tip can also be used as an STM.<sup>257</sup>

Further still the Gross group at IBM Zürich have functionalised the tip by adding a carbon monoxide molecule to the end. This has improved the tip further so that high resolution images can be obtained (Figure 37).<sup>257, 258</sup> Here the carbon monoxide molecule is flexible, therefore if the tip is too close to the sample it will simply bend rather than a metal tip which can damage or break the sample and the tip itself.

### 1.8.5 Uses

Recently STM and AFM have been used to image molecules for a number of reasons including looking at defects, how molecules have been assembled, general structure and their electron density patterns.<sup>259</sup> However, one dominant species which has been used in this field has been PAHs. This is because most PAHs are flat and are therefore much easier to image compared to other molecules which have groups protruding out at different angles.<sup>260</sup>

### 1.8.6 Compound identification and characterisation

Advances in atomic-scale surface characterisation, have allowed a revolution in structure analysis from when it was first developed. Usually an image of an outline of the structure in question is what was commonly produced without much detail. Nevertheless, one of the key advances in this field was the imaging of pentacene **24**.<sup>258, 261-263</sup> Pentacene was first imaged in 2004 by Lagoute *et al.* by STM where the rod-like shape was seen.<sup>261</sup> After more developments Gross *et al.* in 2009 published an exceptionally clear image of pentacene **24** by AFM (Figure 37).<sup>258</sup>

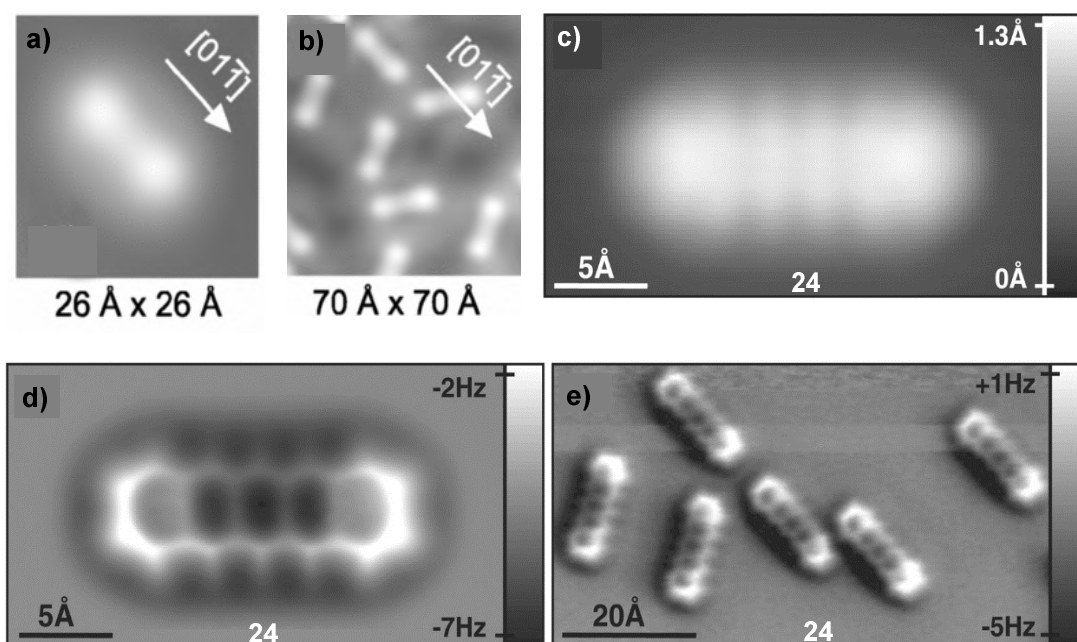


**Figure 37:** a) and b) are images of pentacene by constant current STM by Lagoute *et al.* c) is a constant current STM image of pentacene by Gross *et al.*, d) and e) are constant height NC-AFM of pentacene by Gross *et al.*<sup>258, 261</sup>

These images of pentacene had provided previously unseen atomic resolution. Only a handful of groups have been able to obtain resolution this clear due to the meticulous nature of the STM/AFM setup. In spite of this, these groups have managed to image a number of compounds using these techniques, including recent advances in NC-AFM which can provide atomic level resolution images.<sup>258, 264-276</sup>

Another interesting compound, hexabenzocoronene (HBC) **100** was imaged by Gross *et al.* in 2012 (Figure 38), again showing great clarity.<sup>275</sup> The results of this compound in particular were interesting as it was imaged to measure the bond lengths of the compound to see if it coincides with Clar's sextet rule. As a fully benzenoid structure HBC has seven 'fixed' aromatic rings within the structure and the AFM shows that the C-C bonds linking the sextets are longer (1.687 Å) than that of the C-C bonds which are part of the sextet (1.417 Å).<sup>275</sup> Furthermore, the seven Clar sextets were also seen to be brighter than the rest of the structure which

indicates that these areas are more electron rich which supports the Clar representation of HBC.<sup>37, 275</sup>

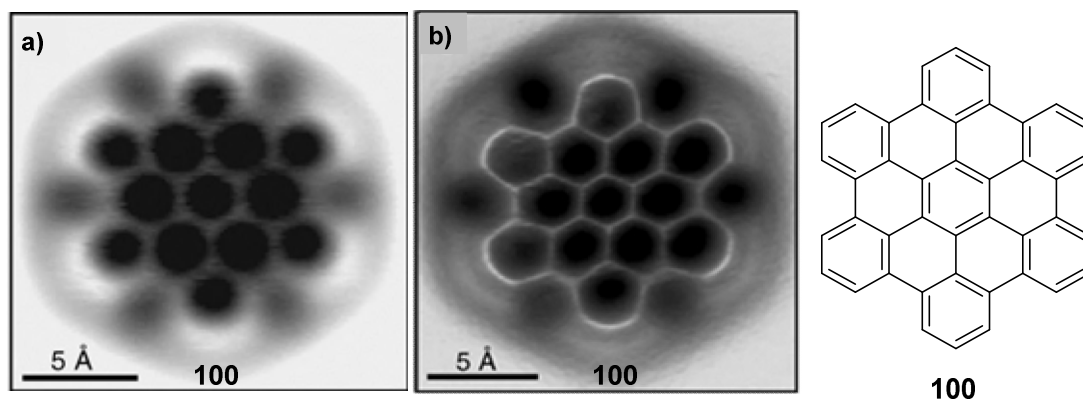
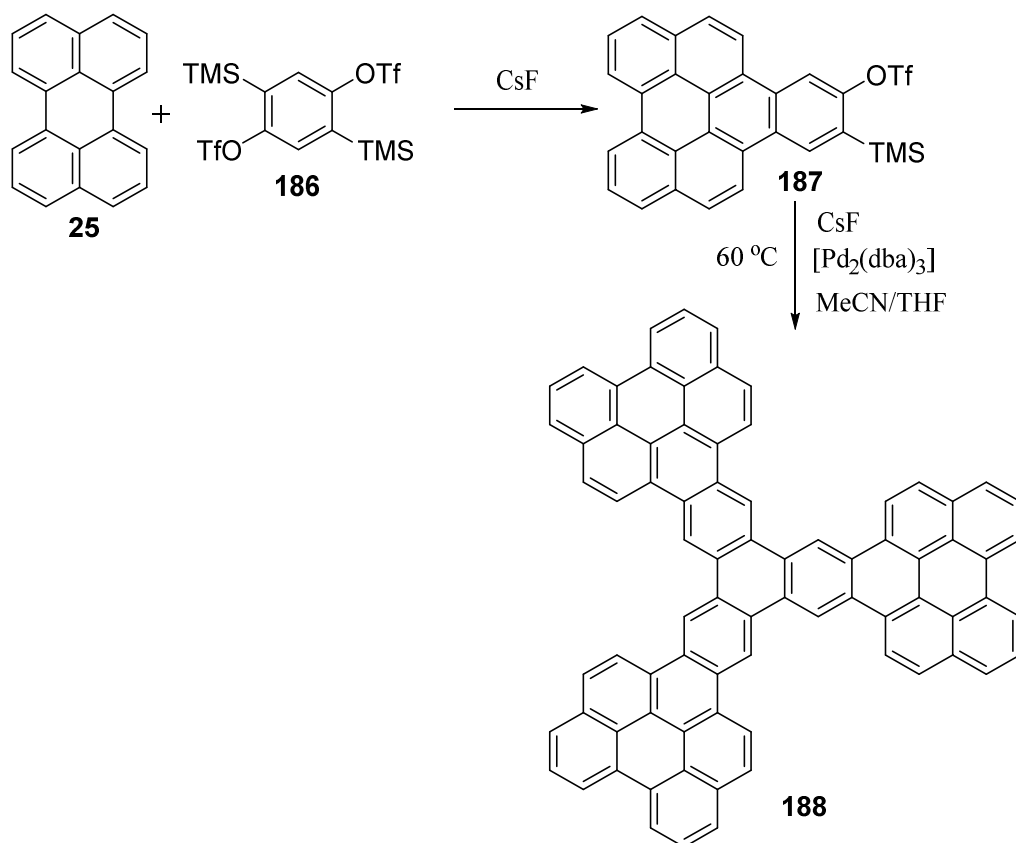


**Figure 38:** a) and b) are constant height NC-AFM images of HBC 100, by Gross *et al.*<sup>275</sup>

In 2012 Schuler *et al.* synthesised a 22-ring aromatic nanographene **188** in an easily accessible one pot method with 46 % yield (Scheme 27).<sup>277</sup>



**Scheme 27: Synthesis of a cyclotrimer nanographene 188, firstly by a [4+2] cycloaddition followed by a [2+2+2] cycloaddition.<sup>277</sup>**

However, due to the size of the PAH and its insolubility it was hard to characterise the compound, as this ruled out liquid-phase NMR spectroscopy. Indeed, MALDI mass spectroscopy suggested the correct molecular mass but another isomer may have been formed. AFM was therefore used to characterise the compound which provided conclusive evidence because of the clarity of the image, overcoming the problems associated when forming nanographenes (Figure 39).<sup>277</sup>

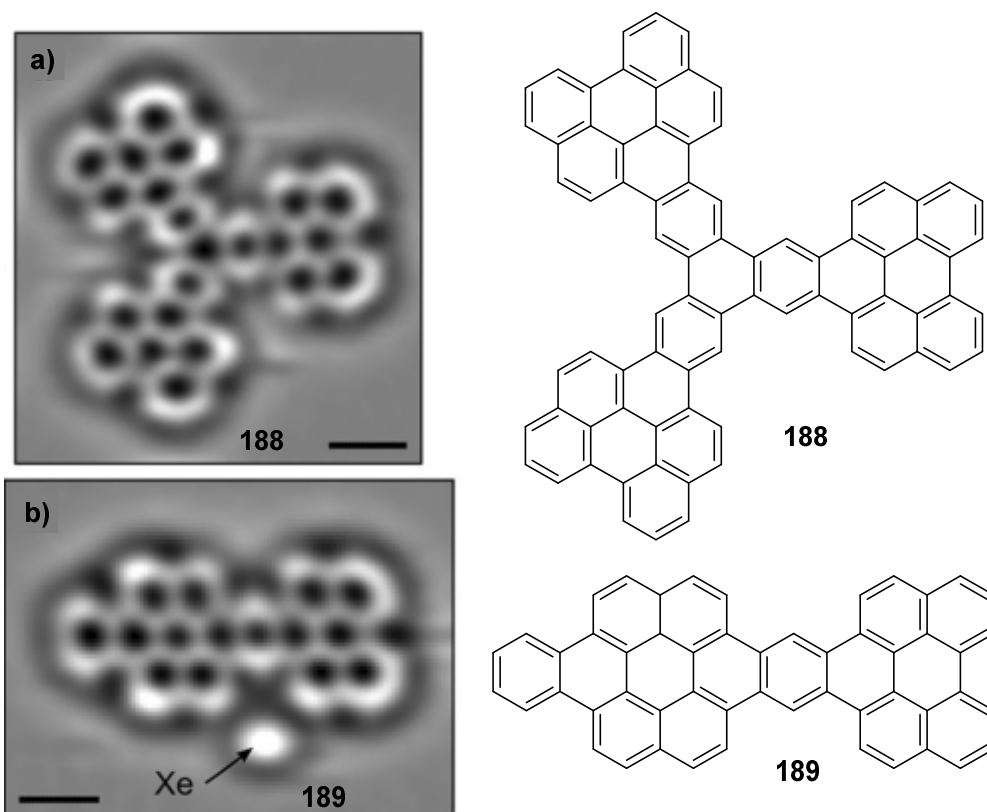


**Figure 39: The reaction product 188 expected (a) visualised under constant height NC-AFM, while (b) was an unexpected compound 189 found in the mixture formed as a by-product. Image taken from Schuler *et al.*<sup>277</sup>**

### 1.8.7 Natural products and stereochemical determination

Even though planar molecules are ideal, this technique can also be used to image non-planar compounds which may be difficult to characterise or when only a small amount has been isolated but insufficient for crystallography. This is because when the molecules lie on the surface they are at different orientations so some may be easy to see and some not, therefore some luck is required for these type of molecules to lie in a favourable orientation. In addition, stereochemical determination of chiral molecules have been resolved using this technique (Figure 40).<sup>274, 276, 278-284</sup>

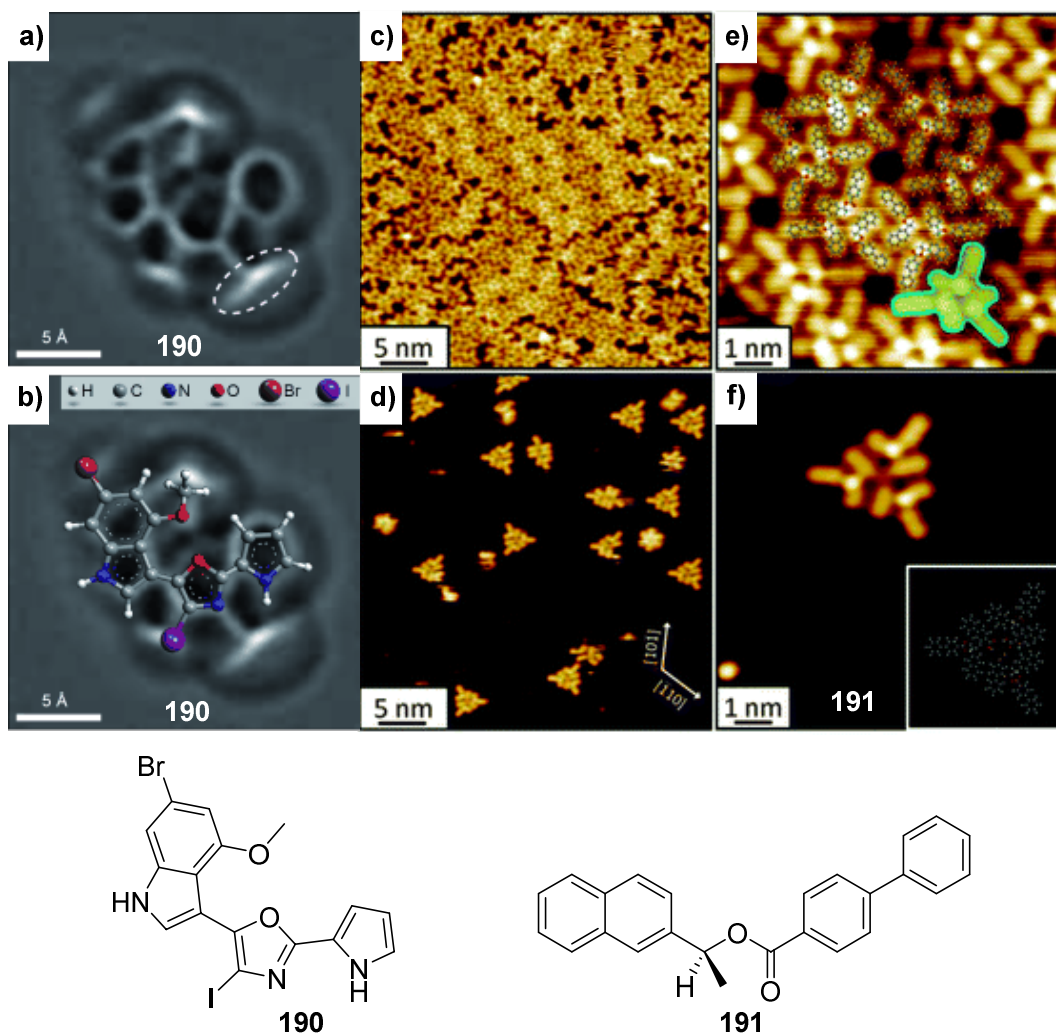


**Figure 40:** NC-AFM image (a) of natural product Breitfussin 190 with an overlaid structure (b).<sup>274</sup> STM images (c-f) of (*S*)-1-(2'-naphthyl)ethyl-(4-phenylbenzoate) (NEP) 191 which can cluster in a triangular form.<sup>278</sup> The molecule consists of a short and long arm which can be identified in the STM image to make characterisation easier.

### 1.8.8 Surface reactions

The advances in this area have been exceptional such that surface reactions are undertaken and studied by STM/AFM.<sup>249, 259, 260, 262, 285-290</sup>

In 2008 Hla *et al.* used an STM tip to manipulate all steps in the reaction of biphenyl from iodobenzene on a copper surface.<sup>287</sup> Pure iodobenzene was placed on the copper surface, the STM tip was placed above the molecule and electrons were injected into it by changing the voltage to a known value. The C-I bond is cleaved when the tunnelling current changes and it is recognised that C-H and C-C bonds

were not cleaved as they require a higher voltage due to the strength of these bonds. Thereafter the tunnelling current was increased substantially and the tip was moved along a path between two phenyls to bring them in close proximity to one another. The STM tip was then placed above the centre of both phenyls and the voltage changed for a certain period until the phenyls joined to form biphenyl, the bond length was then measured establishing that biphenyl had been made.<sup>287</sup>

Azobenzene, a well-known dye, can undergo reversible *trans-cis* isomerisation under UV light. Compounds of these types are of further interest as molecular switches in potential electronic applications. In 2006 Henzl *et al.* used a derivative of azobenzene, ‘disperse orange 3’ **192**, with a nitro and an amine substituent at either end.<sup>286</sup> An STM tip was placed above the molecule and energy was transferred by ‘inelastically’ tunnelling electrons which turned the more stable *trans* isomer **192** into the *cis* **193** as the linear image could now be seen bent (Figure 41).<sup>286</sup>

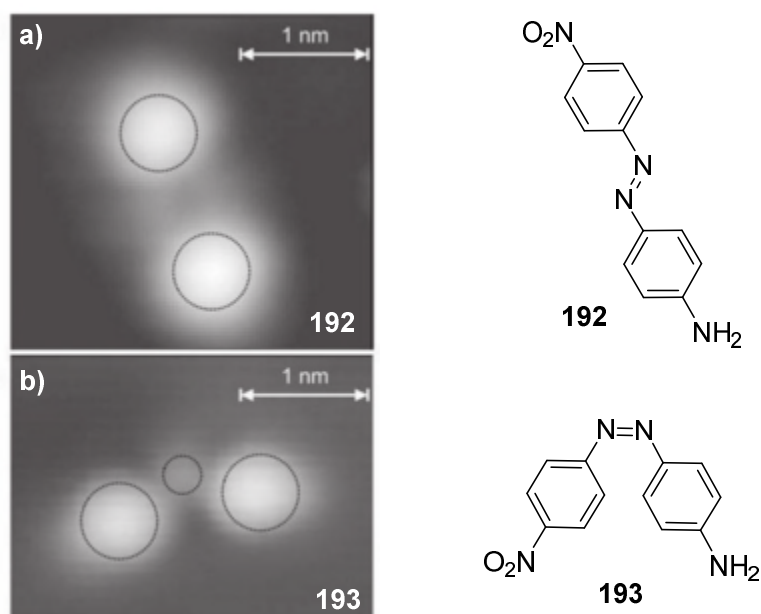


**Figure 41: Disperse orange 3 on a gold surface with (a) before and (b) after *trans* to *cis* STM images.**<sup>286</sup>



Fullerenes have been of interest since the first synthesis of C<sub>60</sub> fullerene **155** in 2002 and different methods have been pursued to attempt to increase the poor 1 % yield in the final cyclodehydrogenation step. In 2008, Otero *et al.* improved on this method by using efficient surface catalysed chemistry to cyclodehydrogenate the precursor into fullerenes in higher yields.<sup>289</sup> After loading the desired precursor onto the platinum surface it was heated to 750 K for approximately 20 minutes and the cyclodehydrogenation was monitored by STM imaging. Both C<sub>60</sub> and triazafullerenes **195** were made in high yields of approximately 100 %, but this was a purely qualitative estimate as this yield was determined by looking at before and after pictures of the surface by STM (Figure 42). Further analysis confirmed that the desired product had been formed.<sup>289</sup>

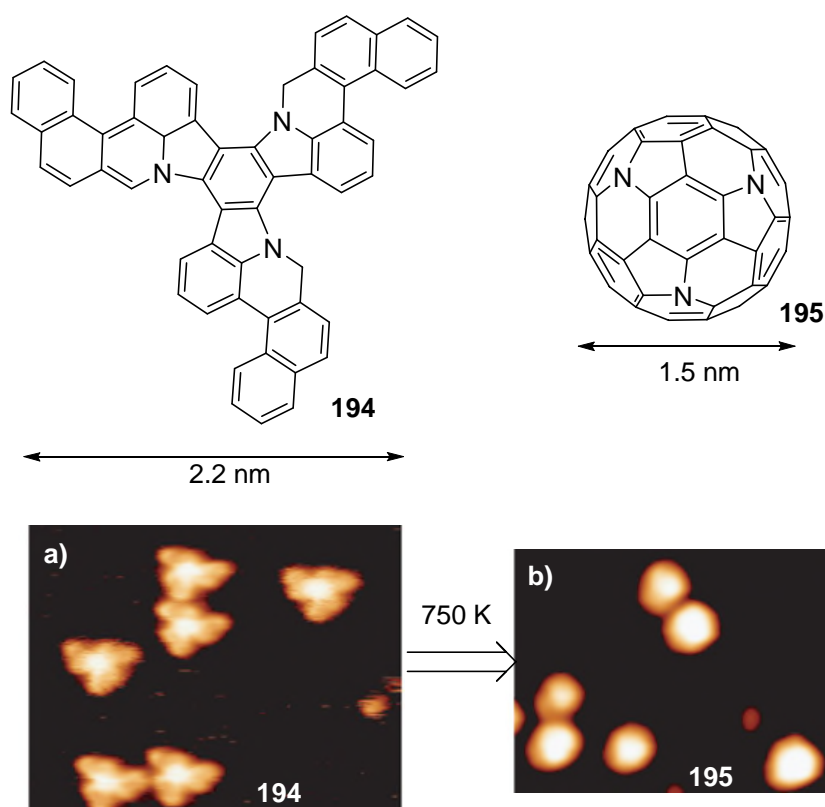
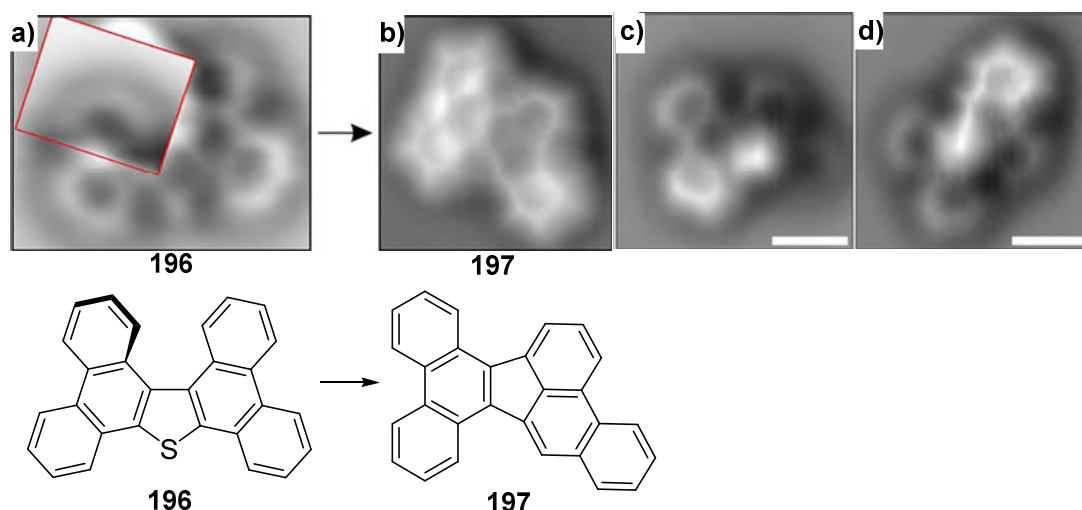


**Figure 42:** STM images before and after cyclodehydrogenation of the precursor molecules of triazafullerene (C<sub>57</sub>H<sub>33</sub>N<sub>3</sub>) **195** by Otero *et al.*<sup>289</sup> The precursor **194** can be seen in a triangular shape while the product can be seen as more of a round shape which is smaller in diameter.

A recent article in 2015 by Albrecht *et al.* has shown even greater advances in AFM, as they were able to image in 3-dimensions (3D) the protruding part of a structure.<sup>259</sup> The point of this study was to determine what products were formed during the reaction and therefore help determine a reaction pathway in addition to determining if 3D imaging can be fulfilled.

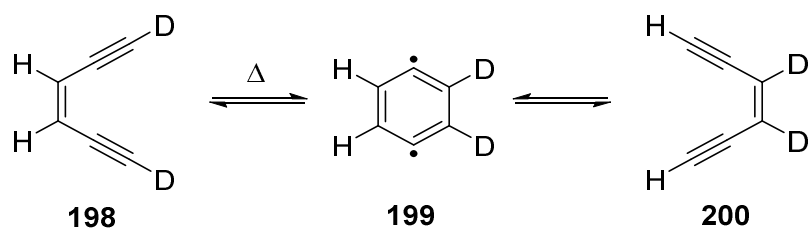
The starting material diphenanthro[9, 10-*b*:9', 10'-*d*]thiophene (DPAT) **196** was placed on a copper surface and heated to 200 °C for two minutes. Three different reaction products were observed and partially characterised by AFM. The reaction pathway was determined to have a C-S bond cleavage, a rotation of one phenanthrene moiety and aromatisation by dehydrogenation (Scheme 28).<sup>259</sup>



**Scheme 28: The main planar compound 197 can be identified by NC-AFM (b). c) and d) show almost planar side-products which have similar structural arrangement and include a sulfur atom though unclear where and what the structure is exactly.<sup>259</sup>**

There is evidently some promise in 3D microscopy, however significant improvements need to be made before the resolution is comparable to that of planar compounds.

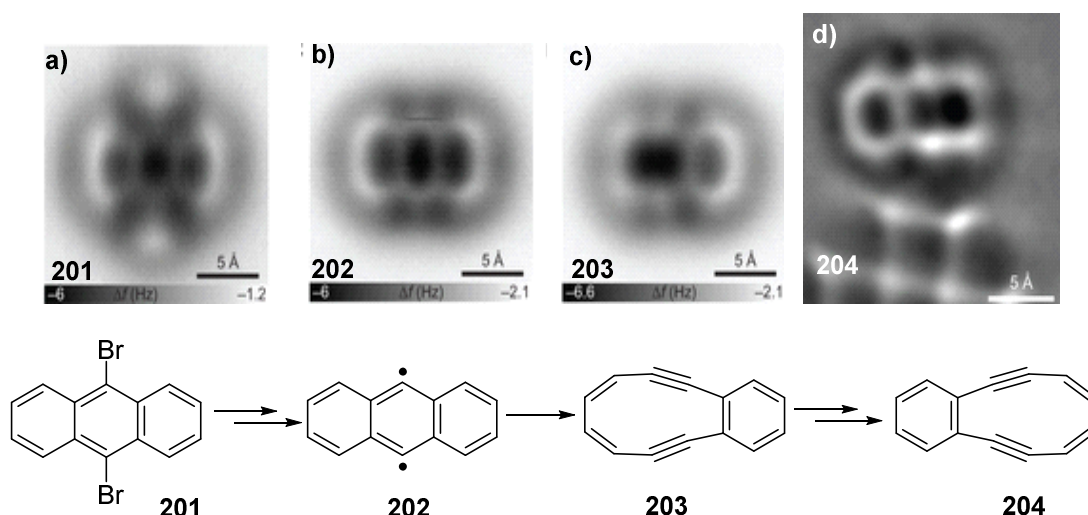
In 1972 Jones and Bergman reported that *cis*-1,5-hexadiyn-3-ene **198** undergoes a rearrangement through the diradical species benzene-1,4-diyl **199** by using deuterium labelling (Scheme 29).<sup>291</sup>



**Scheme 29: The original Bergman cyclisation, using heat to cyclise the product. The diradical **199** was observed to abstract hydrogens from the solvent 2, 6, 10, 14-tetramethylpentadecane to form benzene. In addition, when  $\text{CCl}_4$  was used as a solvent 1,4-dichlorobenzene was observed.**<sup>291, 292</sup>

This type of reaction is now commonly known as a Bergman cyclisation. Generally, it is the cyclisation of an enediyene by either heat or light, to produce a substituted arene in the presence of a hydrogen donor.

After 44 years, the Bergman cyclisation reaction has now been studied with extraordinary results where the intermediates and products of the reaction are imaged during the cyclisation, as reported by Schuler *et al.* (Scheme 30).<sup>292</sup> In this report STM was used to selectively trigger the Bergman cyclisation of an anthracene diradical **202**. Firstly, 9-10-dibromoanthracene **201** was placed on the surface and each bromine taken off sequentially by the STM tip to provide the diradical species. Secondly a voltage pulse was directed onto one of the C-C bond in between benzenes on the diradical species forming the enediyene **203**. The reversibility of this mechanism was also shown by this method and a diradical intermediate was always observed during conversion.<sup>292</sup>



**Scheme 30:** NC-AFM images of the (a) dibromo species 201 (b) the diradical 202, (c) enediyene 203. (d) Reversible manipulation formed the opposite enediyene 204. Images taken from Schuler *et al.*<sup>292</sup>

In summary, AFM and STM are powerful techniques in compound identification, stereochemical determination and in surface reactions, where a ‘before’ and ‘after’ atomic image can be observed. However, there are also limitations to this type of analysis, for example how non-planar compounds can be difficult to characterise due to their orientation on the surface. Furthermore, these techniques are already being used to study graphene<sup>247, 293-295</sup> and smaller related PAHs.<sup>258, 264, 274-277, 296</sup> This is because unknown polyaromatic molecules can be difficult to identify due to the high number of possible isomers, solubility and overlapping NMR signals.<sup>169, 258, 286, 294</sup> STM and AFM can thus distinguish single molecules of such isomers and are therefore set to become extremely powerful analytical tools in synthetic and materials chemistry.

## 1.9 Project outline

The project includes the synthesis of PAHs and the investigation of their reactivity. The PAHs targeted are those of interest to researchers, mainly non-Kekulé structures as they would pose the most interesting properties for material scientists to investigate. One radical has been identified as *6H*-benzo[*cd*]pyrene due to its resemblance to the Olympic logo and as perylene and pentacene which are two other five-fused benzenoids are already used for their fluorescent properties. The second is triangulene, a triplet-state diradical first postulated by Clar which has yet to be isolated due to its extreme instability. To assist with these aims AFM/STM will be employed to aid the formation of these non-Kekulé structures on the surface and thus, be imaged.

## 2 Chapter 2: Benzo[*cd*]pyrene

### 2.1 Introduction

To be able to form an image of the Olympic rings, the compound which would suit this skeleton most would be that of benzo[*cd*]pyrene. Consequently, this structure is in fact a radical **205** (Figure 43).

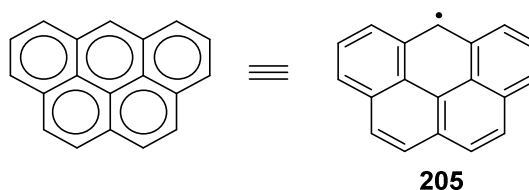
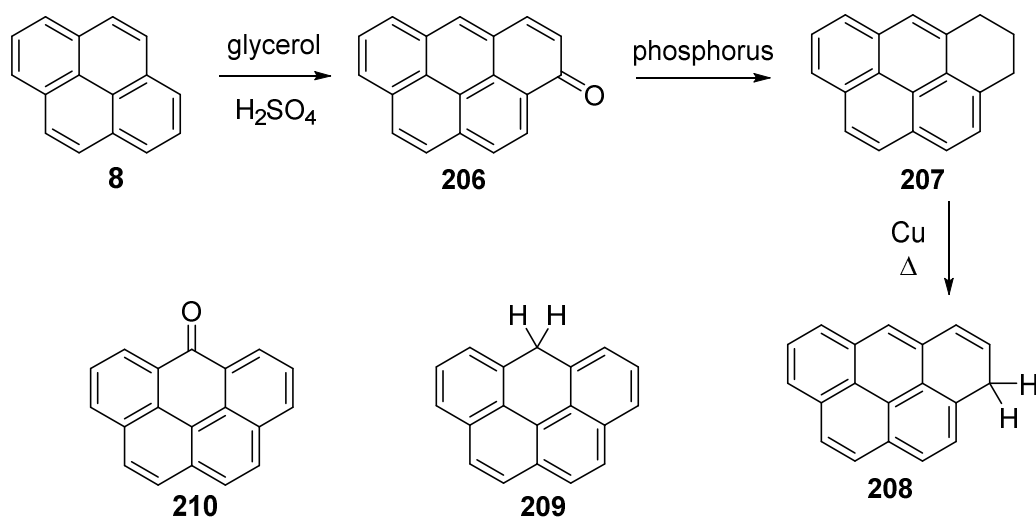


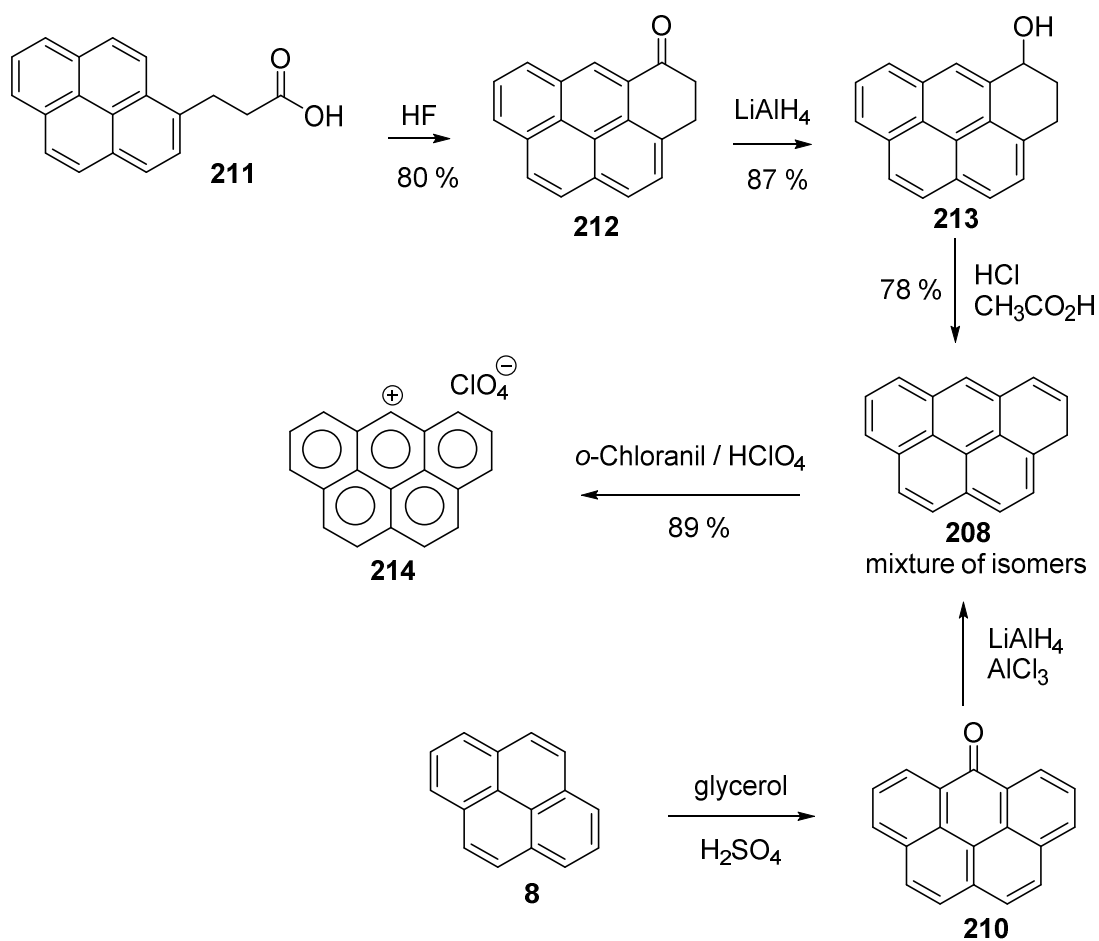
**Figure 43:** The smallest Olympic ring structure is a non-Kekulé structure **205**.

The benzo[*cd*]pyrene radical **205** itself has not been previously synthesised but its precursor, *H*-benzo[*cd*]pyrene and its oxidation products were first synthesised in 1936 by Scholl and Meyer using pyrene **8** as a starting material.<sup>297</sup> Upon reaction with glycerol it was thought to have yielded 3-oxo-3*H*-benzo[*cd*]pyrene **206** isomer, which reacted with phosphorus to yield **207**. Dehydrogenation using copper was thought to yield 3*H*-benzo[*cd*]pyrene **208**. Vollman *et al.* then studied this reaction in 1937 where it became apparent that the end product was in fact 6*H*-benzo[*cd*]pyrene **209** and the ketone intermediate was 6-oxo-6*H*-benzo[*cd*]pyrene **210**, not the isomers stated by Scholl and Meyer (Scheme 31).<sup>297, 298</sup> These reactions have been repeated by a number of chemists.<sup>299-303</sup>



**Scheme 31:** Scholl and Meyers' postulated scheme where later Vollman *et al.* realised that **206** and **208** were not made in fact **210** and **209** were respectively.<sup>297, 298</sup>

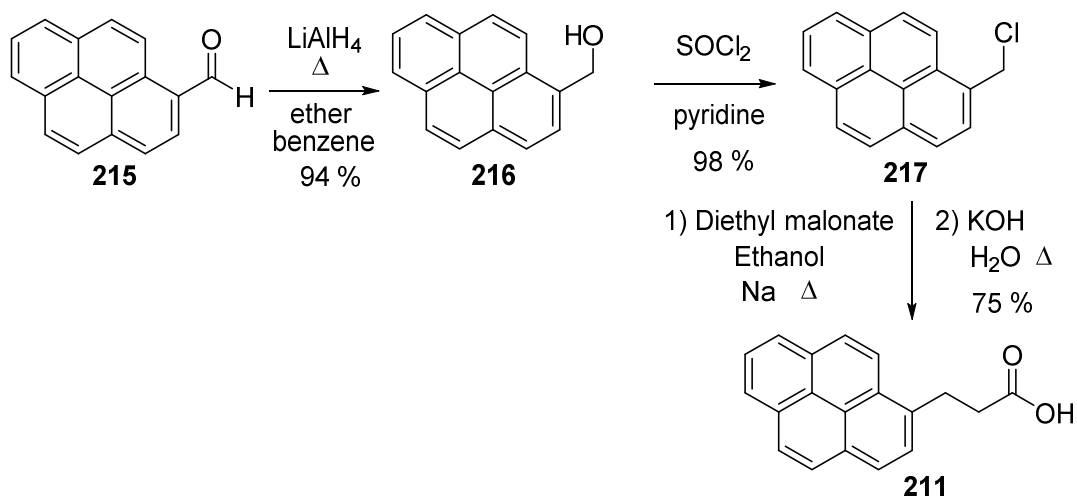
In this project, the starting point for the synthesis of 6*H*-benzo[*cd*]pyrene **209** was based on the 1965 publication by Reid and Bonthron, that also included salt **214** (Scheme 32).<sup>302</sup> However, some of the synthetic steps would need altering as they are very hazardous; for example the ring closure using liquid HF. The work described herein started with a repeat of Reid and Bonthron's synthesis but using modified ring-closure conditions.<sup>302</sup>



Scheme 32: A synthetic route towards 6*H*-benzo[*cd*]pyrenium cation **214** by Reid and Bonthron.<sup>302</sup>

In the 1965 paper the starting material **211** was synthesised in three steps from 1-formylpyrene **215** (Scheme 33) and ketone **210** was synthesised *via* the condensation of pyrene **8** with glycerol and sulfuric acid (Scheme 32).<sup>302</sup>

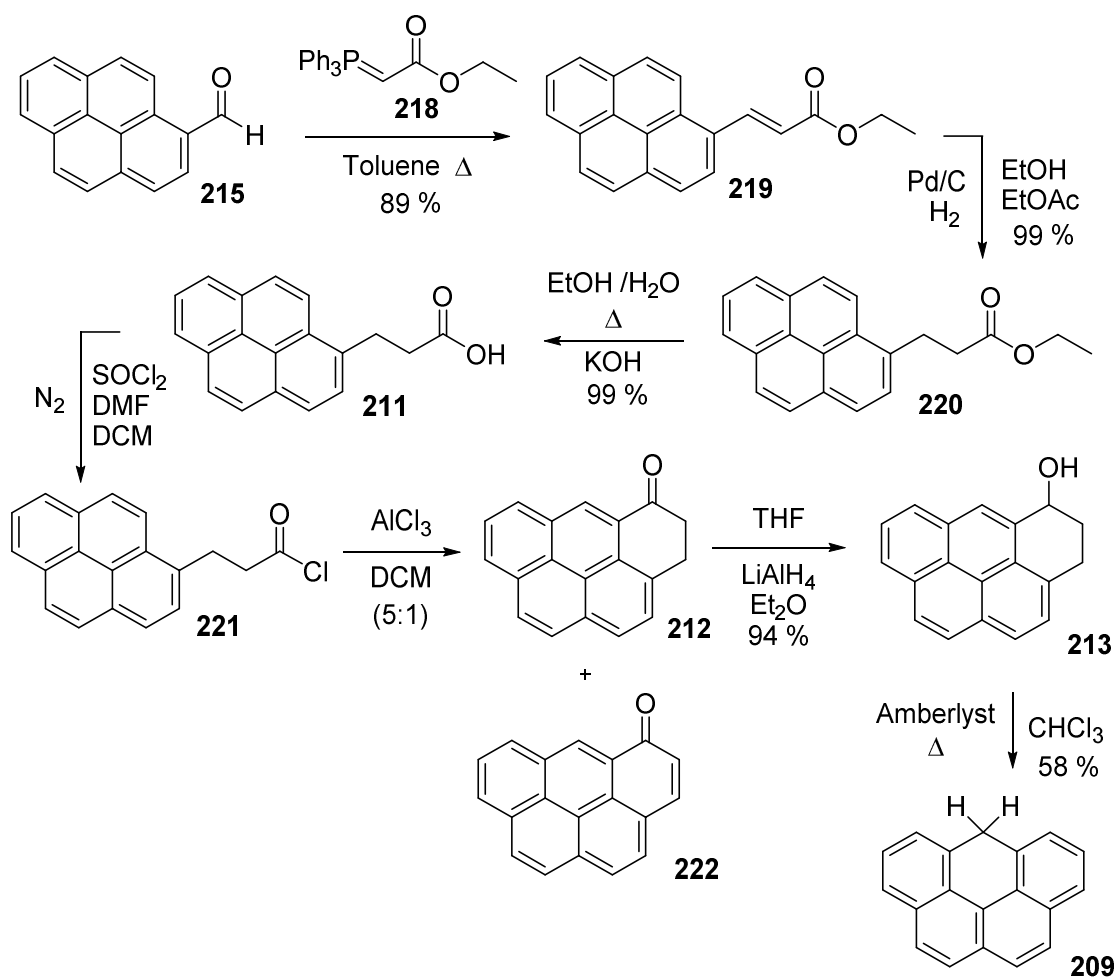




**Scheme 33: Formation of starting material 211, 1-formylpyrene 215 used by Reid and Bonthron to synthesise 6H-benzo[cd]pyrene.<sup>302</sup>**

## 2.2 The synthesis of 6H-benzo[cd]pyrene

In light of Reid and Bonthron's work, a new route was designed and tested (Scheme 34). It uses similar synthetic steps but with materials which are commercially available, less hazardous and more cost effective.<sup>304-311</sup>

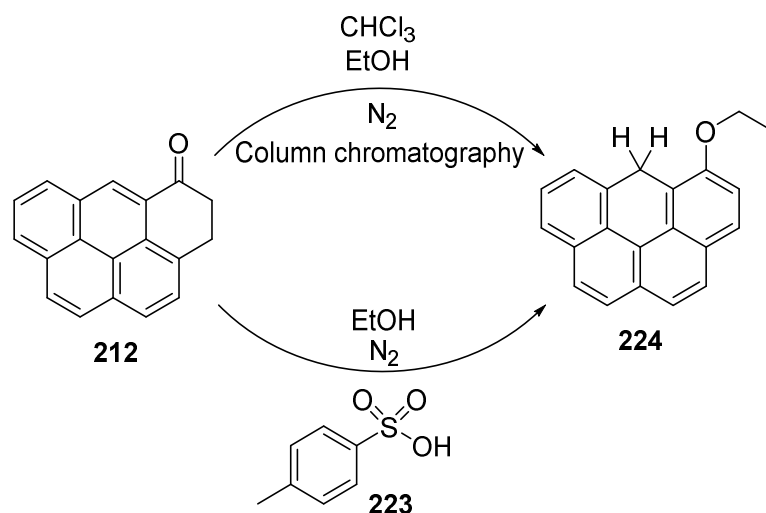


**Scheme 34:** A new route towards the synthesis of 6*H*-benzo[*cd*]pyrene **209**, where **211** was used immediately to form the major product **212**.<sup>304-311</sup>

The Wittig reagent was prepared by reacting the commercially available ethyl bromoacetate with triphenylphosphine. This salt was then deprotonated in base (NaOH) to form the ylid **218**, which was reacted with 1-pyrenecarboxaldehyde **215** under reflux conditions and purified to produce ethyl 3-(1-pyrenyl)acrylate **219**.<sup>305</sup> The double bond of **219** was then hydrogenated and optimising the reaction conditions (including adding ethyl acetate to dissolve **219** fully) gave a good yield of ethyl 3-(1-pyrenyl)propanoate **220**.<sup>308, 309</sup> In addition, the required palladium catalyst loading is as low as 2 mol % which was initially 10 mol %.

Ethyl 3-(1-pyrenyl)propanoate **220** was then hydrolysed to produce 3-(1-pyrenyl)propionic acid **211**.<sup>304, 305</sup> The acid chloride **221** was produced and used immediately for cyclisation due to its instability.<sup>310</sup> A Friedel-Crafts cyclisation using AlCl<sub>3</sub> furnished 3,4-dihydro-5*H*-benzo[*cd*]pyren-5-one **212** which was reduced immediately due to its unstable nature to **213**.<sup>307, 310, 311</sup>

Upon repeating the Friedel-Crafts cyclisation on a larger scale, a very unstable, air sensitive, bright green solid was also obtained during purification by column chromatography. After repeating purification under an inert atmosphere this unknown product was isolated in trace amounts and fully characterised. The data showed that 5-ethoxy-6*H*-benzo[*cd*]pyrene **224** was produced (Scheme 35), even though nothing in the NMR spectrum of the crude material or mechanistic theory supported the formation of this compound. There were no reagents or solvents used in the reaction that could provide an acetate/ethyl group. It was suggested that the compound could have been formed during column chromatography. This is because the eluent chloroform is known to contain small amounts of ethanol as an oxidation scavenger. On a large scale in combination with the acidic conditions of the silica gel a small reaction could take place. To help support this theory **212** was added to a mixture of chloroform and ethanol (9:1) and silica gel under an inert atmosphere, to try and mimic the conditions. However, the reaction was either too slow or did not proceed suggesting that something else was catalysing the reaction. Therefore, different conditions were used in ethanol and toluene sulfonic acid **223** under a dinitrogen atmosphere, 5-ethoxy-6*H*-benzo[*cd*]pyrene **224** could be observed by NMR spectroscopy (Scheme 35).



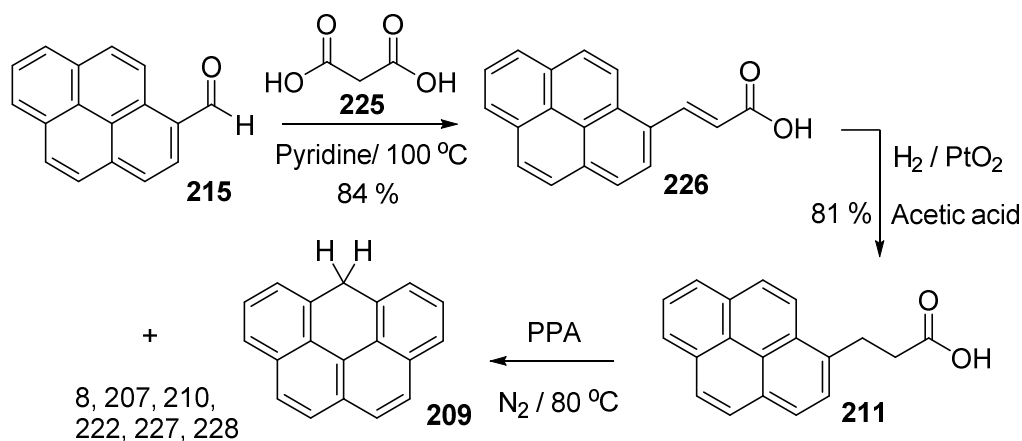
**Scheme 35: Pathways to the production of 5-ethoxy-6H-benzo[cd]pyrene 224.**

Reduction of ketone **212** to alcohol **213** was followed by acid catalysed dehydrogenation. Using acetic acid/hydrogen bromide by the method of Reid and Bontrone, 6H-benzo[cd]pyrene **209** was produced (and not **208** as stated by the literature) but with several other unknown compounds, thus making purification difficult.<sup>302</sup> Optimisation of this step resulted in the use of a solid-supported catalyst, Amberlyst 15. This reaction was much cleaner as it produced mainly 6H-benzo[cd]pyrene **209** with the addition of a small amount of ketone **210** and starting material. Furthermore, it was quickly realised that **209** was very unstable and oxidised quickly into 6-oxo-6H-benzo[cd]pyrene **210**, therefore the compound had to be kept under an inert atmosphere.

### 2.2.1 Optimisation of the synthesis of 6H-benzo[cd]pyrene

Even though the Reid and Bontrone method had been improved with the use of safer reagents and a better route to 3-(1-pyrenyl)propionic acid **211**, further improvements could easily be made. Firstly, utilising the works of Mizushima *et al.* (Scheme 36) 1-pyrenecarboxaldehyde **215**, which is commercially available, was treated with malonic acid, in a Doebner modification of a Knoevenagel

condensation, to form 3-(1-pyrenyl)acrylic acid **226** in good yield.<sup>312</sup> This was subsequently reduced to the desired 3-(1-pyrenyl)propionic acid **211** in acetic acid.<sup>312</sup>



**Scheme 36:** A three-step synthesis of 6H-benzo[cd]pyrene **209**, where a number of additional products are formed (8, 207, 210, 222, 227, 228).<sup>312</sup>

Cyclisation of acid **211** was attempted directly instead of *via* the acid chloride. Use of methane sulfonic acid produced mainly 5-oxo-5H-benzo[cd]pyrene **222** with significant starting material recovered and similar results were obtained when using Eaton's reagent or H<sub>2</sub>SO<sub>4</sub>.<sup>302</sup> Polyphosphoric acid (PPA) produced more favourable results, producing mainly 6H-benzo[cd]pyrene **209** and 6-oxo-6H-benzo[cd]pyrene **210**. Consequently, the unexpected formation of 6H-benzo[cd]pyrene **209** as a major product considerably shortened the synthetic pathway into a three-step route (Scheme 36).

Even though the acid catalysed cyclisation of 3-(1-pyrenyl)propionic acid **211** with PPA did not yield the ketone 3,4-dihydro-5H-benzo[cd]pyren-5-one **212**, the <sup>1</sup>H NMR spectrum of the crude product also showed small amounts of other compounds formed.

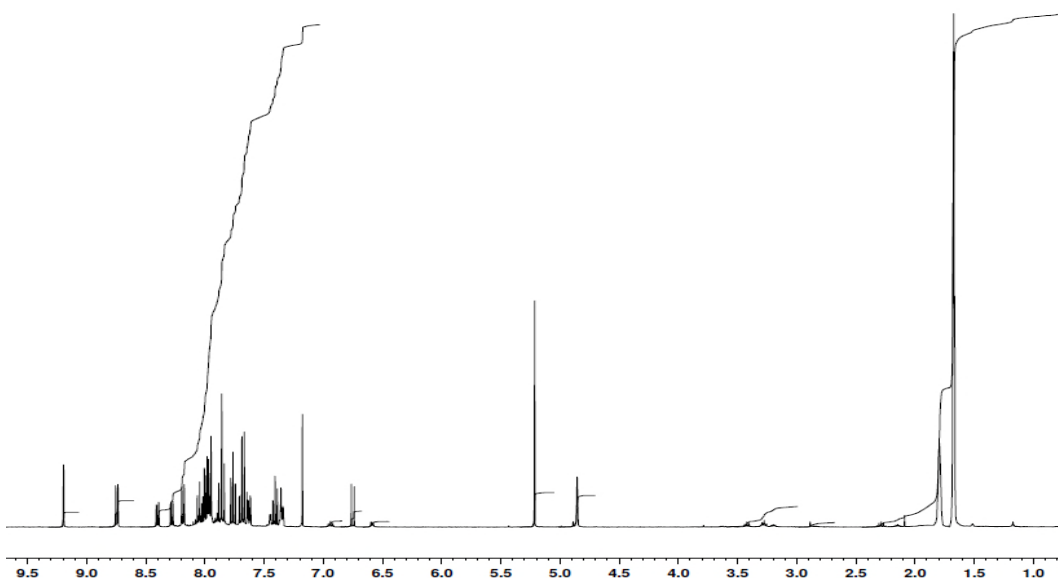
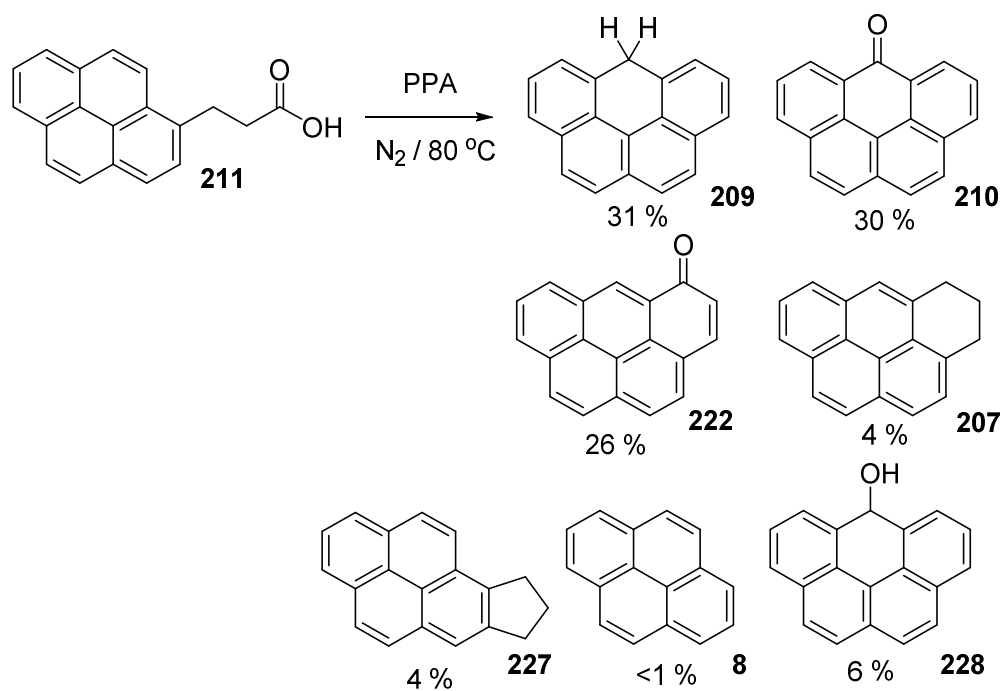


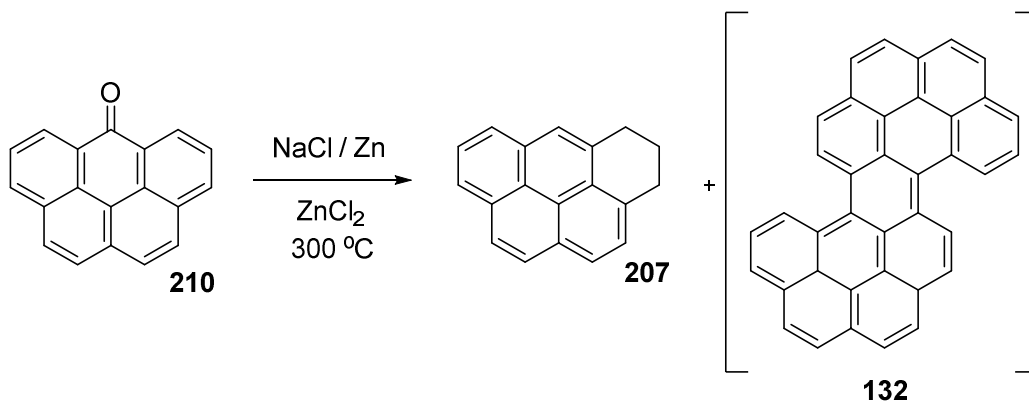
**Figure 44:**  $^1\text{H}$  NMR spectrum of the crude product of the PPA mediated reaction, conducted at  $80\text{ }^\circ\text{C}$  for overnight, under  $\text{N}_2$  (with adamantane as a standard).

Upon extensive gradient column chromatography methods under an inert atmosphere, the major products isolated were confirmed to be 6*H*-benzo[*cd*]pyrene **209**, 6-oxo-6*H*-benzo[*cd*]pyrene **210** and 5-oxo-5*H*-benzo[*cd*]pyrene **222** with data in good agreement with that published.<sup>301, 313, 314</sup> In addition to these compounds, other minor products were isolated in trace quantities including, 4,5-dihydro-3*H*-benzo[*cd*]pyrene **207**, 7,8-dihydro-9*H*-cyclopenta[*a*]pyrene **227** and pyrene **8** (Scheme 37).<sup>315-317</sup>



**Scheme 37:** Compounds formed from the ring cyclisation using PPA at 80 °C under a dinitrogen atmosphere overnight. Compounds **209**, **210** and **222** were the major components isolated.

4,5-Dihydro-3*H*-benzo[*cd*]pyrene **207** was synthesised independently using Clar and Stewart's zinc melt conditions (Scheme 38) for data comparison.<sup>316</sup>



**Scheme 38:** The independent formation of 4,5-dihydro-3*H*-benzo[*cd*]pyrene **207** by the method of Clar and Stewart.<sup>316</sup>

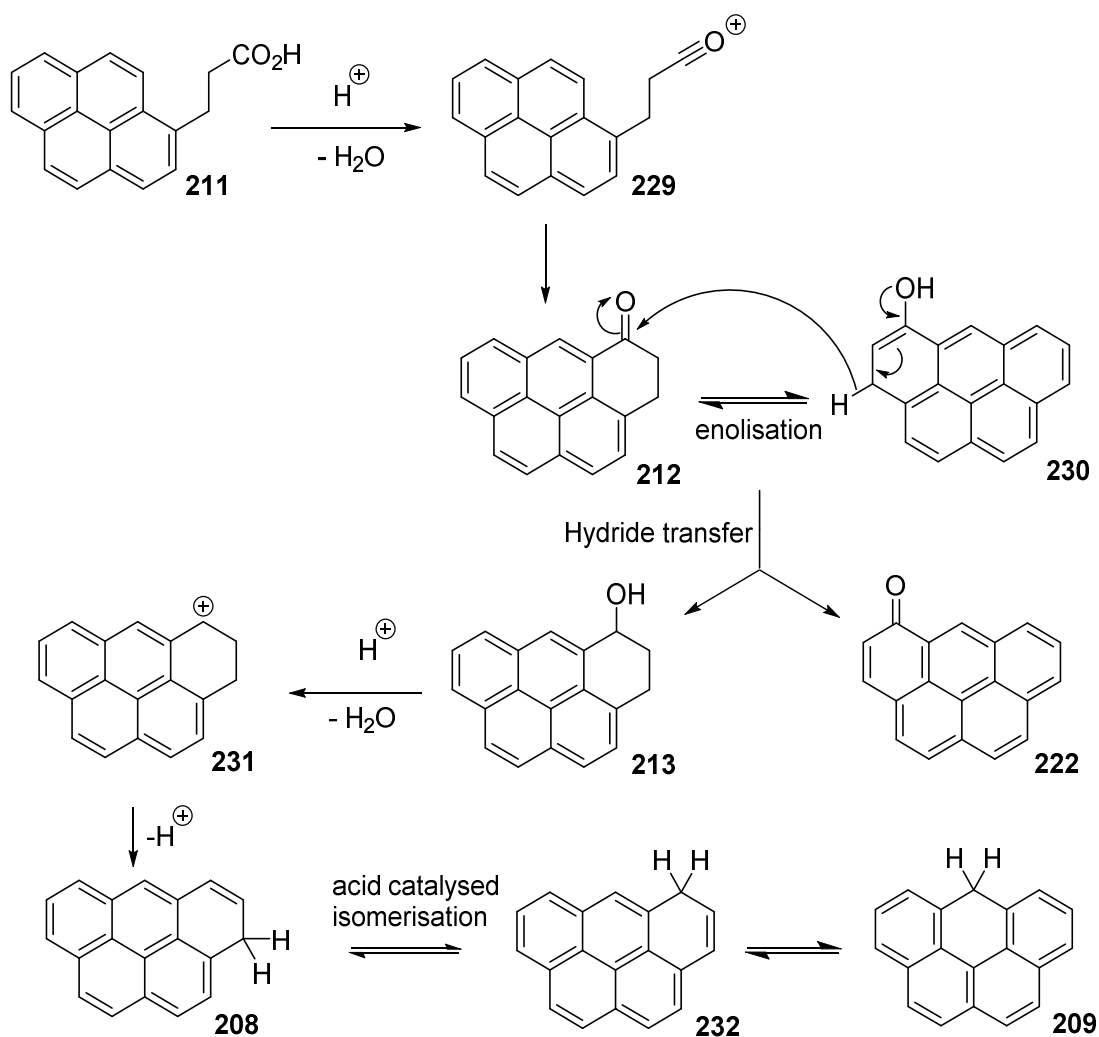
This reaction also contained trace amounts of dimer (when completed using >0.8 g of **210**), dibenzo[*jk, uv*]dinaphtho[2,1,8,7-*defg*-2', 1', 8', 7'-*opqr*]pentacene **132** (Scheme 38).<sup>318</sup>

The isolation of compound **228** is described later in relation to a formal disproportionation reaction.

The compounds which were isolated from the PPA-mediated cyclisation of acid **211** are shown in Scheme 37. Further analysis of the <sup>1</sup>H NMR spectrum of the crude product of the PPA reaction resulted in the following ratios of each product: **209**, 31 %; **210**, 30 %; **222**, 26 %; **228**, 6 %; **207**, 4 %; **227**, 4 %, including a trace quantity of pyrene **8**.

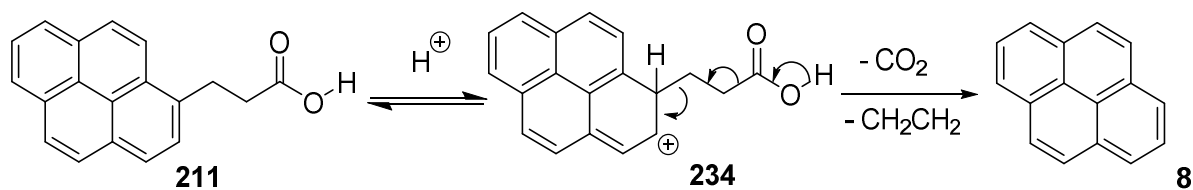
After purification of the crude PPA mixture, none of the expected cyclised ketone of 3,4-dihydro-5*H*-benzo[*cd*]pyren-5-one **212** was observed. However, we believe that the acid initially cyclises to form this compound, but it reacts further. To prove this, 3,4-dihydro-5*H*-benzo[*cd*]pyren-5-one **212** was subjected to the usual PPA reaction conditions where the same plethora of reaction products were observed from Scheme 37, with the exception of 7,8-dihydro-9*H*-cyclopenta[*a*]pyrene **227**. A reaction mechanism is proposed in Scheme 39 for a formal disproportionation of ketone **212**. Here, the acid first protonates and loses water to form a reactive acylium ion **229** which undergoes cyclisation to form ketone **212**. In the highly acidic conditions at elevated temperatures the enol form, **230**, can transfer a hydride to the keto-form to produce **213** and **222**. Acid mediated removal of water produces the cation intermediate **231** which can lose a proton and rapidly isomerise to the more stable isomer 6*H*-benzo[*cd*]pyrene **209**.





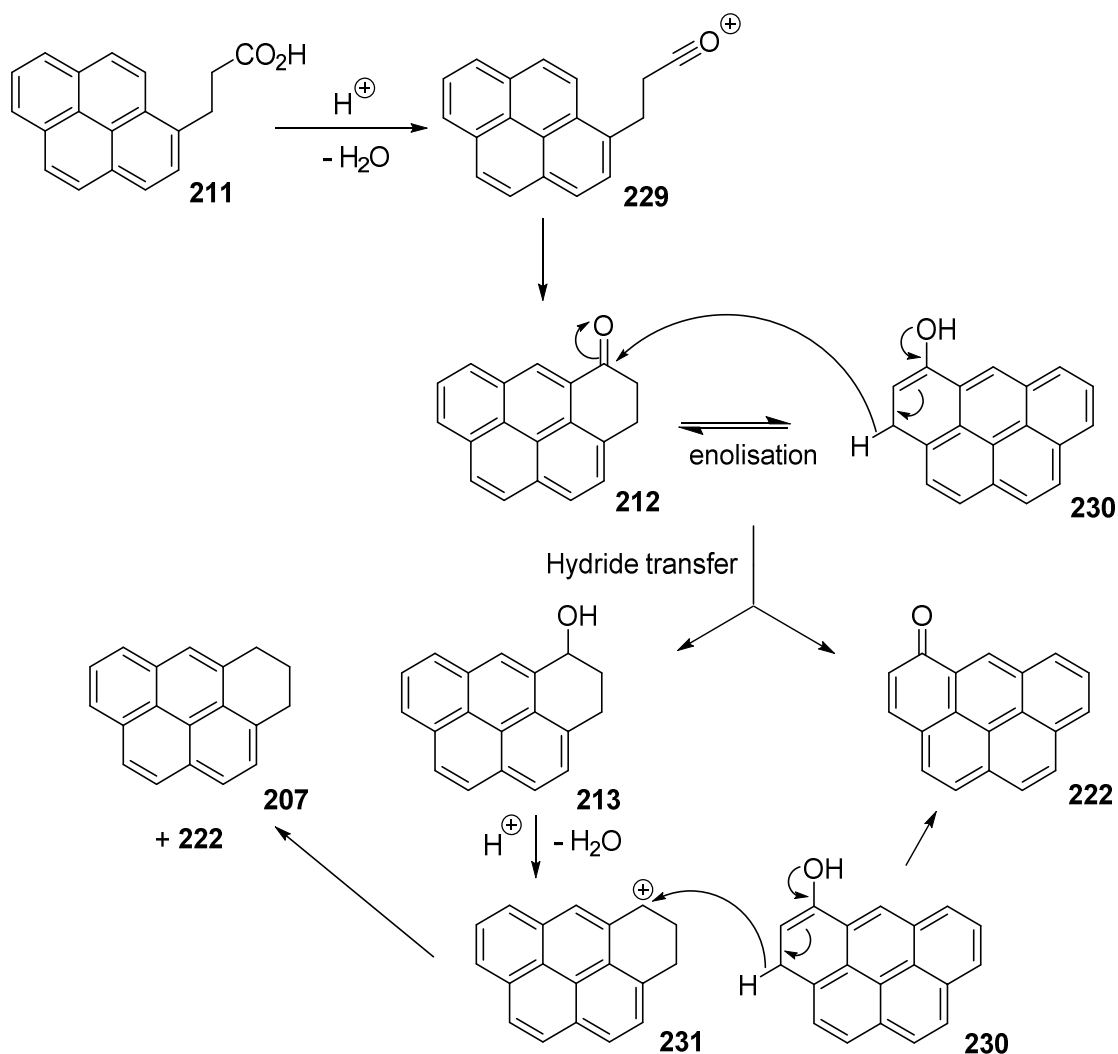
**Scheme 39:** Possible mechanism in which ketone 212 is formed and then reacts further by disproportionation.

The production of the minor compounds can also be explained, for example pyrene **8** can be produced by an acid-catalysed de-alkylation, where ethylene and carbon dioxide are lost (Scheme 40).



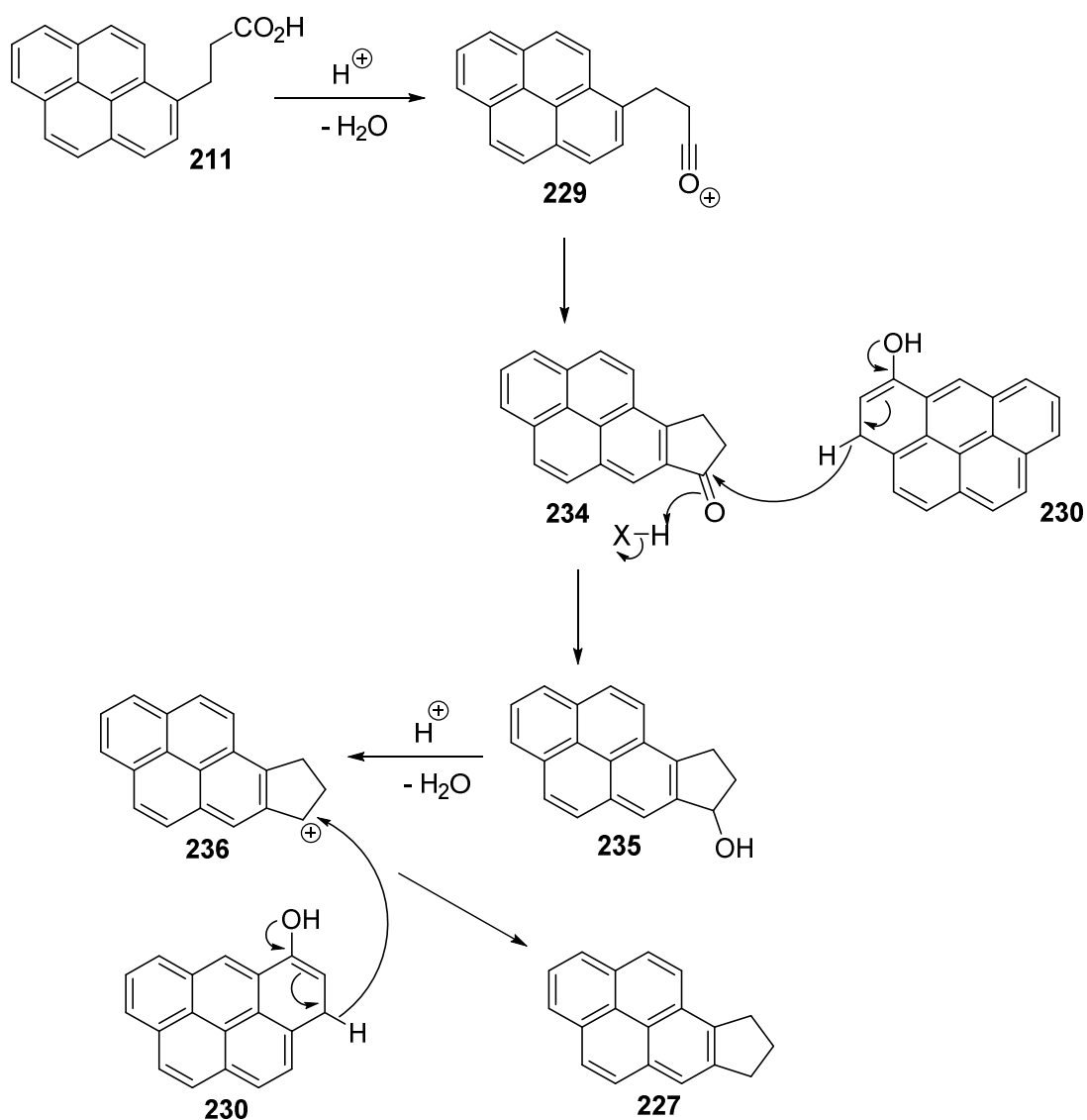
**Scheme 40:** Possible mechanism of formation of pyrene **8** from the starting material 211.

The production of 4,5-dihydro-3*H*-benzo[*cd*]pyrene **207** can occur by the reduction of the cation **231** as shown in Scheme 39 by using enol **230** (or **209** or **228** may also be used) for example.



**Scheme 41:** The possible mechanism of formation of 4,5-dihydro-3*H*-benzo[*cd*]pyrene **207**.

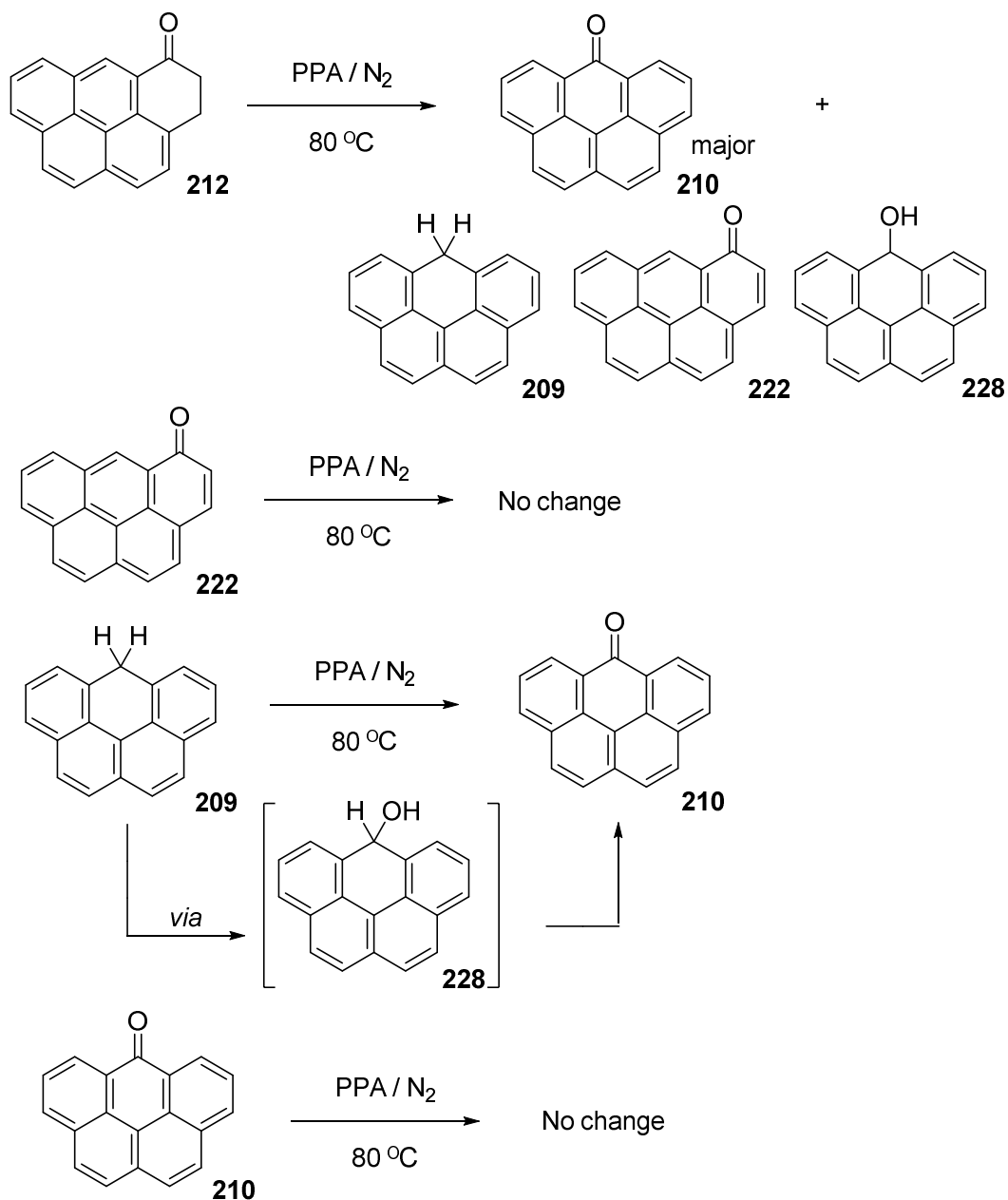
The formation of the 7,8-dihydro-9*H*-cyclopenta[*a*]pyrene **227** can be rationalised by the acylium ion **229** cyclising in the opposite direction, to form a five ring as shown in Scheme 42.



**Scheme 42: Possible mechanism for the formation of 7,8-dihydro-9H-cyclopenta[a]pyrene 227.**

Whilst studying this reaction extensively, it became apparent that 6H-benzo[cd]pyrene **209** oxidises to 6-oxo-6H-benzo[cd]pyrene **210** due to the relatively weak methylene C-H bonds.<sup>319</sup> A further observation which was not reported before was the isomerisation of 5-oxo-5H-benzo[cd]pyrene **222** to 6-oxo-6H-benzo[cd]pyrene **210**.<sup>302, 313</sup> To prove this isomerisation 3,4-dihydro-5H-benzo[cd]pyren-5-one **212**, 6H-benzo[cd]pyrene **209** and 5-oxo-5H-benzo[cd]pyrene **222** were independently heated under the usual PPA reaction conditions. The results

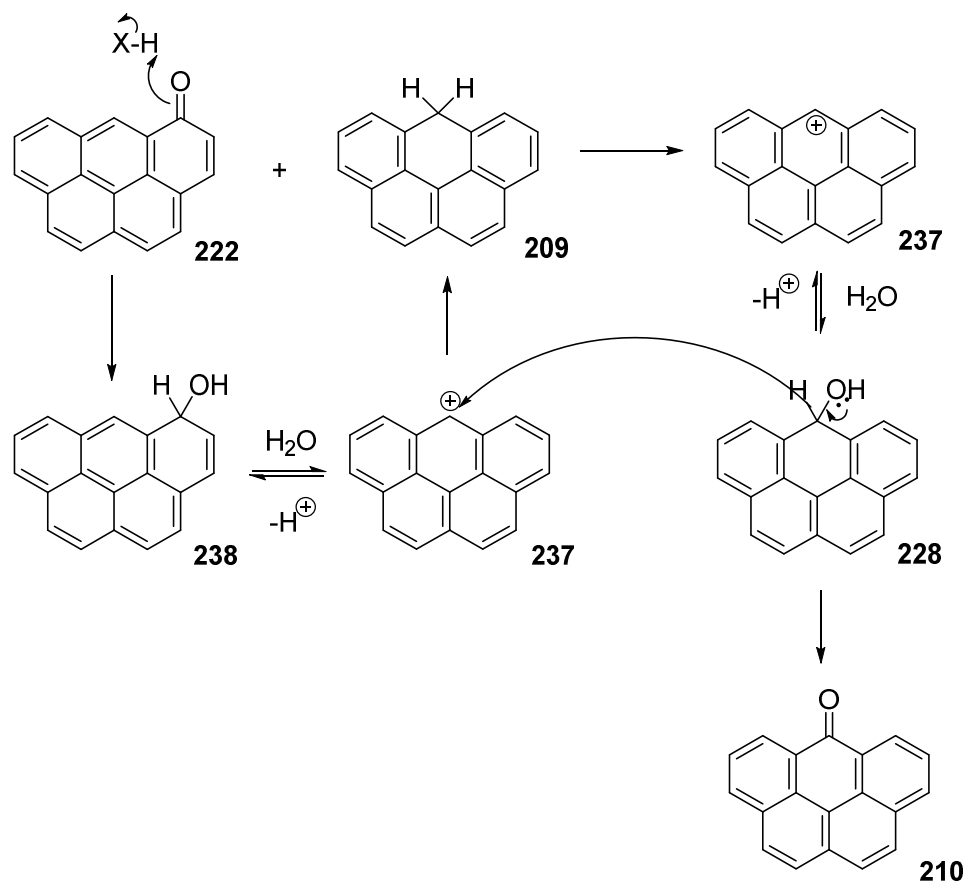
(Scheme 43) shows that 3,4-dihydro-5*H*-benzo[*cd*]pyren-5-one **212** gave a similar range of products to that of the acid catalysed reaction (excluding **227**). 6*H*-Benzo[*cd*]pyrene **209** completely oxidised to 6-oxo-6*H*-benzo[*cd*]pyrene **210**, but no reaction occurred with the 5-oxo-5*H*-benzo[*cd*]pyrene **222** which remained unchanged.<sup>302</sup>



**Scheme 43: Independent PPA reactions; 3,4-dihydro-5*H*-benzo[*cd*]pyren-5-one **212**, 5-oxo-5*H*-benzo[*cd*]pyrene **222**, 6*H*-benzo[*cd*]pyrene **209** and 6-oxo-6*H*-benzo[*cd*]pyrene **210**.**<sup>302</sup>

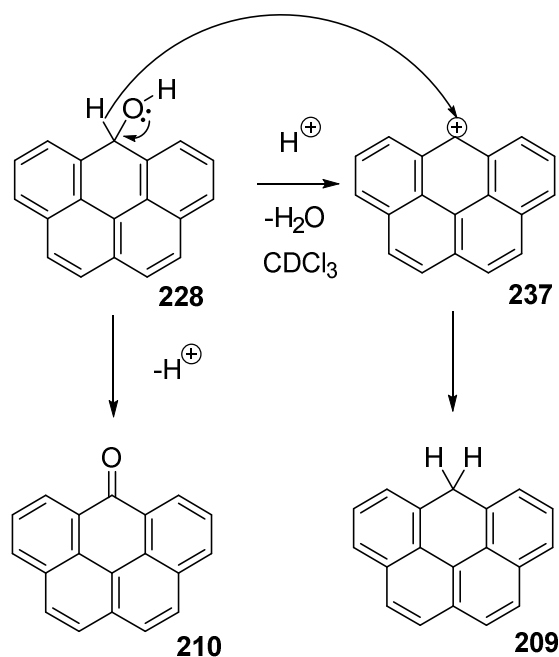
These observations support the proposed theory that 3,4-dihydro-5*H*-benzo[*cd*]pyren-5-one **212** is a key, highly reactive intermediate in the reaction (disproportionation of compounds **213** and **222** in Scheme 39) but not that of the isomerisation of 5-oxo-5*H*-benzo[*cd*]pyrene **222**. Thus, another catalyst was being used for the isomerisation in this reaction.

Hydride donation was postulated before in Scheme 39, therefore we believe that 6*H*-benzo[*cd*]pyrene **209** can also act as a catalytic hydride donor, which has also been mentioned by Morgenthaler *et al.*<sup>301, 320</sup> To support this mechanism 5-oxo-5*H*-benzo[*cd*]pyrene **222** was added to 6*H*-benzo[*cd*]pyrene **209** and heated under the usual PPA reaction conditions with adamantane added as a quantification. The progress was monitored by NMR spectroscopy where it was observed that isomerisation did occur and that 6-oxo-6*H*-benzo[*cd*]pyrene **210** was generated (Scheme 44). Signals related to **228** were also observed.



**Scheme 44: The isomerisation of 222 to 210, with 209 being the source of the hydride which is regenerated.**

Further to this, Reid and Bonthron have previously reported the redox disproportionation of the benzo[*cd*]pyrenium cation **237** into 6*H*-benzo[*cd*]pyrene **209** and 6-oxo-6*H*-benzo[*cd*]pyrene **210**.<sup>302</sup> During this disproportionation (Scheme 45) they proposed that it progressed through an intermediate alcohol **228**, however they never managed to isolate this due to its high reactivity.<sup>302</sup>



**Scheme 45: Disproportionation of alcohol 228 into 209 and 210.**<sup>302</sup>

During purification by column chromatography under an inert atmosphere (including collection and storage), an unknown reactive product was isolated. But it was found that this compound degrades in base-washed and dried  $\text{CDCl}_3$  making analysis extremely difficult. However, after quick preparation and analysis by NMR spectroscopy, it was found that this extremely unstable compound isolated was the alcohol **228** which Reid and Bonthron postulated, though no one has isolated.<sup>302</sup> Within hours of preparation for NMR analysis, the sample soon started to produce different signals and upon analysis the next day the sample had 6*H*-benzo[*cd*]pyrene **209** and 6-oxo-6*H*-benzo[*cd*]pyrene **210** in the redox disproportionation reaction mentioned previously (Scheme 45)<sup>302</sup>

### 2.3 AFM/STM imaging

Scanning tunnelling microscopy and atomic force microscopy (STM/AFM) can be used to image planar molecules, therefore the compounds synthesised in this project

were ideal candidates. A sample of 6*H*-benzo[*cd*]pyrene **209** was imaged by the Gross group at IBM Zürich, where a hydrogen was abstracted from the molecule to create a radical (Figure 45). This was completed by a voltage pulse being applied while the STM tip was above the dihydride group. The compound was chemisorbed onto the copper surface, which caused a slight tilt of the compound. The benefit of this technique is that the structure including carbon-carbon bonds can be seen, as well as being able to form unstable molecules containing radicals in this case.

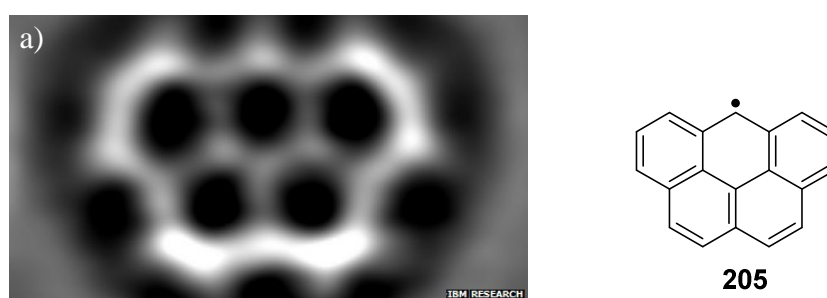


**Figure 45: a) AFM image of benzo[*cd*]pyrene radical 205.<sup>321</sup>**

Additionally, the final step of the reaction which produced a crude mixture of 6*H*-benzo[*cd*]pyrene was also analysed by AFM. A number of isomers both dihydride and oxidative products were imaged as shown in Figure 46.



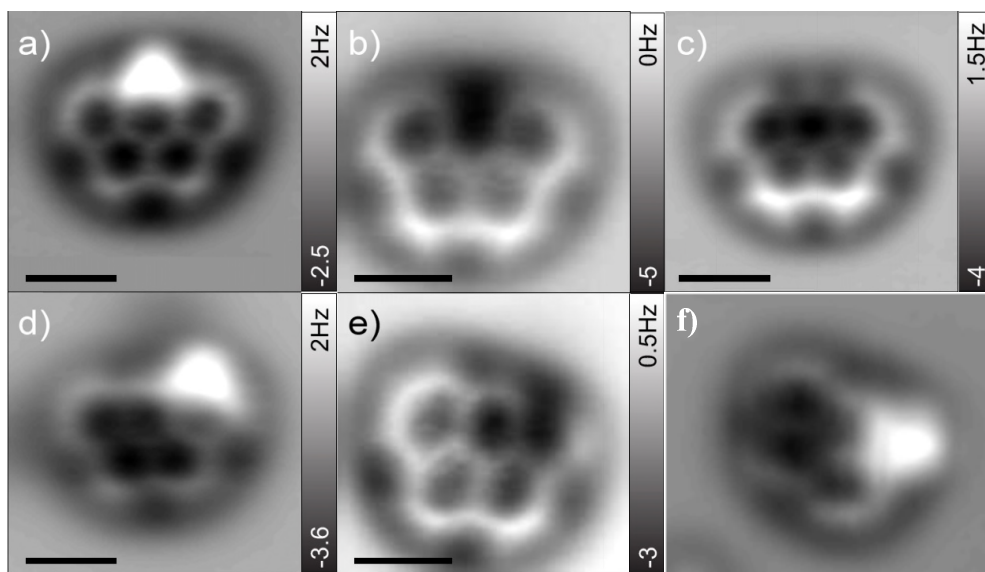


**Figure 46:** NC-AFM images of a) 6*H*-benzo[*cd*]pyrene 209, b) 6-oxo-6*H*-benzo[*cd*]pyrene 210, c) benzo[*cd*]pyrene radical 205, d) 5*H*-benzo[*cd*]pyrene 232, e) 5-oxo-5*H*-benzo[*cd*]pyrene 222, f) 4,5-dihydro-3*H*-benzo[*cd*]pyrene 207. The dark areas in images b and c are the C=O regions and the bright areas on images a, d and f are that of the CH<sub>2</sub> regions.<sup>321</sup>

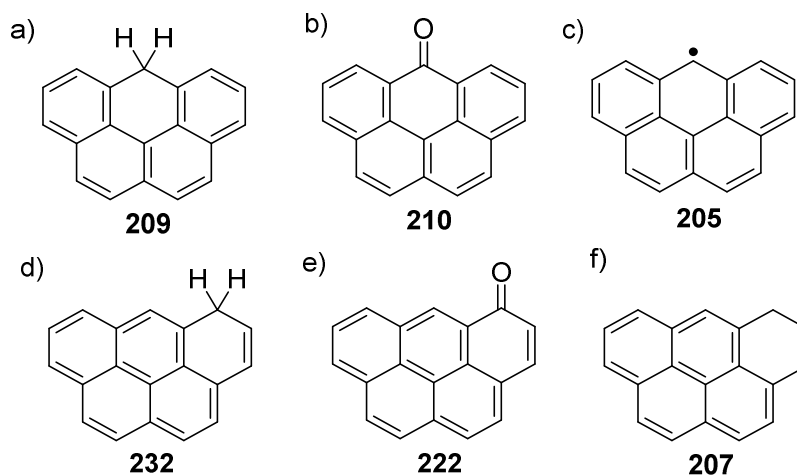


**Figure 47:** Corresponding structures to the AFM images from Figure 46.

Constant height AFM was used and the images were captured at 5 K with a CO tip on a copper surface. The bright spots are the CH<sub>2</sub> hydrogen atoms (repulsive interactions) whilst the dark spots are electron withdrawing ketones (attractive interactions).

Furthermore, a very unstable isomer 5*H*-benzo[*cd*]pyrene **232**, was also seen, which has never been observed before. This result suggests that the 5*H*-position is probably the next most stable isomer as both 5*H*-benzo[*cd*]pyrene **232** and 5-oxo-5*H*-benzo[*cd*]pyrene **222** were imaged but none of the other isomers were found.

Reid and Bonthron have already reported that the six-position is primarily the favoured site of reaction for radicals, anions and cations.<sup>302</sup> In addition, Figure 48 shows that isomers **209**, **232** and **208**, contain two Clar sextets and are therefore more likely to be stable. Furthermore, Valentine *et al.* have studied the benzo[*cd*]pyrene skeleton computationally.<sup>322</sup> They have deduced that 6*H*-benzo[*cd*]pyrene **209** is the most stable isomer thus, this isomer is predominantly seen in the reactions conducted.<sup>322-324</sup> Thereafter **208** (24.5 KJ mol<sup>-1</sup>) and **232** (29.7 KJ mol<sup>-1</sup>) are the next isomers which are low in energy compared to the rest which correlate with the Clar's sextet theory.<sup>11</sup>

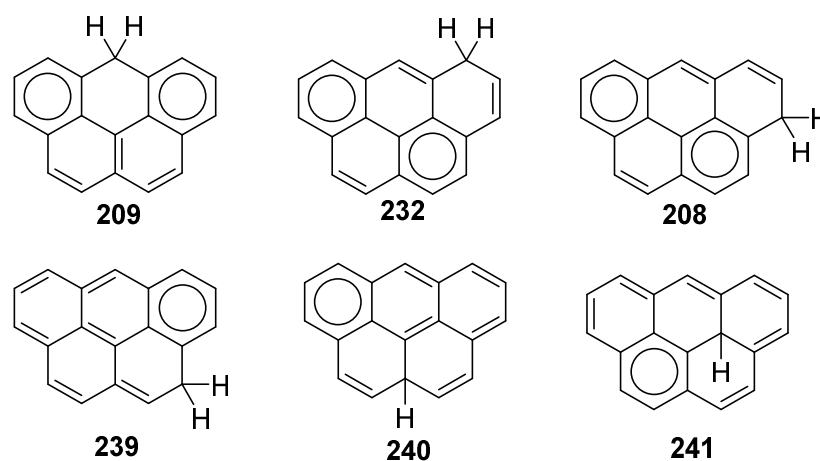
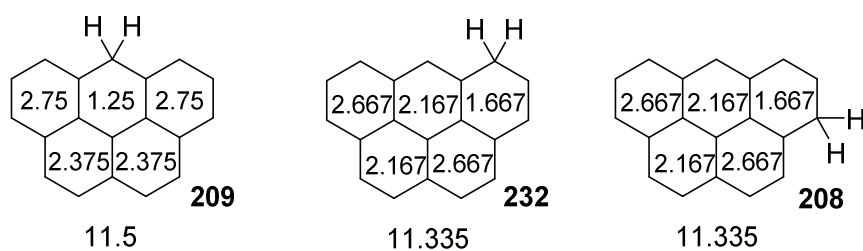


Figure 48: Isomers of benzo[*cd*]pyrene.<sup>11, 322-324</sup>

Pauling RBOs were also calculated on the three isomers which contained two Clar sextets, where the 6*H* position showed slightly more aromatic character than the other two isomers (Figure 49).<sup>80, 84, 85</sup>



**Figure 49: Pauling bond orders of the 6*H*-isomer 209, 5*H*-isomer 232 and 3*H*-isomer 208 of benzo[*cd*]pyrene.**

These results ultimately demonstrate that AFM/STM is a powerful tool, not just in molecule manipulation but also for the characterisation of compounds.

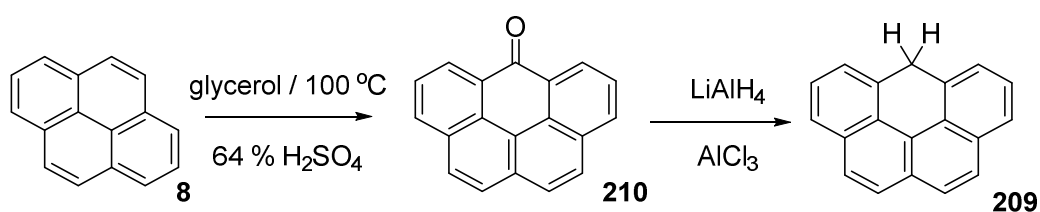
## 2.4 Summary

A new synthesis of 6*H*-benzo[*cd*]pyrene has been described. STM/AFM has been utilised to abstract a hydrogen from 6*H*-benzo[*cd*]pyrene to form a clear image of the olympicene molecule. In addition, better understanding of the reaction has accounted for the other products formed within the cyclisation step in PPA. The isolation of unstable compounds such as 6*H*-benzo[*cd*]pyren-ol has further proved theories which were postulated previously in literature. The disproportionation of products as well as the discovery of the isomerisation of 5*H*-oxo-benzo[*cd*]pyrene using 6*H*-benzo[*cd*]pyrene as a hydrogen transfer catalyst has been discussed. AFM has also been used to identify products within the mixture of the cyclisation step where the unstable 5*H*-benzo[*cd*]pyrene compound has been imaged for the first time along with other more stable compounds.

### 3 Chapter 3: *Peri*-condensation reactions

#### 3.1 Introduction

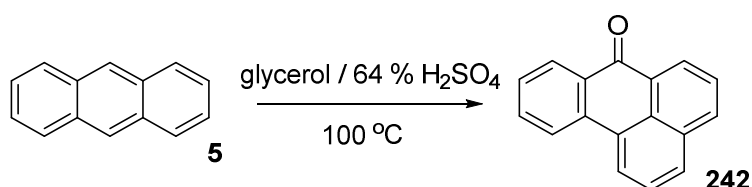
There exists a short two-step synthesis of 6*H*-benzo[*cd*]pyrene **209** from pyrene **8**. The first step was first published by Scholl and Meyer in 1935, whilst the second was published by Vollman *et al.* in 1937 (Scheme 46).<sup>297, 298</sup>



Scheme 46: An alternative synthesis of 6*H*-benzo[*cd*]pyrene **209**.<sup>297, 298</sup>

While this reaction seems simple, the yield for the intermediate 6-oxo-6*H*-benzo[*cd*]pyrene **210** was only 40 %, which poses two questions: i) Firstly, why is the yield low for such a reaction? ii) Secondly, is the conversion low or are there any other products formed which are previously unreported?

In 1904 BASF used this type of reaction with anthracene **5** as the starting material instead of pyrene, again it yielded the addition of a single ring to produce 7*H*-benz[*de*]anthracen-7-one **242** (Scheme 47) as the only reported product.<sup>325, 326</sup>



Scheme 47: The synthesis of benzanthrone **242**, with glycerol and sulfuric acid which was used as a common red dye.<sup>325, 326</sup>

BASF patented benzantrone **242** and its derivatives as it was used as a common red dye during the 1900s. Glycerol was used as a cheap reagent and thus these reactions were carried out on a large scale, although they did not publish any yields.<sup>325, 326</sup>

This type of addition was interesting as it not only involved the addition of a ring onto a stable compound, but also because of the simplicity of the reagents. For these reasons we decided to investigate this style of reaction to gain further insight into the reactivities of PAHs.

### 3.2 Synthesis of 6H-benzo[cd]pyrene using glycerol

An updated version of Scholl and Meyers' reaction published by Morgenthaler and R uchardt was initially employed. The main difference was that 80 % H<sub>2</sub>SO<sub>4</sub> was used instead of 64 %.<sup>301</sup> The reaction uses simple and cheap reagents to produce compounds which may be beneficial to the organo-electronic field and graphene, by growing structures with the addition of aromatic rings. Glycerol is a commercially available reagent, a by-product of biodiesel production and can be found in numerous sectors from the food to the cosmetics industries. Glycerol can be converted into another in-demand product glycidol, by dehydration.<sup>327-329</sup> Glycidol is also used in many applications in the pharmaceutical industry and as a surface coating. Due to the epoxide, it is more reactive than glycerol. Morgenthaler *et al.* stated that the workup was time consuming ('filter for three days'), the conversion was low (approximately 30 % yield) and after four hours some starting material was recovered.<sup>301</sup>

Therefore, this work started with the optimisation of reaction conditions; firstly, glycerol was replaced with the more reactive glycidol, the temperature was reduced to 80 °C and left to react overnight. The workup was simplified to minutes by

neutralising the reaction mixture with 5 M NaOH to pH 7. Finally, the number of equivalents of glycerol and sulfuric acid were changed from 4.4 to 8.0 equiv. and to 33 to 10 equiv. respectively.

The reaction was repeated with the changes made, but the conversion was still low; however, a large amount of black solid was isolated from the reaction which could be a possible reason for the low yield. In addition, NMR analysis of the product showed not only 6-oxo-6*H*-benzo[*cd*]pyrene **210** but a small amount of 6*H*-benzo[*cd*]pyrene **209** was also present.

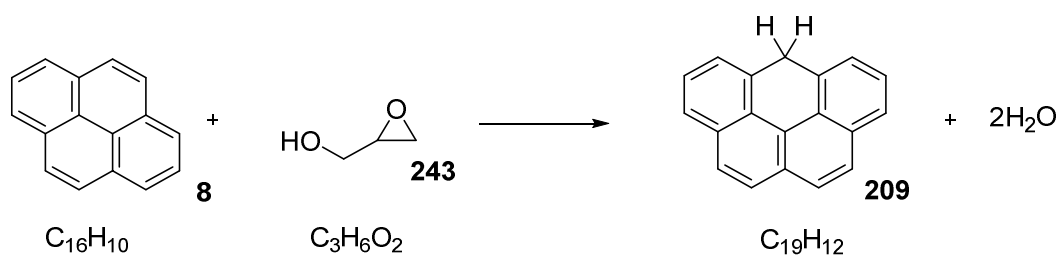
These results raised a few questions, such as:

1. Is there an intermediate formed before 6-oxo-6*H*-benzo[*cd*]pyrene **210** is produced?
2. What is the mechanism of the reaction?
3. What is the black solid which is formed and is this what is causing the low yield?

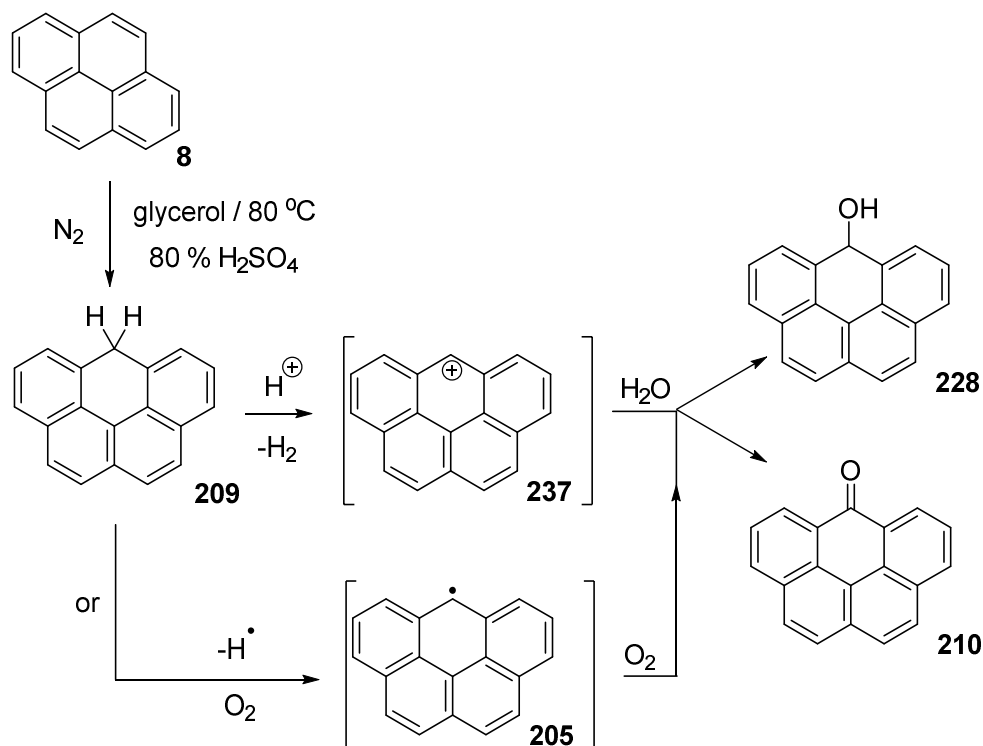
To understand the first question, the reaction with pyrene was completed under an inert atmosphere, where pyrene was dissolved in a minimum amount of chloroform first; as a cautionary step as the slow addition of reagents would generally be quite violent. This mixture and glycidol were subsequently added drop-wise to a stirring solution of 80 % H<sub>2</sub>SO<sub>4</sub>, and left to react at 80 °C overnight.

The NMR spectrum of the crude reaction product showed that the majority of the product formed was 6*H*-benzo[*cd*]pyrene **209** and 6-oxo-6*H*-benzo[*cd*]pyrene **210** (almost equal amounts of each), with small amounts of alcohol **228**. This result suggests that there is an intermediate before ketone **210** is formed. From this evidence, one can deduce that after the formation of **209** a hydrogen can be lost to

form either a radical **205** which can then be oxidised, or a cation intermediate **237**, to form the alcohol **228** and/or ketone **210** (Scheme 49). Trace amounts of alcohol **228** were recovered due to its instability, as it can disproportionate into 6*H*-benzo[*cd*]pyrene **209** and ketone **210** which is previously shown in the results of Chapter 2. Furthermore, the reaction to form the ketone is an oxidation, whereas the formation of the dihydride is not (Scheme 48).



**Scheme 48:** Formation of the dihydride **209** using glycidol **243** with a balanced equation.



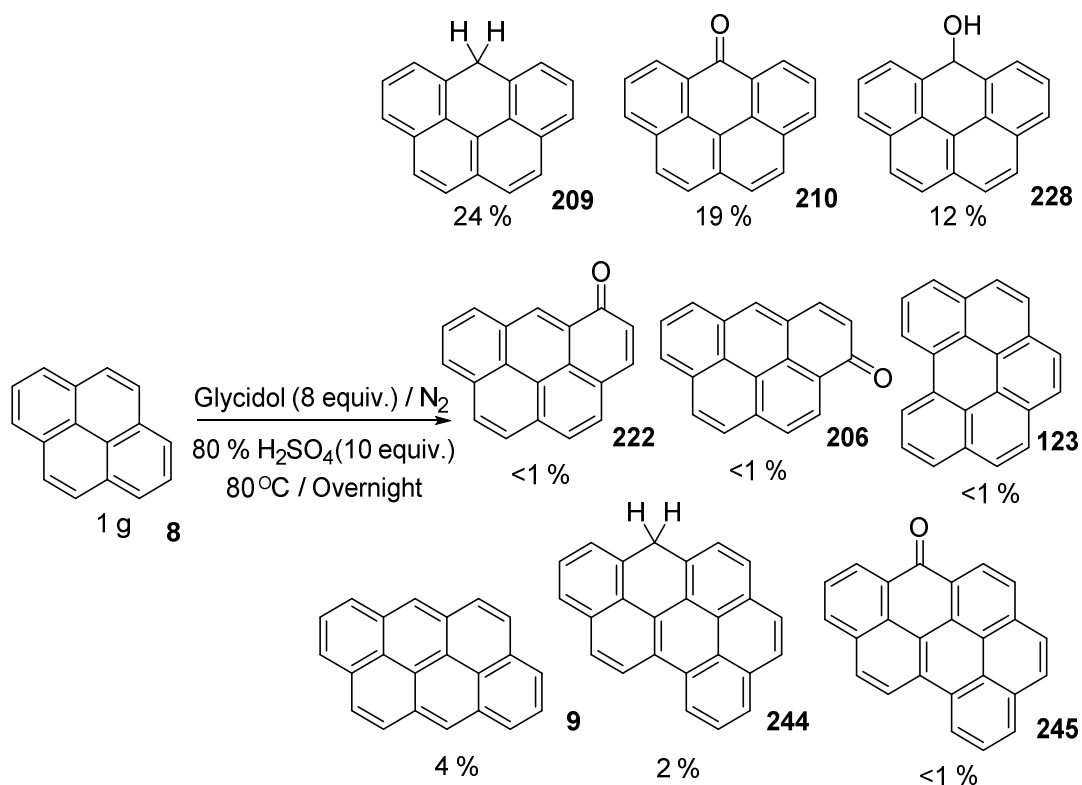
**Scheme 49:** A possible route to explain why **209** is a major product along with ketone **210** in this reaction.

These results, especially the notion that 6*H*-benzo[*cd*]pyrene is produced before 6-oxo-6*H*-benzo[*cd*]pyrene, have not been mentioned before in the published literature. The most recent literature by Morgenthaler and Rüchardt in 1999, also did not state that multiple products were formed; however, this would probably be due to the changed experimental parameters.<sup>301</sup> Notably, after their three day work up, **6** would have oxidised into **5**.<sup>297-299, 301, 302</sup>

The modified work-up neutralised the highly acidic solution with base (NaOH) and this thick viscous solution was filtered through a Büchner funnel. Large amounts of a black-tar like solid was separated from the crude mixture which was easily dissolved in halogenated solvents.

Furthermore, undertaking a large scale reaction under an inert atmosphere produced small amounts of different products, as observed from the <sup>1</sup>H NMR spectrum of the crude reaction product. After laborious purification using silica column chromatography, a number of different products were isolated (Scheme 50).

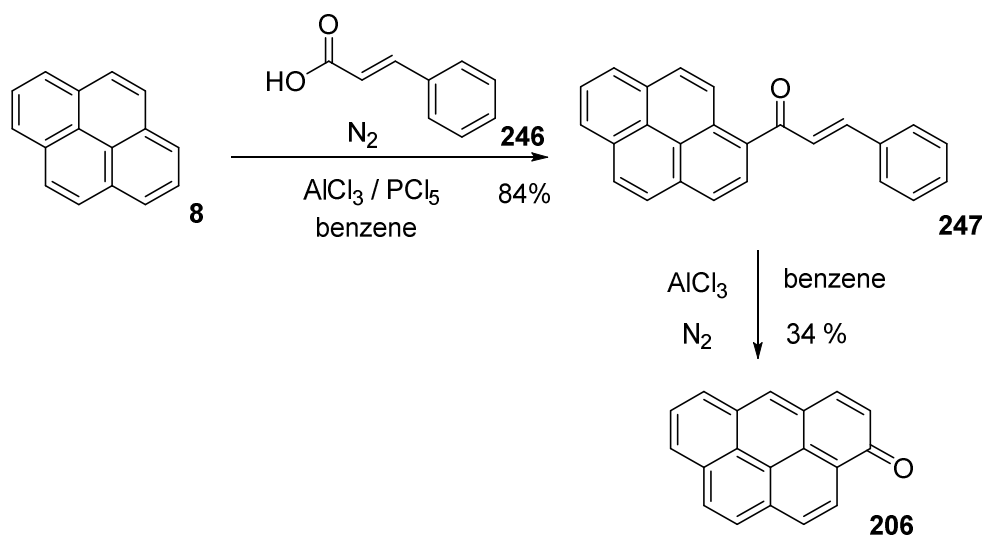




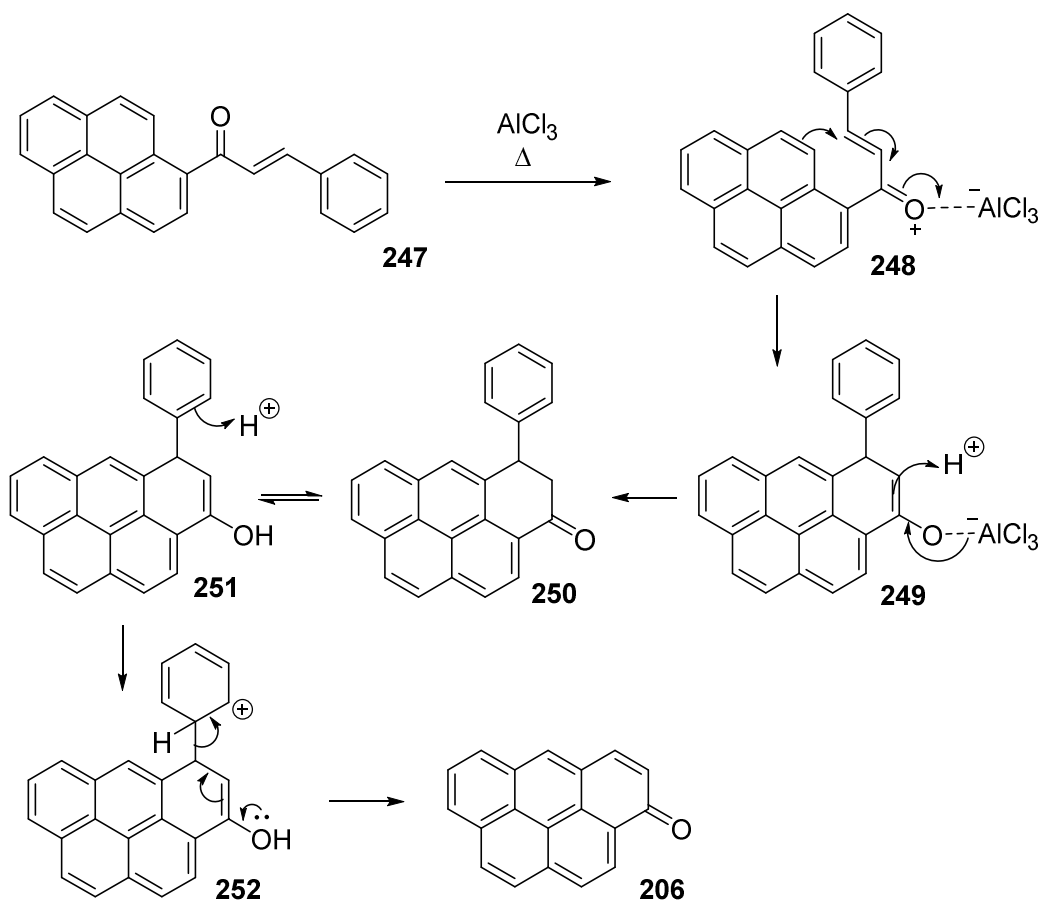
**Scheme 50:** Various compounds isolated from the reaction of pyrene with glycidol in 80 % H<sub>2</sub>SO<sub>4</sub>, approximately 2.0 g of black solid was also obtained. Percentages worked out from the <sup>1</sup>H NMR spectrum and are representative from each pyrene molecule used from the starting material.

Compounds **209**, **210**, **222** and **228** have all been previously characterised before (Chapter 2), compounds **123** and **9** were fully characterised, with the data matching that of known literature of Shen *et al.* and Cremonesi *et al.* respectively.<sup>152, 330</sup>

Trace amounts of impure compound **206** were isolated and fully characterised by NMR spectroscopy. To confirm the assignment further, the synthesis of **206** by Didenko *et al.* which was published without NMR data was undertaken.<sup>331</sup> Pyrene and aluminium chloride was added to a mixture of phosphorus pentachloride and cinnamic acid **246**, to produce cinnamoylpyrene **247**. After purification, ketone **247** was treated with aluminium chloride to produce 3-oxo-3*H*-benzo[*cd*]pyrene **206** (Scheme 51). Full analysis was performed and the data was consistent with the data gained from the product of the glycidol reaction.



**Scheme 51:** The independent synthesis of 3-oxo-3H-benzo[cd]pyrene **206** by the method of Didenko *et al.*<sup>331</sup>



**Scheme 52:** Mechanism for the synthesis of **206** using the method of Didenko *et al.*<sup>331</sup>

Compounds **244** and **245** were larger PAH species and were therefore more difficult to characterise. However, the  $^1\text{H}$  NMR spectrum showed that when compound **244**

was left to oxidise in air it would turn into **245**, thus, these were related redox compounds. Using 2D NMR experiments the structures of **244** and **245** were determined (Figure 50).

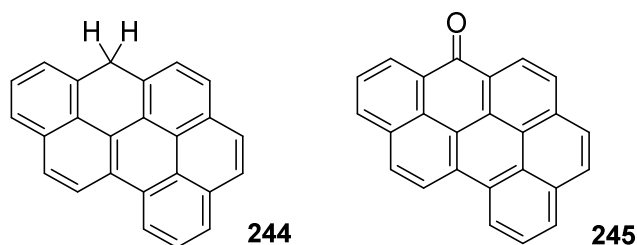


**Figure 50: The characterisation data pointed to compounds 244 and 245 having seven-fused ring structures.**

These new compounds were sent to IBM Zürich for NC-AFM analysis to confirm their structures. The group encountered difficulties during sample preparation for AFM/STM analysis. Nevertheless, a relatively large amount of this material was produced within the pyrene condensation reaction (Figure 51). This compound also correlates to the structural data confirmed by NMR of compounds **244** and **245**.

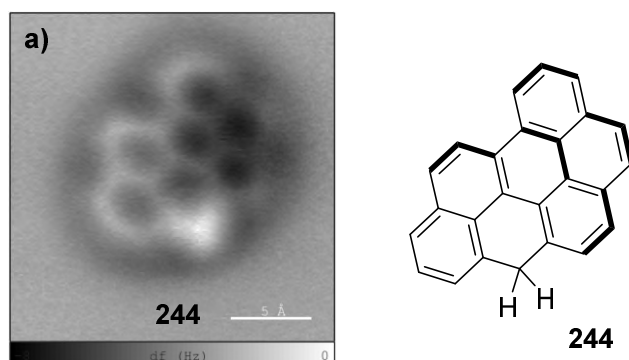


**Figure 51: a) AFM image of 244, which was prominent in the mixture.<sup>321</sup>**

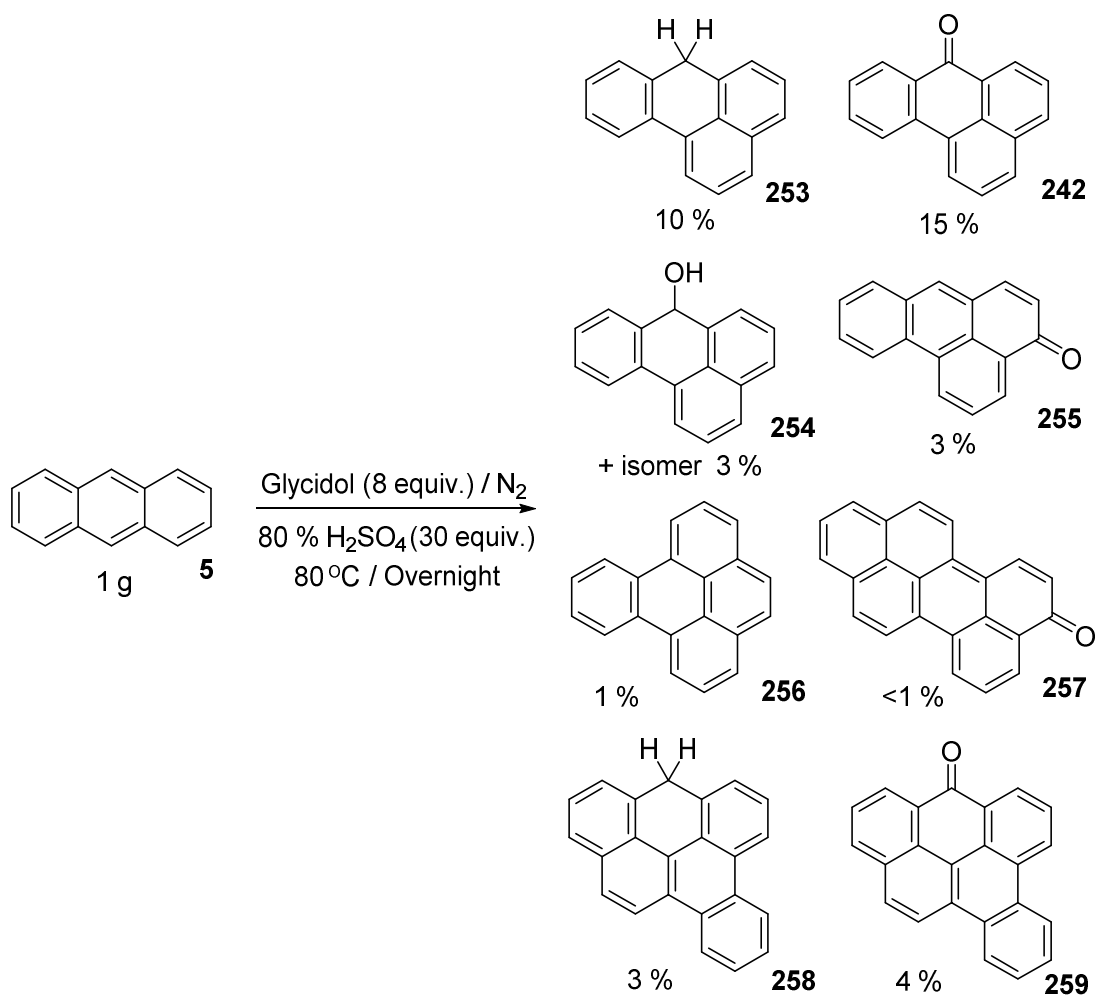
Along with the isolated compounds, a considerable amount of black insoluble powder was also isolated after filtration. This solid was collected *via* a Büchner funnel during workup but for completeness it can be fully collected by centrifuging

the mixture and washing it with water. These washings were collected but were kept separately at the time as this was an unknown substance.

### 3.3 Anthracene

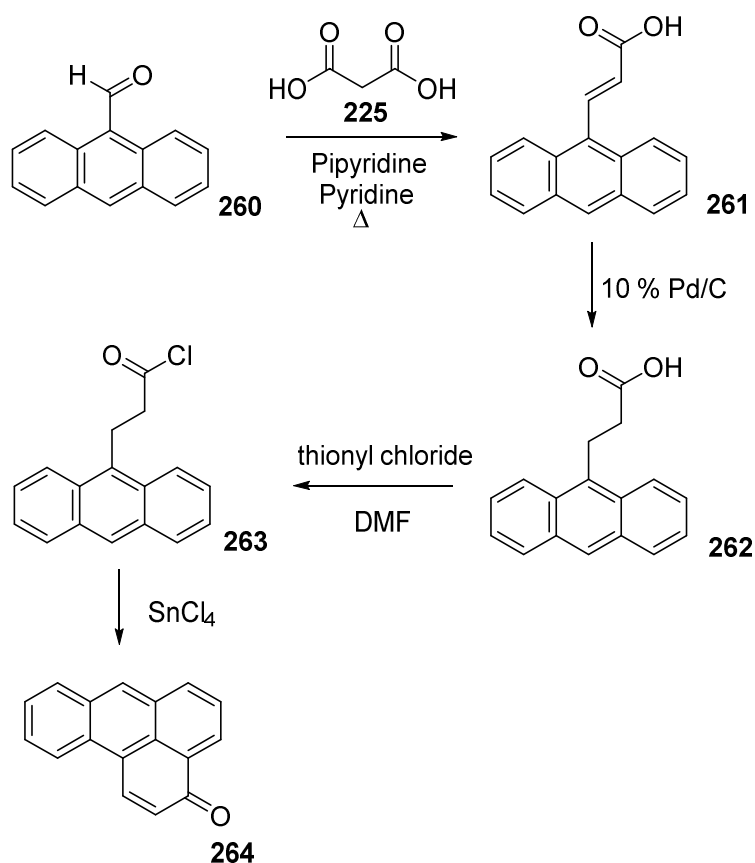
Due to the findings from the pyrene-glycidol reactions in the previous section, anthracene **5** was used as another PAH starting material. The modified procedure developed in the previous section was used. The only notable change from the pyrene reaction is that 30 equivalents of sulfuric acid were used due to the solubility of anthracene.

After the usual workup, the  $^1\text{H}$  NMR spectrum of the crude reaction mixture seemed to show that the dihydride *7H*-benz[*de*]anthracene **253** was formed, in addition to the ketone *7H*-benz[*de*]anthracen-7-one **242** as a major product. Furthermore, there were also a number of minor peaks suggesting additional multiple minor products. These were isolated by column chromatography purification (Scheme 53).



**Scheme 53: Various compounds isolated from the reaction of anthracene with glycidol in 80 % H<sub>2</sub>SO<sub>4</sub>, approximately 1.5 g of black solid was also obtained. Percentages worked out from the <sup>1</sup>H NMR spectrum and are representative from each anthracene molecule used from the starting material.**

Compounds **242**, **253**, **256** and **257** were fully characterised and were consistent with the reported data.<sup>332-335</sup> NMR analysis suggested the structure of compound **255** but to alleviate any doubt an independent synthesis of an alternative isomer **264** was completed (Scheme 54).<sup>336</sup> The data of **264** did not match that of **255**, thus proving that **255** was made.



**Scheme 54: Synthesis of 3-oxo-3H-benz[de]anthrone 264, method taken from Cameron *et al.*<sup>336</sup>**

Column chromatography under an inert atmosphere of the anthracene crude mixture also resulted in the collection of an unknown unstable compound. NMR spectroscopy suggested that there were two compounds which eluted simultaneously, both showing a typical secondary alcohol CH-peak in the  $^{13}\text{C}$  NMR spectrum at 58 ppm. We believe these compounds to be benz[de]anthracen-ol **254** isomers which are highly unstable. The sample disproportionated and oxidised to 7H-benz[de]anthracen-7-one **242** along with a small amount of 7H-benz[de]anthracene **253**. This result suggests that these compounds underwent the same disproportionation reaction as 6H-benzo[cd]pyren-6-ol **228** (Chapter 2). Therefore, one could assume that one of the isomers could be that in the 7H-position **254** and the other isomer is unknown. Due to the instability of **254**, only NMR data

were obtained. The 7*H*-isomer of the alcohol **254** has been reported by Clar *et al.* but only a melting point was given.<sup>337</sup>

Compounds **258** and its oxidation product **259** were difficult to analyse by 2D NMR spectroscopy due to overlapping signals. The data suggested the possible structures of the compounds but these were sent to IBM Zürich to be analysed by NC-AFM for structure determination (Figure 52).

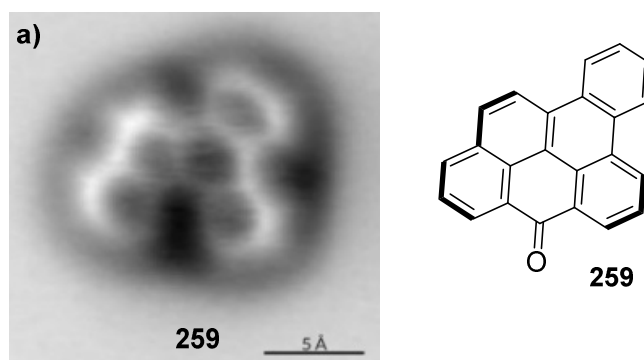
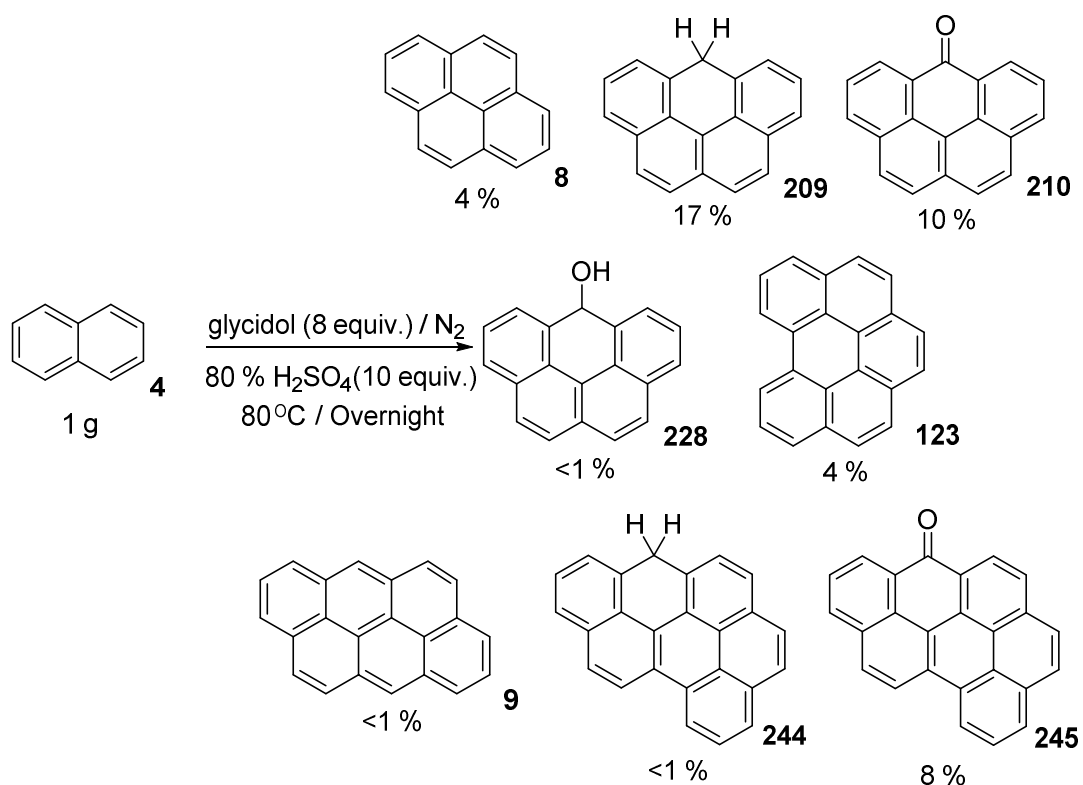


Figure 52: Compound **259** characterised by AFM (a).<sup>321</sup>

In addition to this, 1.5 g amount of black powdered solid was also collected in the same way as the pyrene reaction, as a side-product.

### 3.4 Naphthalene

Naphthalene **4** was also used as a starting material in the same reaction. Interestingly, the isolated products from this reaction were exactly the same as that of the pyrene **8** reaction (Scheme 55).



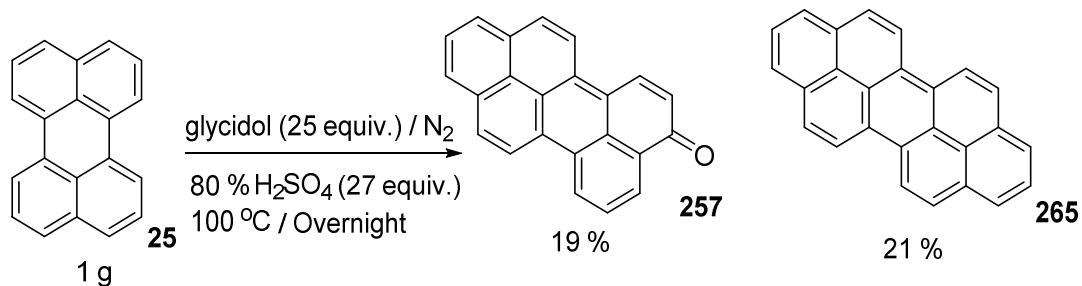
**Scheme 55:** Various compounds isolated from the reaction of naphthalene with glycidol in 80 % H<sub>2</sub>SO<sub>4</sub>, approximately 1.7 g of black solid was also obtained. Percentages worked out from the <sup>1</sup>H NMR spectrum and are representative from each naphthalene molecule used from the starting material.

All these compounds have been characterised from the pyrene condensation reaction where the data is consistent. Likewise, there was a large amount of black powdered solid side-product obtained (1.7 g).

### 3.5 Perylene

Perylene **25** was the largest arene used as a starting material. With the same reaction conditions employed (the only changes were that there were 25 and 27 equivalents of glycidol and sulfuric acid added), there were not as many compounds isolated (Scheme 56).





**Scheme 56:** Compounds isolated from the reaction of perylene with glycidol in 80 % H<sub>2</sub>SO<sub>4</sub>, approximately 3.1 g of black solid was also obtained. Percentages worked out from the <sup>1</sup>H NMR spectrum and are representative from each perylene molecule used from the starting material.

The results show the formation of **257**, which has been characterised before as it is present in the anthracene mixture.<sup>333</sup> Peropyrene **265** is formed when two rings are added on either side of perylene **25**.<sup>338</sup> Again, like the rest of the reactions a large amount of black solid (3.1 g) was also obtained during filtration.

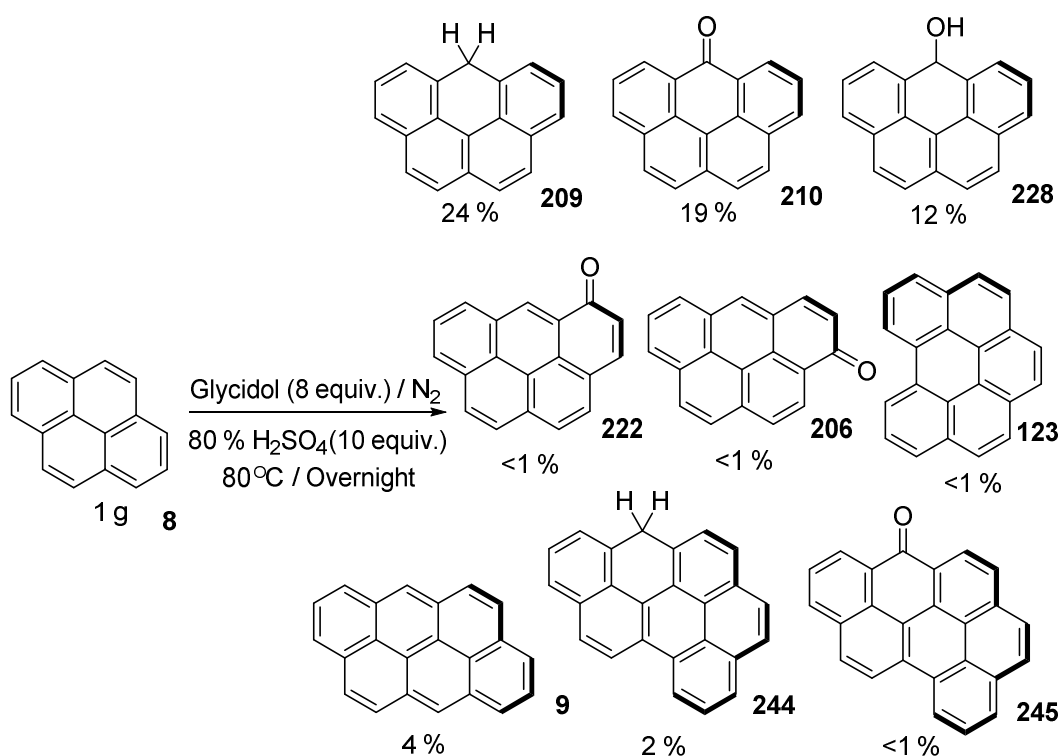
### 3.6 Multiple ring addition – ‘glycidol units’

Examining all four sets of results from the condensation reactions of pyrene, naphthalene, anthracene and perylene, a number of compounds with multiple rings were discovered. All of the additional rings produced are however six-membered rings. Appreciating that one ring can be added to pyrene to form 6*H*-benzo[*cd*]pyrene **209**, if another ring were to be added, compounds **9** and **123** can be produced. Furthermore, the compounds formed from naphthalene are the same as those from the pyrene reaction due to pyrene being formed in the naphthalene reaction.

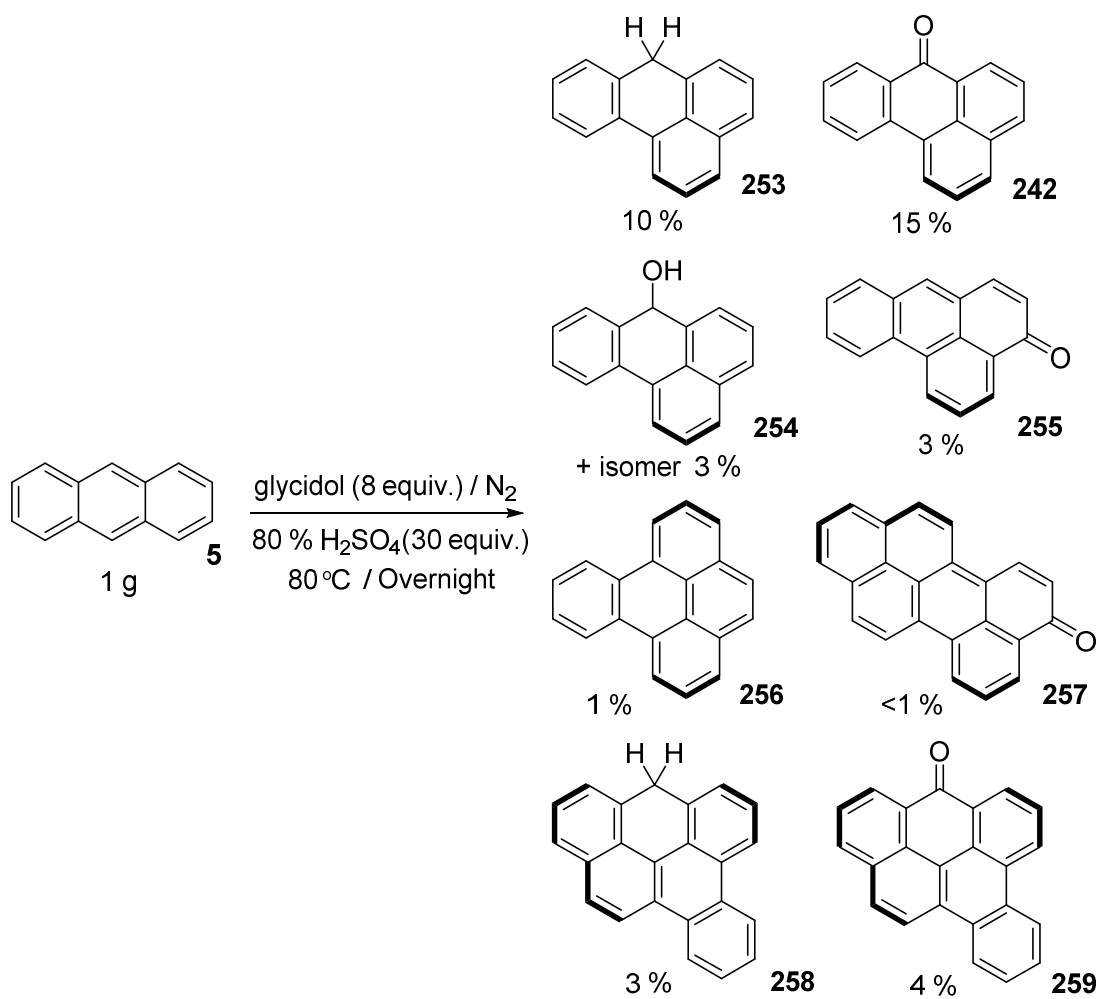
These products are all consistent with the addition of either a single or multiple three carbon unit(s) having added to the starting arene, which are shown in bold on the products in Scheme 57, 58, 59 & 60.

For the annulation to occur, two adjacent ‘*peri*’ positions must be available where the ring can add, and it can be seen that all of the arene starting materials possess this

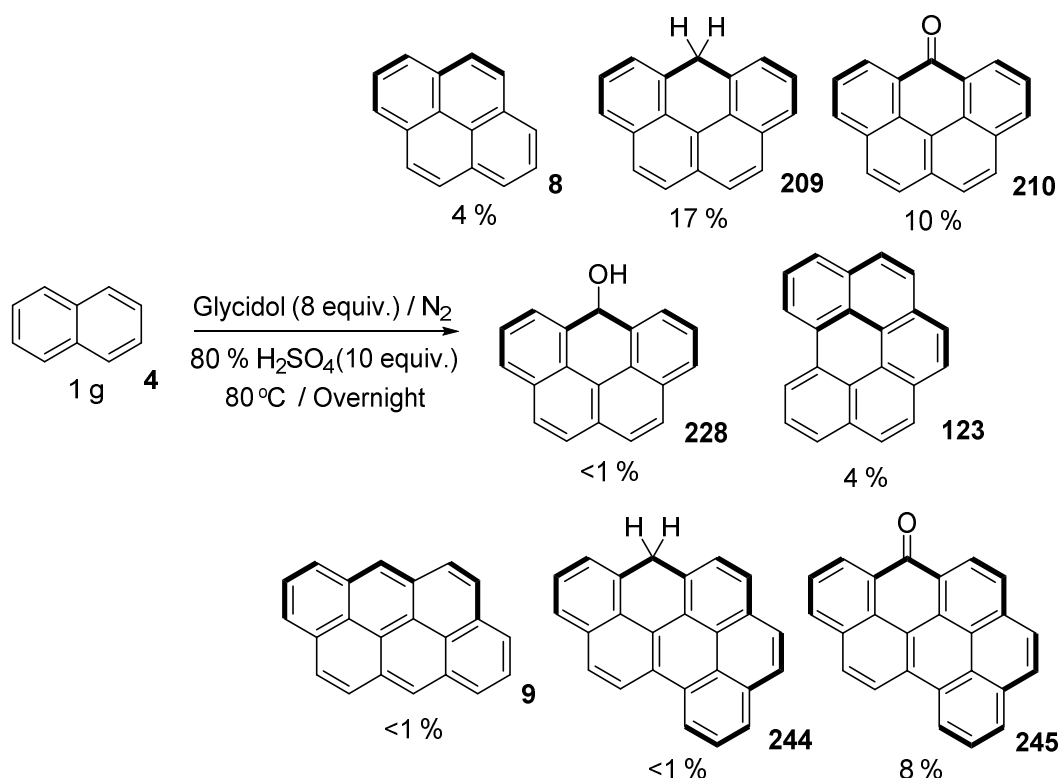
feature. Moreover, there are multiple ways of adding these units onto the ‘*peri*’ positions however, for simplicity, only one method of addition is shown.



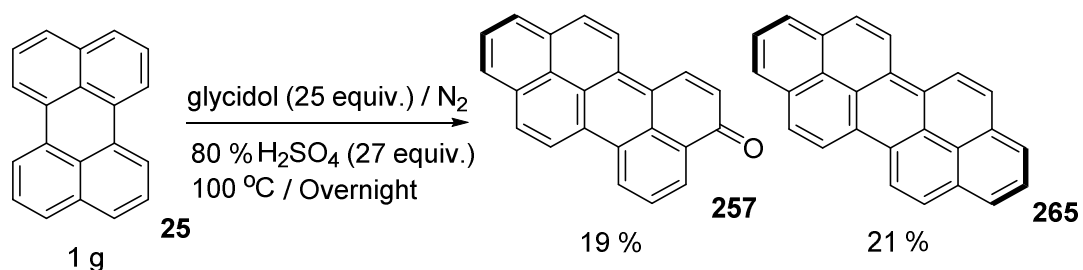
**Scheme 57:** The multiple addition at the ‘*peri*’ positions are shown in bold, only one method of addition is shown.



**Scheme 58:** The multiple addition at the 'peri' positions are shown in bold, only one method of addition is shown.

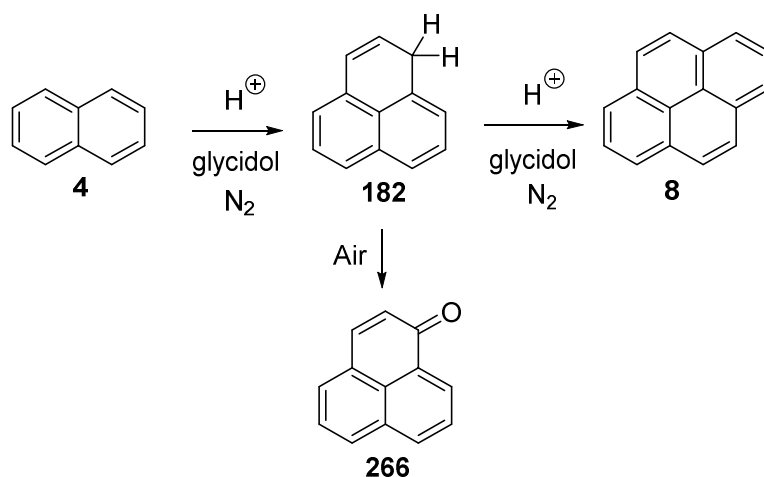


**Scheme 59:** The multiple addition at the 'peri' positions are shown in bold, only one method of addition is shown.



**Scheme 60:** The multiple addition at the 'peri' positions are shown in bold, only one method of addition is shown.

However, if the system does add one ring at a time onto the starting material, phenalene **182** should be observed in the naphthalene **4** condensation products. As it is not observed it probably signifies that phenalene is too reactive. Thus, the reaction was conducted in air rather than an inert atmosphere in the hope of oxidising the intermediate phenalene. This indeed worked, as the <sup>1</sup>H NMR spectrum of the crude reaction mixture showed that perinaphthanone **266** was formed, which is consistent with phenalene **182** being a reactive intermediate (Scheme 61).

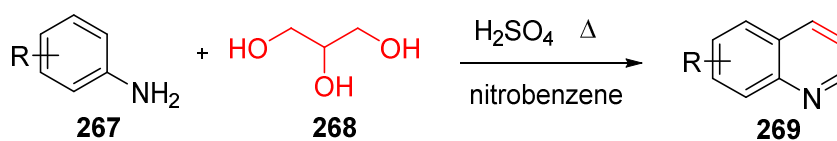


Scheme 61: The formation of the reactive phenalene 182 intermediate.

### 3.7 Possible mechanism of reaction

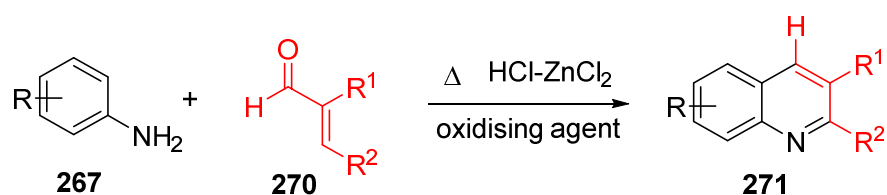
Both glycerol **268** and glycidol **243** can be used in these condensation reactions and with the assumption that a ‘three carbon unit’ (glycidol) adds each time across a pair of ‘peri’ positions on the arene, a reaction mechanism can be proposed.

In 1880 the Czech chemist Z. H. Skraup published a synthesis of quinoline **269**, involving heating glycerol **268** and aniline **267** in sulfuric acid with an oxidising agent such as nitrobenzene (Scheme 62).<sup>339-341</sup>



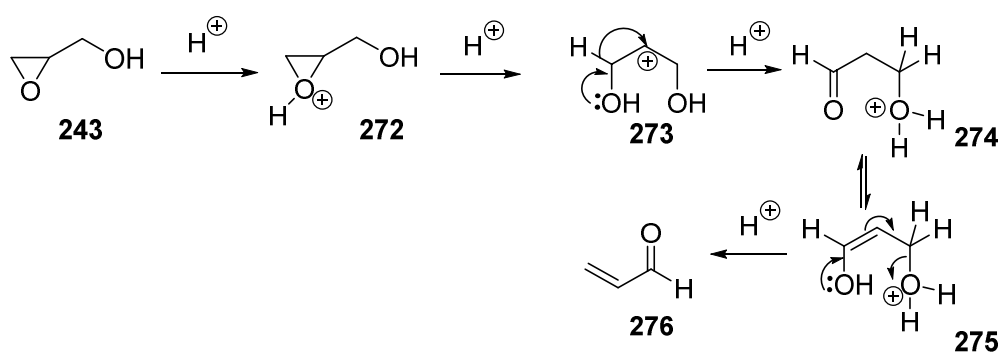
Scheme 62: Skraup's quinoline synthesis also uses glycerol as a three-unit addition.<sup>339, 340</sup>

Soon after this discovery O. Doebner and W. Miller carried out the synthesis of quinolines **271** using similar reaction conditions, but using  $\alpha,\beta$ -unsaturated aldehydes **270** as a substitute for glycerol (Scheme 63).<sup>342-348</sup>



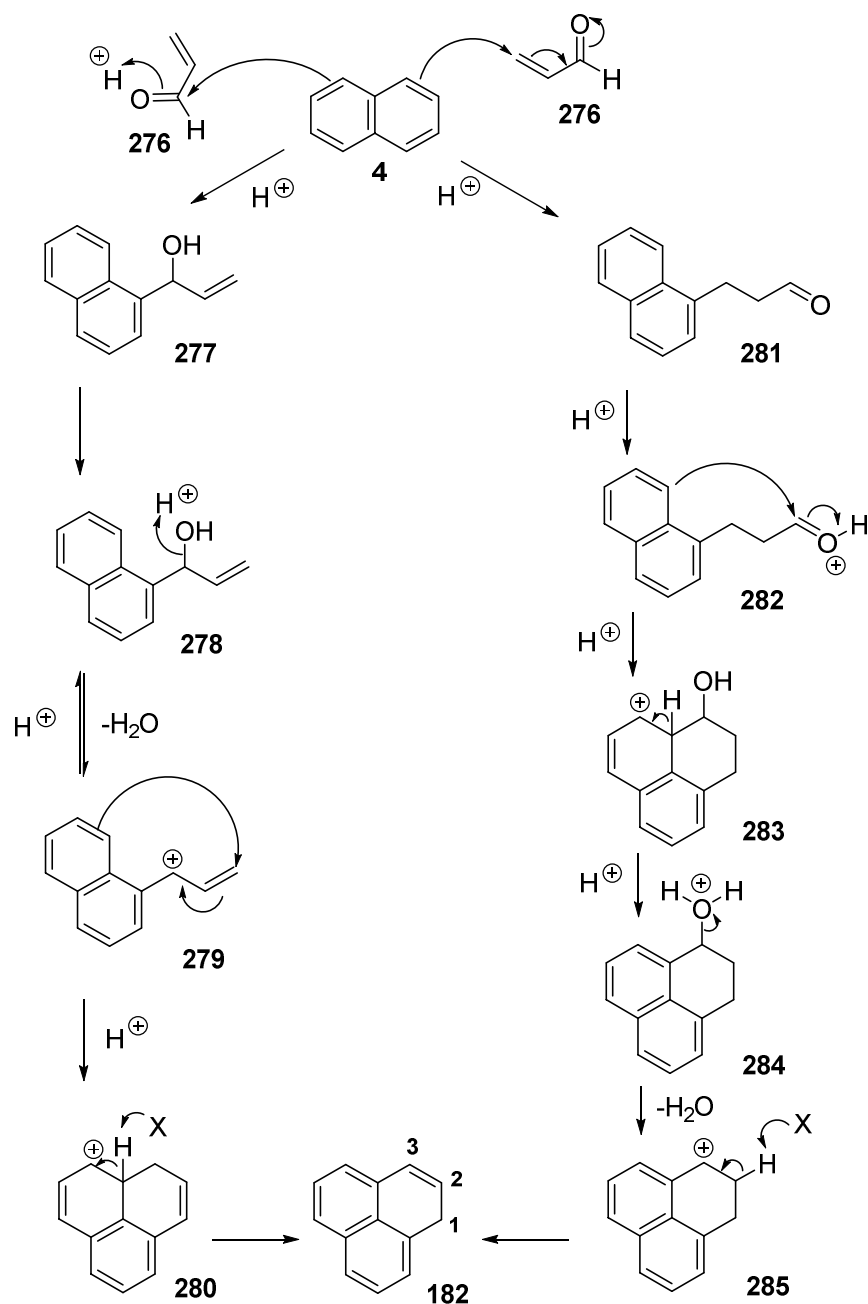
Scheme 63: Substituted quinolines produced by replacing the glycerol by Doebner and Miller.<sup>342, 343, 348</sup>

Acrolein **276** can be synthesised from glycerol (and therefore glycidol **243**) by acid catalysis (Scheme 64).<sup>348-354</sup> Condensation with aniline and oxidative cyclisation is known as the Skraup-Doebner-Von-Miller quinoline synthesis.<sup>339-348</sup>



Scheme 64: The acid catalysed formation of acrolein **276** from glycidol **243**.<sup>348-354</sup>

We believe that the *peri*-condensation reactions proceed *via* the  $\alpha,\beta$ -unsaturated aldehyde acrolein **276** like the Skraup-Doebner-Von-Miller synthesis. For example, naphthalene **4** is most reactive at the one position and this is where the first *peri* addition occurs. It can add one of two ways in a polar mechanism (Scheme 65).<sup>355</sup>



**Scheme 65:** The possible acid catalysed mechanisms, annulation of naphthalene **4** with acrolein **276**.

The formation of a ring onto naphthalene produces a non-Kekulé structure, phenalene **182**. The addition of the next ring to reform a Kekulé PAH can either proceed by a polar or radical mechanism. If it is a polar mechanism, the most nucleophilic site of phenalene **182** would seem to be the two position. Density functional theory (DFT) calculations by Dr David Fox show that there are multiple

sites which an electrophilic attack can occur from, not just the two position (Figure 53). However, the DFT calculation for the phenalenyl radical **7** show that the most prominent sites of attack are the *peri*-positions (Figure 53). It is known that the methylene C-H bond of phenalene is weak.<sup>289, 302, 319, 356</sup> Phenalene **182** and 6*H*-benzo[*cd*]pyrene **209** have a bond dissociation energy (BDE) of 58.1 and 66.8 kcal/mol respectively, compared to the BDE of the methyl C-H toluene 88.5 kcal/mol and diphenylmethane 81.4 kcal/mol.<sup>319, 356, 357</sup> These bonds can easily dissociate and form a radical, which in turn would form a six membered ring in the *peri* positions by a radical addition mechanism. A possible mechanism is shown in Scheme 66. With radical character only present at *peri*-positions in the reactive intermediates, only six-membered ring products are possible. Radical reactions to form six membered rings in aromatic and C=O species are well known and therefore support this mechanistic proposal.<sup>358-362</sup>

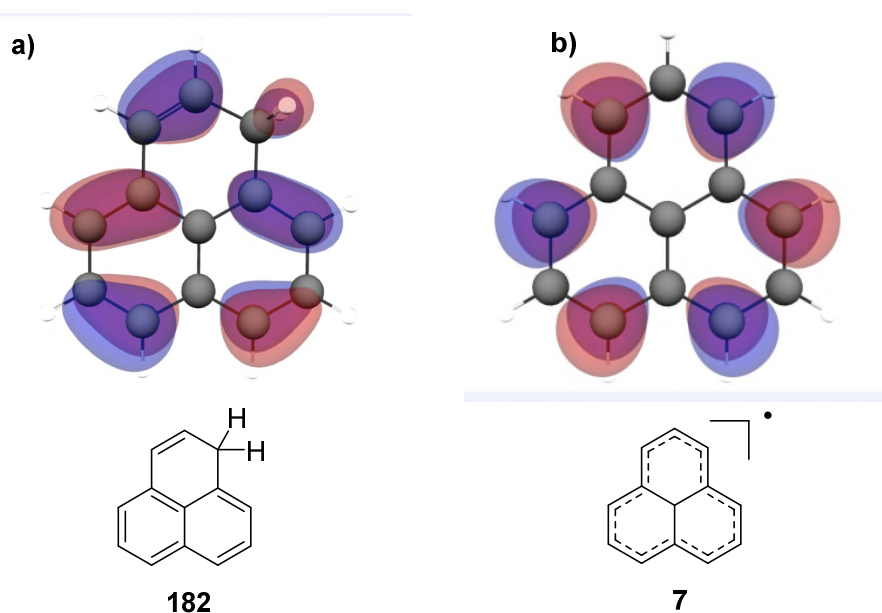


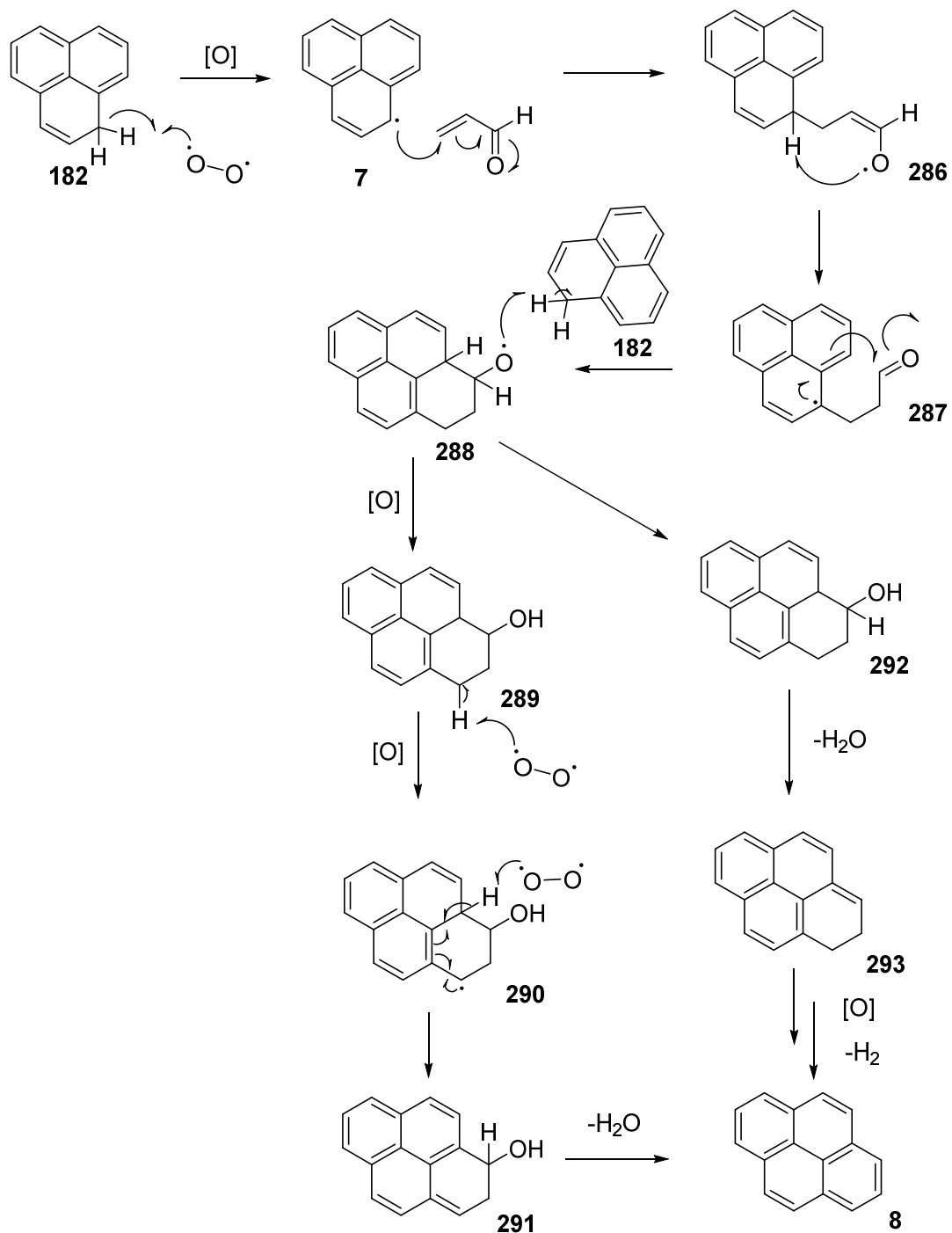
**Figure 53: DFT calculations: a) HOMO of phenalene 182, b) SOMO of the phenalenyl radical 7.**

An alternative polar reaction involving the nucleophilic addition of the most reactive carbon onto acrolein would produce a two-substituted phenalene. This would then



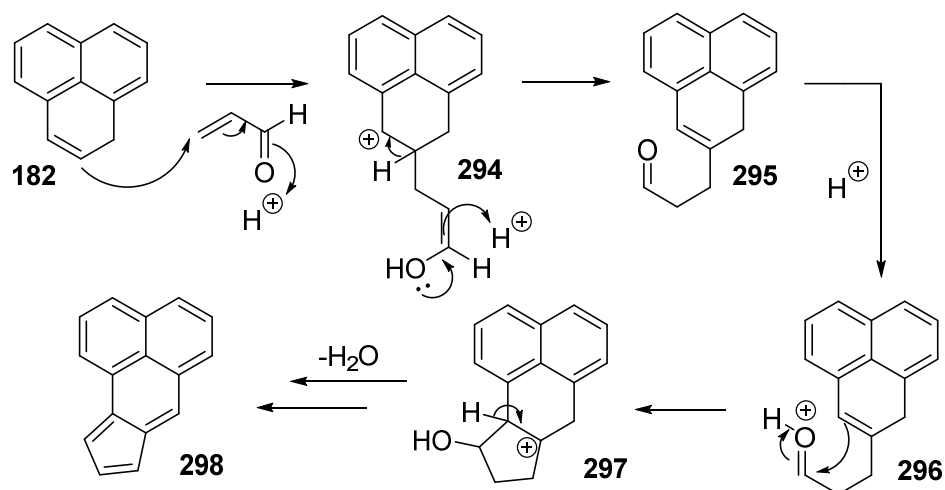
only react further to produce five-membered ring containing compounds which are not observed in the product mixture (Scheme 67).

**Radical**



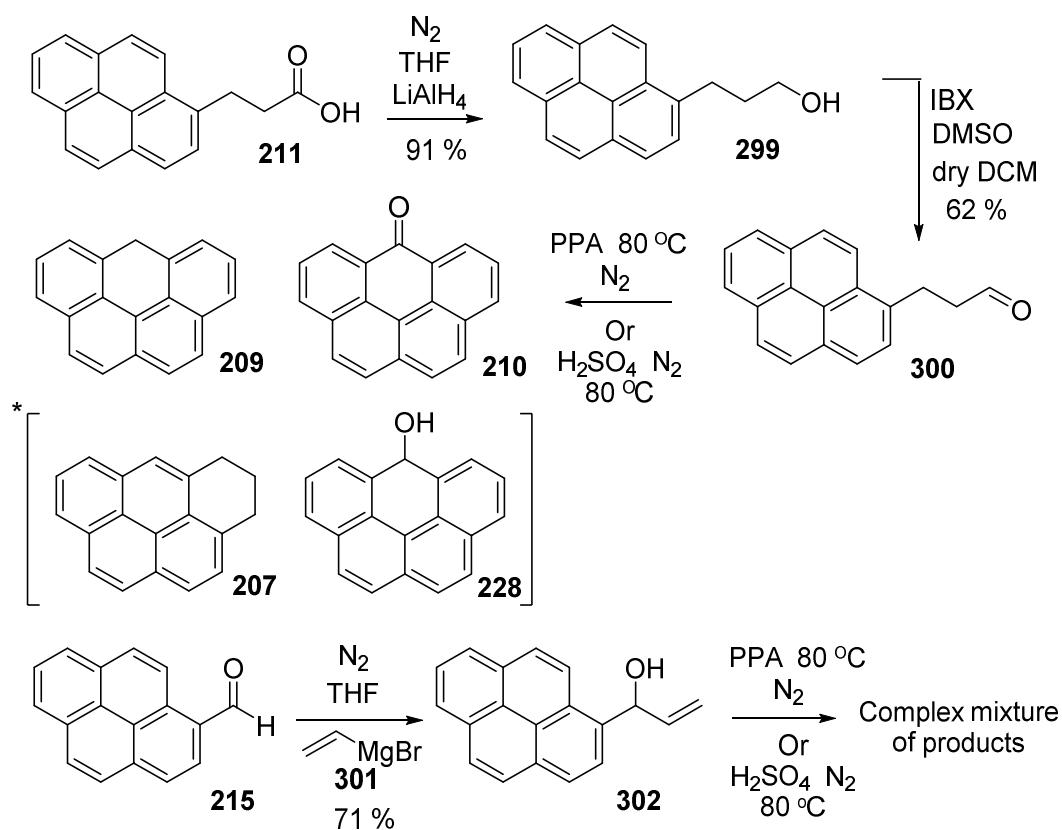
**Scheme 66: Possible acid catalysed radical reaction of the formation of a Kekulé structure pyrene 8.**

**Polar**



**Scheme 67: If the reaction from a non-Kekulé species proceeded from a polar reaction only a five-membered ring would be made.**

To confirm the orientation of the initial reaction of acrolein in our mechanism (Scheme 68), the two possible 1,2- and 1,4 addition intermediates were independently synthesised and reacted. Both 3-(1-pyrenyl)propionaldehyde **300** and 1-(pyrene-1-yl)prop-2-en-1-ol **302** were reacted in PPA and (80 %) sulfuric acid under an inert atmosphere separately, to see if they produce similar cyclic products (Scheme 68).<sup>324, 363-365</sup>



**Scheme 68: Possible intermediates 300 & 302 in the mechanism of the formation of 6H-benzo[cd]pyrene 209. \*Observable in the PPA reaction.**

3-(1-Pyrenyl)propionaldehyde **300** produced the same cyclic products (**209** and **210** were major products) under these conditions, but 1-(pyrene-1-yl)prop-2-en-1-ol **302** did not. This result suggests the mechanism is more likely to go *via* conjugate addition of the arene to acrolein.

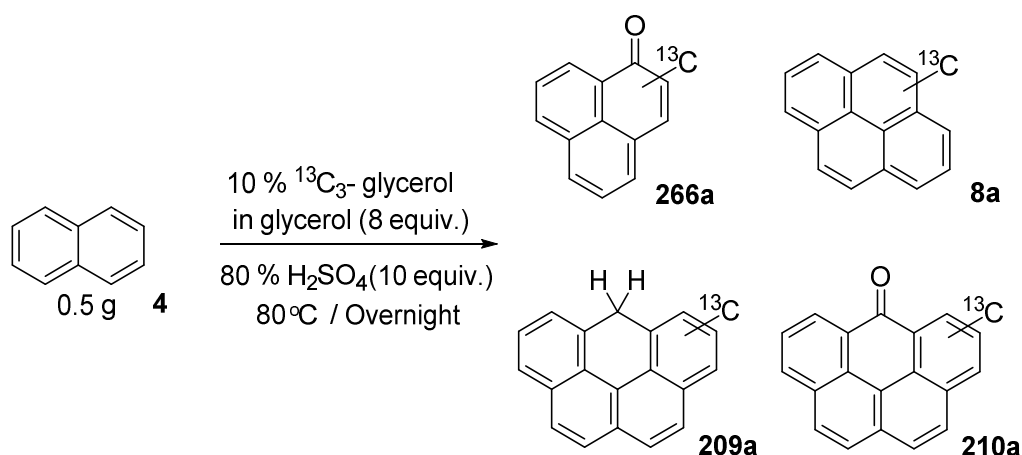
Furthermore, in the early 1900s Bally and Scholl studied the addition of ring(s) to anthracene using glycerol and sulfuric acid, where they believed that a Skraup type reaction took place and that acrolein was an intermediate.<sup>366</sup> They assumed that the cyclisation proceeded from an alkene intermediate but in 1939 Calcott *et al.* and Weinmayr *et al.* proposed an aldehyde intermediate.<sup>367, 368</sup> These works from 1939 also studied the addition of ring(s) on anthracene, phenanthrene and other substituted polyarenes but by using HF and acrolein after studying Scholl and Meyer's work

with glycerol and sulfuric acid.<sup>297, 367, 368</sup> Weinmayr *et al.* also produced perylene from phenanthrene, which is an addition of two rings from acrolein. Calcott *et al.* used the term ‘*peri* condensation’ for these types of reactions as they proceeded to give the products expected as with the conditions of Scholl and Meyer.<sup>297, 367, 368</sup> In addition, it was mentioned that starting materials contained at least two benzene rings (possible reference to *peri*-positions) and that ‘higher or non-fusible’ products which could not be determined were probably formed. This again supports our theory (see Section 3.2) as well as others who have suggested ‘*peri*-condensation’ reactions with PAHs.<sup>366-372</sup>

*Peri* annulation continually produces an arene which can react further. However, further DFT calculations and stability judgements need to be completed, as it is difficult to predict why/if one *peri* site is more reactive than another.<sup>373, 374</sup>

### 3.8 Carbon-13 labelling experiments.

To further investigate the mechanism of poly-annulation and to confirm that the ‘ring’ addition was coming from an intact three carbon unit (glycidol), <sup>13</sup>C-labelling experiments were undertaken. Naphthalene **4** was used as the starting arene as it would provide reaction products which are easier to analyse and collect with multiple ring additions and also includes the largest number of ring additions.



**Scheme 69:** Reaction of naphthalene **4** with glycerol doped with  $^{13}\text{C}_3$ -labelled glycerol (10 %), to produce labelled products **8a**, **209a**, **210a**, **266a**.

The glycerol was doped with 10 %  $^{13}\text{C}_3$ -labelled glycerol, and after undertaking the reaction in air, product purification was completed by column chromatography where  $^{13}\text{C}$ -labelled perinaphthanone **266a**, pyrene **8a**, 6H-benzo[cd]pyrene **209a** and 6-oxo-6H-benzo[cd]pyrene **210a** were isolated.

Initial analysis showed that perinaphthanone **266a** and 6-oxo-6H-benzo[cd]pyrene **210a** could be analysed by NMR spectroscopy, however due to magnetic inequivalence both pyrene **8a** and 6H-benzo[cd]pyrene **209a** could not.

### 3.8.1 Carbon labelled Perinaphthanone (**266a**)

There are three isomers of perinaphthanone possible for the single *peri*-condensation of a  $\text{C}_3$ -unit onto naphthalene (Figure 54).

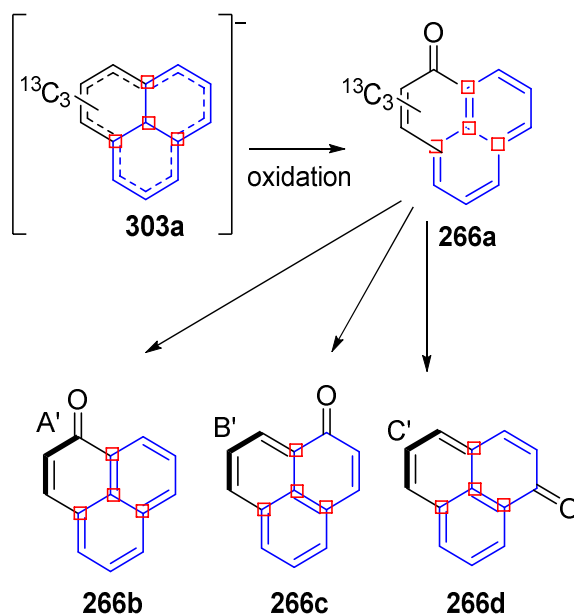


**Figure 54:** The three possible additions of a ring onto naphthalene 266b-d, where the squares show the carbons which will never be labelled.

The carbon assignments were fully assigned for perinaphthanone. Then each peak in the  $^{13}\text{C}$  NMR spectrum was analysed to see if the carbon is labelled (Figure 55).

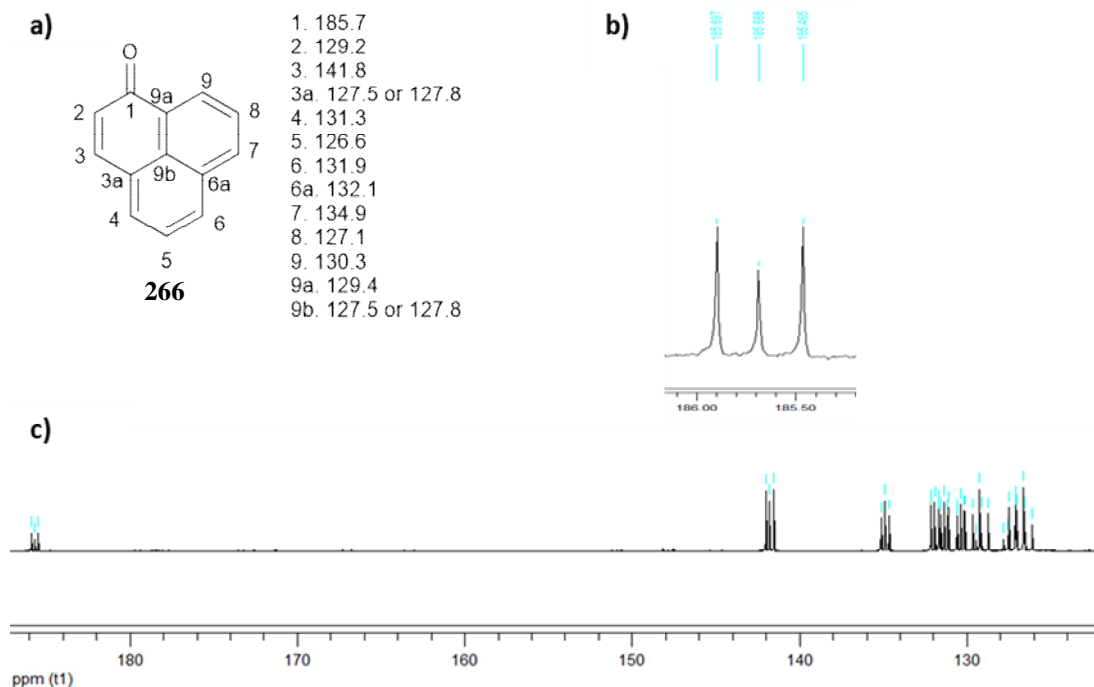


**Figure 55:** a) Assigned perinaphthanone 266 compound (ppm), b) Expanded section of carbonyl peak, c)  $^{13}\text{C}$  NMR of partially labelled perinaphthanone 266a.

The carbonyl carbon region at 185.7 ppm has three peaks (Figure 55b). The middle peak is due to the non-adjacently  $^{13}\text{C}$ -labelled product while the peaks either side are a 54.5 Hz doublet, which is within the typical values for C-C coupling.<sup>375-377</sup> Importantly, as only one doublet is observed, only one adjacent carbon is  $^{13}\text{C}$  enriched, and one intact  $\text{C}_3$  unit has added and has not dissociated during the reaction. The proposed addition mechanism suggests that the carbonyl  $^{13}\text{C}$ -labelled carbon has the possibility of one neighbouring carbon which can be labelled (assuming no scrambling of  $^{13}\text{C}_3$  unit), as the quaternary carbons on the other side would not be labelled (Figure 54). Indeed, a single doublet is observed which represents the  $^{13}\text{C}$ -labelled carbons overlapping along with the singlet from the non-adjacent labelled carbons. The centre of the doublet is not exactly at the same chemical shift as the singlet due to a small isotopic shift.

The relative intensity of the singlet and doublet peaks in the NMR spectrum can be explained. The sample was doped with 10 %  $^{13}\text{C}_3$  labelled glycerol. Therefore, there is a possibility of 10 %  $^{13}\text{C}$ -labelled and 90 % of non-labelled carbon in the product. Furthermore, there are three different arrangements (**226b**, **266c** & **266d**) which the  $^{13}\text{C}$ -labelled compounds can acquire (Figure 56) each with an approximate proportion of 3.3 %.

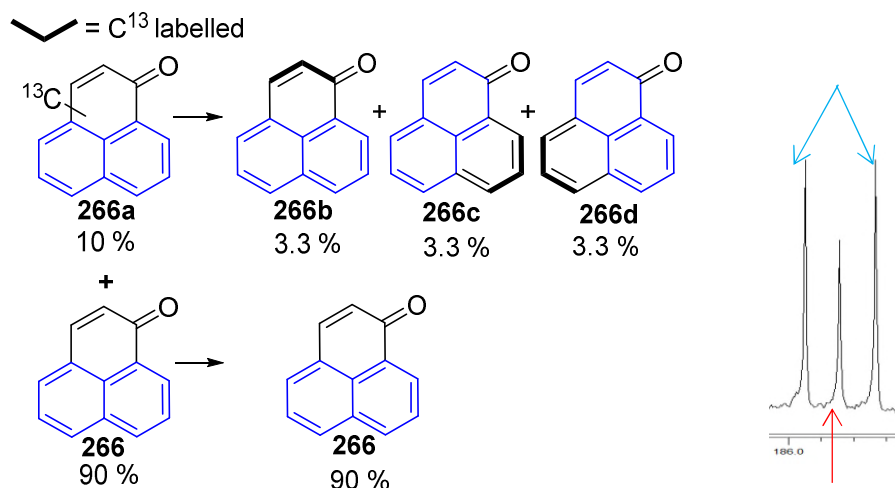


**Figure 56: The proportion of labelled to non-labelled signals expected. The top arrows showing the doublet and the bottom non-labelled portion 266.**

For example, one out of the three arrangements can be labelled in the carbonyl position (Figure 56, top arrows). Hence the doublet peak can be said to be 100 %  $^{13}\text{C}$  of 3.3 %. In addition, roughly 1.1 % of natural carbon contains isotopic carbon therefore the singlet (Figure 56, bottom arrow) is 1.1 % of the remaining 96.7 % of the product. This explains why the doublet is more intense than that of the singlet by a factor of roughly 3.1.

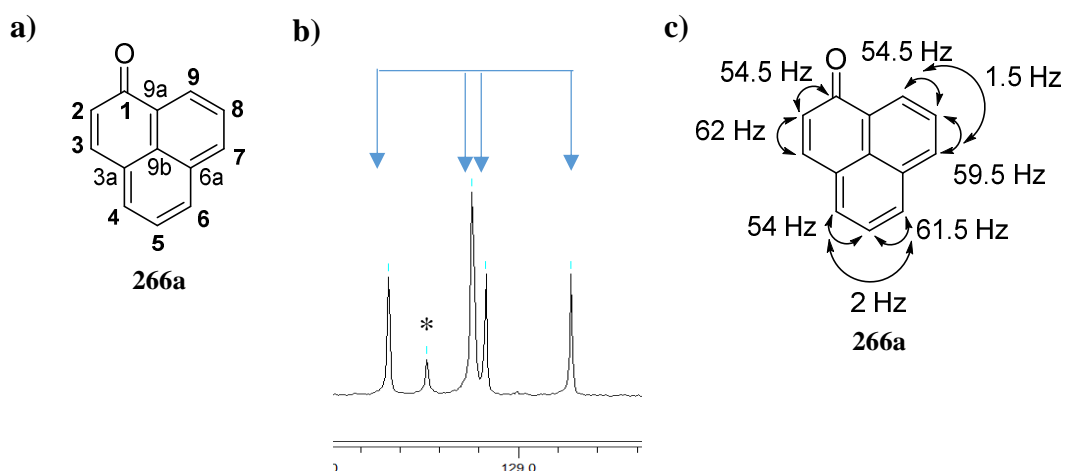


**Figure 57: a) Carbon 2 and its neighbours, b) the  $^{13}\text{C}$  NMR spectrum for C2, c) the observed coupling constants of the labelled perinaphthone.**



The  $^{13}\text{C}$  peak at 129.2 ppm corresponds to the C2 peak, next to the carbonyl which is a singlet overlapping with a double-doublet peak (Figure 57). The double-doublet (represented by the arrows) is due the coupling of two neighbouring non-identical labelled carbons with J values of 62.0 and 54.5 Hz. Again due to the NMR isotope shift the double-doublet peak is not exactly centred to that of the unlabelled carbon singlet. The \* peak can be ignored in this case as it belongs to the quaternary C9a. After complete analysis, all J values for the three different  $^{13}\text{C}_3$  environments can be deduced (Figure 57c).

Furthermore, if the mechanism is correct, there should be four quaternary carbon singlets in the NMR spectrum that are never  $^{13}\text{C}$ -labelled, which is observed (Figure 58).

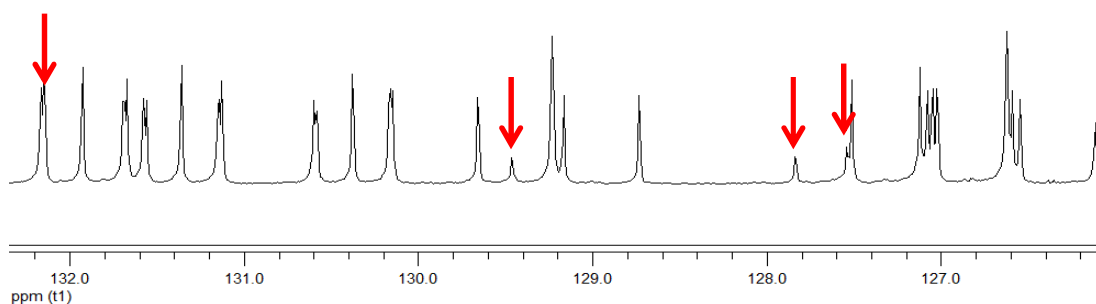


**Figure 58: The arrows showing the quaternary carbons, which are all singlets and therefore not labelled.**

In addition to the 1D  $^1\text{H}$  and  $^{13}\text{C}$  spectra, an INADEQUATE  $^{13}\text{C}$ - $^{13}\text{C}$  correlation experiment was performed to support the assignment of the  $^{13}\text{C}$  spin systems of perinaphthanone.

The INADEQUATE shows coupling between neighbouring carbons which can determine spin systems. Perinaphthanone **266** has three spin systems, carbons 1, 2, 3, carbons 4, 5, 6 and carbons 7, 8, 9. The signal is represented by a contoured circle, and those which are on the same horizontal axis are those which are coupling

together. Figure 59 shows two lines; the first shows two strong signals at 129.2 and 141.8 ppm which represents the coupling of carbons 2 and 3. The second line shows two strong signals at 129.2 and 185.7 ppm which correspond to the coupling of carbons 1 and 2. Collating these results concludes that carbon 1, 2 and 3 are part of the same spin system. The rest of the spin systems can also be determined in this way (Figure 60). The scale on the right hand side of the INADEQUATE is the double quantum frequency which is made up of the sum of the two correlating frequencies.

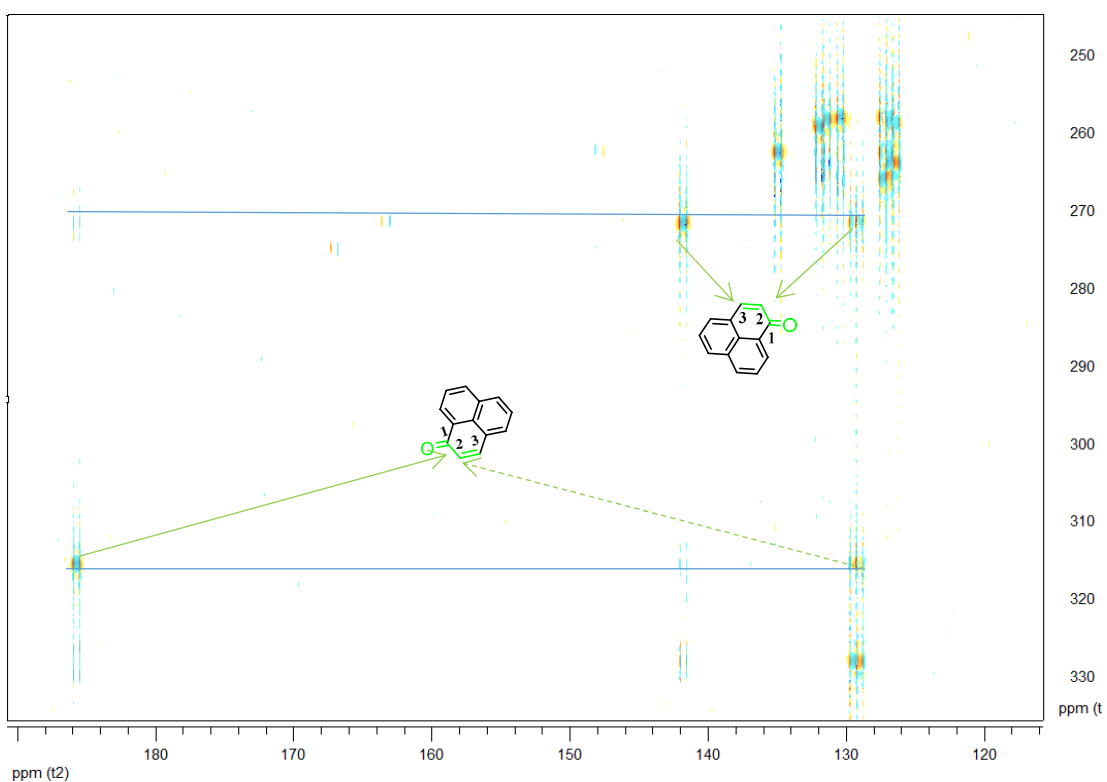


**Figure 59: INADEQUATE of perinaphthanone 266a, showing the assignments on the carbonyl ring, where the signals ‘spots’ which are in line with each other are from the same spin system (lines).**

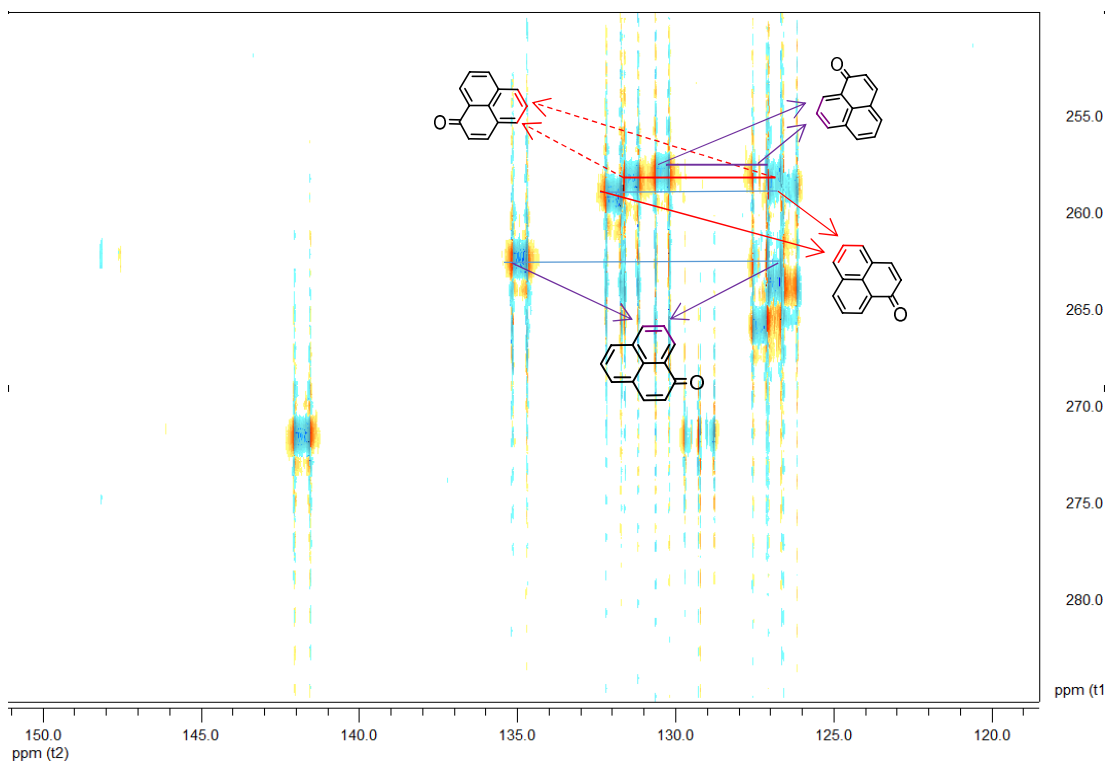


**Figure 60: INADEQUATE of perinaphthanone 266a showing the rest of the spin systems.**

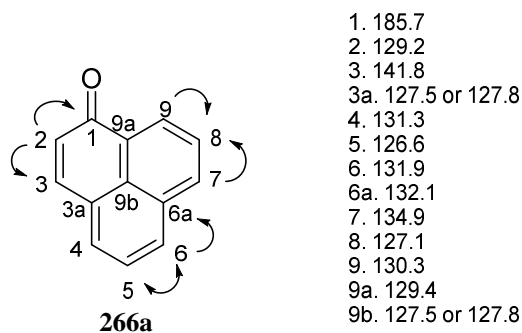


**Figure 61: The analysis of the ADEQUATE results of perinaphthanone 266a, carbons 3, 4 and 8 had overlapping signals.**

Furthermore, an ADEQUATE experiment was also undertaken which deduces which are neighbouring carbons. Figure 61 shows a summary of all of the measured  $^{13}\text{C}$ - $^{13}\text{C}$  coupling patterns. This is also in agreement with the INADEQUATE results.

As well as  $^{13}\text{C}$  NMR spectroscopy, mass spectrometry is also a valuable method for the analysis of labelled compounds.

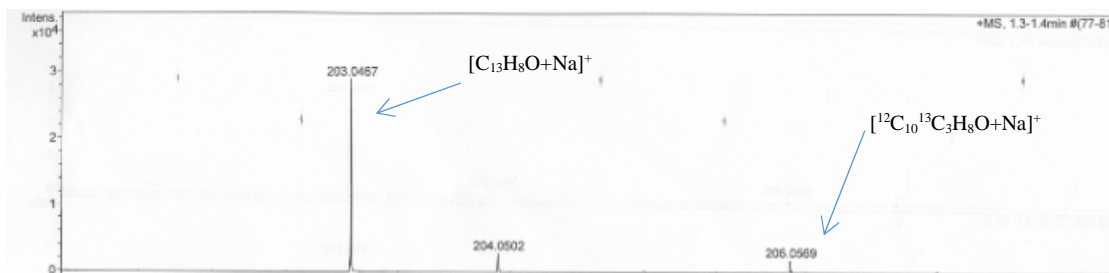


**Figure 62:** Mass spectrometry of the  $^{13}\text{C}$ -labelled perinaphthanone **266a** where the  $^{13}\text{C}_3$  mass can be seen.

Perinaphthanone **266** has a molecular mass of 180.06 and the labelled version **266a** with  $^{13}\text{C}_3$  is 183.03455, the corresponding peaks can be seen in Figure 62.

### 3.8.2 Carbon labelled 6-oxo-6*H*-benzo[*cd*]pyrene

Also from the  $^{13}\text{C}$  labelled reaction, 6-oxo-6*H*-benzo[*cd*]pyrene **210a** was analysed.

The different ring additions onto naphthalene **4** are shown in Figure 63.

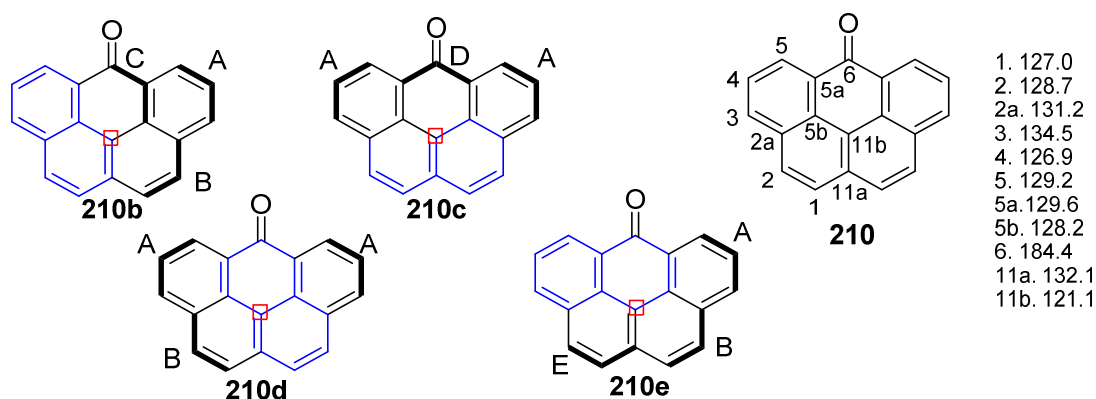


**Figure 63:** The possible additions of rings on the naphthalene starting material (**210b-e**) to make 6-oxo-6*H*-benzo[*cd*]pyrene **210a**. The different letters represent the different type of single additions encountered (A-E). In addition, the full assignment of 6-oxo-6*H*-benzo[*cd*]pyrene **210** is shown (ppm).

After all the carbon signals are characterised the  $^{13}\text{C}$  NMR spectrum was fully analysed (Figure 63) where one of the more interesting peaks was the carbonyl C6. Figure 63 shows the four possible additions which have five different environments (A-E) of  $^{13}\text{C}_3$  units which should be found in the product given the proposed *peri*-condensation pathway.

The C6 peak at 184.4 ppm has three possible environments a C and D spin system as well as an unenriched environment. The splitting in the C spin system would be either a doublet or if  $^2J$  coupling is observed a double-doublet, whilst the peak in the D type system would be a triplet in  $^{13}\text{C}$  NMR spectrum. In the spectrum, both a C (double-doublet) and D (triplet) type environment are observed (Figure 64).

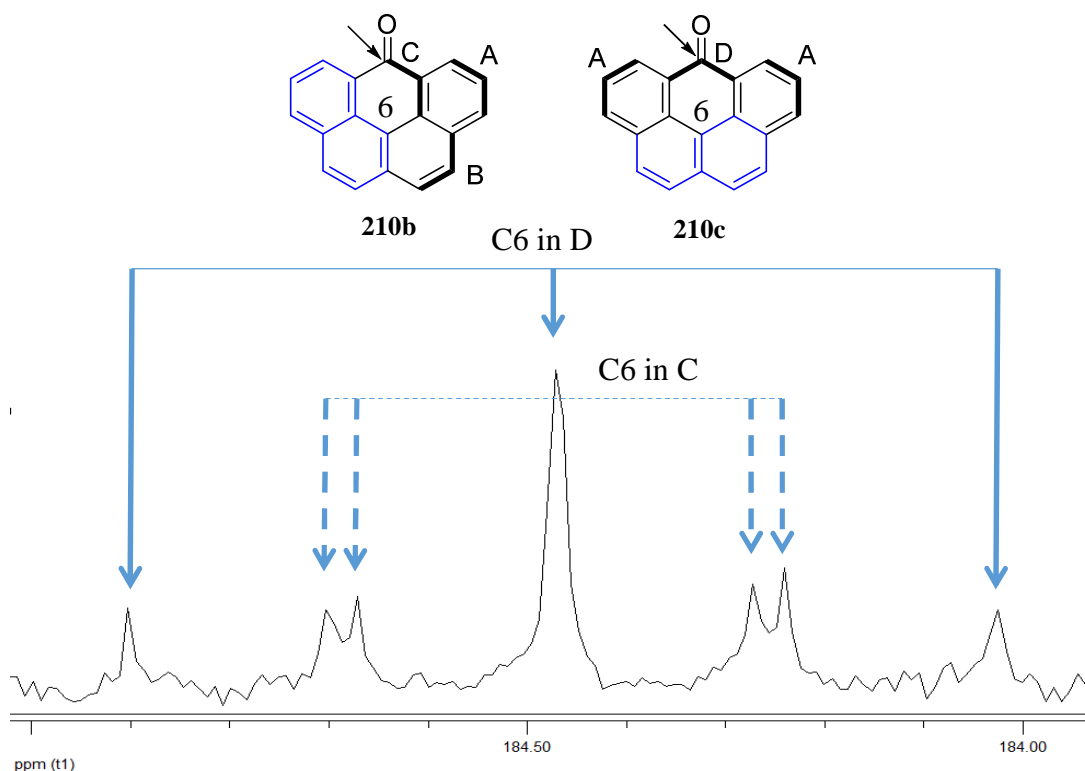


**Figure 64:** The C6 peak, two types of additions can occur C (double-doublet: 54.5, 4.0 Hz – dashed arrows) and D (triplet: 55.0 Hz – solid arrows) where both can be seen with the non-labelled singlet in the centre.

The signal at 134.5 ppm is the C3 carbon, which has only an A type environment, a double-doublet is seen with coupling to C4 and C5 (Figure 65).

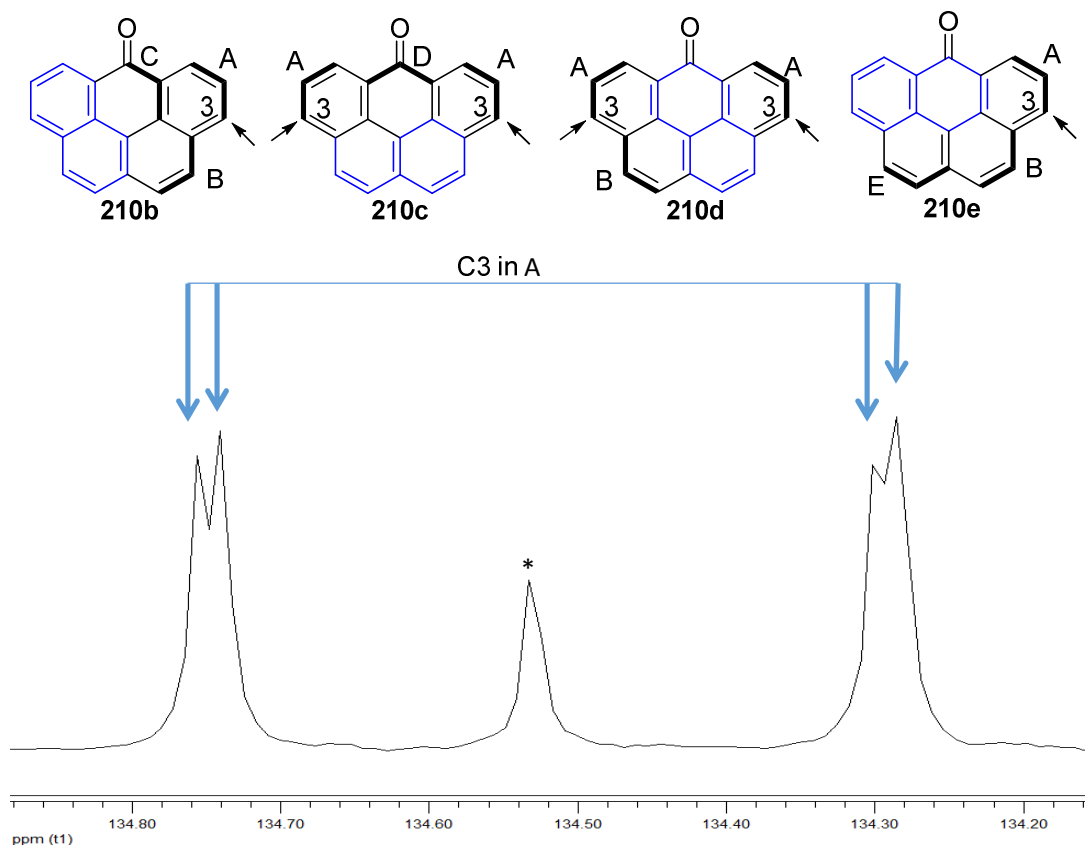


**Figure 65: C3 (double-doublet: 57.0, 1.5 Hz) coupling to C4 and C5, \*peak in the middle is the non-labelled singlet.**

The C4 peak at 126.8 ppm is a double-doublet in an A type environment coupling to C3 and C5.

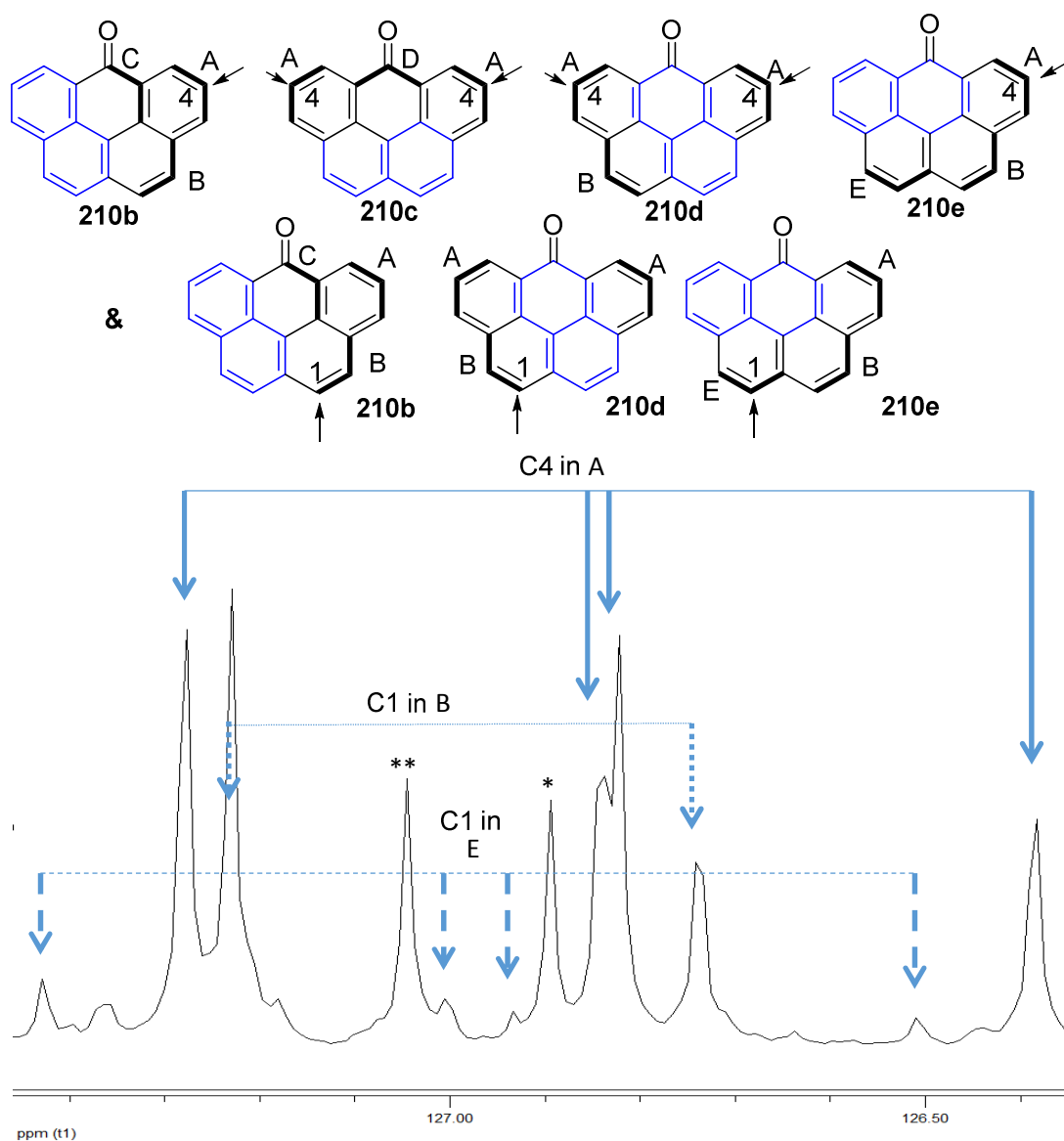


**Figure 66:** Type A environment of C4 (double-doublet: 57.0, 55.0 Hz – solid arrows), \*peak is the non-labelled C4 singlet. In addition, C1 is observed here, with a B type (doublet: 61.5 Hz – dotted line) and an E type environment (double-doublet: 62.5, 53.0 Hz – dashed line), \*\*peak is the non-labelled C1 singlet.

The C1 signal at 126.9 ppm is overlapped with that of C4, where it is part of a B type and E type environment (Figure 66).

The peaks C2 at 128.7 ppm is in the same B and E spin systems as C1, with a doublet and a double-doublet observed in the spectrum respectively (Figure 67).

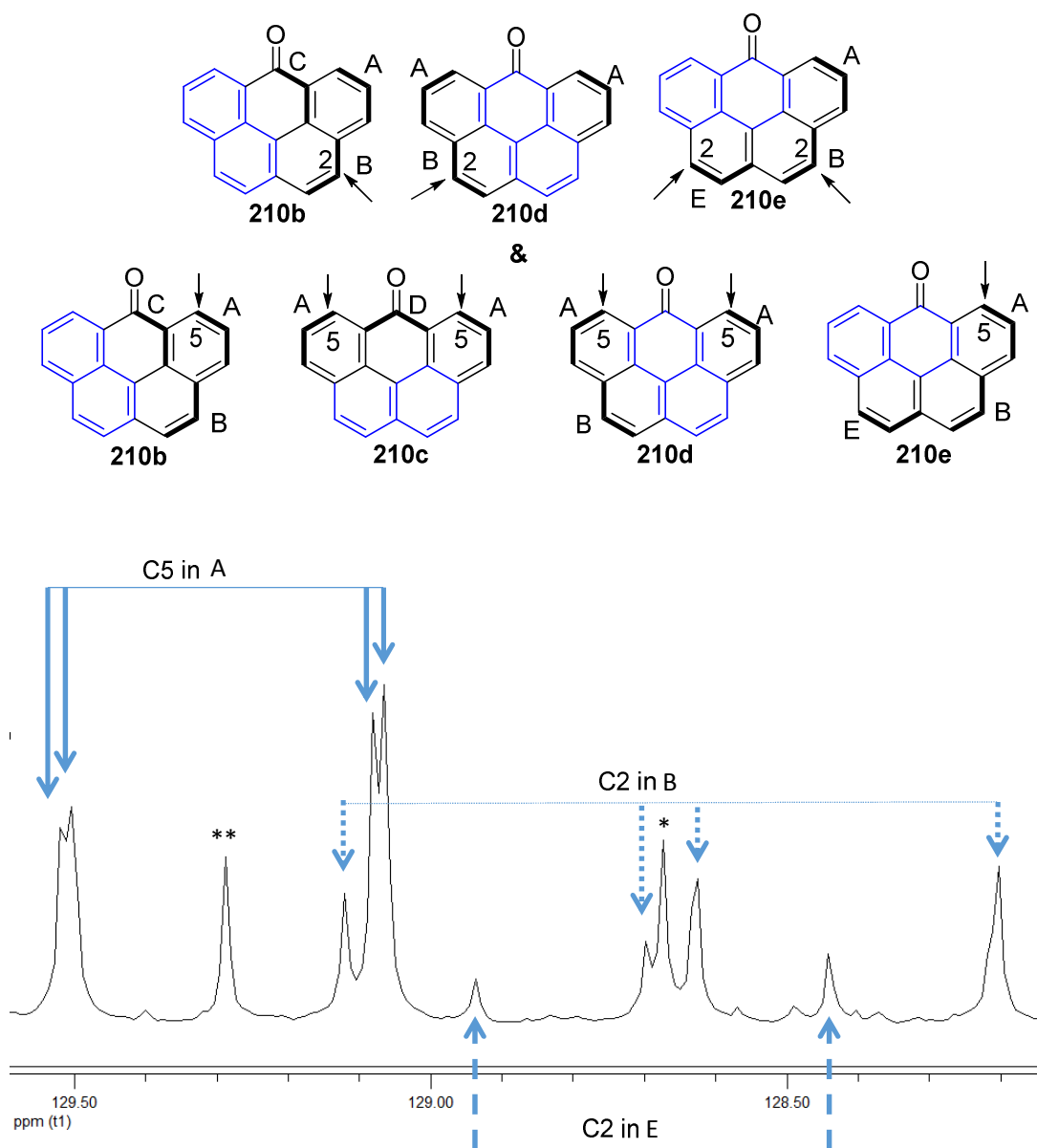


**Figure 67:** C2 at 128.7 ppm has both a B (doublet: 62.5 Hz – dotted lines) and E type (double-doublet: 62.0, 53.5 Hz – dashed lines), \*peak is the C2 non-labelled singlet. C5 at 129.3 ppm, A type environment (double-doublet: 55.0, 1.5 Hz – solid line), \*\*peak is the non-labelled C5 singlet.

The C5 peak at 129.3 ppm are in the A type spin system and is split into a double-doublet as it couples to C4 and C3. The splitting pattern is overlapped with C1 and can be observed in Figure 67.

Consequently, the *peri*-addition can incorporate some quaternary carbons from the molecule (Figure 68).



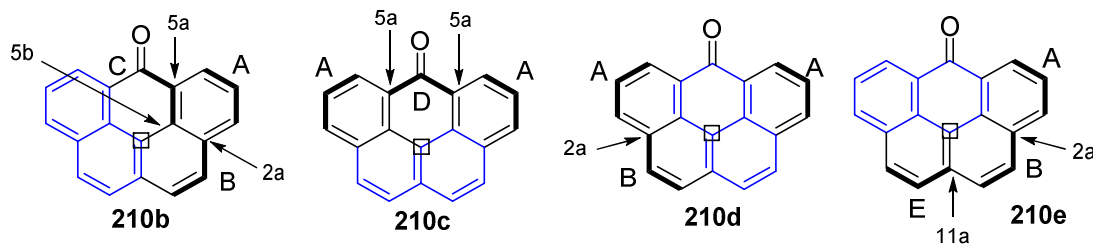


**Figure 68: Summary of the quaternary carbons which are labelled with the proposed mechanism, the square represents the C11b which is not labelled.**

The C5a peak at 129.8 ppm is part of a C and a D type spin system, therefore a double-doublet and a doublet is expected respectively, however due to overlapping peaks and signal strength only a doublet can be observed in the spectrum. The quaternary carbons of C2a at 131.2 ppm and C11a at 132.1 ppm, are always at the end of a  $^{13}\text{C}_3$  unit therefore a doublet is seen for both (Figure 69). C5b splitting is not observed due to overlapping peaks.

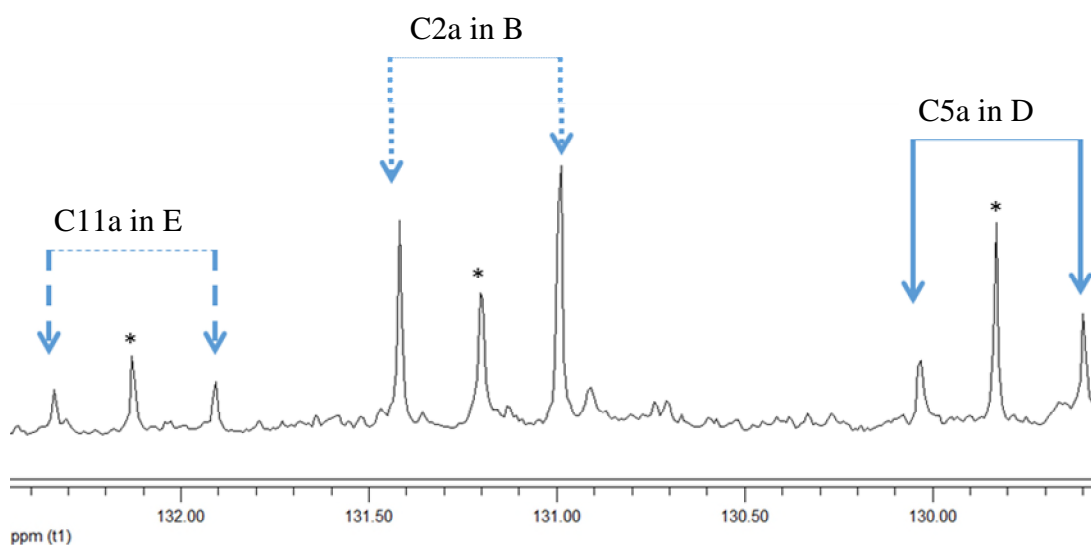


**Figure 69:  $^{13}\text{C}$  NMR spectrum showing C11a, E type (doublet: 54.0 Hz-dashed line), C2a, B type (doublet: 54.0 Hz-dotted line) and C5a D type spin systems (54.5 Hz-solid line). \*peaks are the respective non labelled singlets.**

Note that one quaternary carbon C11b at 121.1 ppm is never labelled (Figure 68) using the  $^{13}\text{C}_3$  unit addition and in the  $^{13}\text{C}$  spectrum only a singlet is observed, which further supports the *peri*-condensation mechanism.

A coupling constant map can be produced after collating all the information from the  $^{13}\text{C}$  spectral data (Figure 70).

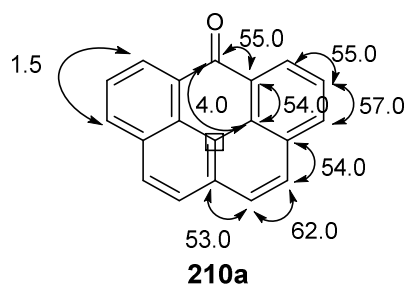


**Figure 70: Coupling constant map of  $^{13}\text{C}$ -labelled 6-oxo-6H-benzo[cd]pyrene 210a, all J values are in Hertz.**

Due to only 10 % carbon labelled doping of glycerol the probability of more than one  $^{13}\text{C}_3$  unit adding onto one naphthalene is very low (1 % or 0.1 %). Hence, further coupling is not observed in the  $^{13}\text{C}$  NMR spectrum. In addition to the 1D  $^1\text{H}$  and  $^{13}\text{C}$  spectra, an INADEQUATE  $^{13}\text{C}$ - $^{13}\text{C}$  correlation experiment and ADEQUATE was performed which supports the assignment of the  $^{13}\text{C}$  spin systems of 6-oxo-6H-benzo[cd]pyrene.

A mass spectrum was also performed on  $^{13}\text{C}_3$  doped 6-oxo-6H-benzo[cd]pyrene **210a**. The non-labelled **210** has a molecular mass of 254.0732 and can be seen at 277.0625 with sodium. The labelled molecule **210a** with one  $^{13}\text{C}_3$  unit is seen at 280.0725 with sodium, the corresponding peaks can be seen in Figure 71.

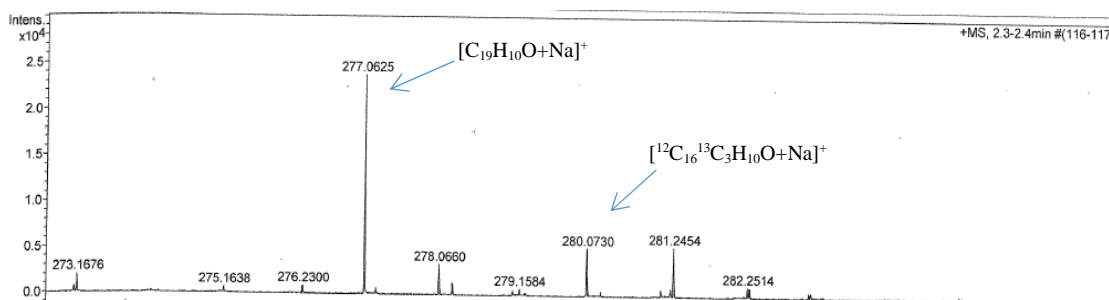


**Figure 71: Mass spectrum of  $^{13}\text{C}$ -labelled sample of 6-oxo-6H-benzo[cd]pyrene 210a.**

Additionally, the peak at 278.0660 represents the 1 % of  $^{13}\text{C}$  part of the natural abundance peak (predicted: 278.0657) and the same can be seen for  $[\text{M}+\text{H}]^+$  signal.

These results obtained suggest that a '3+3' annulation of adjacent '*peri*' positions occurs rapidly when available and that the ketone products proceed *via* their dihydride precursors. Carbon labelled glycerol experiments were undertaken proving the addition of rings was from the glycerol and not scrambled, supporting the mechanism proposed. The analysis was also further supported by INADEQUATE and mass spectrometry experiments.

### 3.9 The solid black powder product of the annulation reactions

The black solid which was produced in all the reactions; naphthalene **4**, anthracene **5**, pyrene **8** and perylene **25**, were analysed. As there was low conversion rate into the expected products and high amounts of this solid obtained, it was necessary to determine if this is a side-product and therefore, what the structural composition of this material is.

Due to the solubility issues no relevant NMR data could be obtained as the material would not dissolve in solvents including DMSO, DMF and DMS. Thereafter, a soxhlet extraction was performed, however only the higher molecular weight compounds purified from the crude mixture were obtained. Therefore, techniques using solid samples were used, including those which were typically used for graphene oxide analysis (all spectra can be found in the experimental section).

#### 3.9.1 Infra-red spectroscopy

The IR spectra of the black solid obtained from all the different reaction mixtures are very similar with characteristic peaks around  $3400\text{ cm}^{-1}$  (O-H stretch),  $2900\text{ cm}^{-1}$  (C-H stretch),  $1700\text{ cm}^{-1}$  (C=O stretch),  $1600\text{ cm}^{-1}$  (C=C stretch) and  $1000\text{ cm}^{-1}$  (C-O

stretch). This has not provided much more information about the structure of the material.

### **3.9.2 Raman spectroscopy**

Raman uses vibrational frequencies of the material, where they are displayed as a band in the spectrum which are very specific to the orientation and weight of atoms in question. The Raman spectrum shows two broad peaks which are 'D' and 'G' bands (see experimental section 6.3.4) attributed to graphene oxide-like compounds according to literature.<sup>378-382</sup> Alternatively, the mixture contains a variety of compounds with very similar structures, this difference in frequency is smaller than the resolution that the instrument provides. Thus the resulting peak will be an average for all vibrations with similar energy.<sup>383, 384</sup>

Due to the similarities of all the data collected so far of the black powder from the different starting materials, the pyrene condensation reaction black solid product was the only solid fully analysed further.

### **3.9.3 Solid state NMR (ssNMR) spectroscopy**

Due to the poor solubility of the black solid, solution state NMR spectroscopy could not be conducted. Therefore, solid state NMR spectroscopy was performed by Dr M. Reddy on the black solid to gain a more accurate analysis of the chemical composition. A strong broad peak around 115 - 150 ppm was present, which can be attributed to high proportion of sp<sup>2</sup> carbons within the structure. There is also a small peak around 20 - 40 ppm which is attributed to CH<sub>2</sub>/CH<sub>3</sub> groups.

### **3.9.4 Thermogravimetric analysis (TGA)**

Thermogravimetric analysis measures the weight difference as a function of temperature where plots can be compared with standards to help determine any

changes in properties. It can be seen (Figure 72) that an initial small mass loss around 200 °C is due to decomposition of functional groups such as carbonyls and alcohols. The main mass loss around 550 °C is due to the decomposition of the core of the structure which can be considered similar to graphitic-type compounds.<sup>380, 385.</sup>

386

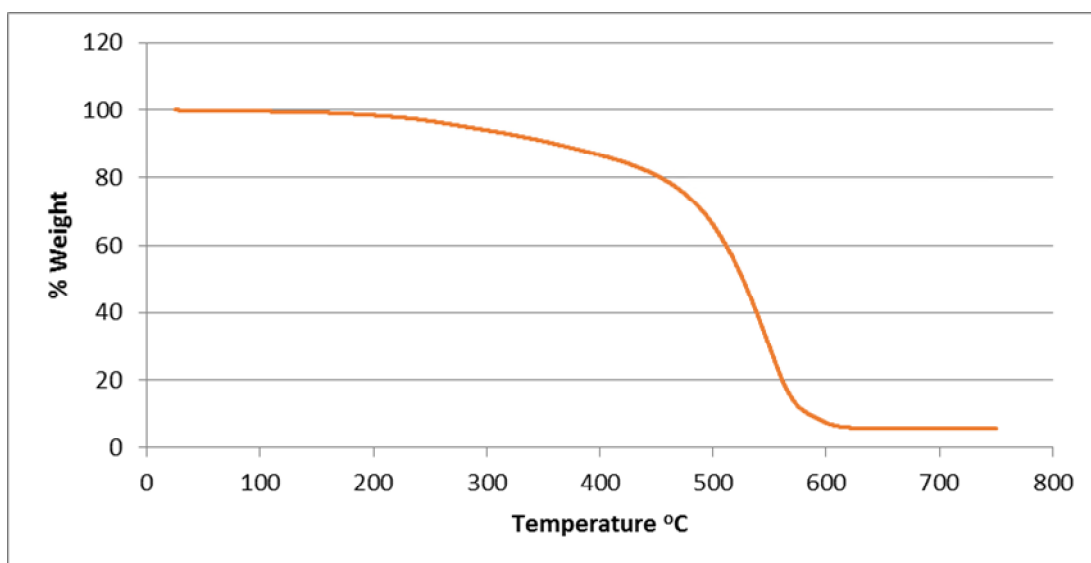


Figure 72: TGA plot of the black powder where the temperature was raised at 10 °C/min from 25 °C - 800 °C.

### 3.9.5 Energy dispersive X-ray spectroscopy (EDX)

Energy dispersive x-ray spectroscopy is a form of elemental analysis using x-rays emitted from the sample. This analysis was completed by Dave Burnett which was used to determine the ratio of carbon to oxygen in the sample, the results show a C:O:S ratio of 87:11:2. The sulfur detected is probably due to residual sulfuric acid.

### 3.9.6 X-ray photoelectron spectroscopy (XPS)

X-ray photoelectron spectroscopy is another form of elemental analysis which gathers information from the photoelectrons emitted from the material, which was performed by Dr M. Walker. The results detected carbon, oxygen and sulfur from the

sample in a ratio of 85:14:1, respectively. The results match closely to that of the EDX ratio.

### **3.9.7 Scanning electron microscopy (SEM)**

Scanning electron microscopy uses an electron beam which scans over the sample in question, whereby the signal collected forms an image of the topology of the sample. The images, obtained by Helen Thomas, show that there are no large graphitic sheets present and that the material is clumped together probably due to  $\pi$ -stacking.

### **3.9.8 Transmission electron microscopy (TEM)**

Transmission electron microscopy passes a beam of electrons through a sample, which ideally is thin. The TEM images obtained by Dr R. Beanland show that the black powder is made up of small structures of seemingly amorphous carbon due to no diffraction pattern observed.

The use of these different techniques has not provided any new information relating to the structural arrangement of the material.

### **3.9.9 AFM/STM analysis by IBM Zürich group**

Analysis by NC-AFM showed that the black product contained a mixture of PAHs (including isomers) containing up to 11 rings (Figure 73), but it was difficult to examine the whole sample so other PAHs may also be formed in the reaction.

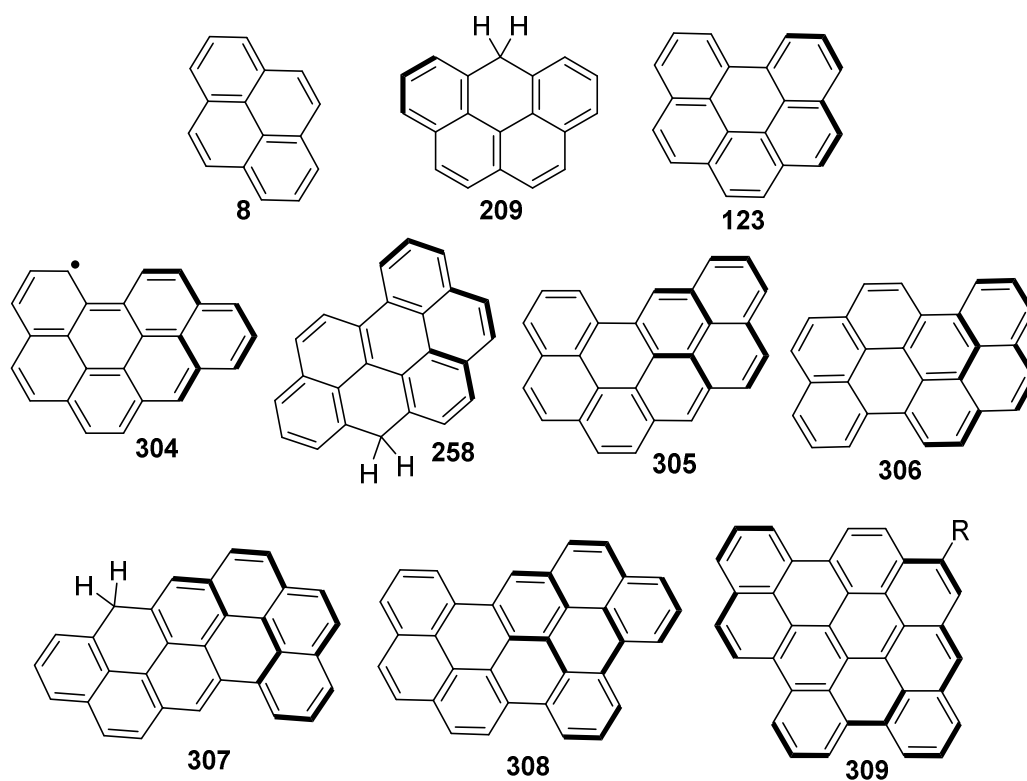
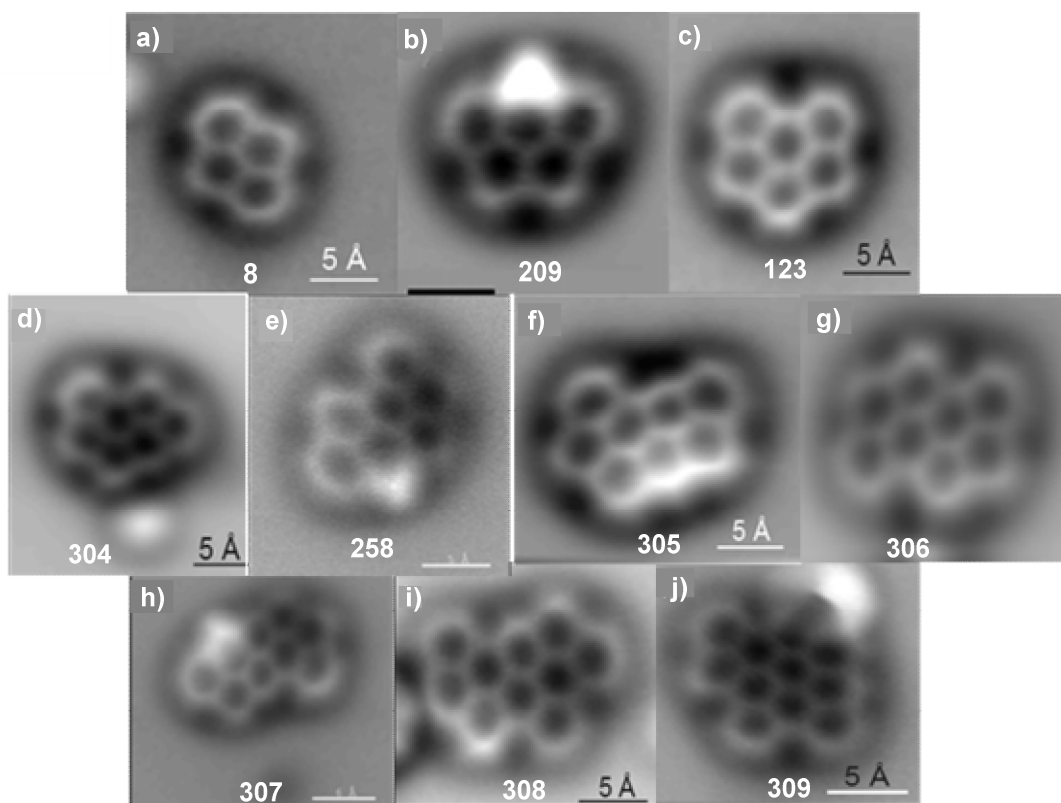
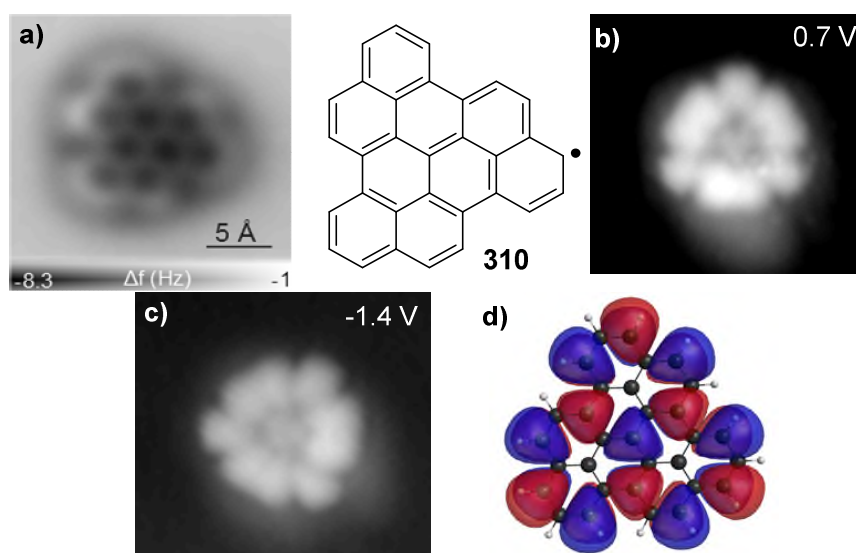


Figure 73: Selected AFM images (a-j) of the black powder from the pyrene reaction, with correlating structures.<sup>321</sup>

The NC-AFM images obtained showed a number of compounds produced including isomers **305** & **306** (Figure 73), dihydrides **209**, **258**, & **307**, ketones and radicals **304**. In addition, they are all consistent with the proposed three-carbon *peri*-addition mechanism, starting from pyrene **8** (Figure 73).

Due to the conditions of AFM/STM including ultra-high vacuum and low temperature, observation of very unstable intermediates such as a  $C_3$ -symmetric nine-ring structure **310** was also possible (Figure 74). To prove that this compound was a radical, scanning tunneling spectroscopy (STS) was performed. STS probes the electronic structure to show information about the density of states in the molecule by using negative (NIR) and positive ion resonance (PIR). For example, to prove **310** (Figure 74) is a radical, an electron was both independently inserted (NIR) and removed (PIR) from the SOMO. The results are shown by STM, where both the NIR and PIR orbital images are identical, thus proving that this compound is indeed a radical as it involves the same molecular orbital (Figure 74).



**Figure 74:** a)  $C_3$ -symmetric radical **310** observed by AFM from the black powder. b) STM of the negative ion resonance (NIR) and c) the positive ion resonance (PIR) of **310**.<sup>321</sup> d) is the DFT calculated SOMO of **310** by Dr D. Fox.



Furthermore, the mixture also contained some PAHs with side chains. Through this method the structure of the side chains could not be determined. However, one can postulate that these could possibly be due to failed ring closures, which look to be on the *peri*-positions of the molecules (Figure 75).

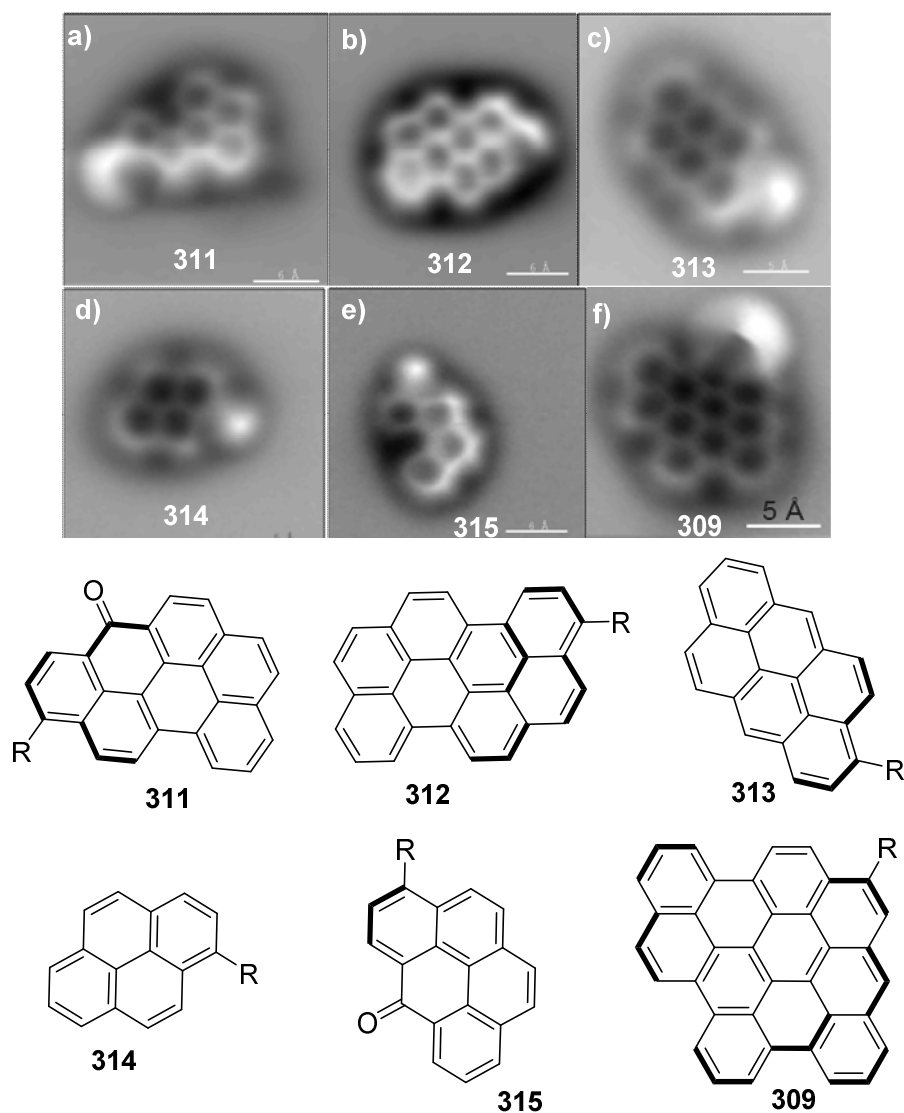


**Figure 75: Selected AFM images (a-f) of compounds found with side chains from the black powder mixture, with the related PAHs shown with addition units (bold). R = unknown side chain.<sup>321</sup>**

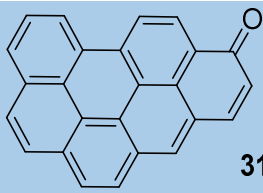
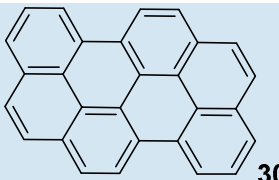
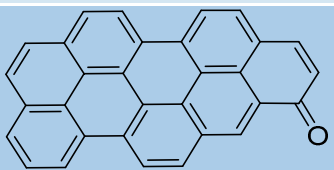
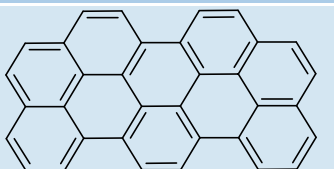
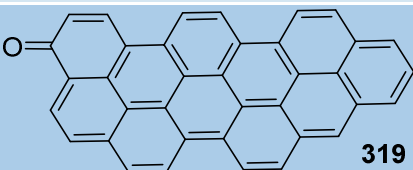
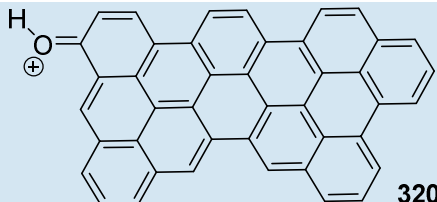
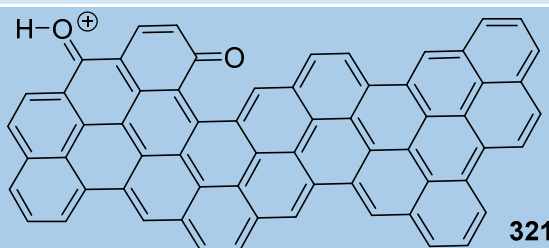
These results show that the previous techniques used can be interpreted in multiple ways, and that the images produced by AFM/STM can either confirm or decline some of the assumptions made to provide a clearer analysis. NC-AFM in this case

alleviated the uncertainty with impressive imagery of various PAHs in a mixture, including novel ones.

#### **3.9.10 Mass spectrometry**

ESI mass spectrometry was undertaken on the black powder samples beforehand but because most PAHs do not contain groups to be ionised easily they are not observed. Therefore, a different method was developed by using the published work of Simpson *et al.* where a solid sample was attached onto a MALDI plate and the readings measured in this way.<sup>169</sup> With this type of direct ionisation of a sample the mass readings were not particularly accurate, but did suggest structures for species which could have been formed.

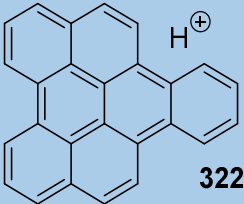
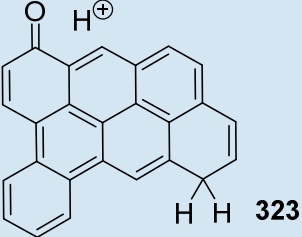
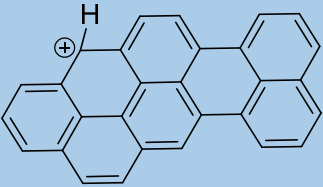
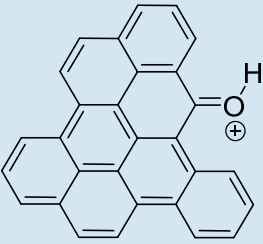
The mass spectrometry results for the pyrene derived black solid product are below. There were also a number of unidentified peaks but these were probably those that did not cyclise fully and can have different substituents on the side chains. In addition, the mass spectrometry results can also provide information concerning the size of the PAHs, albeit some of the larger ones will have a very low signal intensity.

<i>m/z</i> observed	<i>m/z</i> of possible compound	Possible compound (Only one isomer drawn)
328.0635	328.0888	 <b>316</b>
350.0837	350.1096	 <b>306</b>
402.0903	402.1045	 <b>317</b>
424.1134	424.1252	 <b>318</b>
477.1420	476.1201	 <b>319</b>
551.1640	551.1430	 <b>320</b>
825.2073	825.1849	 <b>321</b>

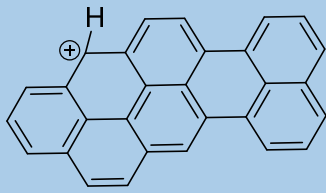
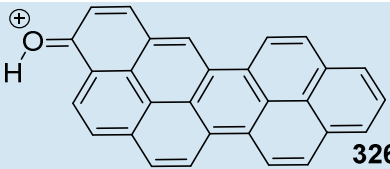
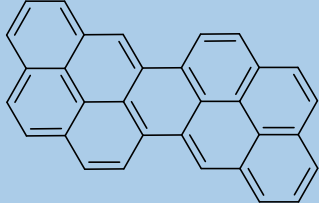
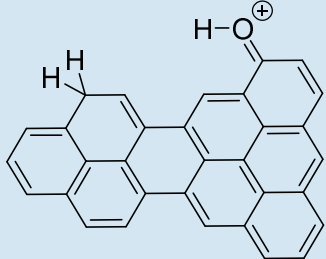
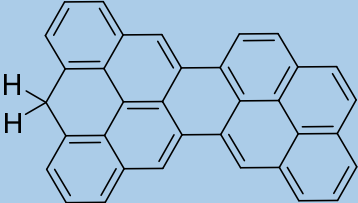
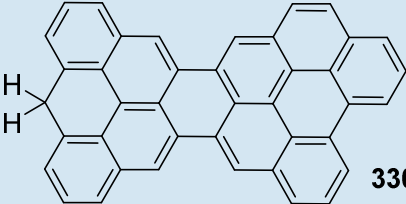
**Table 1: Mass spectrometry results of pyrene derived black powder, where proposed structures are drawn in accordance with the mass observed; pyrene *m/z* peaks were detected at just over 800.**

The first three compounds in Table 2 (at  $m/z$  328, 350 and 402) were also detected by the AFM as the images can be seen above (Figure 73).

The anthracene and perylene derived samples were also similarly analysed (Table 2 & 3).

$m/z$ observed	$m/z$ of possible compound	Possible compound (Only one isomer drawn)
327.157	327.1168	 322
343.177	343.1117	 323
363.212	363.1179	 324
379.237	379.1123	 325

**Table 2: Mass spectrometry results from anthracene derived black powder, where proposed structures are drawn in accordance with the mass observed; anthracene  $m/z$  peaks were detected at just over 530.**

<i>m/z</i> observed	<i>m/z</i> of possible compound	Possible compound (Only one isomer drawn)
363.001	363.1179	 324
379.017	379.1117	 326
400.048	400.1252	 327
417.077	417.1274	 328
438.100	438.1409	 329
512.174	512.1565	 330

**Table 3: Mass spectrometry results from perylene derived black powder, where proposed structures are drawn in accordance with the mass observed; perylene *m/z* peaks were detected at just over 510.**

### 3.10 Summary

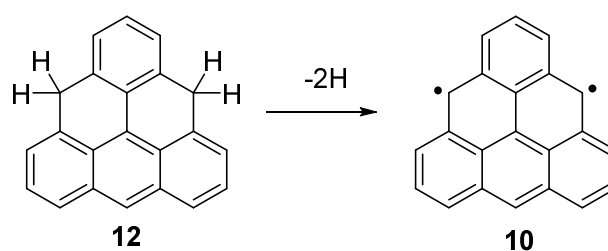
The *peri*-condensation reactions on naphthalene, anthracene, pyrene and perylene produced numerous products due to poly-annulation, which were purified and characterised. The glycidol units can add onto PAHs which contain *peri* positions multiple times rather than only once, with the increasing ring sizes being harder to form. Pyrene has been observed to react to produce products with up to seven additional rings. Where not all the cyclisations are completed, side chains can remain. A mechanism was proposed in relation to the Skraup-Doebner von Miller quinolone synthesis, where experiments including  $^{13}\text{C}_3$  carbon labelling were conducted to help support this. This has yielded better understanding of the reaction and thus, the characterisation of the black solid product has now been completed which was of unknown chemical composition.

STM/AFM was utilised successfully where other analytical methods failed to help characterise unknown compounds especially those which were difficult to dissolve in common organic solvents. Hopefully STM/AFM can be used more regularly in the future for the characterisation of difficult compounds which may be difficult to analyse under normal conditions.

## 4 Chapter 4: Synthesis of triangulene

### 4.1 Introduction

Having synthesised and imaged the benzo[*cd*]pyrene radical by means of AFM/STM, we would attempt to image triangulene **10**. This would require the abstraction of two hydrogens from the parent dihydro-triangulene **12** rather than one to form the reactive diradical (Scheme 70).



**Scheme 70:** Abstraction of two hydrogens from dihydro-triangulene **12** to form triangulene **10**.

The potential existence of triangulene **10** can be dated back to 1941 when it was first discussed by Clar and thus, it is commonly known as Clar's hydrocarbon.<sup>387</sup> This  $D_{3h}$ -symmetric compound is the smallest triplet ground state polybenzenoid and due to its arrangement it is impossible to draw a Kekulé structure.<sup>388</sup> Triangulene's open-shell triplet ground-state is an estimated 20 kcal mol<sup>-1</sup> lower than its singlet state.<sup>29, 389</sup> Thus, it is of great interest to many material scientists for its use in organo-electronics, since this field attempts to exploit spin and molecular electronics of such compounds.<sup>389, 390</sup> Triangulene **10** is part of a triangular shaped series of PAHs with increasing ground-state multiplicity, with the phenalenyl radical **7** the smallest member (Figure 76).

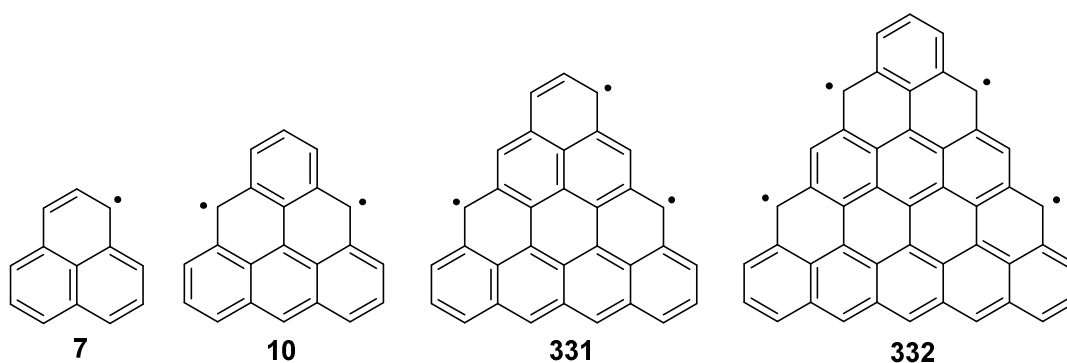
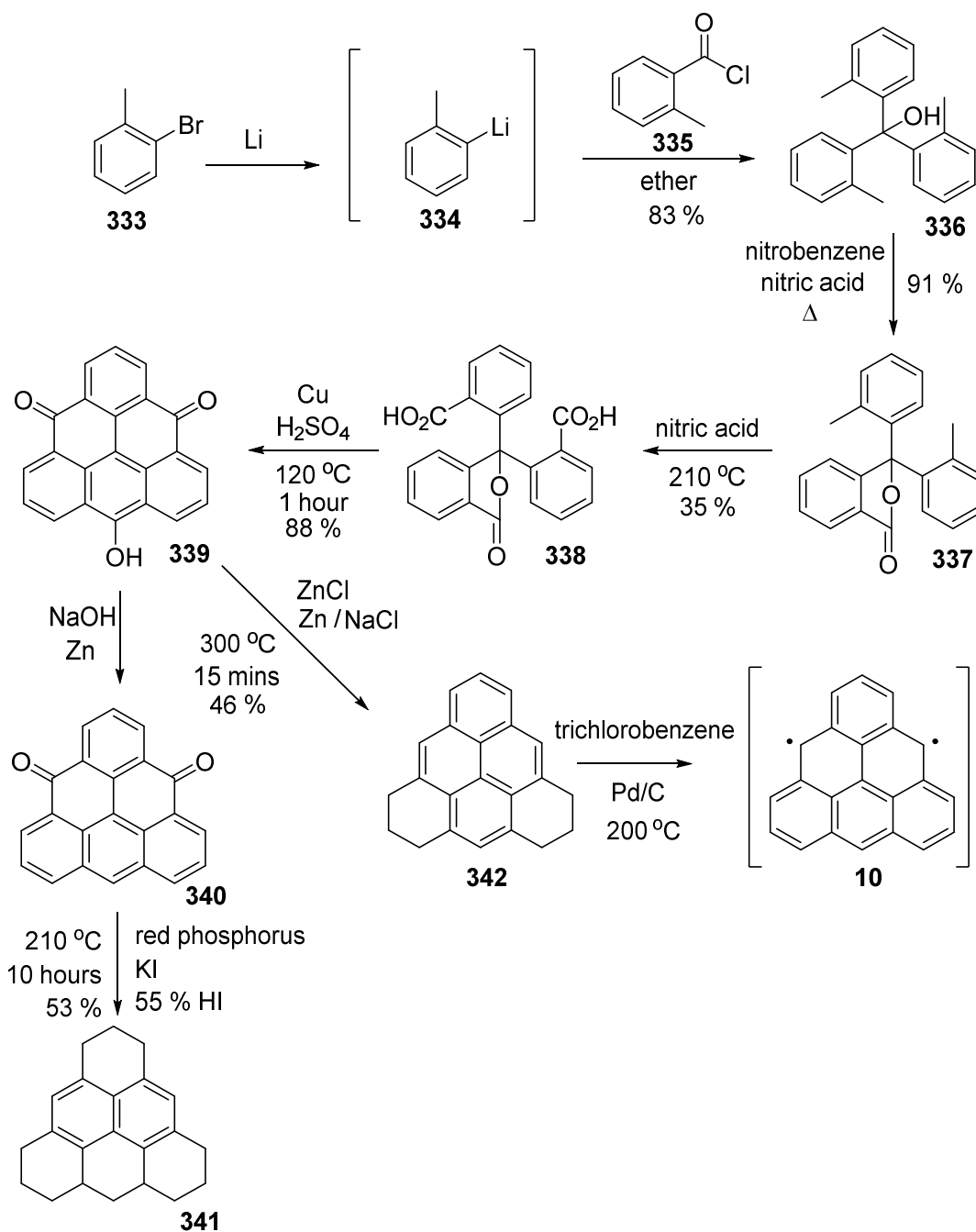


**Figure 76: The triangular series of graphene fragments which due to their structure, do not have a singlet ground-state. The first structure is the phenalenyl radical **7** and the second is the triangulene diradical **10**.**

Triangulene **10** is yet to be isolated due to its open-shell nature it is considered to be highly reactive and unstable.<sup>29, 387-390</sup> Clar could not isolate triangulene, although he synthesised numerous derivatives. Others have attempted but have only been able to form substituted and more stable triangulenes. Clar attempted to form triangulene by many synthetic methods with one of his shorter routes summarised in Scheme 71.<sup>316, 391</sup> In the last step where 1,2,3,5,6,7-hexahydro-dibenzo[*cd,mn*]pyrene **342** was dehydrogenated, Clar reported that during the reaction 4,8-dihydro-4*H*,8*H*-dibenzo[*cd,mn*]pyrene **12** was observed *via* UV spectroscopy. However, at the end of the reaction a brown solid was obtained with a very small quantity of the starting material persisting and nothing else identifiable.<sup>316</sup> With this result, Clar concluded that triangulene **10** was probably generated but because of its instability and high reactivity it polymerised immediately and therefore he was unable to isolate it.<sup>316, 392</sup> Clar proceeded with further work in this area, predominantly working to produce different derivatives with the core of the triangulene structure in attempts to understand these compounds further and to identify a different synthetic route to triangulene.<sup>316, 393</sup> Unfortunately Clar was unable to isolate triangulene with the equipment available in the 1950s.

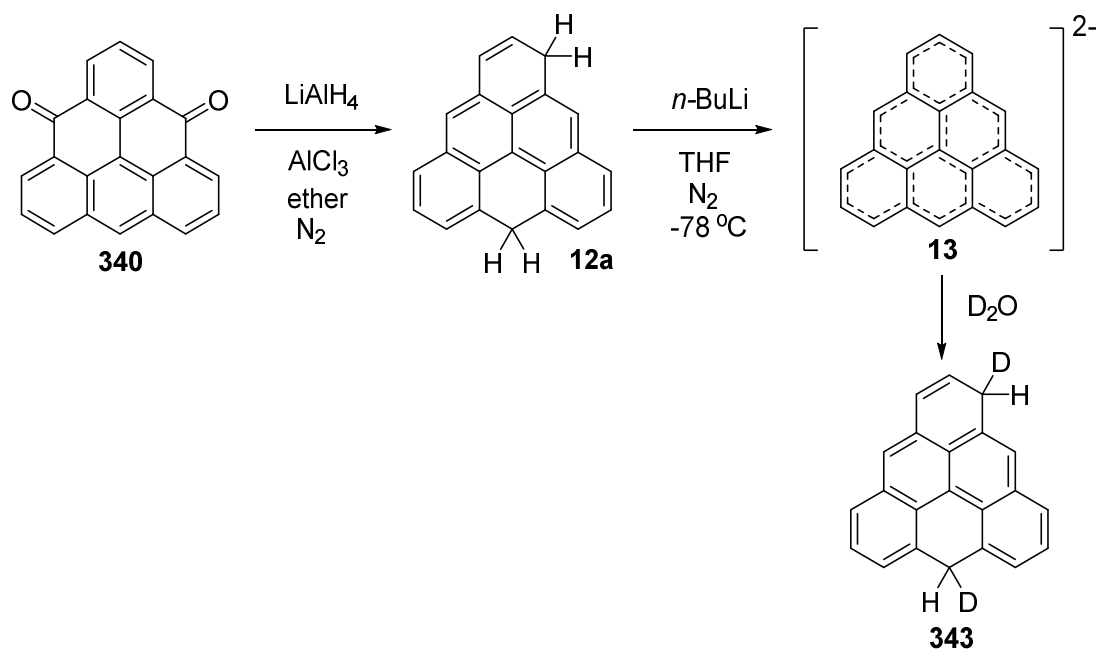




Scheme 71: One of Clar's first synthetic attempts to form triangulene **10**.<sup>316, 391</sup>

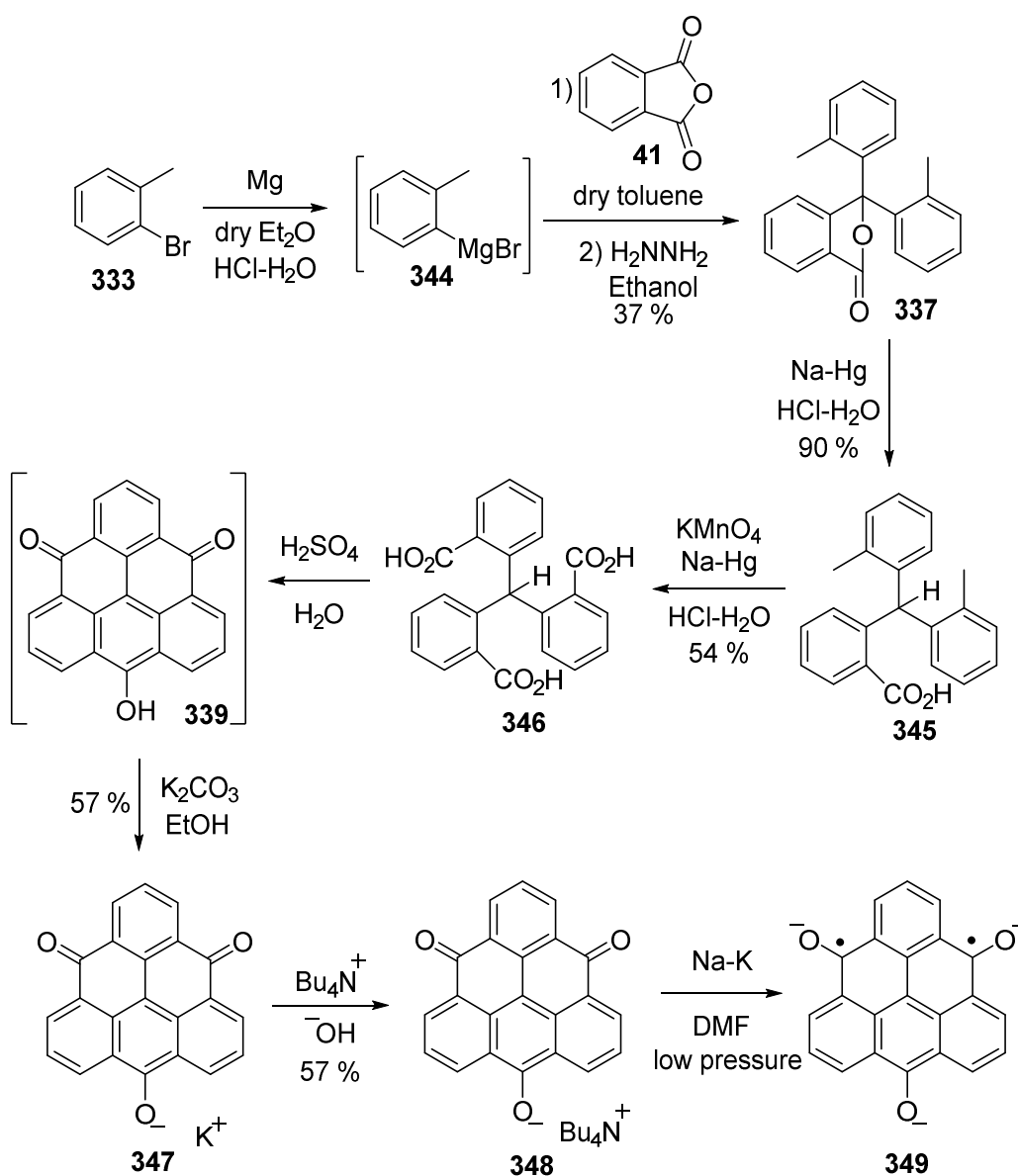
The next significant step in triangulene chemistry was completed by Hara *et al.* in 1977 where they were able to successfully obtain the triangulene dianion **13** with analysis by NMR spectroscopy at  $-50\text{ }^\circ\text{C}$  in deuterated THF.<sup>26</sup> 4,8-Dioxo-4*H*,8*H*-dibenzo[*cd,mn*]pyrene **340** (diketo-triangulene) was reduced with lithium aluminium hydride and treated with butyl lithium at  $-78\text{ }^\circ\text{C}$  to produce the dianion **13**.<sup>26</sup> The

anion was then quenched in D<sub>2</sub>O adding two deuteriums; one at each dihydride site producing species **343** as confirmed by mass spectrometry.<sup>26</sup>



**Scheme 72: The formation of the dianion 13 by Hara *et al.* with NMR spectroscopy confirmation.**

In the 1990s Allinson *et al.* were interested in making non-Kekulé PAH radicals for the potential use as organic molecular magnets.<sup>134, 388, 394, 395</sup> A number of structures were considered with one of the frontrunners being triangulene **10**. Allinson *et al.* reported the first synthesis of a stable tri-substituted triangulene derivative, the trioxytriangulene trianion **349** (Scheme 73).<sup>134, 388, 395</sup>



**Scheme 73:** Allinson *et al.* synthetic route to a stable trioxytriangulene derivative **349**.<sup>134, 388, 395</sup>

The synthesis of this triplet state trioxy derivative was similar to the synthetic route of Clar but most of the more hazardous reagents were substituted with more contemporary reagents.<sup>388</sup> The trioxytriangulene derivative **349** was analysed by electron paramagnetic resonance (ESR) readings, where the triplet ground-state was observed.<sup>29, 388, 395</sup>

In the most recent work of Inoue *et al.* another derivative of triangulene was synthesised; tri-*tert*-butyl-triangulene **350**.<sup>29</sup> This ground state triplet compound was

formed to mimic similar electronics to triangulene although it is stabilised by the three *tert*-butyl groups. These groups were chosen as they would provide the least effect in terms of electronics when compared to heteroatoms such as oxygen which were used by Allinson *et al.*<sup>29, 388</sup> ESR was used to detect the diradical triplet ground state of the tri-*tert*-butyl triangulene species **350**.<sup>29</sup>

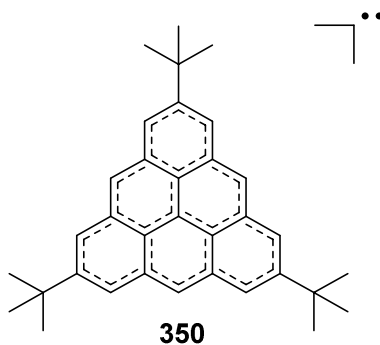
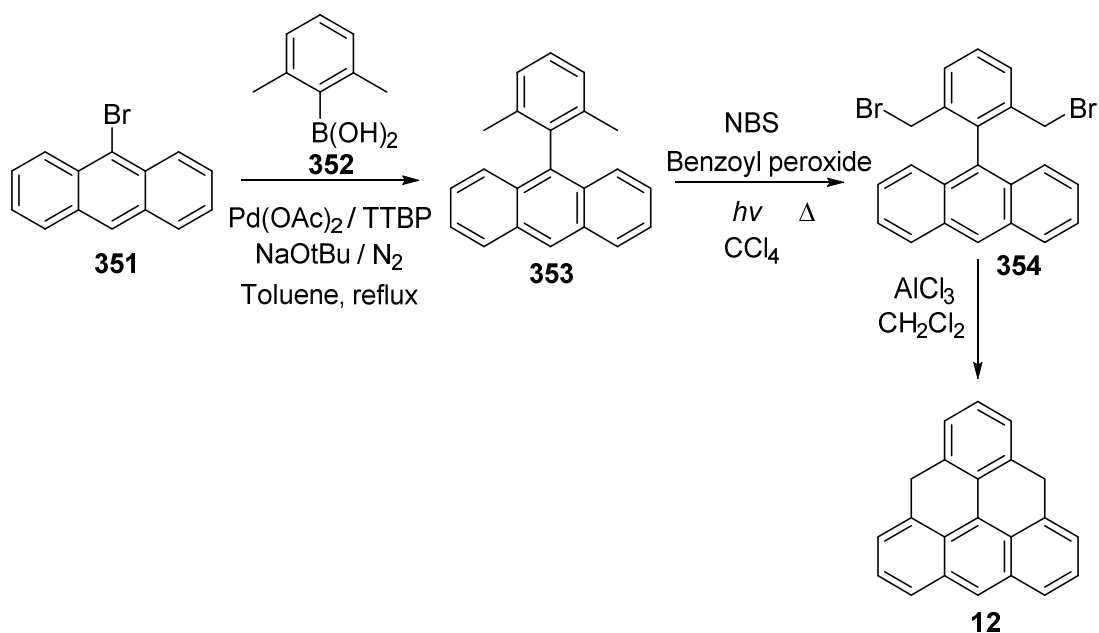


**Figure 77:** Tri-*tert*-butyl triangulene species **350** synthesised by Inoue *et al.*<sup>29</sup>

Since the 1950s triangulene has been of interest to many scientists especially due to its potential use in material science, but due to its instability it has yet to be isolated in the triplet form without any stabilising substituents.

#### 4.2 Route 1: Coupling reactions

We proposed a significantly shortened synthetic route to triangulene **10** *via* the dihydride (4,8-dihydro-4*H*,8*H*-dibenzo[*cd,mn*]pyrene) **12** (Scheme 74).



**Scheme 74: Proposed scheme for the synthesis of 4,8-dihydro-4H,8H-dibenzo[cd,mn]pyrene 12.**

In the proposed synthesis, a Suzuki palladium cross coupling reaction would generate the main framework of the triangulene molecule. The product **353** is tetra-*ortho*-substituted which is very sterically demanding with limited coupling methods available.<sup>396</sup> Literature predominantly suggests that using a very bulky ligand is needed for good yields but most ligands are very expensive to make or buy.<sup>397-403</sup> Due to the uncertainty in success surrounding this route, a cheaper alternative was pursued as this step could be optimised later in development. During extensive screening of the palladium catalyst reaction conditions, modest results and a cheaper alternative ligand was found. Raders *et al.* used a tri-*tert*-butylphosphine (TTBP) ligand, which provided a moderate yield of 36 % of the product **353** (Table 4).<sup>396, 404</sup> In addition a negligible amount of *bis*-anthracene was also produced. The optimised conditions are summarised in Scheme 74.

Reagent	Pd(OAc) <sub>2</sub> mol%	TTBP mol%	24 hours % yield	48 hours % yield
Experiment 1	2	3	19 %	21 %
Experiment 2	3	4	25 %	30 %
Experiment 3	4	5	27 %	36 %

**Table 4: Optimisation of catalyst and ligand conditions.**

Due to the steric hindrance, it was thought that the selective mono-bromination of each methyl group would be difficult, and this proved to be the case (Figure 78). A range of brominated products were formed including at the ten-position of the anthracene. This made purification of the products difficult and reduced the overall yield of the desired product **354** (Scheme 75).

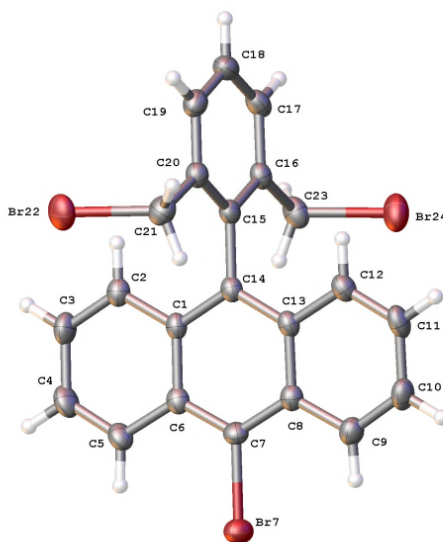
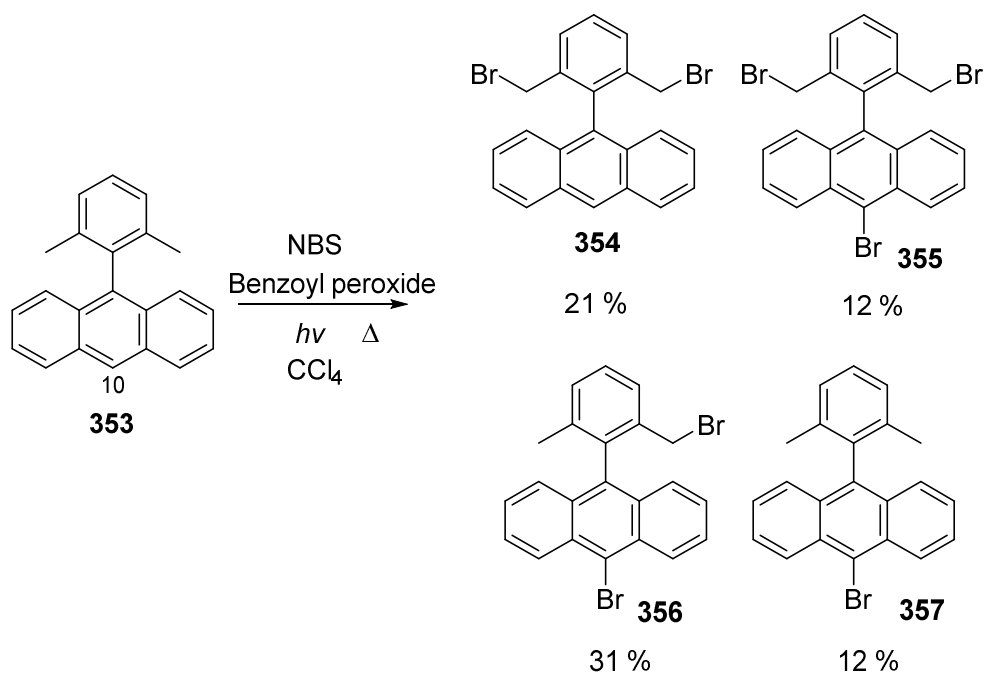


**Figure 78: Crystal structure of 9-bromo-10-(2,6-bis(bromomethyl)phenyl)anthracene 355.**



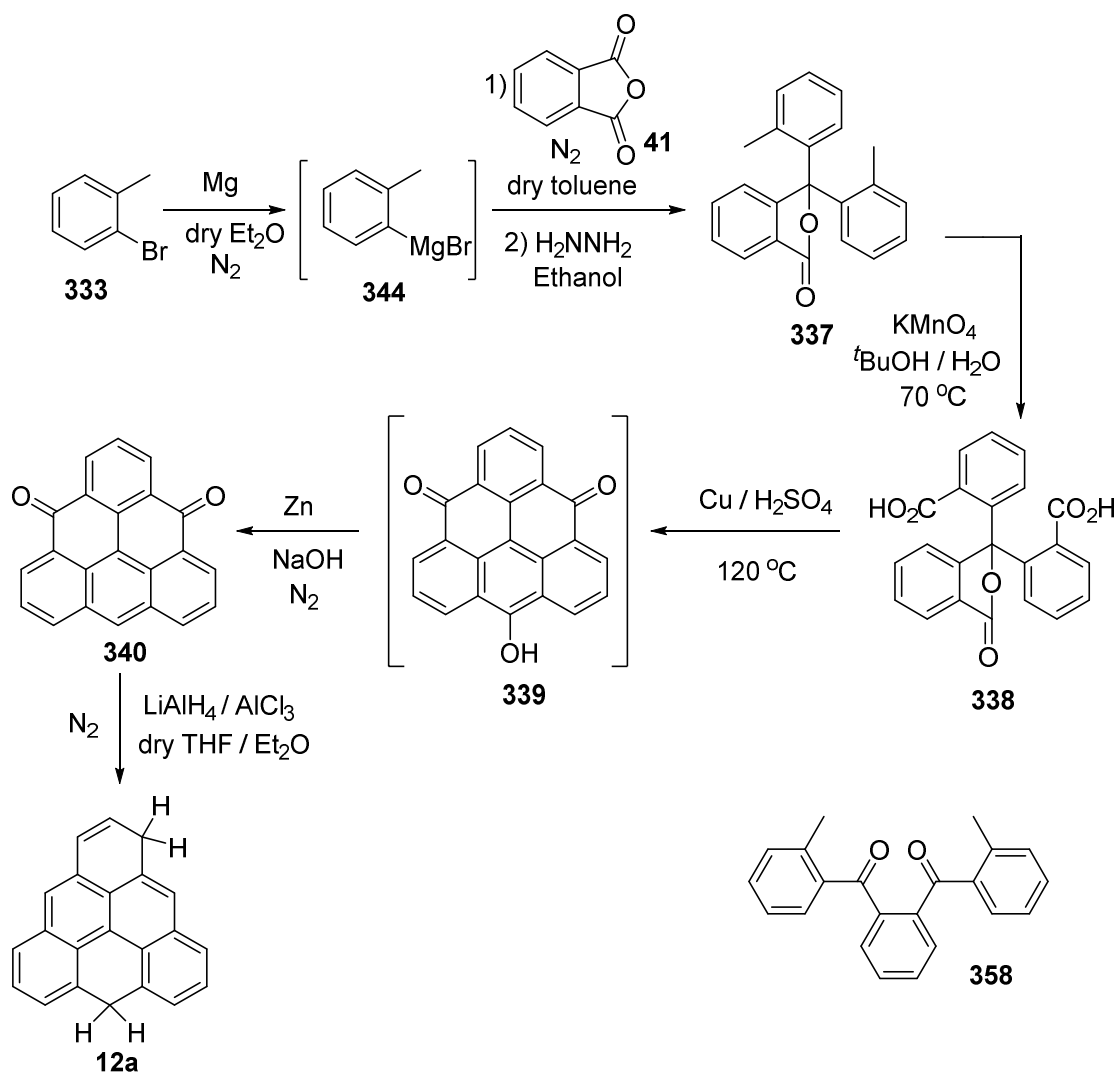
**Scheme 75: The different products produced when brominating 9-(2,6-dimethylphenyl)anthracene 353 in the presence of NBS, benzoyl peroxide and light in CCl<sub>4</sub>.**<sup>405</sup>

A Friedel-Crafts cyclisation was attempted on product **354**, however the desired product was not obtained with the reaction producing a complex mixture. After the low yielding steps and the difficulties met in bromination of the hindered substrate, including purification and the initially unsuccessful cyclisation, a previously successful pathway reported in literature would be pursued.<sup>388</sup>

### 4.3 Route 2: Cyclisation method

3,8-Dihydro-3*H*,8*H*-dibenzo[*cd,mn*]pyrene (dihydro-triangulene) **12a** is a known compound though only Hara *et al.* in 1977 has published any data related to it (basic <sup>1</sup>H NMR spectroscopy and mass spectrometry only).<sup>26</sup> The synthetic route was not mentioned by Hara *et al.* but unsuccessful attempts by Clar have contributed to forming the main skeletal structure of dihydro-triangulene.<sup>316</sup> Furthermore, Allinson *et al.* improved some of the synthetic steps which Clar published in their synthesis of the trioxytriangulene derivative **349**.<sup>388</sup> Therefore using a combination of these

synthetic steps a simplified synthetic pathway to form a dihydro-triangulene species **12a** could be proposed (Scheme 76).

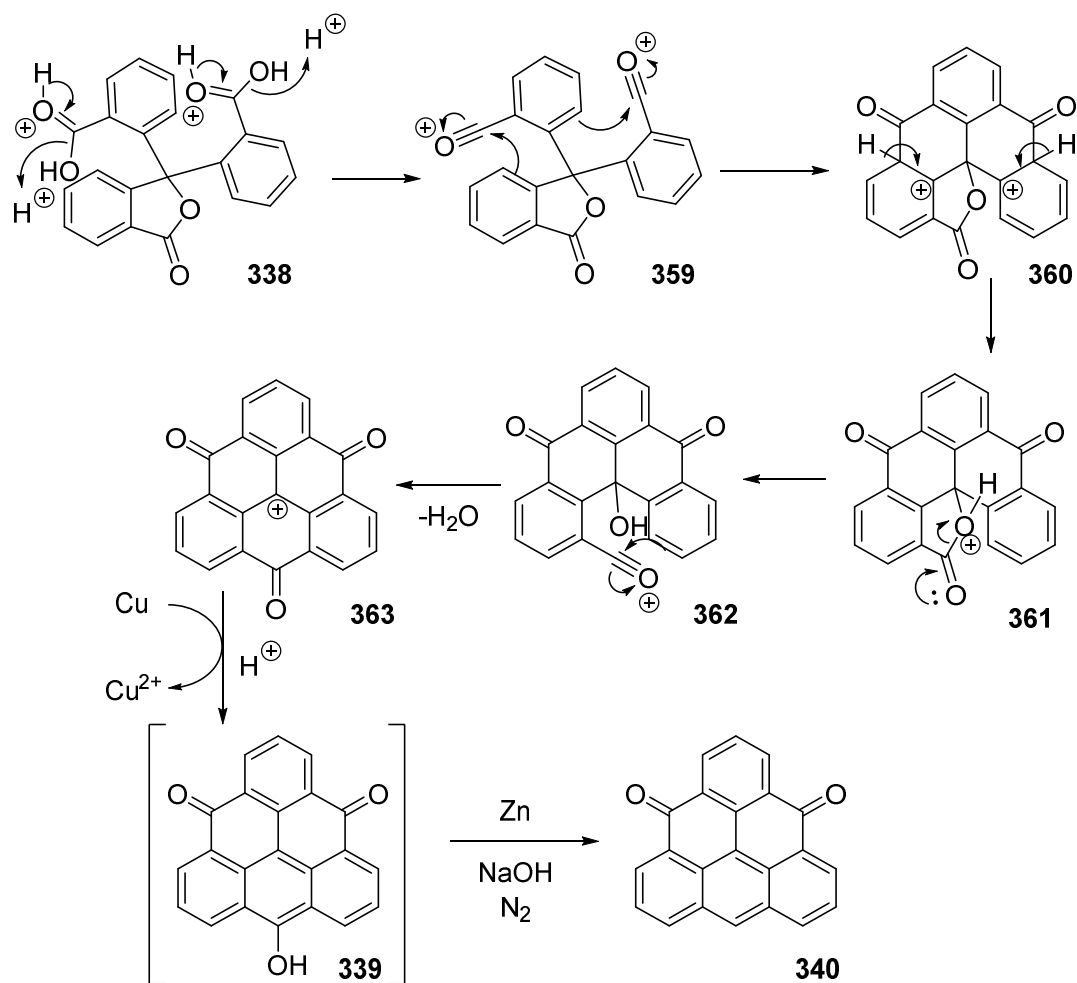


**Scheme 76:** An amalgamation of previous synthetic steps in an effort to synthesise dihydro-triangulene **12a**.<sup>316, 388</sup>

The first step produces a Grignard reagent from 2-bromotoluene **333** which is then reacted immediately with phthalic anhydride **41** to produce 3,3-di-*o*-tolyl-1,3-dihydro-2-benzofuran-1-one **337**.<sup>388</sup> This method was taken from Allinson *et al.*, which was an improvement of Clar's earlier work, where hydrazine monohydrate was added to solubilise the other major diketone impurity **358** whilst **337** could be collected as a solid.<sup>316, 388</sup>



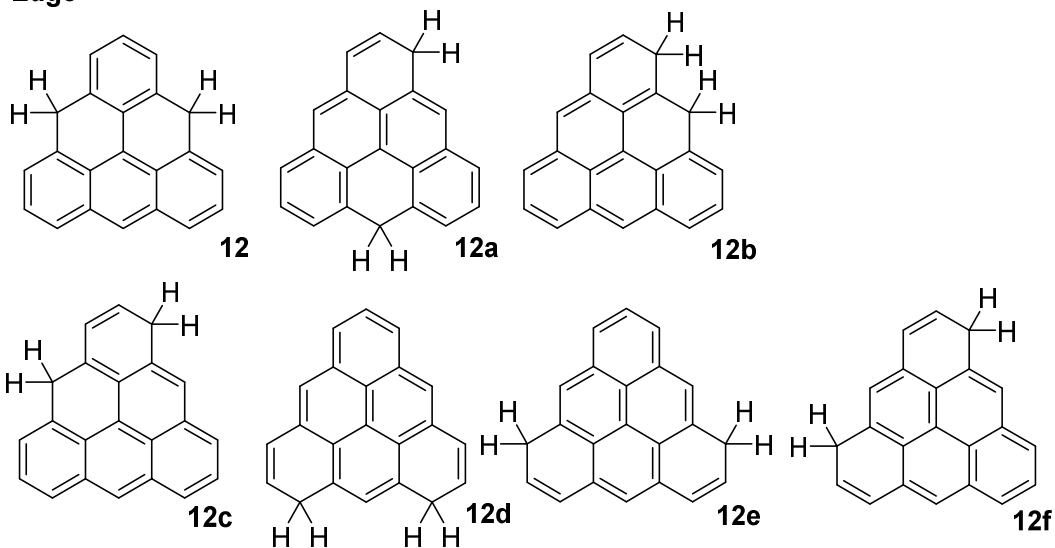
The use of sodium amalgam from the Allinson *et al.* synthesis was avoided by using potassium permanganate to oxidise the methyl groups by the method of Ye *et al.*<sup>388</sup>.<sup>406</sup> The oxidising agent (2.5 equiv.) was added twice, 2 hours apart, at room temperature in between heating, since potassium permanganate is known to decompose under heating.<sup>406</sup> After acidification, a pure white precipitate of di-(*o*-carboxyphenyl)-phthalide **338** was collected in a good yield of 72 %, requiring no further purification. The cyclisation step was completed by Clar's method, using copper powder in concentrated sulfuric acid with heat (Scheme 77).<sup>316</sup> A Friedel-Crafts type cyclisation occurred on both carboxylic acids, which formed water as a leaving group in strongly acidic conditions. A stable tertiary carbocation is then produced in the middle of the symmetrical structure **363** which is reduced by copper, and with further tautomerisation, produces the stable intermediate **339**. This intermediate was reduced with zinc, in base without further purification.<sup>316</sup> After column chromatography a bright red solid of pure 4,8-dioxo-4*H*,8*H*-dibenzo[*cd,mn*]pyrene **340** was obtained.



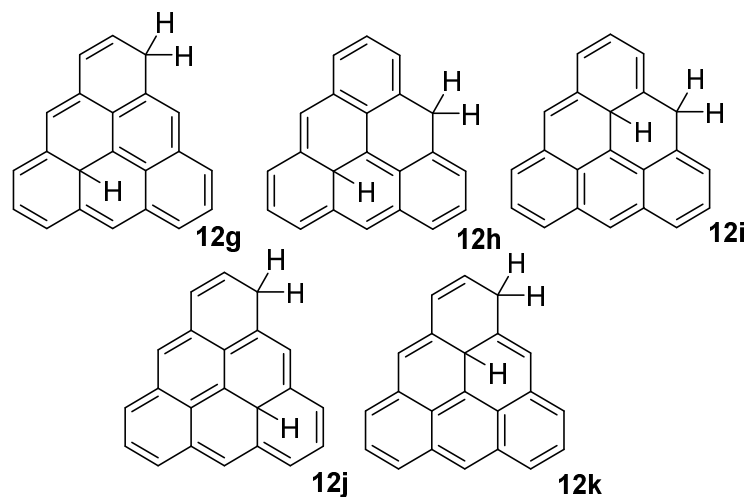
**Scheme 77:** Cyclisation mechanism of 338 where a stable carbocation is produced and the structure tautomerises to make the intermediate 339, this is then reduced by zinc to produce compound 340.

4,8-dioxo-4*H*,8*H*-dibenzo[*cd,mn*]pyrene **340** was reduced by using lithium aluminium hydride and aluminium chloride complex under an inert atmosphere, as reported by Hara *et al.*<sup>26</sup> One would assume that the reduction would produce isomer **12** (Figure 79) where the dihydrides have substituted the ketones, as Clar stated. However, upon completion of the reaction the  $^1\text{H}$  NMR spectrum did indeed show isomer **12a** as the major component which Hara *et al.* observed.

### Edge



### Edge and Inner



### Inner

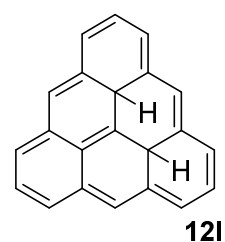


**Figure 79:** All possible dihydro-triangulene isomers 12-12l: 12a is observed whilst 12 was expected.

Furthermore, the  $^1\text{H}$  NMR spectrum also showed that other minor products were present which appeared to be different isomers, however these were difficult to distinguish due to overlapping peaks. The  $^{13}\text{C}$  NMR spectrum showed that the minor product also contained characteristic dihydride peaks. The NMR spectrum was measured immediately after work-up as dihydro-triangulene **12a** started oxidising within hours and had completely oxidised in a sealed NMR tube in deuterated chloroform within 5 days. Unfortunately, in an attempt to investigate the unknown

isomers and purify the mixture, column chromatography under an inert atmosphere was attempted, however the material oxidised rapidly.

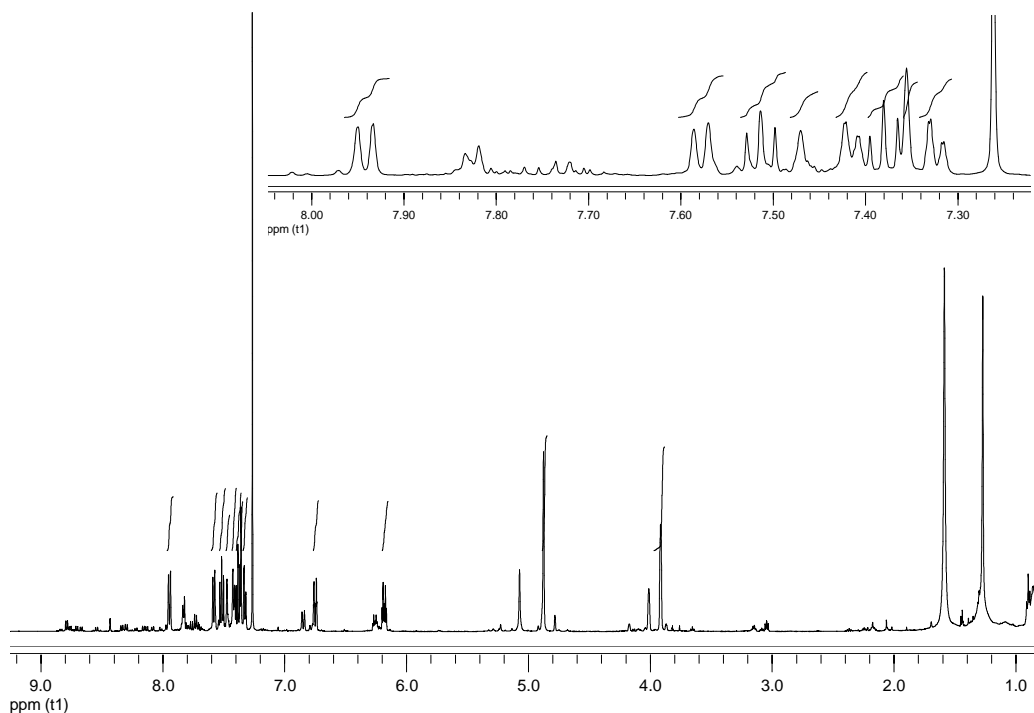


**Figure 80:**  $^1\text{H}$  NMR spectrum of dihydro-triangulene **12a**, the major isomer (integrated). Other minor peaks can also be seen of what is expected to be other isomers. An expanded version of the aromatic region is also shown where each peak is almost distinguishable.

NOE experiments were undertaken to distinguish the isomers of **12a**. The  $^1\text{H}$  NMR spectrum shows the minor isomer has a similar pattern to that of the major isomer **12a**, even though the aromatic region is overlapping and difficult to distinguish. Further up-field next to the major doublet of triplets (6.34 ppm) there is another minor doublet of triplets (6.81 ppm). Next to the other major doublet of triplets (6.18 ppm) there is another minor doublet of triplets (6.22 ppm) (Figure 81). The same occurs next to the two broad singlets (4.87 & 3.90 ppm), a minor broad singlet can be seen directly next to these (5.08 & 3.98 ppm) with integrals which match the ratio of these peaks, indicating this minor product is most likely to be isomer **12b** or **12c** (Figure 79).

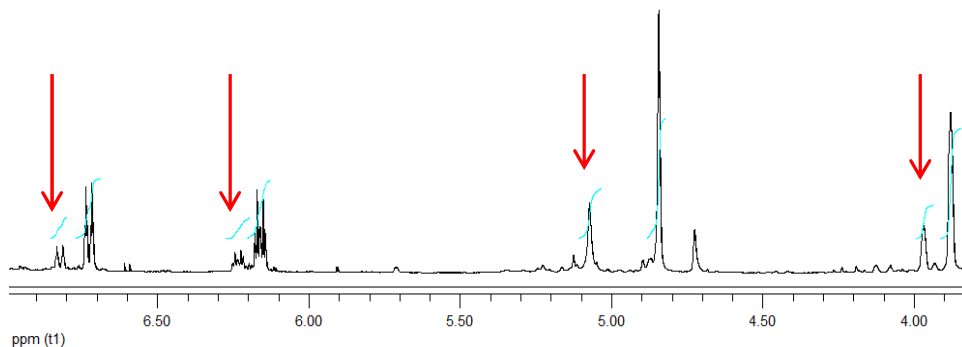


**Figure 81:**  $^1\text{H}$  NMR spectrum of dihydro-triangulene **12a** where another minor isomer can be seen. This isomer has the same two broad singlets (5.08 & 3.98 ppm) and two doublet of triplets (6.81 & 6.22 ppm) in close proximity to the major isomer **12a**.

Surprisingly the NOE experiments did not provide any signals of note, even when irradiation occurred at adjacent protons.

After the dihydro-triangulene **12a** sample was left to completely oxidise, the NMR spectroscopy data showed both isomers turned into ‘diketo-triangulenes’. However, isomer **12a** did not turn back to 4,8-dioxo-4*H*,8*H*-dibenzo[*cd,mn*]pyrene **340**. The specific isomer could not be determined due to unsuccessful purification, as the isomers eluted together during column chromatography. Furthermore, the minor isomer also oxidised into a ‘diketo-triangulene’ as identified by the NMR spectrum, but again the structure could not be determined due to the mixture of isomeric peaks.

During the analysis of dihydro-triangulene two isomers **12** and **12a** were always considered as the two most stable isomers. To help distinguish which would be more stable, Pauling Bond Order analysis was undertaken.<sup>80, 84, 85</sup> This determined that both isomers had the same degree of bonding (Figure 82) which suggested they were very similar in energy. On the other hand, DFT calculations by Dr D. Fox suggest that the unsymmetrical isomer **12a** is more stable than the symmetrical isomer **12** by  $4.5 \text{ kJ mol}^{-1}$ .<sup>407</sup>

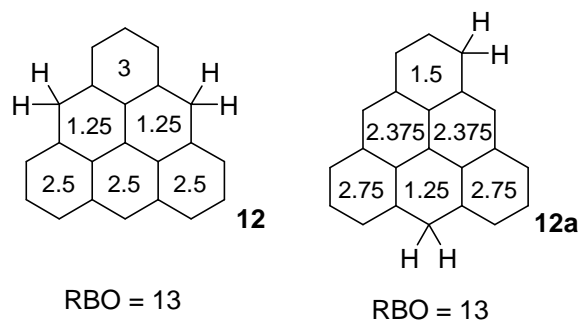
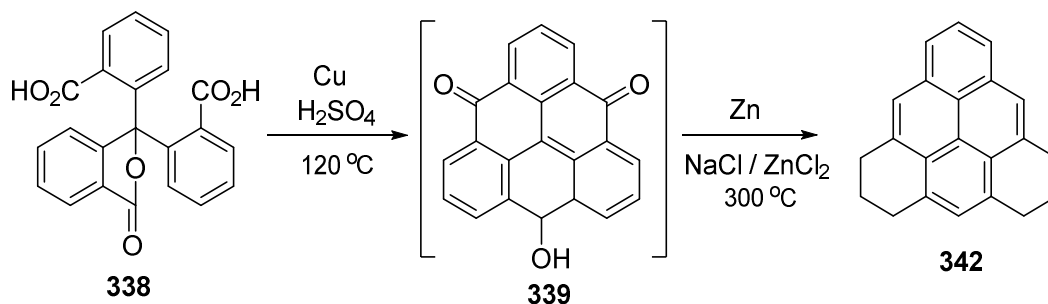


**Figure 82: Pauling Ring Bond Order of two of the main isomers of dihydro-triangulene 12 & 12a.**

### 4.3.1 Triangulene sample 1

Dihydro-triangulene **12a** was synthesised and sent for analysis to IBM. In addition, 1,2,3,5,6,7-hexahydro-dibenzo[*cd,mn*]pyrene **342**, was also synthesised, with the prospect that should dihydro-triangulene **12a** be too unstable, IBM would be able to cleave off four hydrogens from this stable compound. The synthesis of 1,2,3,5,6,7-hexahydro-dibenzo[*cd,mn*]pyrene **342** was undertaken using Clar's zinc-dust reduction from intermediate **339** (Scheme 78).



**Scheme 78: Clar's zinc reduction reaction produced 1,2,3,5,6,7-hexahydro-dibenzo[*cd,mn*]pyrene 342, a stable derivative of the triangulene series.**

The imaging results show that the sample had oxidised, as at least one ketone was always observed (Figure 83).

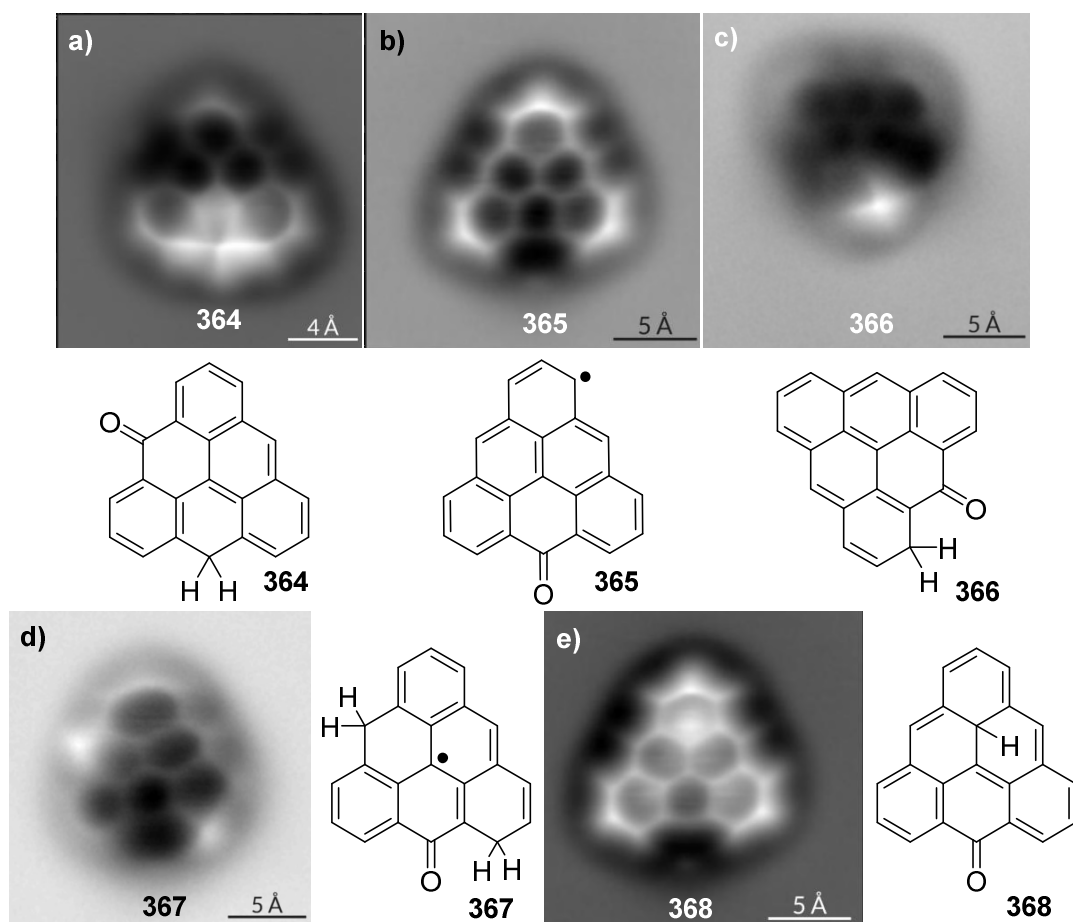


**Figure 83:** AFM images on NaCl (100) of oxidised samples a-e, with a possible radical structure shown 367. AFM image of 368 on Cu (111) where the compound shows a bright spot on an inner carbon suggesting an inner hydrogen present.<sup>321</sup>

A dihydride and ketone triangulene radical **367** was also identified, as well as a possible ‘mono-ketone triangulene’ **368**; where an inner hydrogen seems to be present. The sublimation stage of sample preparation for AFM analysis may result in the modification of some molecules, such as **367** and **368**. These compounds would not have been isolated if it was not for the existence of STM/AFM.

As for 1,2,3,5,6,7-hexahydro-dibenzo[*cd,mn*]pyrene **342**, the IBM group found it difficult to abstract the desired number of hydrogens. This was due to the number of dihydride groups in close proximity which destabilised the position of the compound and hence it was unsuccessful.

### 4.3.2 Triangulene sample 2

To circumvent the issue of oxidation in transit, the reduction of 4,8-dioxo-4*H*,8*H*-dibenzo[*cd,mn*]pyrene **340** was completed at IBM in Switzerland and placed in the AFM/STM vacuum chamber immediately.

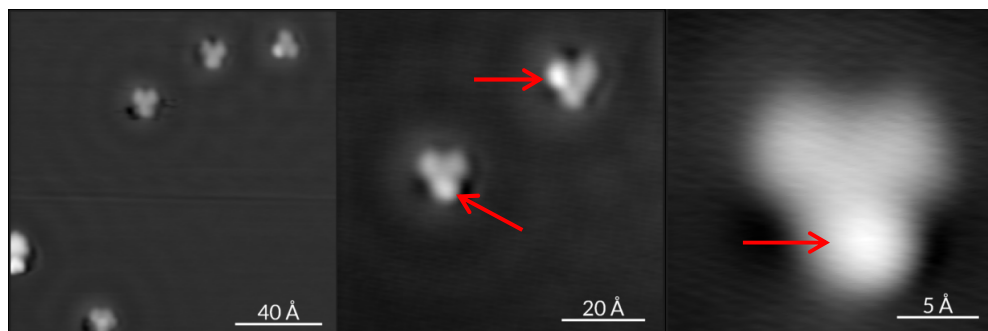


**Figure 84:** STM images on a Cu(111) surface where the dihydride group of **12a** can be clearly seen as a very bright spot on the images.<sup>321</sup>

Dihydro-triangulene **12a** was dehydrogenated by pulsing a current of specific energy over the bright dihydride region with the STM tip. After the hydrogen is cleaved, the same is completed on the second dihydride (Figure 84). Thus, triangulene **10** is formed (Figure 85). In addition to the observed dihydro-triangulene isomers, some oxidised products were also visualised (Figure 85). This illustrates how unstable the precursor dihydride **12a** is given that it was prepared with little exposure to air.



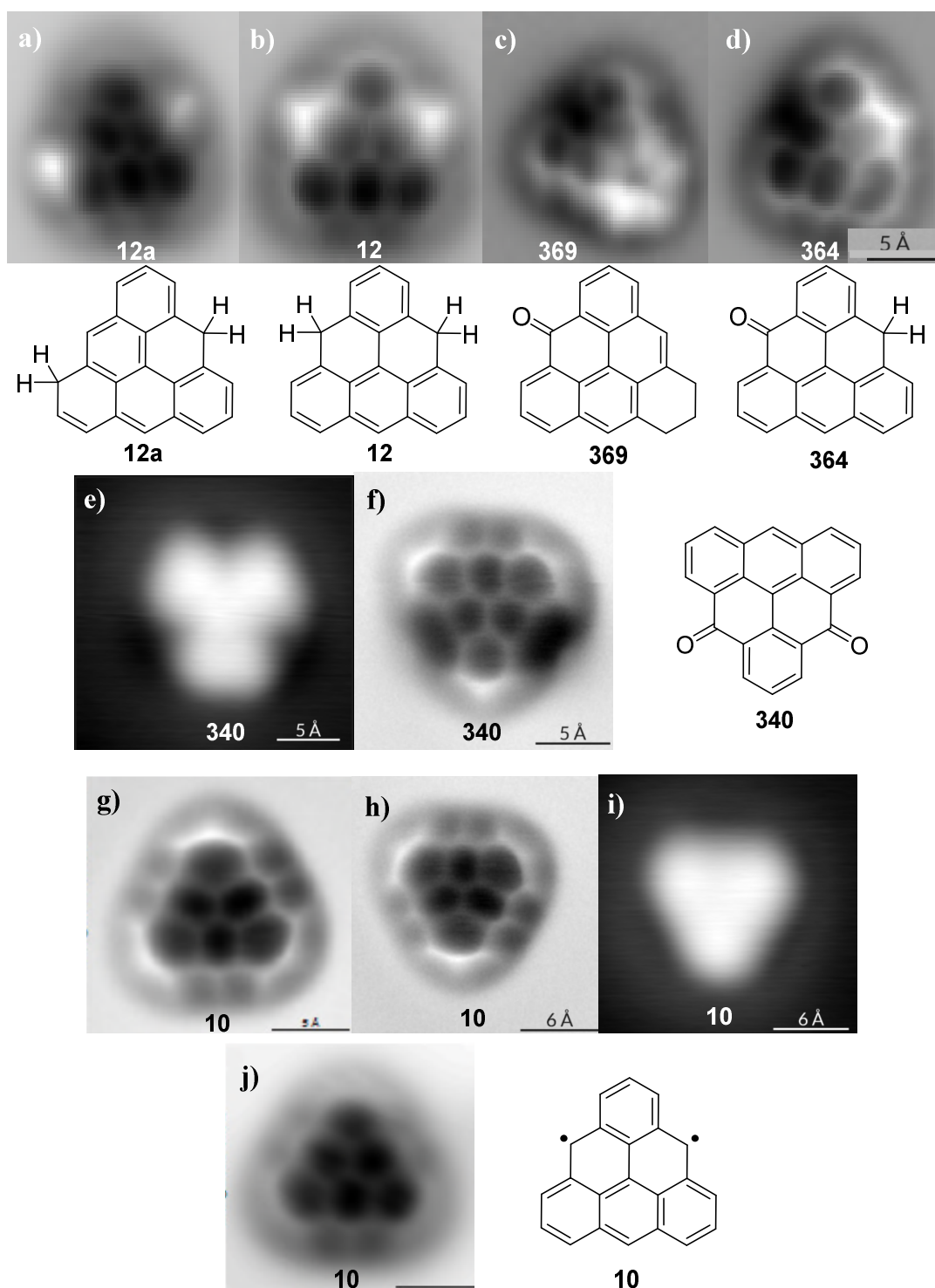


**Figure 85:** AFM images of molecules observed on NaCl (100) surface; (a-b) dihydro-triangulene isomers. (c-e) oxidised species including 4,8-dioxo-4*H*,8*H*-dibenzo[*cd,mn*]pyrene (f) with its STM image (e). Images on Cu (111) surface of triangulene (g-h) and the corresponding STM (i). Image of triangulene on Xe (111) surface (j).<sup>321</sup>

The STM image relates to the AFM image in the same way, where the bright area contains more electron density than the darker areas. For example, the STM image of triangulene is triangular, though the dark patches of the ketones appear to have indented either side of the image for 4,8-dioxo-4*H*,8*H*-dibenzo[*cd,mn*]pyrene **340** (Figure 85). Triangulene was produced on a xenon surface at 5 K, as this crystal formation is inert and will create the least perturbation of the structure, thus forming a realistic image of triangulene.

Furthermore, STS and STM orbital imaging were performed on triangulene using the same method as compound **310** (see Chapter 3, Figure 74). Using NIR and PIR, both orbital images were identical, thus proving the triplet state of triangulene (Figure 86).

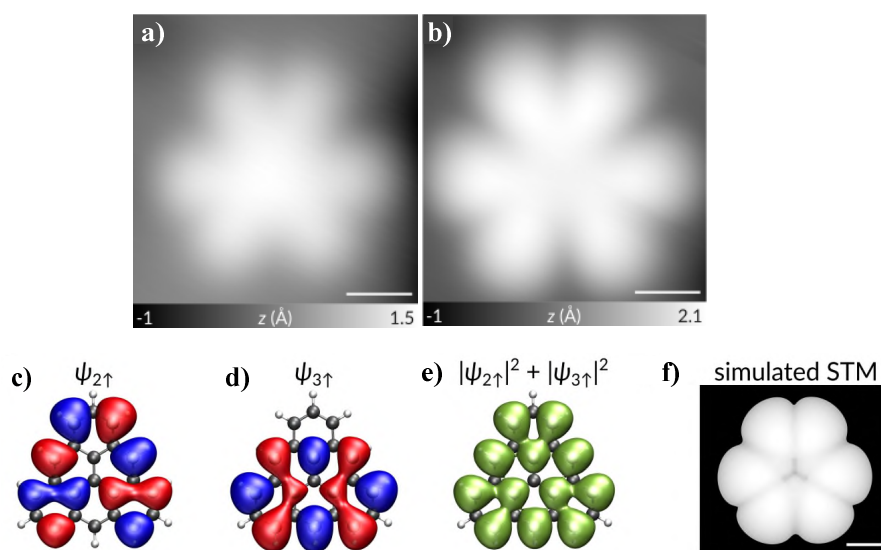


**Figure 86:** a) STM image of the PIR (-1.4 V), b) STM image of the NIR (1.85 V) of triangulene **12a**. DFT calculation of c) SOMO 1, d) SOMO 2 and e) SOMO 1 & 2 combined. f) the simulated image of (e) under the STM tip, where the actual images can be seen in (a) & (b). All data and calculations provided by IBM Zürich.<sup>319, 412</sup>

#### 4.4 Summary

After the initial setback in the synthetic route, the formation of the very unstable triplet-state of triangulene, by the combination of synthesis and STM/AFM was successfully completed. It has been over 74 years since Clar first mentioned triangulene, including many remarks stating that it cannot exist due to its non-Kekulé nature. Nevertheless, STM/AFM is a powerful tool in producing and characterising unstable and sensitive molecules for material and organic chemists.

## 5 Chapter 5: Conclusions and future work

Successful synthesis of the 6*H*-benzo[*cd*]pyrene radical and the imaging of the olympicene molecule by the use of AFM/STM was accomplished. Optimisation of the synthetic route led to the discovery that 6*H*-benzo[*cd*]pyrene is produced first but oxidises in the reaction conditions to 6-oxo-6*H*-benzo[*cd*]pyrene. From this, different arene starting materials were tested in glycidol and sulfuric acid (naphthalene, anthracene and perylene) and the discovery of further reactions were observed. Furthermore, it is suggested that *peri*-condensation reactions occur on the starting materials until the products formed precipitate out of the solution due to their insolubility. Carbon labelled studies have supported this view. The mechanism has also been proposed for ring addition, as a sequential two-stage polar and radical reaction onto each starting material with agreeable DFT calculations. AFM/STM proved to be the best technique to identify most of the products formed in the reactions, including the larger PAHs which were created due to multiple ring additions (black solid) where previous literature did not analyse this.

Another target was also accomplished in that of triangulene, where an optimised method of an older synthesis was utilised. The unstable diradical was isolated and imaged for the first time since its proposal in 1941 by the use of AFM/STM. It has become apparent that PAHs are difficult compounds to study, due to the simple structure they possess and therefore, many have found them difficult to characterise. Here, AFM/STM has served as an invaluable technique to fully characterise PAHs and also for the production of reactive non-Kekulé structures. In the future, this technique is sure to become increasingly popular to the wider scientific field, for example synthetic chemistry, to characterise compounds which are not just planar,

but also challenging to identify and difficult to prepare by common techniques in order to alleviate any doubt about their structure.

Future work would include more analysis and calculations on the mechanism of *peri*-condensation ring addition with the suggested polar and radical pathways. The production of structures with different side chains to be observed under the STM/AFM to help distinguish side-groups of compounds. Furthermore, imaging different molecules with heteroatoms to gain a better understanding of how different elements look under the microscopy techniques, such as poly-thiazoles. Synthesise a library of difficult but interesting PAHs such as other triplet state compounds of interest and possibly those in the triangulene series. Finally, to consider how graphene could be synthesised *via* this *peri*-condensation reaction so there are less defects within the structure than current methods.

## 6 Experimental

### 6.1 Experimental synthetic chemistry

Reactions were carried out at room temperature unless otherwise stated. Column chromatography purifications were carried out using silica gel LC60A40-63 micron. Melting points were recorded twice on a Stuart SM10 instrument. Infra-red spectra were recorded on a Perkin-Elmer paragon 1000 FT-IR spectrophotometer. Hydrogen and carbon NMR were recorded on a Bruker Advanced DPX-300 MHz, DPX-400 MHz, DRX-500 MHz, AVIII-600 MHz or AVII-700 MHz Fourier transform spectrometers and all samples were submitted in deuterated  $\text{CDCl}_3$  unless otherwise stated. All coupling constant ( $J$ ) values are quoted in Hertz (Hz) and are rounded to the nearest 0.5 Hz and all chemical shift are in parts per million (ppm). Hydrogen-decoupled carbon NMR spectra were taken using PENDANT (polarization enhancement during attached nucleus testing), HMQC (heteronuclear multiple quantum coherence), HMBC (Heteronuclear multiple-bond correlation spectroscopy), INADEQUATE (incredible, natural-abundance double-quantum transfer experiment) and COSY (correlation spectroscopy) to further assist in compound analysis. Mass spectra were obtained on a micrOTOF 87 instrument using mass electrospray ionization with positive ion polarity unless otherwise stated and a Varian 3800-4000 GC-MS/MS (EI) Advion CMS instrument with an ASAP source.

EDX & SEM: SEM images of the samples were collected using Zeiss SUPRA 55VP FEG scanning electron microscope. A working distance of 10 mm and a gun voltage of 10 kV were used. Energy Dispersive X-ray Analysis was also performed using the SEM in order to determine the elemental composition of the materials.

TGA were recorded using on a Mettler-Toledo DSC1-Star system at a heating rate of 10 °C/min from 25 °C – 800 °C under air, unless otherwise stated.

Raman measurement were taken on a Renishaw inVia Reflex Raman Microscope machine, under 633 nm excitation with a 20x microscope objective lens. All samples were deposited in powder form without use of any solvents.

TEM images were taken using a JEOL 2100 TEM operating at 200 kV with a Gatan Orius SC600 digital camera.

Solid-state NMR experiments were performed using Bruker Avance III NMR spectrometer operating at a  $^1\text{H}$  Larmor frequency of 500.1 MHz for  $^{13}\text{C}$ - $^1\text{H}$  experiments ( $^{13}\text{C}$  Larmor frequency of 125.8 MHz). A Bruker 4 mm triple-resonance Magic-Angle Spinning (MAS) probe operating in a double-resonance mode was used, with 36 mg of Gace packed into the rotor. One-pulse  $^1\text{H}$ ,  $^{13}\text{C}$ ,  $^{13}\text{C}$  CPMAS and  $^{13}\text{C}$ - $^1\text{H}$  heteronuclear correlation experiments were performed. 64 coadded transients for the  $^1\text{H}$  experiments using a relation delay of 5 s to overall acquisition of 5 minutes. For the  $^{13}\text{C}$  one pulse experiments, 5120 coadded transients were acquired using a relation delay of 10 s to an overall recording time, 11 h, whereas  $^{13}\text{C}$  CPMAS experiments were acquired with 2048 coadded transients using a recycle delay of 6 s to an overall acquisition time of 4 h. In all cases,  $^{13}\text{C}$  experiments were performed at variable spinning frequencies; 10 kHz and 12.5 kHz in order to identify spinning sidebands. In  $^{13}\text{C}$ - $^1\text{H}$  correlation and in CP MAS experiments, SPINAL64  $^1\text{H}$  heteronuclear decoupling with a pulse duration of 5  $\mu\text{s}$  was applied for an acquisition time of 40 ms. The  $^1\text{H}$  nutation frequency for pulses and decoupling was 100 kHz, where the  $^1\text{H}$  90 degree pulse duration was 2.5  $\mu\text{s}$ . For  $^{13}\text{C}$  pulses, the  $^{13}\text{C}$  90 degree pulse length was 4.0 ms. Data was zero filled to 2048 points prior to

Fourier Transformation.  $^{13}\text{C}$  and  $^1\text{H}$  chemical shifts are referenced with respect to neat TMS using adamantane as a secondary reference (38.5 ppm for the higher-ppm  $^{13}\text{C}$  resonance and 1.85 ppm for the  $^1\text{H}$  resonance). For the 2D  $^1\text{H}$ - $^{13}\text{C}$  correlation experiment, eDUMBO-122 homonuclear decoupling was employed during the  $^1\text{H}$  evolution period and the  $t$  and  $t\phi$  spin-echo durations. The 32 ms eDUMBO-122 cycle was divided into 320 steps of 100 ns. Pulse sequences employing  $^1\text{H}$  homonuclear decoupling use pre-pulses to take into account the tilting of the effective field away from the  $x, y$  plane of the rotation frame using a pre-pulse duration of 0.8 ms was used.

XPS: The samples investigated in this study were mounted on Omicron sample plates using carbon tape and loaded in to the vacuum chamber. During the experiments the samples were stored in a 12-stage storage carousel, located between the preparation and main analysis chambers, for storage at pressures of less than  $2 \times 10^{-10}$  mbar. The x-ray photoemission spectroscopy (XPS) measurements were performed in the main analysis chamber (base pressure  $2 \times 10^{-11}$  mbar), with the sample being illuminated using an XM1000 monochromatic Al  $K\alpha$  x-ray source (Omicron Nanotechnology). The measurements were conducted at room temperature and at a take-off angle of  $90^\circ$  with respect to the surface parallel. The photoelectrons were detected using a Sphera electron analyser (Omicron Nanotechnology), with the core levels recorded using a pass energy of 10 eV (resolution approx. 0.47 eV). The spectrometer work function, resolution and binding energy scale were calibrated using the Fermi edge and  $3d_{5/2}$  peak recorded from a polycrystalline Ag sample immediately prior to the commencement of the experiments. An Omicron CN10 charge neutraliser was used throughout the experiment in order to prevent surface charging. As a result, all binding energies were referenced with respect to the



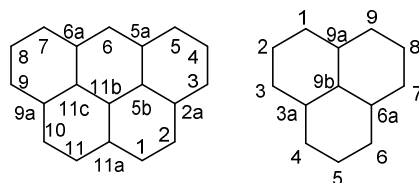
adventitious carbon component in the C 1 s region at 284.6 eV. The data were analysed using the CasaXPS package, with Voigt (Gaussian-Lorentzian) lineshapes and Shirley backgrounds used throughout. For compositional analysis, the analyser transmission function has been determined using Ag, Au and Cu foils to determine the detection efficiency across the full binding energy range to an accuracy of better than 2 %.

AFM and STM: The experiments were carried out in a homebuilt combined STM and AFM operating under ultrahigh vacuum conditions (base pressure  $p < 10^{-10}$  mbar) at a temperature  $T = 5$  K. The microscope was equipped with two different qPlus sensors (1, 2) with eigenfrequencies of 31036 Hz and 25035 Hz, respectively, a stiffness of  $k = 1800$  N/m and Q values on the order of  $10^5$ . The voltage  $V$  was applied to the sample. The AFM was operated in frequency-modulation mode (3), and an oscillation amplitude of  $A = 50$  pm was used. STM images were recorded in constant-current mode (closed feedback loop) and show the topography  $z$ . AFM images were performed in constant-height mode (open feedback loop) and show the frequency shift  $\Delta f$ . A height offset  $\Delta z$  with respect to an indicated STM set point above the bare surface (Cu, NaCl, Xe) is given for each AFM image. Positive height offsets refer to a distance decrease. Scanning tunneling spectra, that is  $I(V)$  curves, were also recorded in constant-height mode. The differential conductance,  $dI/dV (V)$ , was then obtained by numerical differentiation of the  $I(V)$  signal. STM and AFM images, as well as numerically obtained  $dI/dV (V)$  curves were post-processed using Gaussian low-pass filters (FWHM corresponding to 4 to 6 image pixels for raw data of  $160 \times 160$  to  $640 \times 640$  pixels). The tip had been terminated with a CO molecule for all AFM images. STM images and STS spectra were acquired with metal-terminated tips, except where stated otherwise. CO

molecules were picked up from NaCl islands, or on Xe monolayers from step edges to two-layer-thick Xe islands. Sample preparation for AFM/STM: Cu(111) single crystals were cleaned by sputtering and annealing cycles. Experiments were performed on the bare Cu(111) surface, on 2 monolayer (ml) thick islands of NaCl and on 1-ml-thick islands of Xe. NaCl islands were grown by sublimation from a crucible onto the cleaned Cu(111) surface held at a temperature of 270 K (4). This resulted in (100)-terminated NaCl islands of 2 mL to 3 mL thickness. Closed-packed Xe films were grown by Xe adsorption onto the Cu(111) crystal while the sample was inside the microscope head at temperatures below 15 K. A background Xe pressure of  $2 \times 10^{-5}$  mbar was maintained in the UHV chamber, and a shutter to the microscope head was opened for about 30 s. This resulted in Xe islands of 1 mL to 2 mL thickness. Precursor molecules were thermally sublimed in a two-step procedure. First, the compound was filled into crucibles made from tantalum, which were inserted into the load-lock of the UHV chamber, and evacuated to a pressure better than  $1 \times 10^{-4}$  mbar. Next, the compound was sublimed from the crucible onto a mobile evaporator in the load- lock (at  $p \sim 10^{-8}$  mbar) of the UHV chamber. Then, this evaporator was introduced into the STM chamber ( $p < 10^{-10}$  mbar), and the compound was deposited by means of flash sublimation onto the cold sample (below 10 K) placed in the microscope head. In addition, low coverages of CO molecules (for tip preparation) were dosed onto the cold sample.

Glycerol ( $^{13}\text{C}_3$ , 99 %) was purchased from Goss Scientific to help undertake carbon labelled experiments.

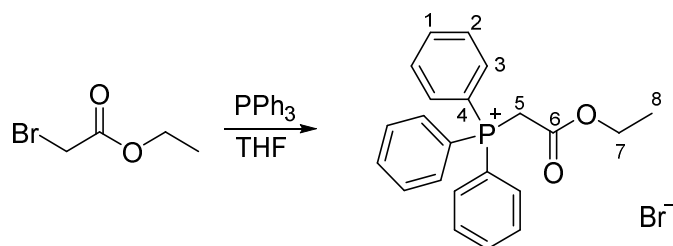
PAH Compound carbons are numbered according to the standard numbering scheme below for five- and three-fused rings:



## 6.2 Experimental for Chapter 2

### 6.2.1 Synthesis of 6*H*-benzo[*cd*]pyrene: Method 1

#### 6.2.1.1 (Ethoxycarbonylmethyl)-triphenylphosphonium bromide (370)



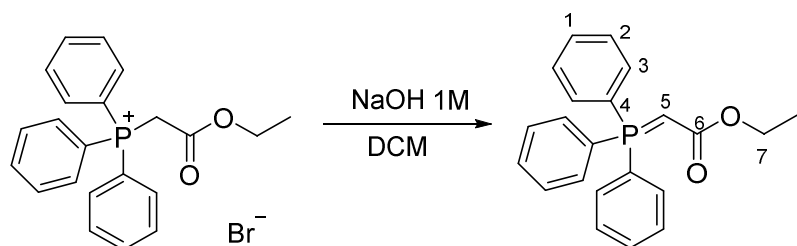
By the method of Popaj and Hesse.<sup>408</sup>

Ethyl bromoacetate (5.00 mL, 45.0 mmol) was added to a solution of triphenylphosphine (11.8 g, 45.0 mmol) in THF (65.0 mL) and the mixture was heated at 60 °C overnight. A white precipitate was observed and diethyl ether was added to aid precipitation. The mixture was filtered, washed with diethyl ether, dried over Na<sub>2</sub>SO<sub>4</sub> and concentrated *in vacuo* to produce a white powder (18.5 g, 96 %).

$\nu_{\max}/\text{cm}^{-1}$ : 3038, 2991 (CH), 1714 (CO), 1588 (aromatic), 1440 (P-Ph), 1307, 880 (aromatic ring); melting point: 158 - 161 °C (lit. 153 - 155 °C)<sup>408</sup>;  $\delta_{\text{H}}$  (400 MHz, CDCl<sub>3</sub>): 7.77 - 7.52 (15H, m, H-1, 2, 3), 5.25 (2H, d, *J* 14.0, H-5), 3.87 (2H, q, *J* 7.0, H-7), 0.89 (3H, t, *J* 7.0, H-8);  $\delta_{\text{C}}$  (100 MHz, CDCl<sub>3</sub>): 163.9 (d, <sup>2</sup>*J*<sub>CP</sub> 3.5, C-6), 134.9 (d, <sup>4</sup>*J*<sub>CP</sub> 3.0, C-1), 133.5 (d, <sup>3</sup>*J*<sub>CP</sub> 11.0, C-2), 129.9 (d, <sup>2</sup>*J*<sub>CP</sub> 13.0, C-3), 117.4 (d, <sup>1</sup>*J*<sub>CP</sub>

89.0, C-4), 62.5 (C-7), 32.7 (d,  $^1J_{CP}$  56.5, C-5), 13.3 (C-8); HRMS (ESI)  $m/z$  ( $C_{22}H_{22}O_2P$   $[M-Br]^+$  requires 349.1352) found 349.1356. This compound is previously reported and data are consistent with these reports.<sup>408</sup>

### 6.2.1.2 Ethyl (triphenylphosphoranylidene)acetate (218)

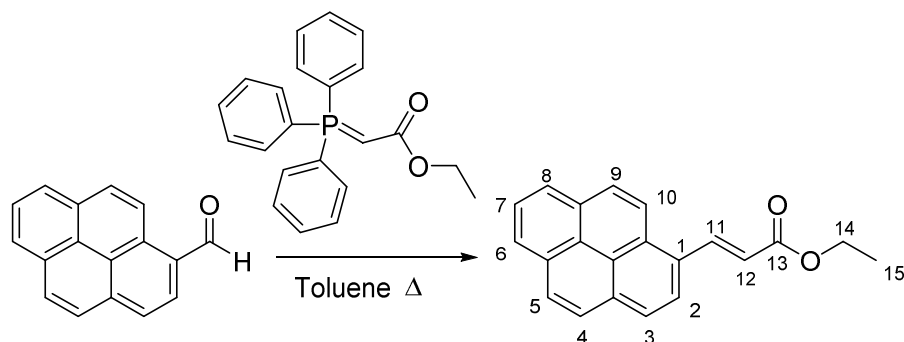


By the method of Sadhukhan *et al.*<sup>409</sup>

(Ethoxycarbonylmethyl)-triphenylphosphonium bromide (0.5 g, 1.16 mmol) was dissolved in dichloromethane and aqueous sodium hydroxide (1.0 M, 20 mL) solution was added and left to react for 15 minutes with vigorous stirring. The organic layer was separated and the aqueous layer was extracted with dichloromethane (3 x 15 mL). The organic layers were collected, dried over  $Na_2SO_4$  and concentrated *in vacuo* to give a white solid (0.4 g, 98 %).

$\nu_{max}/cm^{-1}$ : 3056, 2977 (CH), 1603 (CO), 1436 (P-Ph), 1370 ( $CH_3$  deformation), 1328, 890 (aromatic ring); melting point: 126 - 130 °C (lit. 128 - 130 °C)<sup>410</sup>;  $\delta_H$  (400 MHz,  $CDCl_3$ ): 7.68 - 7.61 (6H, m, H-aryl), 7.56 - 7.50 (3H, m, H-aryl), 7.47 - 7.41 (6H, m, H-aryl), 4.08 - 3.81 (2H, br. s, H-7), 2.98 - 2.72 (1H, br. s, H-5), 1.08 - 0.52 (3H, br. s, H-8);  $\delta_C$  (125 MHz,  $CDCl_3$ ): 171.1 (d,  $^2J_{CP}$  10.0, C-6), 132.5 (d,  $^2J_{CP}$  10.0, C-3), 131.5 (C-1), 128.3 (d,  $^3J_{CP}$  12.0, C-2), 126.3 (d,  $^1J_{CP}$  89.0, C-4), 57.4 (C-7), 29.6 (d,  $^1J_{CP}$  129.5, C-5), 14.6 (C-8); HRMS (ESI)  $m/z$  ( $C_{22}H_{21}O_2PNa$   $[M+Na]^+$  requires 371.1171) found 371.1177. This compound is previously reported and data are consistent with these reports.<sup>409</sup>

### 6.2.1.3 Ethyl 3-(1-pyrenyl)acrylate (219)



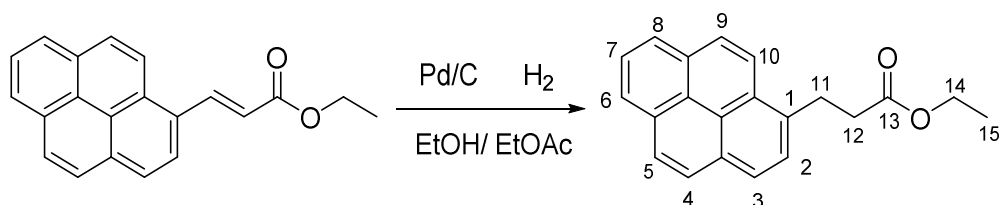
By the method of Hermans *et al.*<sup>411</sup>

1-Pyrenecarboxaldehyde (1.13 g, 4.90 mmol) was added to a solution of ethyl (triphenylphosphoranylidene)acetate (1.71 g, 4.90 mmol) in toluene (80.0 mL) and the reaction mixture was heated under reflux for 96 hours. The mixture was left to cool and the solvent was removed *in vacuo* to form a crude yellow/orange solid. The crude product was purified by column chromatography using chloroform : petroleum ether 40 - 60 °C (8:2) to yield yellow granules (1.30 g, 89 %).

$\nu_{\max}/\text{cm}^{-1}$ : 2980, 2905 (CH), 1705 (C=O), 1620, 1595 (aromatic), 1459 (C-H deformations), 1372 (CH<sub>3</sub> deformation), 1278, 838 (aromatic ring) 971 (alkene); melting point: 106 - 109 °C (lit. 102 - 103 °C)<sup>317</sup>;  $\delta_{\text{H}}$  (400 MHz, CDCl<sub>3</sub>): 8.83 (1H, d, *J* 15.5, H-12), 8.49 (1H, d, *J* 9.5, H-aryl), 8.29 - 8.00 (8H, m, H-aryl), 6.71 (1H, d, *J* 15.5, H-11), 4.37 (2H, q, *J* 7.0, H-14), 1.42 (3H, t, *J* 7.0, H-15);  $\delta_{\text{C}}$  (125 MHz, CDCl<sub>3</sub>): 167.1 (C-13), 141.2 (C-12), 132.6 (C-aryl), 131.2 (C-aryl), 130.6 (C-aryl), 129.6 (C-aryl), 128.4 (C-aryl), 128.2 (C-aryl), 127.2 (C-aryl), 126.2 (C-aryl), 125.9 (C-aryl), 125.7 (C-aryl), 124.9 (C-aryl), 124.8 (C-aryl), 124.5 (C-aryl), 124.1 (C-aryl), 122.4 (C-aryl), 120.2 (C-11), 60.6 (C-14), 14.4 (C-15) \*one <sup>13</sup>C peak missing due to overlapping peaks; HRMS (ESI) *m/z* (C<sub>21</sub>H<sub>17</sub>O<sub>2</sub> [M+H]<sup>+</sup> requires 301.1223)

found 301.1230. This compound is previously reported and data are consistent with these reports.<sup>317</sup>

#### 6.2.1.4 Ethyl 3-(1-pyrenyl)propanoate (220)



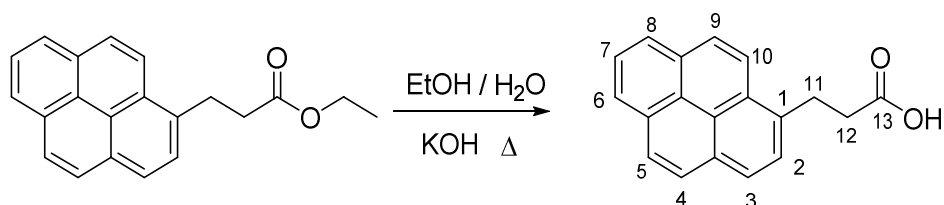
By the method of Hermans *et al.*<sup>411</sup>

Ethyl 3-(1-pyrenyl)acrylate (3.02 g, 10.1 mmol) was dissolved in ethyl acetate (70 mL). Ethanol (70 mL) and 10 % Pd/C (2 mol %) were then added to the mixture and the air in the system was replaced with hydrogen. The reaction was left under a hydrogen balloon at room temperature for 29 hours. The reaction mixture was then filtered through a pad of celite with ethyl acetate and the solvent was removed *in vacuo* to yield a dark yellow solid (3.02 g, 99 %).

$\nu_{\max}/\text{cm}^{-1}$ : 2989, 2916 (CH), 1728 (C=O), 1603, 1586 (aromatic), 1456 (C-H deformations), 1372 (CH<sub>3</sub> deformation), 1287, 846 (aromatic ring); melting point: 160 - 162 °C (lit. 168 °C)<sup>412</sup>;  $\delta_{\text{H}}$  (400 MHz, CDCl<sub>3</sub>): 8.25 (1H, d, *J* 9.0, H-aryl), 8.17 - 8.13 (2H, m, H-aryl), 8.10 - 8.05 (2H, m, H-aryl), 8.02 - 7.96 (3H, m, H-aryl), 7.87 (1H, d, *J* 8.0, H-aryl), 4.17 (2H, q, *J* 7.0, H-14), 3.70 (2H, t, *J* 8.0, H-11), 2.86 (2H, t, *J* 8.0, H-12), 1.25 (3H, t, *J* 7.0, H-15);  $\delta_{\text{C}}$  (125 MHz, CDCl<sub>3</sub>): 172.8 (C-13), 134.3 (C-aryl), 131.2 (C-aryl), 130.6 (C-aryl), 129.9 (C-aryl), 128.3 (C-aryl), 127.3 (C-aryl), 127.2 (C-aryl), 126.8 (C-aryl), 126.6 (C-aryl), 125.6 (C-aryl), 124.8 (C-aryl), 124.7 (C-aryl), 122.7 (C-aryl), 60.4 (C-14), 35.9 (C-12), 28.4 (C-11), 14.1 (C-15)  
\*three <sup>13</sup>C peaks missing due to overlapping peaks; HRMS (ESI) *m/z* (C<sub>21</sub>H<sub>19</sub>O<sub>2</sub>)

[M+H]<sup>+</sup> requires 303.1380) found 303.1384. This compound is previously reported and data are consistent with these reports.<sup>412</sup>

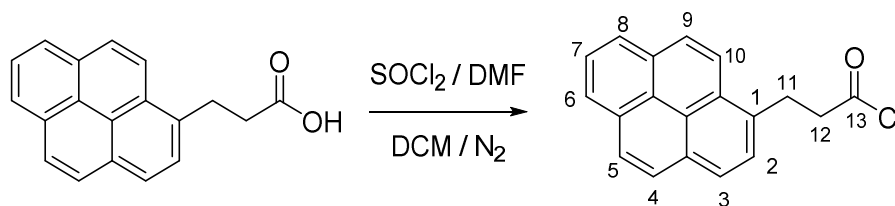
### 6.2.1.5 Ethyl 3-(1-pyrenyl)propionic acid (211)



Under a dinitrogen atmosphere, ethyl 3-(1-pyrenyl)propanoate (0.5 g, 1.6 mmol) was dissolved in warm ethanol (10 mL), then water (1.0 mL) and solid potassium hydroxide (0.18 g, 3.2 mmol) were added and the solution was left to react overnight. The reaction mixture was cooled and the solvent was removed *in vacuo*. Buffer solution (pH 2, 10 mL) was added and the mixture was extracted with ethyl acetate (3 x 10 mL). The combined organics were dried over Na<sub>2</sub>SO<sub>4</sub> and the solvent was removed *in vacuo* to yield an orange crystalline solid (0.45 g, 99 %).

$\nu_{\max}/\text{cm}^{-1}$ : 3037 (OH), 1696 (C=O), 1414 (-CO<sub>2</sub>), 1432 (C-H deformations), 1603, 1586, 1293, 844 (aromatic ring); melting point: 178 - 180 °C (lit.174 - 176 °C)<sup>302</sup>;  $\delta_{\text{H}}$  (400 MHz, CDCl<sub>3</sub>): 8.28 (1H, d, *J* 9.0, H-aryl), 8.21 - 8.11 (4H, m, H-aryl), 8.04 - 7.98 (3H, m, H-aryl), 7.92 (1H, d, *J* 8.0, H-aryl), 3.72 (2H, t, *J* 8.0, H-11), 2.94 (2H, t, *J* 8.0, H-12);  $\delta_{\text{C}}$  (125 MHz, CDCl<sub>3</sub>): 178.7 (C-13), 134.0 (C-aryl), 131.4 (C-aryl), 130.8 (C-aryl), 130.2 (C-aryl), 128.6 (C-aryl), 127.7 (C-aryl), 127.4 (C-aryl), 126.9 (C-aryl), 125.9 (C-aryl), 125.1 (C-aryl), 125.1 (C-aryl), 124.9 (C-aryl), 124.9 (C-aryl), 122.8 (C-aryl), 35.7 (C-12), 28.3 (C-11) \*two <sup>13</sup>C peaks missing due to overlapping peaks; HRMS (ESI) *m/z* (C<sub>19</sub>H<sub>14</sub>O<sub>2</sub> [M+Na]<sup>+</sup> requires 297.0886) found 297.0881. This compound is previously reported and data are consistent with these reports.<sup>312</sup>

### 6.2.1.6 3-(1-Pyrenyl)propanoyl chloride (221)

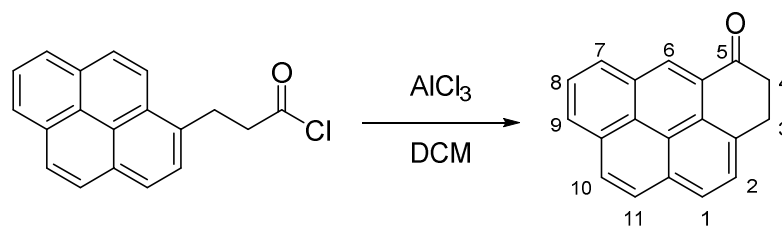


3-(1-Pyrenyl)propionic acid (0.10 g, 0.36 mmol) was dissolved in dichloromethane (15.0 mL) at 0 °C under a dinitrogen atmosphere. Thionyl chloride (0.026 mL, 0.36 mmol) was then added carefully and thereafter DMF (two drops). The reaction was left to react in the inert atmosphere for 1 hour at room temperature. The solvent was removed *in vacuo* to give the acid chloride as an orange crystalline solid (96 %) and was used immediately.

$\nu_{\max}/\text{cm}^{-1}$ : 2915 (CH), 1791 (acid chloride), 1601, 1586 (aromatic), 1205, 840, 757 (substituted benzene rings) 709, 678 (C-Cl); melting point 89 - 92 °C;  $\delta_{\text{H}}$  (400 MHz, CDCl<sub>3</sub>): 8.23 - 7.99 (8H, m, H-aryl), 7.89 (1H, d, *J* 8.0, H-aryl), 3.77 (2H, dd, *J* 8.0, 7.5, H-11), 3.44 (2H, dd, *J* 8.0, 7.5, H-12);  $\delta_{\text{C}}$  (125 MHz, CDCl<sub>3</sub>): 173.0 (C-13), 132.2 (C-aryl), 131.2 (C-aryl), 130.6 (C-aryl), 130.4 (C-aryl), 128.4 (C-aryl), 127.9 (C-aryl), 127.3 (C-aryl), 127.1 (C-aryl), 126.9 (C-aryl), 125.9 (C-aryl), 125.3 (C-aryl), 125.1 (C-aryl), 124.9 (C-aryl), 124.7 (C-aryl), 122.2 (C-aryl), 48.4 (C-11), 28.6 (C-12) \*one <sup>13</sup>C peak missing due to overlapping peaks; HRMS (ESI) *m/z* (C<sub>19</sub>H<sub>13</sub>O [M-Cl]<sup>+</sup> requires 257.0961) found 257.0964. This compound is previously unreported.



### 6.2.1.7 3,4-Dihydro-5H-benzo[cd]pyren-5-one (212)

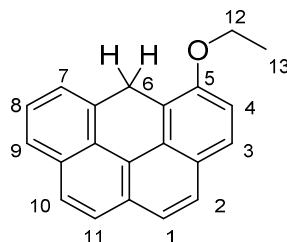


By the method of Weeratunga *et al.*<sup>310</sup>

Anhydrous aluminium chloride (0.17 g, 1.30 mmol) was added to a stirring solution of 3-(1-pyrenyl)propanoyl chloride (0.19 g, 0.65 mmol) in dichloromethane (15.0 mL) at 0 °C under a dinitrogen atmosphere. The reaction was then left for 1 hour under a dinitrogen atmosphere at room temperature. The solvent was removed *in vacuo*, the residue was acidified with HCl (1.0 M) to pH 2 and then extracted with dichloromethane (3 x 10 mL). The combined extracts were collected, dried over Na<sub>2</sub>SO<sub>4</sub> and the solvent was removed *in vacuo* to yield a yellow/orange residue. The crude product ketone **212** was then used immediately without further purification.

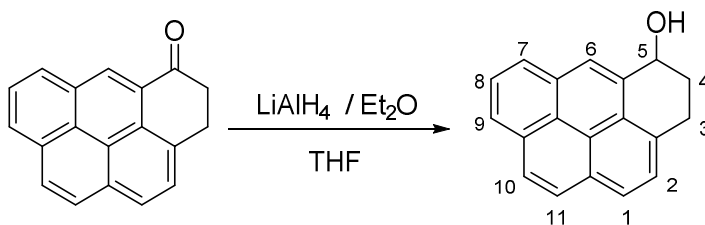
$\nu_{\max}/\text{cm}^{-1}$ : 2919 (CH), 1679 (C=O), 1622, 1545 (aromatic), 1276, 836, 776 (substituted benzene rings); melting point 161 -163 °C (lit. 157 - 158 °C)<sup>302</sup>;  $\delta_{\text{H}}$  (400 MHz, CDCl<sub>3</sub>): 8.81 (1H, s, H-6), 8.36 (1H, d, *J* 7.5, H-7), 8.27 (1H, d, *J* 7.5, H-9), 8.19 (1H, d, *J* 8.0, H-1), 8.09 (1H, d, *J* 9.0, H-11), 8.07 - 8.02 (2H, m, H-8, 10), 7.95 (1H, d, *J* 8.0, H-2), 3.71 (2H, t, *J* 7.0, H-3), 3.17 (2H, t, *J* 7.0, H-4);  $\delta_{\text{C}}$  (150 MHz, CDCl<sub>3</sub>): 199.2 (C-5), 131.4 (C-aryl), 131.3 (C-aryl), 129.8 (C-aryl), 129.7 (C-aryl), 128.8 (C-aryl), 127.9 (C-aryl), 127.7 (C-aryl), 127.7 (C-aryl), 127.7 (C-aryl), 127.6 (C-aryl), 127.2 (C-aryl), 126.7 (C-aryl), 126.6 (C-aryl), 126.5 (C-aryl), 125.9 (C-aryl), 125.2 (C-aryl), 124.7 (C-aryl), 39.1 (C-4), 28.9 (C-3); HRMS (ESI) *m/z* (C<sub>19</sub>H<sub>13</sub>O [M+H]<sup>+</sup> requires 257.0961) found 257.0956. This compound is previously reported but without full characterisation.<sup>302</sup>

### 6.2.1.8 5-Ethoxy-6H-benzo[cd]pyrene (224)



$\nu_{\max}/\text{cm}^{-1}$ : 3045, 2921 (CH), 2851 (CH aryl ether), 1598 (aromatic), 1454, 1439 (CH deformations), 1379 ( $\text{CH}_3$  symmetrical deformation), 1247 (aryl C-O), 1118 (C-O), 1278, 831, 782 (substituted benzene ring); melting point: 57 - 60 °C;  $\delta_{\text{H}}$  (700 MHz,  $\text{CDCl}_3$ ): 7.80 (1H, d,  $J$  8.5, H-aryl), 7.76 - 7.71 (4H, m, H-aryl), 7.62 (1H, d,  $J$  8.5, H-aryl), 7.53 (1H, dd,  $J$  7.0, 1.5, H-aryl), 7.51 (1H, t,  $J$  7.5, H-aryl), 7.25 (1H, d,  $J$  9.0, H-aryl), 4.80 (2H, s, H-6), 4.26 (2H, q,  $J$  7.0, H-12), 1.55 (3H, t,  $J$  7.0, H-13);  $\delta_{\text{C}}$  (175 MHz,  $\text{CDCl}_3$ ):  $\delta_{\text{C}}$  153.4 (C-aryl), 134.0 (C-aryl), 131.8 (C-aryl), 128.9 (C-aryl), 128.1 (C-aryl), 128.1 (C-aryl), 126.9 (C-aryl), 126.7 (C-aryl), 126.6 (C-aryl), 126.4 (C-aryl), 126.3 (C-aryl), 126.2 (C-aryl), 125.7 (C-aryl), 125.3 (C-aryl), 125.3 (C-aryl), 124.1 (C-aryl), 119.7 (C-aryl), 112.5 (C-aryl), 64.1 (C-12), 29.1 (C-6), 15.2 (C-13); HRMS (ESI)  $m/z$  ( $\text{C}_{21}\text{H}_{15}\text{O}$   $[\text{M}-\text{H}]^+$  requires 283.1128) found 283.1117. This compound is previously unreported.

### 6.2.1.9 3,4-Dihydro-5H-benzo[cd]pyren-5-ol (213)

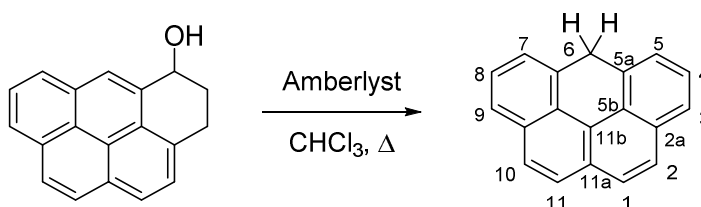


Under a dinitrogen atmosphere, lithium aluminium hydride (3.00 mg, 0.08 mmol) in diethyl ether (3 mL) was stirred at 0 °C. 3,4-Dihydro-5H-benzo[cd]pyren-5-one

(20.0 mg, 0.08 mmol) was dissolved in THF and added to the mixture slowly. The solution was left to react at room temperature for 1 hour. Water and then dilute HCl were added (1:3) sequentially under a dinitrogen atmosphere. The organic layers were collected, dried over Na<sub>2</sub>SO<sub>4</sub> and the solvent was removed *in vacuo* to obtain an orange solid. The reaction product was purified by silica column chromatography using chloroform : ethyl acetate (9:1) to obtain alcohol **213** as a light pink powder (19 mg, 94 %).

$\nu_{\max}/\text{cm}^{-1}$ : 3272 (OH stretch), 2929, 2852 (CH), 1458 (aromatic), 1334 (OH bending), 1072 (CO stretching), 1295, 843, 757 (substituted benzene rings); melting point: 166 - 169 °C (lit. 165 - 168 °C)<sup>302</sup>;  $\delta_{\text{H}}$  (500 MHz, CDCl<sub>3</sub>): 8.17 - 7.96 (7H, m, H-aryl), 7.83 (1H, d, *J* 8.0, H-aryl), 5.29 (1H, dd *J* 7.0, 3.5, H-5), 3.58 (1H, ddd, *J* 16.5, 8.0, 5.0, H-4), 3.37 (1H, ddd, *J* 16.5, 7.0, 5.0, H-4), 2.43 - 2.30 (2H, m, H-3);  $\delta_{\text{C}}$  (125 MHz, CDCl<sub>3</sub>): 136.6 (C-aryl), 133.3 (C-aryl), 131.3 (C-aryl), 130.9 (C-aryl), 129.6 (C-aryl), 127.4 (C-aryl), 126.5 (C-aryl), 126.0 (C-aryl), 125.9 (C-aryl), 125.8 (C-aryl), 124.8 (C-aryl), 124.8 (C-aryl), 124.6 (C-aryl), 123.8 (C-aryl), 69.9 (C-5), 31.6 (C-3), 26.9 (C-4) \*two peaks missing due to overlapping peaks; HRMS (ESI) *m/z* (C<sub>19</sub>H<sub>14</sub>ONa [M+Na]<sup>+</sup> requires 281.0937) found 281.0937. This compound is previously reported but without full characterisation.<sup>302</sup>

#### 6.2.1.10 6H-Benzo[cd]pyrene (209)



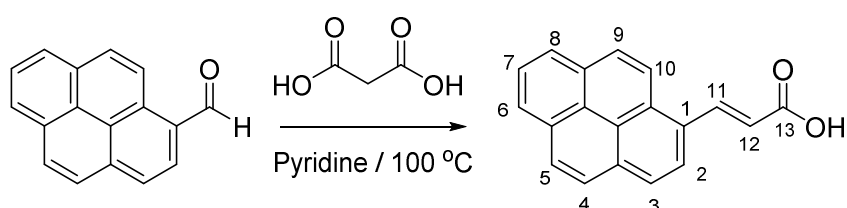
3,4-Dihydro-5H-benzo[cd]pyren-5-ol (100 mg, 0.39 mmol) was dissolved in chloroform (30.0 mL) and Amberlyst 15 (100 mg) was added under a dinitrogen

atmosphere. The reaction was heated to 30 °C and left to react overnight under the inert atmosphere. The solution was then filtered and the Amberlyst 15 was washed with chloroform. The organics were combined and reduced *in vacuo*. The reaction product was purified by silica column chromatography under a dinitrogen atmosphere eluting with chloroform : petroleum ether 40 - 60 °C (1:1) to yield the product as an off white solid (50.0 mg, 54 %).

$\nu_{\max}/\text{cm}^{-1}$ : 2953, 2918 (CH), 1595 (C=C), 1280, 833, 757 (substituted benzene rings); melting point 121 - 124 °C (lit. 123 - 124 °C)<sup>301</sup>;  $\delta_{\text{H}}$  (500 MHz,  $\text{CDCl}_3$ ): 7.81 (2H, d,  $J$  8.5, H-2), 7.77 (2H, d,  $J$  8.5, H-1), 7.74 (2H, dd,  $J$  8.0, 0.5, H-3), 7.51 (2H, t,  $J$  7.5, H-4), 7.46 (2H, dd,  $J$  7.0, 1.5, H-5), 4.98 (2H, s, H-6);  $\delta_{\text{C}}$  (125 MHz,  $\text{CDCl}_3$ ): 133.9 (C-5a), 131.9 (C-2a), 128.0 (C-5b), 127.9 (C-11a), 126.9 (C-2), 126.7 (C-1), 126.4 (C-4), 125.9 (C-11b), 125.5 (C-3), 125.3 (C-5), 24.2 (C-6); HRMS (ESI)  $m/z$  ( $\text{C}_{19}\text{H}_{11}$   $[\text{M}-\text{H}]^+$  requires 239.0855) found 239.0854. This compound is previously reported but HMBC studies show that the peaks for H1 & H2 were previously misassigned.<sup>301</sup>

## 6.2.2 Synthesis of 6H-benzo[cd]pyrene: Method 2

### 6.2.2.1 3-(1-Pyrenyl)acrylic acid (226)



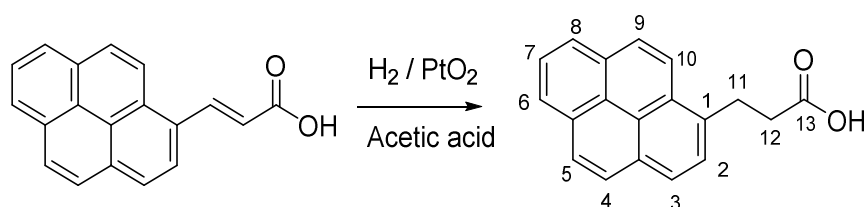
By the method of Mizushima *et al.*<sup>312</sup>

Malonic acid (3.39 g, 32.6 mmol) was added to a solution of pyrenecarboxaldehyde (1.5 g, 6.52 mmol) in pyridine (6.0 mL) and the mixture was left to react at 100 °C. After 2.5 days HCl (1.0 M, 6.0 mL) was added and the mixture was filtered. The

solid was washed with water and petroleum ether 40 - 60 °C and dried in a desiccator to afford a yellow crystalline solid (1.49 g, 84 %).

$\nu_{\max}/\text{cm}^{-1}$ : 3039 (OH), 2818, 2585 (CH), 1670 (C=O), 1419 (CO<sub>2</sub>), 1437 (C-H deformations), 1609, 1279, 835 (aromatic rings), 971 (alkene); melting point: 279 - 282 °C (lit. N/A);  $\delta_{\text{H}}$  (400 MHz, (CD<sub>3</sub>)<sub>2</sub>SO): 8.70 (1H, d, *J* 15.5, H-11), 8.56 - 8.51 (2H, m, H-aryl), 8.39 - 8.30 (4H, m, H-aryl), 8.26 (1H, d, *J* 9.0, H-aryl), 8.22 (1H, d, *J* 9.0, aryl), 8.12 (1H, t, *J* 7.5, H-aryl), 6.83 (1H, d, *J* 15.5, H-12);  $\delta_{\text{C}}$  (100 MHz, (CD<sub>3</sub>)<sub>2</sub>SO): 167.5 (C-13), 139.8 (C-11), 132.0 (C-aryl), 130.8 (C-aryl), 130.1 (C-aryl), 128.8 (C-aryl), 128.6 (C-aryl), 128.4 (C-aryl), 127.8 (C-aryl), 127.3 (C-aryl), 126.6 (C-aryl), 126.1 (C-aryl), 125.8 (C-aryl), 125.3 (C-aryl), 124.6 (C-aryl), 123.9 (C-aryl), 123.7 (C-aryl), 122.2 (C-12), 121.6 (C-aryl); HRMS (ESI) *m/z* (C<sub>19</sub>H<sub>11</sub>O<sub>2</sub> [M-H]<sup>-</sup> requires 271.0765) found 271.0768. This compound is previously reported and data are consistent with these reports.<sup>312</sup>

#### 6.2.2.2 3-(1-pyrenyl)propionic acid (211) – second version



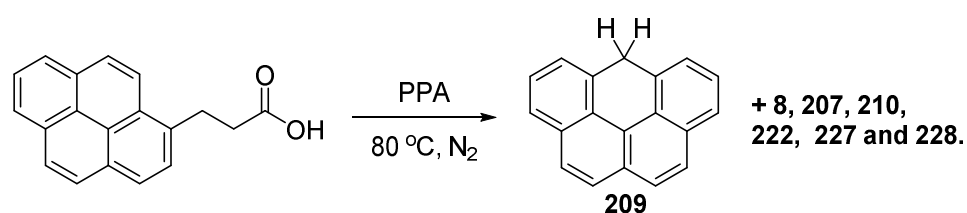
By the method of Mizushima *et al.*<sup>312</sup>

Ethyl 3-(1-pyrenyl)acrylate (0.5 g, 1.84 mmol) was stirred in acetic acid (80 mL) and PtO<sub>2</sub> (1.5 mol %) and left to react at room temperature under a dihydrogen atmosphere. After 1.5 days the acetic acid was removed *in vacuo* and the residue was diluted with dichloromethane. The solution was washed through a pad of celite, then the organics were collected and washed with water, followed by drying over Na<sub>2</sub>SO<sub>4</sub>.

The organic layers were filtered and removed *in vacuo* and the crude product was recrystallised with hexane/dichloromethane to give a yellow/gold crystalline solid (0.41 g, 81 %). Data matches that of compound **211** reported above (see section 6.2.1.5).

### 6.2.2.3 6H-benzo[cd]pyrene

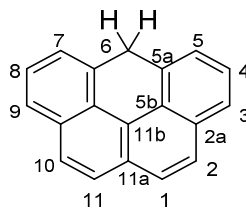
Polyphosphoric acid mediated reaction of 3-(1-pyrenyl)propionic acid **211** producing compounds **8**, **207**, **209**, **210**, **222**, **227** and **228**.



To a stirring solution of polyphosphoric acid (10.3 g) at 80 °C was added 3-(1-pyrenyl)propionic acid (0.10 g, 0.35 mmol). The reaction was heated at 80 °C under a dinitrogen atmosphere for 24 hours. The reaction was cooled using an ice bath, water was added (15.0 mL) and the mixture was extracted with dichloromethane (4 x 20 mL). The organic layers were collected, dried over Na<sub>2</sub>SO<sub>4</sub> and the solvent was removed *in vacuo* to produce a red solid (0.95 g). Analysis by <sup>1</sup>H NMR was consistent with the molar proportions of products to be **209**, 31 % : **210**, 30 % : **222**, 26 % : **228**, 6 % : **207**, 4 % : **227**, 4 % plus a trace of pyrene **8** which could not be quantified due to overlapping peaks.

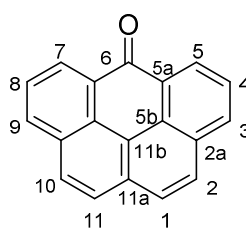
This solid was purified by silica column chromatography under a dinitrogen atmosphere with a gradient system which consisted of: chloroform : petroleum ether 40 - 60 °C (5:95), (2:8), (100:0) and then finally 100 % ethyl acetate. The products were isolated as follows:

#### 6.2.2.4 6H-Benzo[cd]pyrene (209)



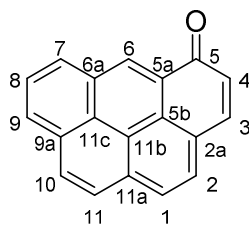
Data matches that of compound **209** reported above (see section 6.2.1.10).

#### 6.2.2.5 6-Oxo-6H-benzo[cd]pyrene (210)



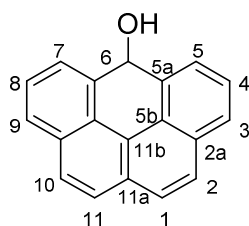
$\nu_{\max}/\text{cm}^{-1}$ : 2921 (CH), 1652 (C=O), 1609, 1570 (aromatic), 1285, 853, 838, 750 (substituted benzene rings); melting point 240 - 245 °C (lit. 243 - 244 °C)<sup>301</sup>;  $\delta_{\text{H}}$  (600 MHz,  $\text{CDCl}_3$ ): 8.87 (2H, d,  $J$  7.5, H-5, 7), 8.32 (2H, d,  $J$  8.0, H-3, 9), 8.10 (2H, d,  $J$  8.5, H-2, 10), 7.99 (2H, d,  $J$  8.5, H-1, 11), 7.88 (2H, t,  $J$  7.5, H-4, 8);  $\delta_{\text{C}}$  (150 MHz,  $\text{CDCl}_3$ ): 184.4 (C-6), 134.5 (C-3), 132.1 (C-11a), 131.2 (C-2a), 129.8 (C-5a), 129.2 (C-5), 128.6 (C-2), 128.2 (C-5b), 127.0 (C-1), 126.9 (C-4), 121.1 (C-11b); HRMS (ESI)  $m/z$  ( $\text{C}_{19}\text{H}_{11}\text{O}$   $[\text{M}+\text{H}]^+$  requires 255.0804) found 255.0802. This compound is previously reported and data are consistent with reports.<sup>301</sup>

### 6.2.2.6 5-Oxo-5H-benzo[cd]pyrene (222)



$\nu_{\max}/\text{cm}^{-1}$ : 3031 (CH), 1642 (C=O), 1614, 1566 (C=C), 1278, 845, 756 (substituted benzene rings); melting point 201 - 204 °C (lit. 218 - 221 °C)<sup>302</sup>;  $\delta_{\text{H}}$  (400 MHz,  $\text{CDCl}_3$ ): 9.36 (1H, s, H-6), 8.56 (1H, d,  $J$  7.5, H-7), 8.43 (1H, d,  $J$  7.5, H-9), 8.22 (1H, d,  $J$  8.0, H-1), 8.18 – 8.11 (4H, m, H-2, 8, 10, 11), 8.02 (1H, d,  $J$  9.5, H-3), 6.86 (1H, d,  $J$  9.5, H-4);  $\delta_{\text{C}}$  (150 MHz,  $\text{CDCl}_3$ ): 186.1 (C-5), 143.1(C-3), 134.4 (C-6), 133.2 (C-11a), 131.0 (C-7), 130.7 (C-9a), 130.3 (C-9), 129.6 (C-6a), 128.5 128.4 128.4 (C-2, 4, 10), 128.3 (C-5a), 127.7 (C-11), 127.1 (C-8), 125.2 (C-1), 125.2 (C-5b), 124.8 124.7 (C-2a, 11c), 123.6 (C-11b); HRMS (ESI)  $m/z$  ( $\text{C}_{19}\text{H}_{11}\text{O}$  [ $\text{M}+\text{H}$ ]<sup>+</sup> requires 255.0804) found 255.0806. This compound is previously reported and data are consistent with reports.<sup>313</sup>

### 6.2.2.7 6H-Benzo[cd]pyren-6-ol (228)

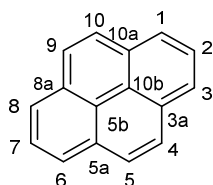


$\nu_{\max}/\text{cm}^{-1}$ : 2916, 2848 (CH), 1484 (aromatic), 1386 (OH bending), 1141 (CO stretching), 1281, 832, 748 (substituted benzene rings); melting point 160 - 164 °C;  $\delta_{\text{H}}$  (700 MHz,  $\text{CDCl}_3$ ): 7.56 (2H, d,  $J$  8.5, H-2, 10), 7.54 (2H, d,  $J$  8.5, H-1, 11), 7.46 (2H, d,  $J$  8.0, H-3, 9), 7.04 (2H, t,  $J$  7.5, H-4, 8), 6.70 (2H, d,  $J$  7.0, H-5, 7), 5.00 (1H, s, H-6 CH);  $\delta_{\text{C}}$  (175 MHz,  $\text{CDCl}_3$ ): 133.2 (C-5a), 130.0 (C-2a), 128.5 (C-5b),



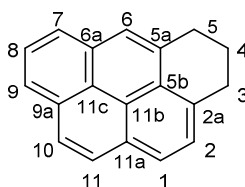
127.5 (C-11a), 126.2 (C-5), 126.1 (C-2), 125.9 (C-3), 125.6 (C-1), 124.9 (C-4), 123.9 (C-11b), 60.4 (C-6); HRMS (ESI)  $m/z$  ( $C_{19}H_{11}$   $[M-H_2O+H]^+$  requires 239.0855) found 239.0853. This compound is previously unreported.

#### 6.2.2.8 Pyrene (8)



$\delta_H$  (400 MHz,  $CDCl_3$ ): 8.19 (4H, d,  $J$  7.5, H-1, 3, 6, 8), 8.09 (4H, s, H-4, 5, 9, 10), 8.01 (2H, t,  $J$  7.5, H-2, 7);  $\delta_C$  (100 MHz,  $CDCl_3$ ): 131.0 (C-3a), 127.3 (C-5), 125.7 (C-2), 124.8 (C-1), 124.6 (C-10b). This compound is previously reported and data are consistent with reports.<sup>315</sup>

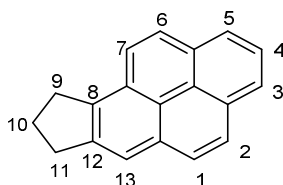
#### 6.2.2.9 4, 5-Dihydro-3H-benzo[cd]pyrene (207)



As a solid (trace quantity);  $\nu_{max}/cm^{-1}$ : 2917, 2849 (CH), 1606, 1583 (aromatic), 1459, 1435 (CH deformations), 1255, 826, 757 (substituted benzene rings), 719 (CH rocking); melting point 98 - 101 °C (lit. 108 - 109 °C)<sup>303</sup>;  $\delta_H$  (700 MHz,  $CDCl_3$ ): 8.11 - 8.05 (3H, m, H-6, 7, 9), 8.02 (1H, d,  $J$  9.0, H-1), 8.00 (1H, d,  $J$  9.0, H-2), 7.95 (1H, t,  $J$  7.5, H-8), 7.82 - 7.78 (2H, m, H-10, 11), 3.39 (2H, t,  $J$  6.0, H-5), 3.31 (2H, t,  $J$  6.0, H-3), 2.25 (2H, quin.,  $J$  6.0, H-4);  $\delta_C$  (175 MHz,  $CDCl_3$ ): 135.3 (C-aryl), 134.6 (C-aryl), 131.4 (C-aryl), 131.3 (C-aryl), 129.6 (C-aryl), 127.6 (C-aryl), 127.4 (C-aryl), 126.4 (C-aryl), 125.9 (C-aryl), 125.8 (C-aryl), 124.8 (C-aryl), 124.5 (C-aryl),

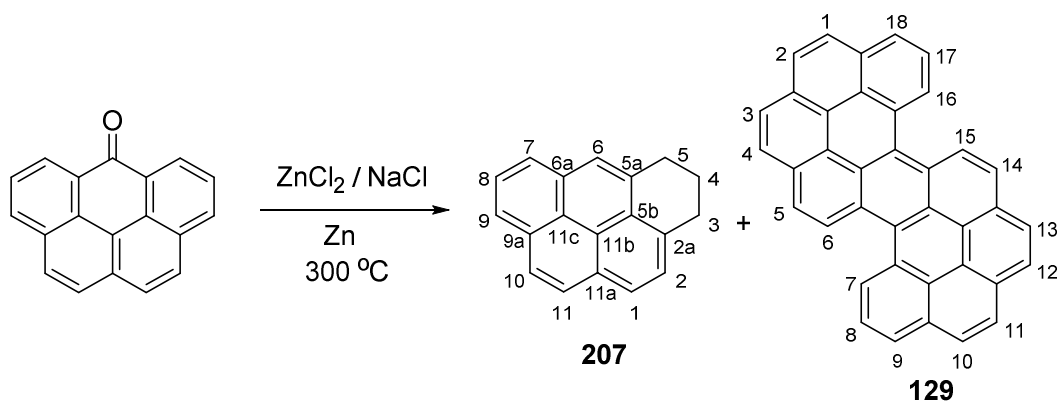
124.1 (C-aryl), 123.7 (C-aryl), 123.6 (C-aryl), 123.6 (C-aryl), 31.8 (C-3), 31.6 (C-5), 23.4 (C-4); HRMS (ESI)  $m/z$  ( $C_{19}H_{15}$   $[M+H]^+$  requires 243.1168) found 243.1180. This compound is previously reported without NMR spectroscopic data.<sup>316</sup>

#### 6.2.2.10 7,8-Dihydro-9H-cyclopenta[*a*]pyrene (227)



$\delta_H$  (400 MHz,  $CDCl_3$ ): 8.21 - 7.93 (8H, m, H-aryl), 3.39\* (2H, br. t, H-9 or 11), 3.31 (2H, br. t,  $J$  6.0, H-9 or 11), 2.25 (2H, quin.,  $J$  6.0, H-10) \*peak at 3.39 ppm is overlapping with the peak at 3.39 ppm of 4,5-dihydro-3H-benzo[*cd*]pyrene as this compound was obtained as a mixture. This compound is previously reported.<sup>317</sup>

#### 6.2.2.11 Synthesis of 4, 5-Dihydro-3H-benzo[*cd*]pyrene (207)

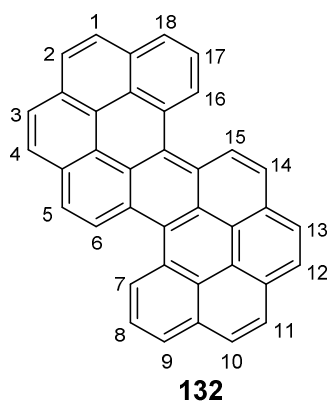


By the method of Clar and Stewart.<sup>316</sup>

Sodium chloride (1.68 g, 2.00 equiv.) and moist zinc chloride (8.40 g, 10.0 equiv.) were added to a mixture of 6-oxo-6H-benzo[*cd*]pyrene (0.84 g, 3.30 mmol) and zinc dust (1.68 g, 2.00 equiv.). The mixture was heated to 300 °C and the melted mixture was left to react for 1 hour with constant stirring. The reaction mixture was cooled,

followed by addition of dilute acetic acid and the layer was then partitioned with dichloromethane (3 x 125 mL) where the organics were collected. The organics were then washed with water (3 x 100 mL), collected and dried over Na<sub>2</sub>SO<sub>4</sub>, filtered and the solvent was removed *in vacuo*. The reaction mixture was purified by silica column chromatography using 100 % petroleum ether 40 – 60 °C to produce **207**, a white solid (0.58 g, 73 %) and **132**, a dark orange/brown solid (6.00 mg, 0.8 %). Characterisation data were identical with the sample isolated from the polyphosphoric acid mediated ring-closure of acid **211** as described above (**207** see section 6.2.2.9).

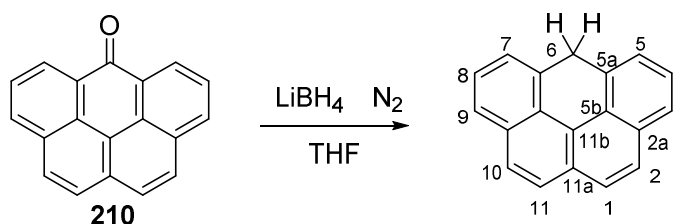
#### 6.2.2.12 Dibenzo[jk,uv]dinaphtho[2,1,8,7-defg-2',1',8',7'-opqr]pentacene (**132**)



$\nu_{\max}/\text{cm}^{-1}$ : 2954, 2921, 2851 (CH), 1607, 1580 (aromatic), 1259, 903, 844, 752 (substituted benzene rings); melting point >300 °C (lit. >300 °C)<sup>318</sup>;  $\delta_{\text{H}}$  (500 MHz, CDCl<sub>3</sub>): 9.53 (2H, d,  $J$  9.0, H-6, 15), 9.34 (2H, d,  $J$  7.5, H-7, 16), 8.58 - 8.53 (4H, m, H-1, 2, 10, 11), 8.43 (2H, d,  $J$  9.0, H-5, 14), 8.37 (2H, d,  $J$  7.5, H-9, 18), 8.35 (2H, d,  $J$  8.5, H-3, 12), 8.30 (2H, d,  $J$  8.5, H-4, 13), 8.18 (2H, t,  $J$  7.5, H-8, 17);  $\delta_{\text{C}}$  (125 MHz, CDCl<sub>3</sub>): 131.7<sub>(quat)</sub>, 129.7<sub>(quat)</sub>, 129.6<sub>(quat)</sub>, 128.9<sub>(quat)</sub>, 128.6 (C-7, 16), 128.0 (C-5, 14), 127.4 (C-3, 12), 127.3 (C-4, 13), 126.8 (C-6, 15), 126.5 (C-5, 14), 126.4<sub>(quat)</sub>, 126.1<sub>(quat)</sub>, 125.9 (C-1 and 10 or C-2 and 11), 125.9 (C-8, 17), 125.6 (C-1

and 10 or C-2 and 11), 125.5<sub>(quat)</sub>, 124.6<sub>(quat)</sub>, 124.2<sub>(quat)</sub>, 123.2<sub>(quat)</sub>; HRMS Orbitrap XL (APCI)  $m/z$  ( $C_{38}H_{19}$   $[M+H]^+$  requires 475.1481) found 475.1477. This compound is previously reported and data are consistent with reports.<sup>318</sup>

#### 6.2.2.13 6H-Benzo[cd]pyrene (209) – from ketone 210.

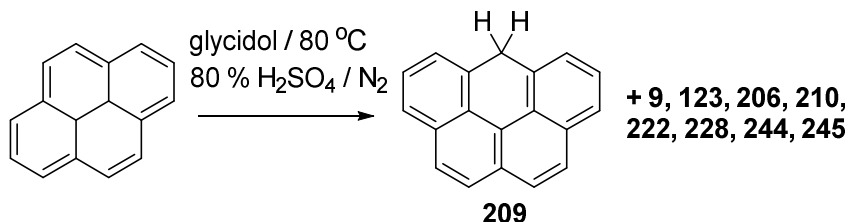


6-Oxo-6H-benzo[cd]pyrene (5.00 mg, 19.7  $\mu\text{mol}$ ) was dissolved in THF and added dropwise to a solution of lithium borohydride (0.86 mg, 39.4  $\mu\text{mol}$ ) in THF (5.00 mL) at 0 °C under a dinitrogen atmosphere. After one hour at room temperature, water and then aqueous HCl were added (1:3) sequentially under a dinitrogen atmosphere. The organic layers were collected, dried over  $\text{Na}_2\text{SO}_4$  and the solvent was removed *in vacuo* to obtain 6H-benzo[cd]pyrene as a white solid (4.30 mg, 84 %) with characterisation data identical to that above (**209** see section 6.2.1.10). \*This reduction also works with  $\text{LiAlH}_4$  instead of  $\text{LiBH}_4$  in the same conditions.

## 6.3 Experimental for Chapter 3

### 6.3.1 Synthesis of 6H-benzo[cd]pyrene: Method 3

#### 6.3.1.1 Synthesis using pyrene



Method modified from literature.<sup>297-299, 301, 302, 325</sup>

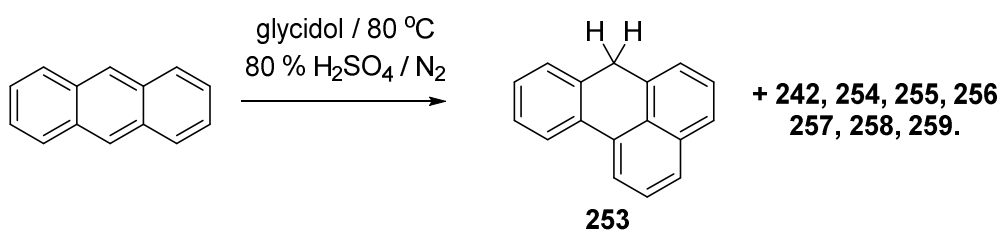
Under a dinitrogen atmosphere, pyrene (0.50 g, 2.47 mmol) was dissolved in minimum chloroform and glycidol (1.31 mL, 19.8 mmol, 8.00 equiv.) was added to this solution. 80 % H<sub>2</sub>SO<sub>4</sub> (1.39 mL, 24.7 mmol, 10.0 equiv.) was then added dropwise to the mixture. The reaction was heated to 80 °C and left to react for 18 hours under a dinitrogen atmosphere. Work up for either products a) or b).

- a) General work up for PAH mixtures – the reaction mixture was cooled and placed into an ice bath where 5.0 M NaOH was added until pH 7. The mixture was filtered through a Büchner funnel with filter paper guide and washed through with dichloromethane (2 x 30 mL). The filtrate mixture was partitioned and the organic layer was collected. The aqueous layer was extracted a further three times with dichloromethane and the organic layers were collected together, dried over Na<sub>2</sub>SO<sub>4</sub> and the solvent was removed *in vacuo* to give the crude product mixture (0.25 g). The mixture was purified by silica column chromatography under a dinitrogen atmosphere using a gradient system of petroleum ether 40 - 60 °C with chloroform and another gradient system of chloroform with ethyl acetate. Several different products

were formed; **(209)** 24 %, **(210)** 19 %, **(228)** 12 %, **(9)** 4 %, **(244)** 2 %, **(222)** <1 %, **(206)** <1 %, **(245)** <1 %.

b) General work up for the black solid – Alternatively, the reaction mixture was placed into an ice bath and water added (20 mL). The mixture was transferred into falcon tubes, diluted with water and centrifuged (10000 rpm for 20 mins) four times, the solid was collected and the water was removed *in vacuo*. The solid was then washed with chloroform (4 x 40 mL) and collected in a Hirsch funnel and left to dry in a desiccator to give a black solid (1.0 g).

### 6.3.1.2 Synthesis using anthracene



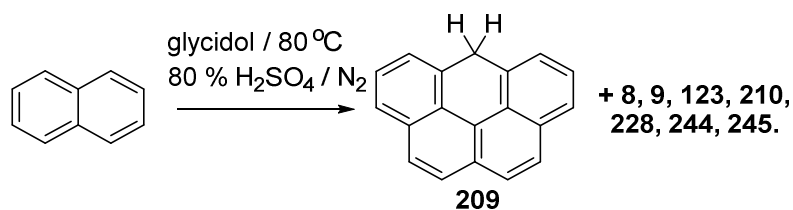
Method modified from literature.<sup>297-299, 301, 302, 325</sup>

Under a dinitrogen atmosphere, anthracene (0.50 g, 2.81 mmol) was added to a mixture of chloroform (0.50 mL) and glycidol (1.49 mL, 22.4 mmol, 8.00 equiv.). 80 % H<sub>2</sub>SO<sub>4</sub> (4.78 mL, 84.3 mmol, 30.0 equiv.) was then added dropwise to the solution. The reaction was heated to 80 °C and left to react for 18 hours under a dinitrogen atmosphere. General work up for either products a) or b) was same as above (see section 6.3.1.1).

a) Obtained 0.20 g of the crude product mixture. Several different products were formed after purification; **(242)** 15 %, **(253)** 10 %, **(259)** 4 %, **(258)** 3 %, **(255)** 3 %, **(254)** 3 %, **(256)** 1 %, **(257)** <1 %.

b) 0.8 g of a black solid powder was obtained.

### 6.3.1.3 Synthesis using naphthalene

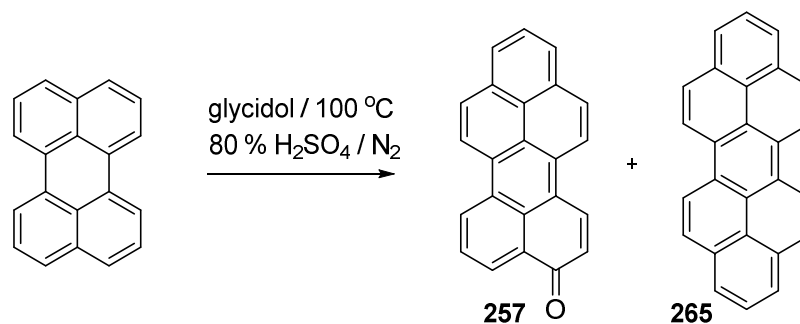


Method modified from literature.<sup>297-299, 301, 302, 325</sup>

Under a dinitrogen atmosphere, naphthalene (0.50 g, 3.90 mmol) was dissolved in minimum chloroform and glycidol (2.07 mL, 31.2 mmol, 8.00 equiv.) was added. 80 % H<sub>2</sub>SO<sub>4</sub> (2.21 mL, 39.0 mmol, 10.0 equiv.) was then added dropwise to the solution. The reaction was heated to 80 °C and left to react for 18 hours under a dinitrogen atmosphere. General work up for either products a) or b) was same as above (see section 6.3.1.1).

- a) Obtained 0.22 g of the crude product mixture. Several different products were formed after purification; **(209)** 17 %, **(210)** 10 %, **(245)** 8 %, **(123)** 4 %, **(8)** 4 %, **(9)** <1 %, **(228)** <1 %, **(244)** <1 %.
- b) 0.9 g of a black powdered solid was obtained.

#### 6.3.1.4 Synthesis using perylene



Method modified from literature.<sup>297-299, 301, 302, 325</sup>

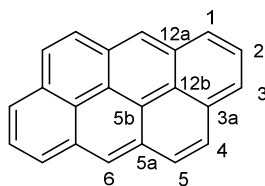
Under a dinitrogen atmosphere, perylene (0.5 g, 1.98 mmol) was dissolved in minimum chloroform and glycidol (3.30 mL, 49.5 mmol, 25.0 equiv.) was added to this solution. Thereafter, 80 % H<sub>2</sub>SO<sub>4</sub> (3.00 mL, 53.5 mmol, 27.0 equiv.) was added dropwise to the mixture. The reaction was heated to 100 °C and left to react for 18 hours under a dinitrogen atmosphere. General work up for either products a) or b) was same as above (see section 6.3.1.1).

- a) Obtained 0.3 g of the crude product mixture. The mixture was purified by silica column chromatography under a dinitrogen atmosphere using 100 % petroleum ether 40 - 60 °C to obtain (**265** peropyrene) and chloroform : ethyl acetate (9:1) to obtain (**257**). Several different products were formed; (**265**) 25 mg, 21 %, (**257**) 40 mg, 19 %, (20 % perylene **25** recovered)
- b) 0.9 g of a black powdered solid was obtained.

\*The characterisation of most of the products from sections 6.3.1.1 and 6.3.1.3 can be found in section 6.2.2, due to repetition of products.

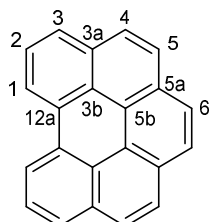


### 6.3.1.5 Dibenzo[cd,jk]pyrene; Anthanthrene (9)



$\nu_{\max}/\text{cm}^{-1}$ : 3033, 2923(CH), 1237, 895, 876 (aromatic rings); melting point: 258 - 261 °C (lit. 261 - 262 °C)<sup>330</sup>;  $\delta_{\text{H}}$  (700 MHz,  $\text{CDCl}_3$ ): 8.81 (2H, s, H-6), 8.54 (2H, d,  $J$  8.0, H-1), 8.22 (2H, d,  $J$  7.0, H-3), 8.16 (2H, d,  $J$  9.0, H-5), 8.15 (2H, t,  $J$  7.5, H-2), 8.08 (2H, d,  $J$  9.0, H-4);  $\delta_{\text{C}}$  (175 MHz,  $\text{CDCl}_3$ ): 131.5 (C-5a or 5b), 130.7 (C-3a or 12b), 130.6 (C-3a or 12b), 128.5 (C-4), 128.3 (C-5), 125.9 (C-1), 125.9 (C-2), 124.3 (C-6), 123.9 (C-3), 123.0 (C-11b), 122.6 (C-5a or 5b); GC-MS (EI) 277  $m/z$  ( $[\text{C}_{22}\text{H}_{12}]^+$ ,  $[\text{M}+\text{H}]^+$ ). This compound is previously reported and data are consistent with reports.<sup>330</sup>

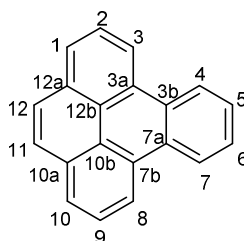
### 6.3.1.6 Benzo[ghi]perylene (123)



$\nu_{\max}/\text{cm}^{-1}$ : 2987, 2901 (CH), 1250, 892, 878 (aromatic rings); melting point: 268 - 271 °C (lit. 268 - 271 °C)<sup>413</sup>;  $\delta_{\text{H}}$  (700 MHz,  $\text{CDCl}_3$ ): 9.04 (2H, d,  $J$  7.5, H-1), 8.38 (2H, s, H-6), 8.21 (2H, d,  $J$  7.5, H-3), 8.15 (2H, d,  $J$  8.5, H-4 or 5), 8.10 (2H, d,  $J$  8.5, H-4 or 5), 8.04 (2H, t,  $J$  7.5, H-2);  $\delta_{\text{C}}$  (175 MHz,  $\text{CDCl}_3$ ): 132.2 (C-3a), 130.4 (C-12a), 129.2 (C-5a), 127.4 (C-4 or 5), 126.5 (C-3), 126.2 (C-2), 125.7 (C-3b), 125.6 (C-6), 123.9 (C-5b), 120.7 (C-1), \*one  $^{13}\text{C}$  peak missing due to overlapping

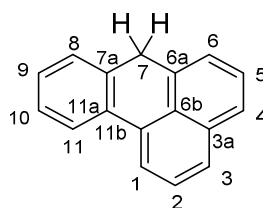
peaks; GC-MS (EI) 277  $m/z$  ( $[C_{22}H_{12}]^+$ ,  $[M+H]^+$ ). This compound is previously reported and data are consistent with reports.<sup>152</sup>

### 6.3.1.7 Benzo[e]pyrene (256)



$\nu_{\max}/\text{cm}^{-1}$ : 2919, 2850 (CH), 1261, 897, 825 (aromatic rings); melting point: 175 - 178 °C (lit. 175 °C)<sup>335</sup>;  $\delta_{\text{H}}$  (700 MHz,  $\text{CDCl}_3$ ): 8.91 (2H, d,  $J$  8.0, H-3), 8.86 (2H, dd,  $J$  6.0, 3.5, H-4 or 5), 8.19 (2H, d,  $J$  7.5, H-1), 8.06 (2H, s, H-12), 8.05 (2H, t,  $J$  7.5, H-2), 7.76 (2H, dd,  $J$  6.0, 3.0, H-4 or 5);  $\delta_{\text{C}}$  (175 MHz,  $\text{CDCl}_3$ ): 131.7 (C-12a), 130.3 (C-3b), 129.3 (C-3a), 127.6 (C-4 or 5), 127.4 (C-12), 126.2 (C-1), 126.1 (C-2), 124.3 (C-12b), 123.8 (C-4 or 5), 120.3 (C-3); GC-MS (EI) 252  $m/z$  ( $[C_{22}H_{12}]^+$ ,  $[M]^+$ ). This compound is previously reported and data are consistent with reports.<sup>335</sup>

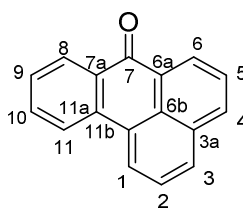
### 6.3.1.8 7H-Benz[de]anthracene (253)



$\nu_{\max}/\text{cm}^{-1}$ : 3037, 2922 (CH), 1593 (C=C), 1455 (CH deformations), 1193, 889, 815, 773 (aromatic rings); melting point: 80 - 82 °C (lit. 81.5 °C)<sup>332</sup>;  $\delta_{\text{H}}$  (400 MHz,  $\text{CDCl}_3$ ): 8.01 (1H, d,  $J$  7.5, H-11), 7.96 (1H, d,  $J$  7.5, H-1), 7.69 (1H, d,  $J$  8.0, H-3), 7.63 (1H, d,  $J$  8.0, H-4), 7.45 (1H, t,  $J$  7.5, H-2), 7.40 (1H, t,  $J$  7.5, H-5), 7.33 (1H, dd,  $J$  7.0, 1.0, H-6) 7.31 - 7.21 (3H, m, H-8, 9, 10), 4.54 (2H, s, H-7);  $\delta_{\text{C}}$  (100 MHz,

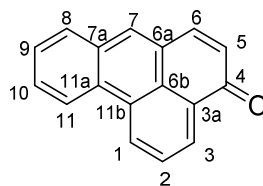
CDCl<sub>3</sub>): 134.3 (C-7a), 133.9 (C-3a), 133.2 (C-6a), 132.3 (C-11a), 131.1 (C-11b), 128.9 (C-8), 128.8 (C-6b), 127.7 (C-9), 127.6 (C-3), 126.8 (C-10), 126.2 (C-2), 125.9 (C-5), 125.5 (C-4), 124.4 (C-6), 123.3 (C-11), 118.6 (C-1), 34.4 (C-7); GC-MS (EI) 216 *m/z* ([C<sub>17</sub>H<sub>12</sub>]<sup>+</sup>, [M]<sup>+</sup>). This compound is previously reported and data are consistent with reports.<sup>332</sup>

### 6.3.1.9 7H-Benzo[de]anthracen-7-one; Benzanthrone (242)



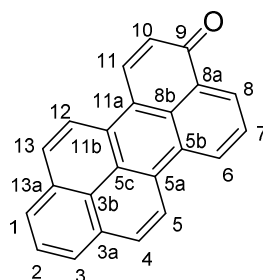
$\nu_{\max}/\text{cm}^{-1}$ : 3054, 2925 (CH), 1646 (C=O), 1599 (C=C), 1191, 877, 796, 780 (aromatic rings); melting point: 168 - 170 °C (lit. 162 - 164 °C)<sup>334</sup>;  $\delta_{\text{H}}$  (400 MHz, CDCl<sub>3</sub>): 8.72 (1H, dd, *J* 7.5, 1.0, H-6), 8.48 (1H, dd, *J* 8.0, 1.5, H-8), 8.37 (1H, d, *J* 7.5, H-1), 8.27 (1H, d, *J* 8.0, H-11), 8.16 (1H, dd, *J* 8.0, 1.0, H-4), 7.94 (1H, d, *J* 8.0, H-3), 7.73 (1H, t, *J* 7.5, H-5), 7.72 - 7.67 (1H, m, H-10), 7.62 (1H, t, *J* 8.0, H-2), 7.52 (1H, td, *J* 7.5, 1.0, H-9);  $\delta_{\text{C}}$  (100 MHz, CDCl<sub>3</sub>): 183.8 (C-7), 136.1 (C-11a), 135.0 (C-4), 133.3 (C-10), 132.9 (C-3a), 131.0 (C-7a), 130.1 (C-3), 129.7 (C-6), 128.4 (C-6a), 128.1 (C-9), 128.0 (C-8), 127.8 (C-6b), 126.7 (C-11b), 126.5 (C-2), 126.5 (C-5), 124.1 (C-1), 122.9 (C-11); HRMS (ESI) *m/z* (C<sub>17</sub>H<sub>10</sub>ONa [M+Na]<sup>+</sup> requires 254.0629) found 254.0630. This compound is previously reported and data are consistent with reports.<sup>334</sup>

### 6.3.1.10 4-Oxo-4H-benz[de]anthracene (255)



$\nu_{\max}/\text{cm}^{-1}$ : 2920, 2850 (CH), 1637 (C=O), 1584 (C=C), 1159, 901, 820, 747 (aromatic rings); melting point: 67 - 69 °C;  $\delta_{\text{H}}$  (700 MHz,  $\text{CDCl}_3$ ): 8.98 (1H, d,  $J$  8.0, H-1), 8.71 (1H, d,  $J$  8.0, H-11), 8.65 (1H, d,  $J$  7.5, H-3), 8.08 (1H, s, H-7), 7.99 (1H, d,  $J$  8.0, H-8), 7.92 (1H, t,  $J$  8.0, H-2), 7.82 (1H, d,  $J$  9.5, H-6), 7.78 (1H, t,  $J$  7.5, H-10), 7.68 (1H, t,  $J$  7.5, H-9), 6.79 (1H, t,  $J$  9.5, H-5);  $\delta_{\text{C}}$  (175 MHz,  $\text{CDCl}_3$ ): 185.9 (C-4), 142.1 (C-6), 134.1 (C-7), 131.6 (C-7a or 11a), 131.5 (C-7a or 11a), 130.2 (C-8), 129.9 (C-3a), 129.6 (C-11b), 129.4 (C-10), 129.1 (C-5), 128.5 (C-3), 128.3 (C-1), 127.7 (C-9), 127.6 (C-2), 127.2 (C-6b), 126.4 (C-6a), 123.0 (C-11); HRMS (ESI)  $m/z$  ( $\text{C}_{17}\text{H}_{11}\text{O}$   $[\text{M}+\text{H}]^+$  requires 231.0804) found 231.0805. The data for this compound is previously unreported.

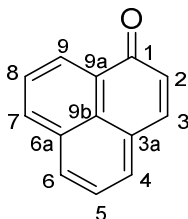
### 6.3.1.11 9-Oxo-9H-benzo[cd]perylene (257)



$\nu_{\max}/\text{cm}^{-1}$ : 2922, 2855 (CH), 1630 (C=O), 1571 (C=C), 1145, 945, 838, 761 (aromatic rings); melting point: 298 - 300 °C (lit. 298 - 300 °C)<sup>333</sup>;  $\delta_{\text{H}}$  (700 MHz,  $\text{CDCl}_3$ ): 9.30 (1H, d,  $J$  7.5, H-6), 9.02 (1H, d,  $J$  9.0, H-5), 8.94 (1H, d,  $J$  6.0, H-8), 8.77 (1H, d,  $J$  10.0, H-11), 8.53 (1H, d,  $J$  9.0, H-12), 8.40 (1H, d,  $J$  9.0, H-4), 8.31

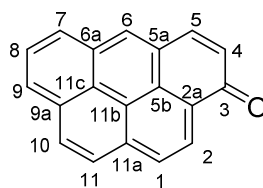
(1H, d,  $J$  7.5, H-3), 8.20 (1H, d,  $J$  6.0, H-1), 8.14 (1H, d,  $J$  9.0, H-13), 8.06 - 8.01 (2H, m, H-2, 7), 6.96 (1H, d,  $J$  10.0, H-10);  $\delta_C$  (175 MHz,  $CDCl_3$ ): 185.4 (C-9), 136.5 (C-11), 132.3 (C-11b), 131.8 (C-13), 131.3 (C-3a or 5b), 131.1 (C-5a), 130.7 (C-4 or 8), 130.6 (C-4 or 8), 130.5 (C-13a), 129.9 (C-8a), 129.4 (C-6), 128.2 (C-3 or 10), 128.1 (C-3 or 10), 127.6 (C-1), 126.9 (C-3a or 5b), 126.8 (C-2 or 7), 126.5 (C-2 or 7), 125.9 (C-8b), 124.9 (C-3b), 123.7 (C-5c), 122.2 (C-5 or 12), 122.1 (C-5 or 12), 120.4 (C-11a); HRMS (ESI)  $m/z$  ( $C_{23}H_{13}O$   $[M+H]^+$  requires 305.0961) found 305.0966. This compound is previously reported and data are consistent with reports.<sup>333</sup>

#### 6.3.1.12 Phenalen-1-one; Perinaphthanone (266)



$\delta_H$  (400 MHz,  $CDCl_3$ ): 8.62 (1H, d,  $J$  7.5, H-9), 8.19 (1H, d,  $J$  8.0, H-7), 8.02 (1H, d,  $J$  8.5, H-6), 7.80 - 7.72 (3H, m, H-3, 4, 8), 7.59 (1H, m, H-5), 6.73 (1H, d,  $J$  10.0, H-2);  $\delta_C$  (100 MHz,  $CDCl_3$ ): 185.6 (C-1), 141.7 (C-3), 134.9 (C-7), 132.1 (C-6a), 131.9 (C-6), 131.3 (C-4), 130.3 (C-9), 129.5 (C-9a), 129.2 (C-2), 127.8 (C-3a or 9b), 127.5 (C-3a or 9b), 127.1 (C-8), 126.6 (C-5). This compound is previously reported and data are consistent with reports.<sup>414</sup>

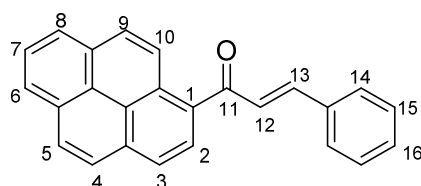
### 6.3.1.13 3-Oxo-3H-benzo[cd]pyrene (206)



$\nu_{\max}/\text{cm}^{-1}$ : 2918, 2850 (CH), 1625 (C=O), 1570 (C=C), 1141, 917, 807, 720 (aromatic rings); melting point: 197 - 203 °C \*(impure) (lit. 204 - 205 °C)<sup>331</sup>;  $\delta_{\text{H}}$  (500 MHz,  $\text{CDCl}_3$ ): 8.96 (1H, d,  $J$  8.0, H-2), 8.50 (1H, s, H-6), 8.44 (1H, d,  $J$  7.5, H-7), 8.42 (1H, d,  $J$  7.5, H-9), 8.40 (1H, d,  $J$  8.0, H-1), 8.29 (1H, d,  $J$  9.0, H-10), 8.23 (1H, d,  $J$  9.0, H-11), 8.12 (1H, t,  $J$  7.5, H-8), 8.02 (1H, d,  $J$  9.5, H-5), 6.96 (1H, d,  $J$  9.5, H-4);  $\delta_{\text{C}}$  (175 MHz,  $\text{CDCl}_3$ ): 185.7 (C-3), 140.9 (C-5), 135.2 (C-11a), 134.1 (C-6), 130.6 (C-9a), 130.0 (C-9), 129.9 (C-6a), 129.9, 129.8, 129.8 (C-4, 7, 10), 127.6 (C-11), 127.6 (C-5a), 126.9 (C-8), 126.9 (C-5b), 126.4 (C-2a), 126.2 (C-1, 2), 123.8 (C-11c), 123.3 (C-11b); HRMS (ESI)  $m/z$  ( $\text{C}_{19}\text{H}_{11}\text{O}$   $[\text{M}+\text{H}]^+$  requires 255.0804) found 255.0798. This compound is previously reported (without NMR) and data are consistent with these reports.<sup>331</sup>

### 6.3.1.14 Synthesis of 3-Oxo-3H-benzo[cd]pyrene: alternative synthesis.

#### 6.3.1.14.1 1-Cinnamoylpyrene (247)



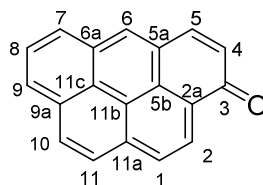
By the method of Didenko and Gerasimenko.<sup>331</sup>

To a solution of cinnamic acid (2.50 g, 16.8 mmol) in benzene (25.0 mL) was added phosphorus pentachloride (3.50 g, 16.8 mmol) and left to react at room temperature

until fully dissolved under a dinitrogen atmosphere. To this mixture, pyrene (3.00 g, 14.8 mmol) and aluminium chloride (3.00 g, 22.5 mmol) were added portion-wise and stirred for two hours at room temperature under a dinitrogen atmosphere. The reaction mixture was then slowly poured into cold dilute HCl. The organic layer was collected and washed with water twice, the organics were dried over Na<sub>2</sub>SO<sub>4</sub> and the solvent was removed *in vacuo*. The crude mixture was purified by silica column chromatography using chloroform: petroleum ether 40 - 60 °C (8:2) to afford a yellow solid (4.10 g, 84 %).

$\nu_{\max}/\text{cm}^{-1}$ : 3031 (CH), 1653 (C=O), 1572 (C=C), 1137, 840, 684 (aromatic rings) 965 (CH out-of-plane deformation); melting point: 110 - 113 °C (lit. 118 - 118.5 °C)<sup>331</sup>;  $\delta_{\text{H}}$  (500 MHz, CDCl<sub>3</sub>): 8.63 (1H, d, *J* 9.5, H-aryl), 8.27 - 8.23 (3H, m, H-aryl), 8.21 (1H, d, *J* 8.0, H-aryl), 8.18 (1H, d *J* 9.5, H-aryl), 8.16 (1H, d, *J* 9.0, H-aryl), 8.09 (1H, d, *J* 9.0, H-aryl), 8.05 (1H, t, *J* 7.5, H-7), 7.66 (1H, d, *J* 16.0, H-13), 7.62 - 7.58 (2H, m, H-15), 7.48 (1H, d, *J* 16.0, H-12), 7.43 - 7.38 (3H, m, H-14, 16);  $\delta_{\text{C}}$  (125 MHz, CDCl<sub>3</sub>): 195.9 (C-11), 145.9 (C-aryl), 134.6<sub>(quat)</sub>, 133.8<sub>(quat)</sub>, 133.2<sub>(quat)</sub>, 131.1<sub>(quat)</sub>, 130.7 (C-aryl), 130.6<sub>(quat)</sub>, 129.3<sub>(quat)</sub>, 129.1 (C-aryl), 129.1 (C-aryl), 128.9 (C-14 or 15), 128.5 (C-14 or 15), 127.4 (C-aryl), 127.1 (C-aryl), 126.3 (C-aryl), 126.2 (C-aryl), 126.1 (C-aryl), 125.9 (C-aryl), 124.9<sub>(quat)</sub>, 124.7 (C-aryl), 124.4<sub>(quat)</sub>, 124.0 (C-aryl); HRMS (ESI) *m/z* (C<sub>25</sub>H<sub>16</sub>ONa [M+Na] requires 355.1093) found 355.1100. This compound is previously reported (without NMR) and data are consistent with these reports.<sup>331</sup>

#### 6.3.1.14.2 3-Oxo-3H-benzo[cd]pyrene (206)

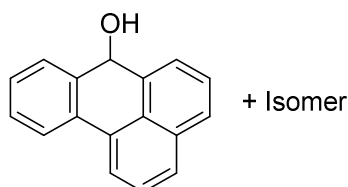


By the method of Didenko and Gerasimenko.<sup>331</sup>

Under a dinitrogen atmosphere to a stirring solution of aluminium chloride (2.00 g, 15.0 mmol) in benzene (15.0 mL), 1-cinnamoylpyrene (1.00 g, 3.01 mmol) was added and left to react under an inert atmosphere. After 30 minutes the reaction was cooled and added carefully to cold dilute HCl and the organics were collected. The organics were washed with water twice, dried over Na<sub>2</sub>SO<sub>4</sub> and reduced *in vacuo*. The crude product was purified by silica column chromatography using a gradient system of chloroform: ethyl acetate (98:2 then 9:1), to produce a light orange solid (0.29 g, 38 %).

Melting point: 204 - 206 °C (lit. 204 - 205 °C).<sup>331</sup> This compound is previously reported (without NMR) and the other data (above – see section 6.3.1.13) are consistent with these reports.<sup>331</sup>

#### 6.3.1.15 Benz[de]anthracen-ol: Dihydro-benzanthrone (254)

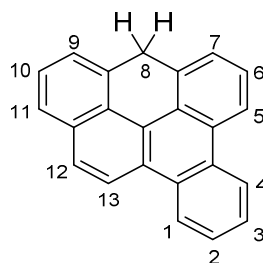


We believe that two isomers are present most likely OH in the 7H position (above) and another isomer which is difficult to predict. Ratio of isomers '254a' and '254b' - 1:1.4



$\delta_{\text{H}}$  (600 MHz,  $\text{CDCl}_3$ ): 7.66 (1H, d,  $J$  8.0, 254b), 7.58 (1H, d,  $J$  8.0, 254a), 7.53 (1H, d,  $J$  8.0, 254a), 7.47 (1H, d,  $J$  8.0, 254a), 7.42 - 7.40 (2H, m), 7.38 (1H, d,  $J$  8.0, 254b), 7.30 (1H, d,  $J$  8.0, 254b), 7.28 - 7.23 (2H, m), 7.16 - 7.09 (3H, m), 7.06 - 7.02 (3H, m), 6.96 (1H, t,  $J$  7.5, 254a), 6.76 (1H, d,  $J$  7.5, 254a), 6.49 (1H, d,  $J$  7.0, 254a), 6.37 (1H, d,  $J$  7.0, 254b), 4.76 (1H, s, 254b), 4.58 (1H, s, 254a).  $\delta_{\text{C}}$  (150 MHz,  $\text{CDCl}_3$ ): 134.9<sub>(quat)</sub>, 134.7<sub>(quat)</sub>, 134.6<sub>(quat)</sub>, 134.3<sub>(quat)</sub>, 132.7<sub>(quat)</sub>, 132.3<sub>(quat)</sub>, 131.7<sub>(quat)</sub>, 131.2<sub>(quat)</sub>, 130.1<sub>(quat)</sub>, 129.6<sub>(quat)</sub>, 129.4 (C-aryl), 129.3 (C-aryl), 129.2<sub>(quat)</sub>, 129.1<sub>(quat)</sub>, 126.9 (C-aryl), 126.9 (C-aryl), 126.9 (C-aryl), 126.8 (C-aryl), 126.7 (C-aryl), 126.5 (C-aryl), 126.2 (C-aryl), 126.1 (C-aryl), 125.9 (C-aryl), 125.8 (C-aryl), 125.4 (C-aryl), 124.9 (C-aryl), 124.8 (C-aryl), 122.5 (C-aryl), 118.2 (C-aryl), 118.1 (C-aryl), 58.5 ( $\underline{\text{C}}\text{H}$ , I1), 58.3 ( $\underline{\text{C}}\text{H}$ , I2). \*two  $^{13}\text{C}$  peaks missing due to overlapping peaks. These compounds are previously reported by Clar but only melting point reported.<sup>337</sup>

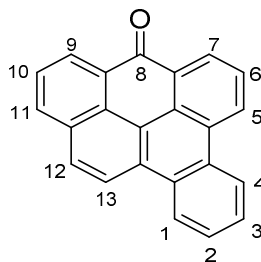
### 6.3.1.16 8H-Benzo[e,jk]pyrene (258)



$\nu_{\text{max}}/\text{cm}^{-1}$ : 2921, 2852 (CH), 1461 (CH deformations), 1041, 822, 765 (aromatic rings); melting point: 134 - 137 °C;  $\delta_{\text{H}}$  (600 MHz,  $\text{CDCl}_3$ ): 8.71 (2H, m, H-aryl), 8.58 (1H, d,  $J$  9.0, H-aryl), 8.54 (1H, d,  $J$  8.0, H-aryl), 7.94 (1H, d,  $J$  9.0, H-aryl), 7.77 (1H, d,  $J$  8.0, H-aryl), 7.72 - 7.66 (2H, m, H-aryl), 7.62 (1H, t,  $J$  7.5, H-aryl), 7.54 - 7.51 (2H, m, H-aryl), 7.49 (1H, dd,  $J$  7.0, 1.0, H-aryl), 4.95 (2H, s, H-8);  $\delta_{\text{C}}$  (150 MHz,  $\text{CDCl}_3$ ): 134.2<sub>(quat)</sub>, 134.1<sub>(quat)</sub>, 132.3<sub>(quat)</sub>, 130.0<sub>(quat)</sub>, 129.9<sub>(quat)</sub>, 129.7<sub>(quat)</sub>, 128.3<sub>(quat)</sub>, 127.6 (C-aryl), 127.2 (C-aryl), 126.9 (C-aryl), 126.8 (C-aryl), 126.6 (C-

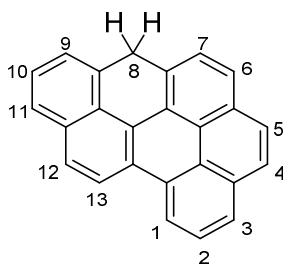
aryl), 126.4 (C-aryl), 125.6 (C-aryl), 125.5<sub>(quat)</sub>, 125.3 (C-aryl), 125.1<sub>(quat)</sub>, 125.1<sub>(quat)</sub>, 123.6 (C-aryl), 123.5 (C-aryl), 121.6 (C-aryl), 120.8 (C-aryl), 34.7 (C-8); HRMS (ESI)  $m/z$  ( $C_{23}H_{13}$   $[M-H]^-$  requires 289.1023) found 289.1014. This compound is previously unreported.

### 6.3.1.17 8-Oxo-8H-benzo[e,jk]pyrene (259)



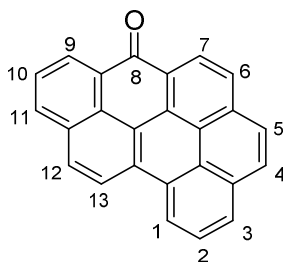
$\nu_{\max}/\text{cm}^{-1}$ : 3059, 2922 (CH), 1645 (C=O), 1598 (C=C), 1216, 948, 826, 750 (aromatic rings); melting point: 201 - 204 °C;  $\delta_{\text{H}}$  (700 MHz,  $\text{CDCl}_3$ ): 8.84 (1H, d,  $J$  8.0, H-5), 8.75 (1H, d,  $J$  7.0, H-9), 8.71 (1H, d,  $J$  7.5, H-7), 8.61 (1H, dd,  $J$  7.0, 2.0, H-1), 8.56 (1H, dd,  $J$  7.0, 2.0, H-4), 8.48 (1H, d,  $J$  9.0, H-13), 8.17 (1H, d,  $J$  7.5, H-11), 7.99 (1H, d,  $J$  9.0, H-12), 7.79 (1H, t,  $J$  7.5, H-6), 7.78 (1H, t,  $J$  7.5, H-10), 7.70 - 7.66 (2H, m, H-2, 3);  $\delta_{\text{C}}$  (175 MHz,  $\text{CDCl}_3$ ): 183.9 (C-8), 134.5 (C-aryl), 131.1<sub>(quat)</sub>, 130.1<sub>(quat)</sub>, 129.9<sub>(quat)</sub>, 129.9<sub>(quat)</sub>, 129.4 (C-aryl), 129.1 (C-aryl), 129.0<sub>(quat)</sub>, 128.9<sub>(quat)</sub>, 128.4 (C-aryl), 128.3 (C-aryl), 127.9 (C-aryl), 127.8<sub>(quat)</sub>, 127.8<sub>(quat)</sub>, 127.6 (C-aryl), 126.9 (C-aryl), 126.6 (C-aryl), 123.9 (C-aryl), 123.3 (C-aryl), 121.6 (C-aryl), 119.9<sub>(quat)</sub>. \*one  $^{13}\text{C}$  peak missing due to overlapping peaks; HRMS (ESI)  $m/z$  ( $C_{23}H_{13}O$   $[M+H]^+$  requires 305.0961) found 305.0974. This compound is previously unreported.

### 6.3.1.18 8H-Dibenzo[cd,ghi]perylene (244)



$\nu_{\max}/\text{cm}^{-1}$ : 2915, 2848 (CH), 1461 (CH deformations), 1052, 836, 727 (aromatic rings); melting point: 165 - 169 °C;  $\delta_{\text{H}}$  (700 MHz,  $\text{CDCl}_3$ ): 8.86 (1H, d,  $J$  8.0, H-aryl), 8.70 (1H, d,  $J$  9.0, H-aryl), 8.16 (1H, d,  $J$  7.5, H-aryl), 8.11 (1H, d,  $J$  8.0, H-aryl), 8.05 (1H, t,  $J$  7.5, H-aryl), 8.02 - 8.00 (2H, m, H-aryl), 7.99 (1H, d,  $J$  9.0, H-aryl), 7.86 (1H, d,  $J$  8.0, H-aryl), 7.79 (1H, d,  $J$  7.5, H-aryl), 7.57 - 7.52 (2H, m, H-aryl), 5.16 (2H, s, H-8);  $\delta_{\text{C}}$  (175 MHz,  $\text{CDCl}_3$ ): 134.4<sub>(quat)</sub>, 132.6<sub>(quat)</sub>, 131.9<sub>(quat)</sub>, 131.7<sub>(quat)</sub>, 129.6<sub>(quat)</sub>, 129.6<sub>(quat)</sub>, 128.7<sub>(quat)</sub>, 127.7 (C-aryl), 127.3 (C-aryl), 126.8 (C-aryl), 126.6 (C-aryl), 126.2 (C-aryl), 126.1 (C-aryl), 125.8 (C-aryl), 125.7<sub>(quat)</sub>, 125.6 (C-aryl), 125.6 (C-aryl), 125.4 (C-aryl), 124.8<sub>(quat)</sub>, 123.8<sub>(quat)</sub>, 121.9 (C-aryl), 120.1 (C-aryl), 34.9 (C-8) \*two  $^{13}\text{C}$  peaks missing due to overlapping peaks; HRMS (ESI)  $m/z$  ( $\text{C}_{25}\text{H}_{13}$   $[\text{M}-\text{H}]^-$  requires 313.1012) found 313.1018. This compound is previously unreported.

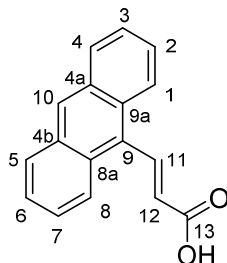
### 6.3.1.19 8-Oxo-8H-dibenzo[cd,ghi]perylene (245)



$\nu_{\max}/\text{cm}^{-1}$ : 2921, 2850 (CH), 1639 (C=O), 1583 (C=C), 928, 812, 718 (aromatic rings); melting point:  $>300\text{ }^{\circ}\text{C}$ ; (700 MHz,  $\text{CDCl}_3$ ): 9.11 - 9.09 (2H, m, H-aryl), 8.97 (1H, d,  $J$  7.5, H-aryl), 8.91 (1H, d,  $J$  9.0, H-aryl), 8.38 - 8.34 (3H, m, H-aryl), 8.30 - 8.26 (2H, m, H-aryl), 8.19 - 8.16 (2H, m, H-aryl), 7.94 (1H, t,  $J$  7.0, H-aryl);  $\delta_{\text{C}}$  (175 MHz,  $\text{CDCl}_3$ ): 183.9 (C-8), 135.3<sub>(quat)</sub>, 134.4 (C-aryl), 131.5<sub>(quat)</sub>, 131.3<sub>(quat)</sub>, 130.9<sub>(quat)</sub>, 130.3 (C-aryl), 129.9 (C-aryl), 129.8<sub>(quat)</sub>, 129.8 (C-aryl), 128.6 (C-aryl), 128.4<sub>(quat)</sub>, 128.1<sub>(quat)</sub>, 128.1<sub>(quat)</sub>, 127.5 (C-aryl), 126.9 (C-aryl), 126.8<sub>(quat)</sub>, 126.7 (C-aryl), 126.3 (C-aryl), 126.2 (C-aryl), 123.8<sub>(quat)</sub>, 123.2 (C-aryl), 122.9<sub>(quat)</sub>, 122.1 (C-aryl), 120.8<sub>(quat)</sub>; HRMS (ESI)  $m/z$  ( $\text{C}_{25}\text{H}_{13}\text{O}$   $[\text{M}+\text{H}]^+$  requires 329.0961) found 329.0958. This compound is previously unreported.

### 6.3.1.20 Synthesis of 3-oxo-3H-benz[*d,e*]anthrone.

#### 6.3.1.20.1 9-Anthraceneacrylic acid (261)



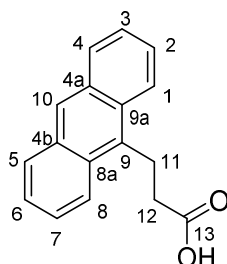
By the method of Atkinson *et al.*<sup>415</sup>

A mixture of 9-anthraldehyde (1.00 g, 4.85 mmol), malonic acid (0.65 g, 6.25 mmol), pyridine (2.50 mL) and piperidine (0.20 mL) was heated at 100 °C for 3 days, and then heated at 190 °C for 30 minutes. The mixture was cooled and poured into cold dilute HCl (2.00 M) where a precipitate was formed and collected by filtration. The precipitate was then dissolved in minimum ethyl acetate and partitioned with aqueous sodium hydroxide (2.00 M), the aqueous layer was collected and acidified with concentrated HCl. The yellow precipitate was collected by filtration, washed with a little water and left to dry. A yellow solid was obtained (0.76 g, 63 %).

$\nu_{\max}/\text{cm}^{-1}$ : 2821 (CH), 1682 (C=O), 1558 (C=C), 1152, 839, 681 (aromatic rings), 969 (CH out-of-plane deformation); melting point: 246 - 248 °C (lit. 244 - 245 °C)<sup>415</sup>;  $\delta_{\text{H}}$  (500 MHz,  $(\text{CD}_3)_2\text{SO}$ ): 8.65 (1H, s, H-10), 8.39 (1H, d,  $J$  16.0, H-11), 8.21 - 8.19 (2H, m, H-1, 8), 8.14 - 8.12 (2H, m, H-4, 5), 7.60 - 7.54 (4H, m, H-2, 3, 6, 7), 6.34 (1H, d,  $J$  16.0, H-12);  $\delta_{\text{C}}$  (125 MHz,  $(\text{CD}_3)_2\text{SO}$ ): 167.3 (C-13), 138.7 (C-11), 130.8 (C-4a, 4b), 130.2 (C-12), 129.5 (C-9), 128.7 (C-4, 5), 128.6 (C-8a, 9a), 127.6 (C-10), 126.4 (C-2, 7), 125.5 (C-3, 6), 124.9 (C-1, 8); HRMS (ESI)  $m/z$

(C<sub>17</sub>H<sub>11</sub>O<sub>2</sub> [M-H]<sup>-</sup> requires 247.0765) found 247.0763. This compound is previously reported and data are consistent with these reports.<sup>416</sup>

### 6.3.1.20.2 3-(Anthracen-9-yl)propanoic acid (262)

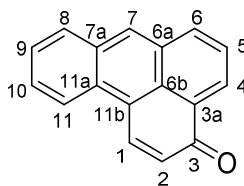


By the method of Atkinson *et al.*<sup>415</sup>

To a solution of 9-anthraceneacrylic acid (0.15 g, 0.60 mmol) in ethanol (5.00 mL) was added 10 % Pd/C (0.05 g) and left to react overnight at room temperature under a dihydrogen atmosphere. The reaction mixture was poured through a pad of celite which was washed through with ethyl acetate and the solvent was removed *in vacuo*. The crude mixture was purified by column chromatography using ethyl acetate : chloroform (55:45) to afford an off-white solid (0.11 g, 73 %).

$\nu_{\max}/\text{cm}^{-1}$ : 2924, 2851 (CH), 1692 (C=O), 1156, 836, 689 (aromatic rings), 726 (CH<sub>2</sub> rocking); melting point: 188 - 191 °C (lit. 192 - 193 °C)<sup>415</sup>;  $\delta_{\text{H}}$  (400 MHz, CDCl<sub>3</sub>): 8.39 (1H, s, H-10), 8.29 (2H, d, *J* 9.0, H-1, 8), 8.03 (2H, d, *J* 8.5, H-4, 5), 7.59 - 7.53 (2H, m, H-3, 6), 7.52 - 7.46 (2H, m, H-2, 7), 4.03 - 3.99 (2H, m, H-11), 2.88 - 2.84 (2H, m, H-12);  $\delta_{\text{C}}$  (100 MHz, CDCl<sub>3</sub>): 178.9 (C-13), 131.9 (C-9), 131.6 (C-4a, 4b), 129.5 (C-8a, 9a), 129.4 (C-4, 5), 126.5 (C-10), 126.1 (C-2, 7), 124.9 (C-3, 6), 123.8 (C-1, 8), 34.9 (C-12), 23.0 (C-11); HRMS (ESI) *m/z* (C<sub>17</sub>H<sub>13</sub>O<sub>2</sub> [M-H]<sup>-</sup> requires 249.0921) found 249.0923. This compound is previously reported and data are consistent with these reports.<sup>417</sup>

### 6.3.1.20.3 3-Oxo-3H-benz[d,e]anthrone (264)



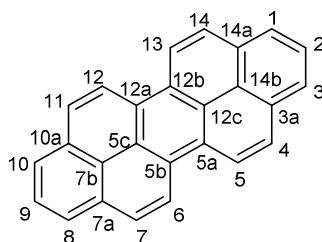
By the method of Pham *et al.*<sup>336</sup>

To a solution of 3-(anthracen-9-yl)propanoic acid (15.0 mg, 59.9  $\mu\text{mol}$ ) in dry dichloromethane (5.00 mL) was added thionyl chloride (5.00  $\mu\text{L}$ , 0.07  $\mu\text{mol}$ ) and DMF (1 drop) and left to react under a dinitrogen atmosphere for 2 hours. The solvent was removed *in vacuo* to leave an orange solid which was used straight away. The solid was re-dissolved in dry chloroform (5.00 mL) with the addition of stannic chloride (0.05 mL, 43.0  $\mu\text{mol}$ ) and the reaction was left to react under a dinitrogen atmosphere overnight. Cold dilute HCl was added and the organic layers were collected, dried over  $\text{Na}_2\text{SO}_4$  and the crude product was purified by silica column chromatography using chloroform : ethyl acetate (90:10). A red solid was obtained (5.00 mg, 36 %).

$\nu_{\text{max}}/\text{cm}^{-1}$ : 3042, 2920 (CH), 1628 (C=O), 1598 (C=C), 1194, 888, 768, 734 (aromatic rings); melting point: 119 - 121  $^{\circ}\text{C}$  (lit. 120  $^{\circ}\text{C}$ )<sup>336</sup>;  $\delta_{\text{H}}$  (500 MHz  $\text{CDCl}_3$ ): 8.84 (1H, dd,  $J$  7.0 1.0, H-4), 8.71 (1H, s, H-7), 8.71 (1H, d,  $J$  10.0, H-1), 8.54 (1H, d,  $J$  9.0, H-8), 8.43 (1H, dd,  $J$  8.0, 0.5, H-6), 8.09 (1H, d,  $J$  8.5, H-11), 7.84 (1H, dd,  $J$  8.0, 7.0, H-5), 7.73 (1H, ddd,  $J$  9.0, 6.5, 1.0, H-9), 7.58 (1H, ddd,  $J$  8.0, 6.5, 0.5, H-10), 6.93 (1H, d,  $J$  10.0, H-2);  $\delta_{\text{C}}$  (125 MHz  $\text{CDCl}_3$ ): 185.3 (C-3), 136.4 (C-1 or 6), 136.3 (C-1 or 6), 133.2 (C-4 or 7), 133.1 (C-4 or 7), 132.2 (C-11a), 131.9 (C-7a), 129.9 (C-3a or 6a), 129.9 (C-11), 129.8 (C-3a or 6a), 129.2 (C-9), 128.6 (C-2), 126.3 (C-5), 126.1 (C-10), 125.9 (C-6b), 122.4 (C-8), \*one  $^{13}\text{C}$  peak missing due to

overlapping peaks (11b); HRMS (ESI)  $m/z$  ( $C_{17}H_{10}ONa$   $[M+Na]^+$  requires 253.0624) found 253.0620. This compound is previously reported and data are consistent with these reports.<sup>418</sup>

### 6.3.1.21 Dibenzo[*cd, lm*]perylene; Peropyrene (265)

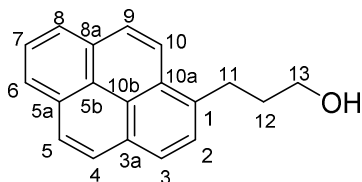


$\nu_{max}/cm^{-1}$ : 2951, 2915, 2847 (CH), 1462 (CH deformations), 1240, 836, 796 (aromatic rings); melting point:  $>300$  °C (lit.  $>300$  °C)<sup>338</sup>;  $\delta_H$  (500 MHz,  $CDCl_3$ ): 9.29 (4H, d,  $J$  9.0, H-5, 6, 12, 13), 8.43 (4H, d,  $J$  9.0, H-4, 7, 11, 14), 8.38 (4H, d,  $J$  7.5, H-1, 3, 8, 10), 8.15 (2H, t,  $J$  7.5, H-2, 9);  $\delta_C$  (125 MHz,  $CDCl_3$ ): 131.3 (C-3a or 5a), 127.8 (C-4, 7, 11, 14), 126.1 (C-2, 9), 125.4 (C-3a or 5a), 125.3 (C-1, 3, 8, 10), 125.3 (C-5c or 7b), 122.9 (C-5c or 7b), 122.9 (C-5, 6, 12, 13);  $m/z$  CMS (ASAP) 326.2 ( $[C_{26}H_{14}]$ ,  $[M]$ ). This compound is previously reported and data are consistent with these reports.<sup>338</sup>



## 6.3.2 Synthesis of intermediates for mechanism determination

### 6.3.2.1 3-(Pyrene-1-yl)propan-1-ol (299)



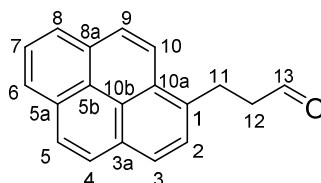
By the method of Horaguchi *et al.*<sup>363</sup>

3-(1-Pyrenyl)propionic acid (0.10 g, 0.36 mmol) was dissolved in minimum THF and was added drop-wise to a stirring solution of lithium aluminium hydride (0.02 g, 0.53 mmol) in THF (10.0 mL) at 0 °C under a dinitrogen atmosphere. The reaction was left to react at room temperature for 3 hours under a dinitrogen atmosphere. The solvent was removed *in vacuo*, followed by addition of water and HCl (1:3) sequentially. The mixture was partitioned with ethyl acetate, thereafter the organics were collected, dried over Na<sub>2</sub>SO<sub>4</sub> and the solvent was removed *in vacuo*. The crude product was purified by silica column chromatography using chloroform : ethyl acetate (9:1) to produce an off-white solid (85.0 mg, 91 %).

$\nu_{\max}/\text{cm}^{-1}$ : 3267 (OH), 2942, 2849 (CH), 1585 (C=C), 1168, 914, 840, 752 (aromatic rings), 720 (CH<sub>2</sub> rocking); melting point: 96 - 98 °C (lit. 67 - 70 °C)<sup>419</sup>;  $\delta_{\text{H}}$  (500 MHz, CDCl<sub>3</sub>): 8.30 (1H, d, *J* 9.0, H-4 or 5), 8.17 (2H, d, *J* 8.0, H-6, 8), 8.11 (1H, d, *J* 7.5, H-3), 8.10 (1H, d, *J* 9.0, H-4 or 5), 8.05 - 8.01 (2H, m, H-9, 10), 8.00 (1H, t, *J* 7.5, H-7), 7.88 (1H, d, *J* 7.5, H-2), 3.78 (2H, t, *J* 6.5, H-13), 3.45 (2H, t, *J* 7.5, H-11), 2.16 - 2.09 (2H, m, H-12);  $\delta_{\text{C}}$  (125 MHz, CDCl<sub>3</sub>): 136.1 (C-10b), 131.4 (C-8a), 130.9 (C-5a), 129.8 (C-10a), 128.6 (C-3a), 127.5 (C-5), 127.3 (C-2), 127.2 (C-9 or 10), 126.6 (C-9 or 10), 125.8 (C-7), 125.1 (C-5b or 1), 124.9 (C-5b or 1), 124.9 (C-6 or 8), 124.8 (C-6 or 8), 124.7 (C-3), 123.3 (C-4), 62.4 (C-13), 34.5 (C-

12), 29.6 (C-11); HRMS (ESI)  $m/z$  ( $C_{19}H_{16}ONa$   $[M+Na]^+$  requires 283.1093) found 283.1090. This compound is previously reported and data are consistent with these reports.<sup>420</sup>

### 6.3.2.2 3-(1-Pyrenyl)propionaldehyde (300)



By the method of Sabitha *et al.*<sup>365</sup>

An ice-cooled solution of IBX (103 mg, 369  $\mu$ mol) in DMSO (2.00 mL) was added to 3-(pyrene-1-yl)propan-1-ol (80.0 mg, 308  $\mu$ mol) in dry dichloromethane (1.00 mL). The mixture was stirred at room temperature for 4 hours and filtered through a celite pad with ethyl acetate. The organics were collected and washed with water and then brine, dried over  $Na_2SO_4$  and the solvent was removed *in vacuo*. The residue was purified by silica column chromatography with chloroform to produce an off-white solid (59.0 mg, 62 %).

$\nu_{max}/cm^{-1}$ : 3037, 2894 (CH), 2851, 2747 (C-H aldehyde) 1709 (C=O), 1584 (C=C), 1183, 891, 841, 754 (aromatic rings), 714 ( $CH_2$  rocking); melting point: 69 - 71  $^{\circ}C$  (lit.72 - 73.2  $^{\circ}C$ )<sup>304</sup>;  $\delta_H$  (500 MHz,  $CDCl_3$ ): 9.89 (1H, s, H-13), 8.17 (3H, m, H-aryl), 8.09 (1H, d,  $J$  9.0, H-aryl), 8.09 (1H, d,  $J$  8.0, H-aryl), 8.04 - 7.99 (3H, m, H-aryl), 7.84 (1H, d,  $J$  8.0, H-aryl), 3.64 (2H, t,  $J$  7.5, H-11), 2.96 (2H, td,  $J$  8.0, 1.0, H-12);  $\delta_C$  (125 MHz,  $CDCl_3$ ): 201.3 (C-13), 134.2<sub>(quat)</sub>, 131.3<sub>(quat)</sub>, 130.7<sub>(quat)</sub>, 130.1<sub>(quat)</sub>, 128.4<sub>(quat)</sub>, 127.6 (C-aryl), 127.4 (C-aryl), 126.9 (C-aryl), 126.8 (C-aryl), 125.9 (C-aryl), 125.1 (C-aryl), 124.9<sub>(quat)</sub>, 124.9 (C-aryl), 124.9 (C-aryl), 124.8<sub>(quat)</sub>, 122.6 (C-aryl), 45.4 (C-12), 25.6 (C-11); HRMS (ESI)  $m/z$  ( $C_{19}H_{14}ONa$   $[M+Na]^+$  requires

281.0937) found 281.0936. This compound is previously reported (without NMR) and data are consistent with these reports.<sup>304</sup>

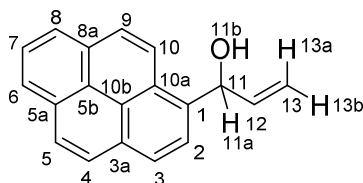
#### 6.3.2.2.1 3-(1-pyrenyl)propionaldehyde reaction with PPA

3-(1-pyrenyl)propionaldehyde (0.165 g, 0.639 mmol) was added to a stirring solution of polyphosphoric acid under a dinitrogen atmosphere and left to react for 18 hours at 80 °C. The reaction was cooled, followed by addition of water and the mixture was partitioned with dichloromethane (3 x 20 mL). The organics were collected, dried over Na<sub>2</sub>SO<sub>4</sub> and the solvent was removed *in vacuo*. The dark orange solid was analysed by <sup>1</sup>H NMR spectroscopy.

#### 6.3.2.2.2 3-(1-pyrenyl)propionaldehyde reaction with sulfuric acid

3-(1-Pyrenyl)propionaldehyde (7.50 mg, 29.1 μmol) was added to a stirring solution of sulfuric acid (80 %) under a dinitrogen atmosphere and left to react for 18 hours at 80 °C. The reaction was cooled, water was added and the mixture was partitioned with dichloromethane (3 x 20 mL). The organics were collected, dried over Na<sub>2</sub>SO<sub>4</sub> and the solvent was removed *in vacuo*. The dark orange solid was analysed by <sup>1</sup>H NMR spectroscopy.

#### 6.3.2.3 1-(Pyrene-1-yl)prop-2-en-1-ol (302)



By the method of Lafrance *et al.*<sup>364</sup>

To a solution of pyrenecarboxaldehyde (0.50 g, 2.17 mmol) in THF (5.00 mL) was slowly added vinyl magnesium bromide (2.60 mL, 2.61 mmol, 1.00 M) in THF at

0 °C under a dinitrogen atmosphere. The mixture was allowed to warm to room temperature and left to react overnight. The solution was then quenched with saturated ammonium chloride and extracted with dichloromethane. The organics were collected, dried over Na<sub>2</sub>SO<sub>4</sub> and the solvent was removed *in vacuo*. The residue was purified by silica column chromatography using chloroform : petroleum ether 40 - 60 °C (8:2) to afford a pale yellow solid (0.40 g, 71 %).

$\nu_{\max}/\text{cm}^{-1}$ : 3240 (OH), 3038 (CH), 1585 (C=C), 1182, 886, 840, 752 (aromatic rings), 1058 (C-O), 987, 918 (RCH=CH<sub>2</sub>); melting point: 101 - 103 °C;  $\delta_{\text{H}}$  (500 MHz, CDCl<sub>3</sub>): 8.21 (1H, d, *J* 9.5, H-10), 8.14 (1H, d, *J* 7.5, H-6 or 8), 8.12 (1H, d, *J* 7.5, H-6 or 8), 8.08 - 8.05 (2H, m, H-2, 3), 7.88 (1H, d, *J* 9.0, H-4 or 5), 7.87 (1H, t, *J* 7.5, H-7), 7.84 (1H, d, *J* 9.5, H-9), 7.83 (1H, d, *J* 9.0, H-4 or 5), 6.29 (1H, ddd, *J* 17.0, 10.5, 5.5, H-12), 6.09 - 6.06 (1H, m, H-11a), 5.43 (1H, dt, *J* 17.0, 1.5, H-13a), 5.27 (1H, dt, *J* 10.5, 1.5, H-13b), 2.80 (1H, br. s, H-11b);  $\delta_{\text{C}}$  (125 MHz, CDCl<sub>3</sub>): 139.7 (C-12), 135.4 (C-1), 131.1<sub>(quat)</sub>, 130.7<sub>(quat)</sub>, 130.4 (C-3b), 127.7<sub>(quat)</sub>, 127.4 (C-aryl), 127.2 (C-aryl), 127.2 (C-aryl), 125.7 (C-aryl), 125.1 (C-aryl), 124.9 (C-aryl), 124.8 (C-aryl), 124.7<sub>(quat)</sub>, 124.6 (C-10a), 123.8 (C-aryl), 122.6 (C-10), 115.3 (C-13), 72.0 (C-11); HRMS (ESI) *m/z* (C<sub>19</sub>H<sub>14</sub>ONa [M+Na]<sup>+</sup> requires 281.0937) found 281.0938. This compound is previously unreported.

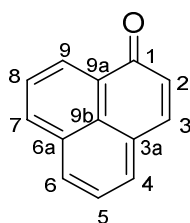
#### 6.3.2.3.1 1-(Pyrene-1-yl)prop-2-en-1-ol reaction with PPA and sulfuric acid

These reactions were treated as the method as above but with 1-(Pyrene-1-yl)prop-2-en-1-ol.

### 6.3.3 Carbon-13 labelled experiments

Naphthalene (0.5 g, 3.90 mmol) was added to a mixture of glycerol (1.42 g, 15.4 mmol) and  $^{13}\text{C}_3$  glycerol (158 mg, 1.66 mmol). Thereafter, 80 %  $\text{H}_2\text{SO}_4$  (5.00 mL, 3.51 mmol) was added dropwise to the mixture and the reaction was heated to 80 °C and left to react for 18 hours. The reaction mixture was cooled and placed into an ice bath where 5.0 M NaOH was added until pH 7. The mixture was filtered through a Büchner funnel with a filter guide and washed through with dichloromethane (2 x 30 mL). The filtrate mixture was partitioned and the organic layer was collected. The aqueous layer was extracted a further three times with dichloromethane and the organic layers were collected together, dried over  $\text{Na}_2\text{SO}_4$  and the solvent was removed *in vacuo* to give the crude product mixture (0.35 g). The mixture was purified by a gradient silica column chromatography using 100 % petroleum ether 40 - 60 °C to chloroform. Labelled phenalen-1-one, pyrene, 6*H*-benzo[*cd*]pyrene and 6-oxo-6*H*-benzo[*cd*]pyrene samples were isolated however each of these samples would contain different labelled three-unit spin systems (As shown in Chapter 3.8).

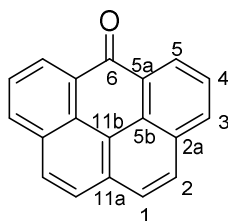
#### 6.3.3.1 $^{13}\text{C}$ -Phenalen-1-one; $^{13}\text{C}$ -Perinaphthanone (266a)



$\delta_{\text{C}}$  (125 MHz,  $\text{CDCl}_3$ ): 185.7 (d,  $J$  54.5, C-1), 141.8 (d,  $J$  62.0, C-3), 134.9 (dd,  $J$  57.5, 2.0, C-7), 131.9 (dd,  $J$  60.0, 2.0, C-6), 131.3 (dd,  $J$  54.0, 2.0, C-4), 130.4 (dd,  $J$  55.0, 1.5, C-9), 129.5 (s, C-9a), 129.2 (dd,  $J$  62, 54.5, C-2), 127.8 (s, C-3a or 9b), 127.5 (s, C-3a or 9b), 127.0 (dd,  $J$  61.5, 54.0, C-8), 126.6 (dd,  $J$  63.5, 54.0, C-5),

\*one  $^{13}\text{C}$  peak missing due to overlapping peaks (132.1 C-6a); HRMS (ESI)  $m/z$  ( $\text{C}_{13}\text{H}_8\text{ONa}$  [ $^{12}\text{C}_{10}^{13}\text{C}_3\text{H}_8\text{O}+\text{Na}$ ] $^+$  requires 206.0569) found 206.0568.

### 6.3.3.2 $^{13}\text{C}$ -6-Oxo-6H-benzo[cd]pyrene (210a)



$\delta_{\text{C}}$  (125 MHz,  $\text{CDCl}_3$ ): 184.5 (t,  $J$  55.5, C-6), 184.5 (dd,  $J$  54.0, 4.0, C-6), 134.5 (dd,  $J$  57.0, 1.5, C-3), 132.1 (d,  $J$  54.0, C-11a), 131.2 (d,  $J$  54.0, C-2a), 129.8 (d,  $J$  54.5, C-5a), 129.3 (dd,  $J$  55.0, 1.5, C-5), 128.7 (d,  $J$  62.5, C-2), 128.7 (dd,  $J$  62.0, 53.5, C-2), 126.9 (d,  $J$  61.5, C-1), 126.9 (dd,  $J$  62.5, 53.0, C-1), 126.8 (dd,  $J$  57.0, 55.0, C-4), 121.2 (s, C-11b), \*one  $^{13}\text{C}$  peak missing due to overlapping peaks (128.2, C-5b); HRMS (ESI)  $m/z$  ( $\text{C}_{19}\text{H}_{10}\text{ONa}$  [ $^{12}\text{C}_{16}^{13}\text{C}_3\text{H}_{10}\text{O}+\text{Na}$ ] $^+$  requires 280.0725) found 280.0730.

## 6.3.4 Analysis of the black powder

### 6.3.4.1 Infra-red spectroscopy

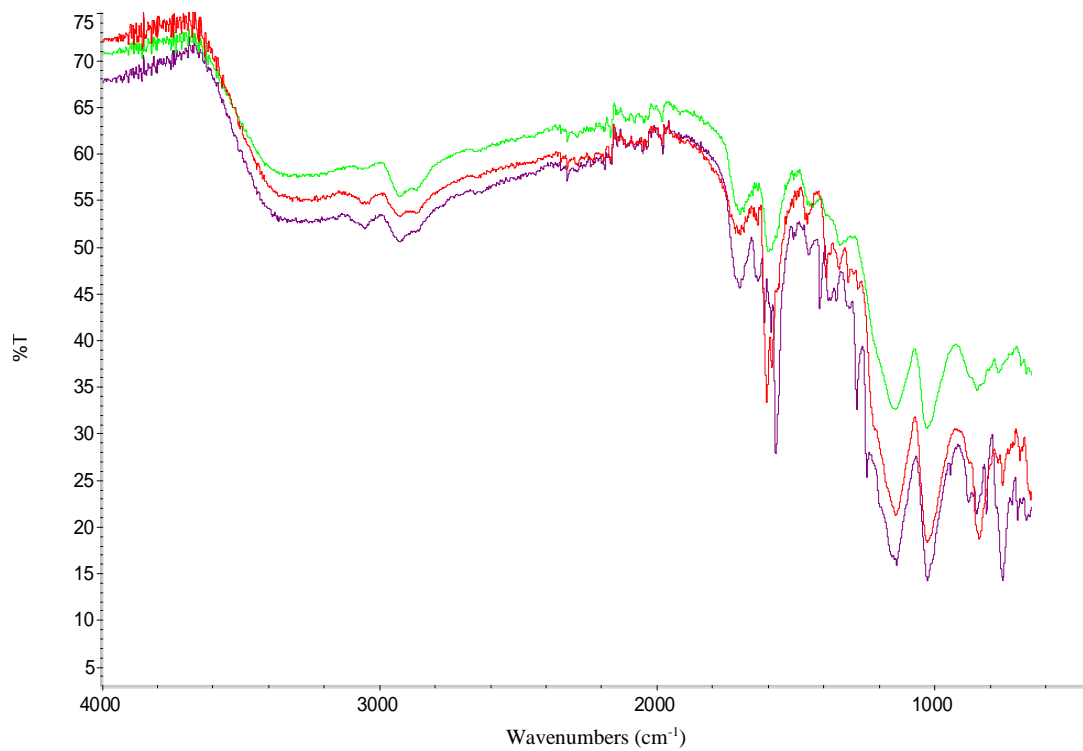


**Figure 87: IR spectrum of the black powder obtained from pyrene, anthracene and naphthalene, all with very similar readings.**

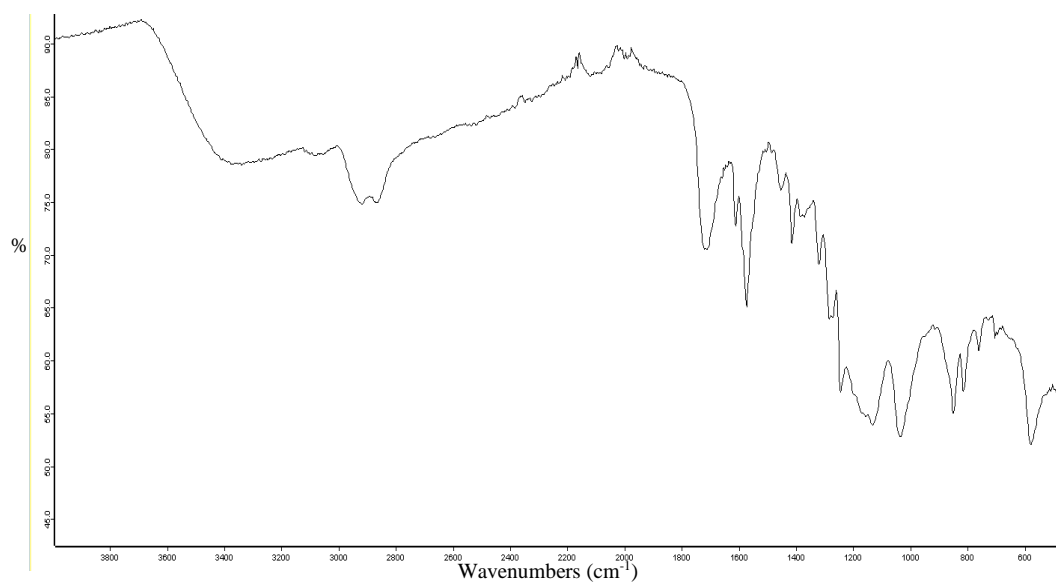


**Figure 88: IR of perylene, with similar reading to the other three peri-condensation black products.**

Graphitic substances have been reported to have very similar IR spectra containing the characteristic peaks as above.<sup>378, 386, 421</sup>

#### 6.3.4.2 Raman spectroscopy

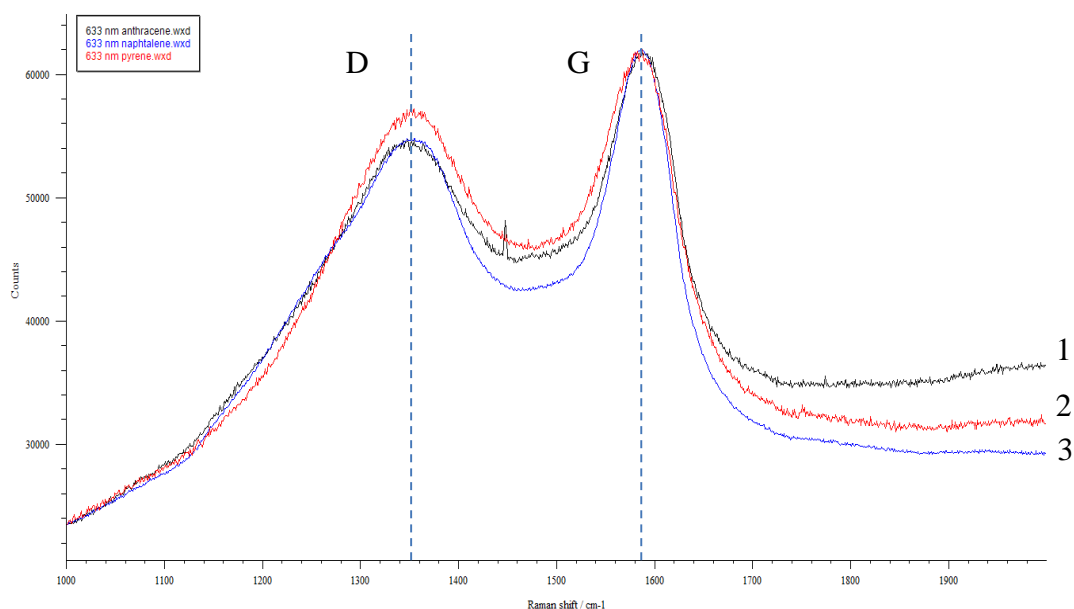


**Figure 89: Raman spectra of the black powder obtained from the reagents anthracene (1), pyrene (2) and naphthalene (3).**

Comparing the Raman spectra to the literature, it shows two broad peaks which are known to be typical graphene oxide-like; a 'G' band at around 1587 cm<sup>-1</sup> and a 'D' band at around 1354 cm<sup>-1</sup>. The 'D' band is caused by the asymmetry of the compound in terms of defects in this case. The 'G' band is due to carbon-carbon bond stretching vibrations and at this shift specific to sp<sup>2</sup> carbons.<sup>378, 379, 381, 382, 384</sup> Alternatively, the Raman results can also be interpreted as; the broad peaks can be attributed to the different compound sizes being in a close range (5-11 rings). This broadening usually occurs in the Raman spectra of big and complex structures such as polymers and proteins. However, the presence of different compounds with fairly similar structures would cause the same effect because similar bonds, such as C=C, in different environments (for example varying number of conjugate states) vibrate



in similar but not the same frequencies.<sup>383, 384</sup> Typically, in a mixture of compounds with very similar structures, this difference in frequency is smaller than the resolution that the instrument provides. Thus the resulting peak will be an average for all vibrations with similar energy.

#### 6.3.4.3 *ssNMR spectroscopy*

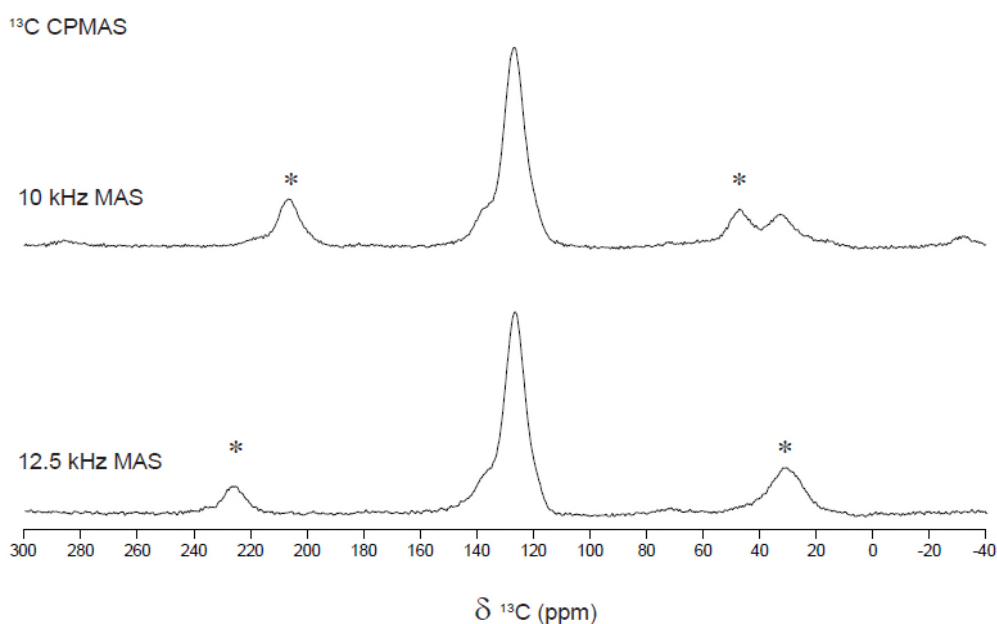


**Figure 90: Shows the 500 MHz Carbon-13 solid state MAS NMR spectra of the insoluble product. Two different spin speeds were used to help deduce real peaks from side bands which are denoted as \*.**

A strong broad peak around 115 - 150 ppm was present, which can be attributed to aromatic rings present within the structure. There is also a small peak around 20 - 40 ppm which is attributed to CH<sub>2</sub>/CH<sub>3</sub> groups. It was imperative that at least two different spinning speeds were used in the ssNMR because these peaks (sidebands) can be easily interpreted as 'real' peaks as part of the structure of the compound in question. In addition, these side bands can also mask other smaller, less intense peaks which can be seen in Figure 90 at around 20 - 40 ppm.

#### ***6.3.4.4 Thermogravimetric analysis (TGA)***

In the TGA spectrum, the small mass loss (15 % wt %) at around 200 °C could be due to the decomposition of some functional groups, such as carbonyls. Consequently, this can also be due to the side products with an alkane chain on from the un-cyclised glycidol as seen in the ssNMR. In addition, the PAHs can be heavily  $\pi$ -stacked which therefore increases the temperature of decomposition. There is also a general trend that upon increasing the number of the aromatics rings the decomposition temperature increases with a few exceptions (e.g. pyrene decomposition is at approximately 330 °C and perylene around 375 °C).<sup>380, 385, 386</sup>

### 6.3.4.5 X-ray photoelectron spectroscopy (XPS)

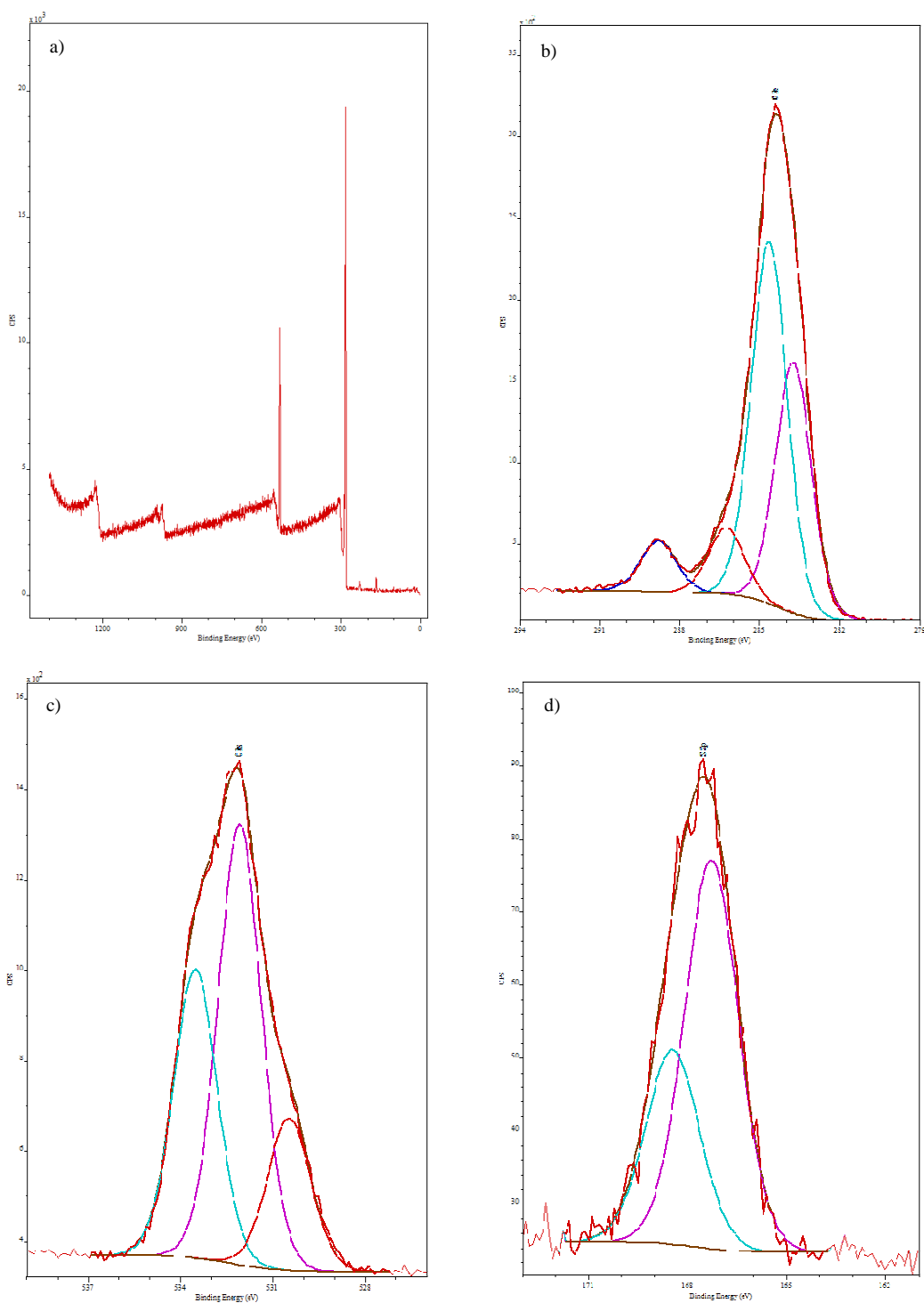


**Figure 91: a) XPS survey spectrum of black powder, b) carbon spectrum, c) oxygen spectrum and d) sulfur spectrum, with the different bonds which can be typically expected plotted underneath the peak of each element.**

The results detected carbon, oxygen and sulfur from the sample in a ratio of 85:14:1, respectively. There is still a high ratio of carbon to oxygen and the results closely match the EDX data. In addition, it can be said that there was a negligible amount of sulfur detected, as XPS is generally more sensitive to sulfur.

#### **6.3.4.6 Scanning electron microscopy (SEM)**

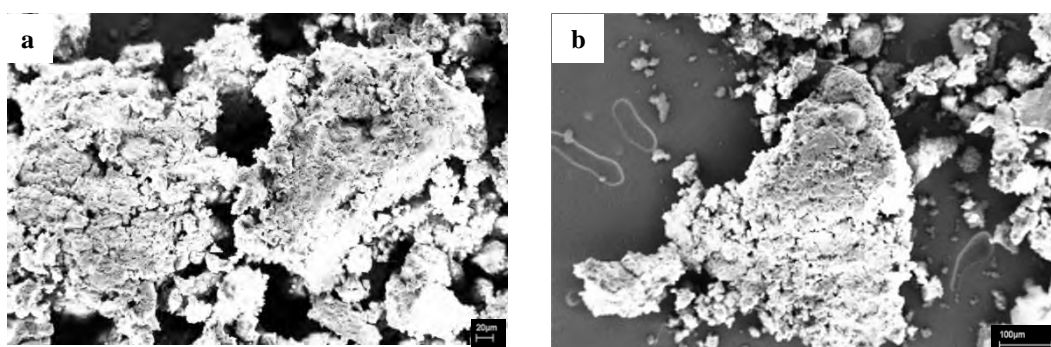


**Figure 92: SEM (a, b) of the black powder formed.**

The SEM images show that there are lots of small particles gathered together and no large sheets exhibited like graphene. In addition, the sample unexpectedly conducts the electron beam hence bright spots can be seen on the images.

#### 6.3.4.7 Transmission electron microscopy (TEM)

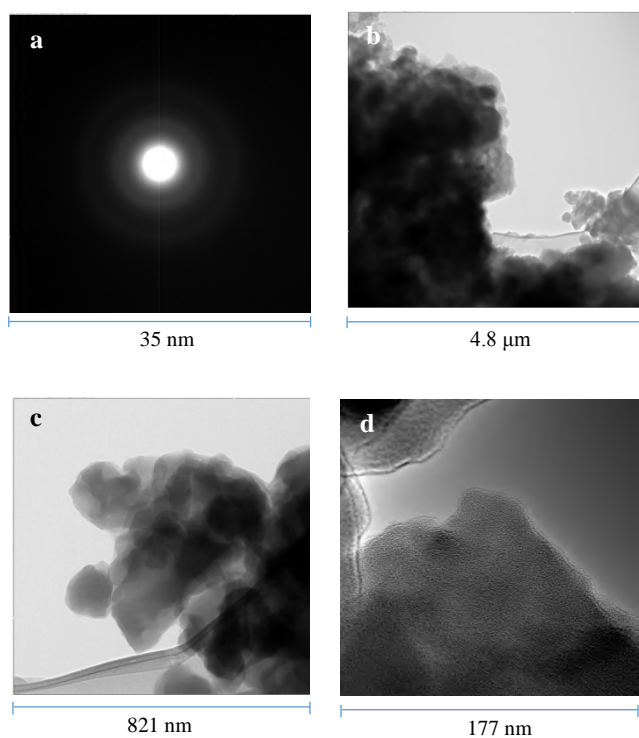


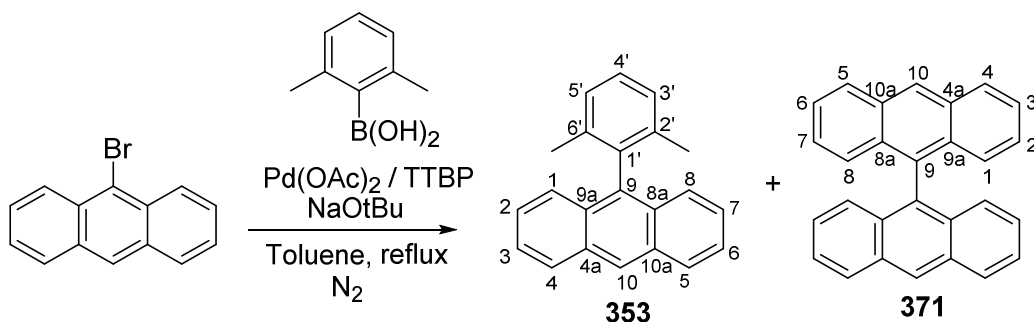
**Figure 93: a) Electron diffraction pattern of the black powder. (b, c, d) TEM of black solid on a lacy carbon support film.**

Due to the insolubility of the black powder in common solvents the powder was deposited onto the lacy carbon by direct transfer of the solid. The selected area electron diffraction pattern (a) shows no diffraction spots and hence there is no order in the structure in terms of large sheets of molecules.

## 6.4 Experimental for Chapter 4

### 6.4.1 Failed triangulene synthesis: Coupling method.

#### 6.4.1.1 9-(2,6-Dimethylphenyl)anthracene (353)



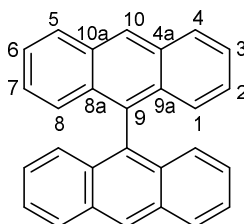
By the method modified from Zhao *et al.* and Raders *et al.*<sup>396, 404</sup>

Degassed toluene (45.0 mL) was added to a mixture of 9-bromoanthracene (2.00 g, 7.77 mmol, 1.00 equiv.), 2,6-dimethylboronic acid (1.51 g, 10.1 mmol, 1.30 equiv.), tri-*tert*-butylphosphine (113 mg, 5 mol %), palladium acetate (69.8 mg, 4 mol %) and sodium *tert*-butoxide (2.24 g, 23.3 mmol, 3.00 equiv.) under a dinitrogen atmosphere and heated at 110 °C. After 48 hours the reaction mixture was cooled and the solvent was removed *in vacuo*, the residue was dissolved in dichloromethane (70.0 mL) and the organic layer was washed with water (2 x 50 mL). The organics were collected, dried over Na<sub>2</sub>SO<sub>4</sub> and the solvent was removed *in vacuo*. The brown solid was purified *via* column chromatography using 100 % petroleum ether 40 - 60 °C where a white crystalline solid was obtained (0.72 g, 32 %).

$\nu_{\max}/\text{cm}^{-1}$ : 3044, 2918 (CH), 1581 (aromatic), 1375 (CH<sub>3</sub> sym. deformations), 1309, 883 (aromatic rings); melting point: 144 - 145 °C (lit. 145 - 146 °C)<sup>403</sup>;  $\delta_{\text{H}}$  (400 MHz, CDCl<sub>3</sub>): 8.53 (1H, s, H-10), 8.10 (2H, d, *J* 8.0, H-4, 5), 7.52 - 7.46 (4H, m, H-1, 3, 6, 8), 7.42 - 7.34 (3H, m, H-4', 2, 7), 7.31 (2H, d, *J* 7.5, H-3', 5'), 1.79 (6H, s, H-7');  $\delta_{\text{C}}$  (100 MHz, CDCl<sub>3</sub>): 137.7 (C-2', 6'), 137.5 (C-1'), 135.5 (C-9), 131.6 (C-8a, 9a),

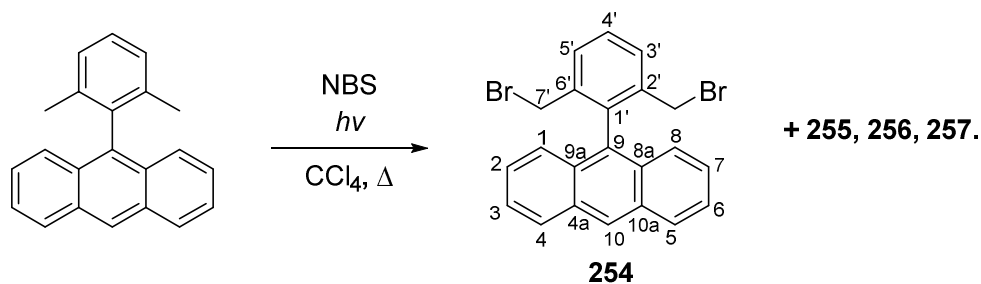
129.5 (C-4a, 10a), 128.6 (C-4, 5), 127.6 (C-4'), 127.4 (C-3', 5'), 126.2 (C-10), 125.8 (C-2, 7), 125.6 (C-1, 8), 125.2 (C-3, 6), 20.1 (C-7'); GCMS (EI):  $m/z$  C<sub>22</sub>H<sub>18</sub> 282 [M]. This compound is previously reported and data are consistent with these reports.<sup>403</sup>

#### 6.4.1.2 Bis-anthracene (371)



This compound was produced from the reaction above as a minor side product (60 mg, 2 %).  $\nu_{\max}/\text{cm}^{-1}$ : 3047 (CH), 1518, 1318, 888 (aromatic ring); melting point:  $>300$  °C (lit. 300 °C)<sup>422</sup>;  $\delta_{\text{H}}$  (400 MHz, CDCl<sub>3</sub>): 8.69 (2H, s, H-10), 8.16 (4H, d,  $J$  8.5, H-4, 5), 7.47 - 7.43 (4H, m, H-3, 6), 7.18 - 7.08 (8H, m, H-1, 2, 7, 8);  $\delta_{\text{C}}$  (100 MHz, CDCl<sub>3</sub>): 133.0 (C-9) 131.6 (C-8a, 9a or 4a, 10a), 131.5 (C-8a, 9a or 4a, 10a), 128.5 (C-2, 7), 127.2 (C-10), 126.8 (C-1, 8), 125.8 (C-2, 7), 125.3 (C-3, 6); GCMS (EI):  $m/z$  C<sub>28</sub>H<sub>18</sub> 354 [M]. This compound is previously reported and data are consistent with these reports.<sup>422</sup>

#### 6.4.1.3 9-(2,6-Bis(bromomethyl)phenyl)anthracene (354)



By the method modified from Lai *et al.* and Stewart *et al.*<sup>423, 424</sup>

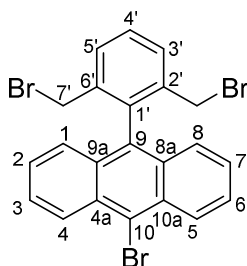
9-(2,6-Dimethylphenyl)anthracene (100 mg, 354  $\mu\text{mol}$ ) was dissolved in  $\text{CCl}_4$  (8.00 mL) and *N*-bromosuccinimide (190 mg, 1.06 mmol) along with benzoyl peroxide (50.0 mg, 0.21 mmol) was added. The reaction was heated to 65  $^\circ\text{C}$ , under a dinitrogen atmosphere and a light source used (7 Watt, LED). The reaction was left for 48 hours to react with benzoyl peroxide was added every 12 hours. After this period the mixture was cooled and filtered, the filtrate was collected and solvent was removed *in vacuo*. The mixture was purified by a gradient silica column chromatography system using 100 % petroleum ether and then petroleum ether 40 - 60  $^\circ\text{C}$  : chloroform (1:1), to produce a pale orange solid (32.0 mg, 21 %). With additional side products (**355** 12 %, **356** 31 %, **357** 12 %).

$\nu_{\text{max}}/\text{cm}^{-1}$ : 2920, 2820 (CH), 1600 (aromatic), 1449 ( $\text{CH}_2$  asym. deformations), 1343, 886 (aromatic ring) 758, 737 (CBr); melting point: 130 - 133  $^\circ\text{C}$  (lit. 132 - 134  $^\circ\text{C}$ )<sup>424</sup>;  $\delta_{\text{H}}$  (500 MHz,  $\text{CDCl}_3$ ): 8.59 (1H, s, H-10), 8.01 (2H, d,  $J$  8.5, H-4, 5), 7.63 (2H, d,  $J$  8.0, H-3', 5'), 7.62 - 7.58 (1H, m, H-4'), 7.49 (2H, ddd,  $J$  8.5, 5.5, 2.0, H-3, 6), 7.39 - 7.35 (4H, m, H-1, 2, 7, 8), 3.94 (4H, s, H-7');  $\delta_{\text{C}}$  (125 MHz,  $\text{CDCl}_3$ ): 138.0 (C-2', 6'), 137.6 (C-1'), 131.4 (C-8a, 9a), 131.0 (C-3', 5'), 130.4 (C-9), 130.3 (C-4a, 10a), 129.3 (C-4'), 128.6 (C-4, 5), 127.9 (C-10), 126.2 (C-1, 8 or C-2, 7), 126.0 (C-1, 8 or C-2, 7), 125.5 (C-3, 6), 31.2 (C-7'); GCMS (EI):  $m/z$   $\text{C}_{22}\text{H}_{16}\text{Br}_2$  440



[M]. This compound is previously reported and data are consistent with these reports.<sup>424</sup>

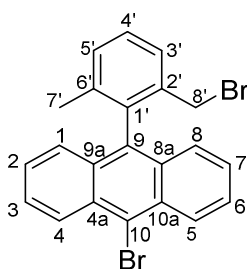
#### 6.4.1.4 9-Bromo(2,6-bis(bromomethyl)phenyl)anthracene (355)



$\nu_{\max}/\text{cm}^{-1}$ : 2920, 2850 (CH), 1572 (aromatic), 1438 ( $\text{CH}_2$  asym. deformations), 1333, 883 (aromatic ring) 753, 728 (CBr); melting point: 136 - 138 °C;  $\delta_{\text{H}}$  (700 MHz,  $\text{CDCl}_3$ ): 8.65 (2H, d,  $J$  9.0, H-4, 5), 7.71 (2H, d,  $J$  8.0, H-3', 5'), 7.63 - 7.60 (3H, m, H-4', 3, 6), 7.42 - 7.39 (4H, m, H-1, 2, 7, 8), 3.91 (4H, s, H-7');  $\delta_{\text{C}}$  (175 MHz,  $\text{CDCl}_3$ ): 137.9 (C-2', 6'), 137.1 (C-1'), 131.2 (C-3', 5'), 131.1 (C-9), 130.9 (C-8a, 9a), 130.4 (C-4a, 10a), 129.6 (C-4'), 128.1 (C-4, 5), 127.4 (C-3, 6), 126.8 (C-1, 8), 126.3 (C-2, 7), 124.4 (C-10), 30.9 (C-7'); GCMS (EI):  $m/z$   $\text{C}_{22}\text{H}_{16}^{79}\text{Br}_2^{81}\text{Br}$  520 [M].

This compound is previously unreported.

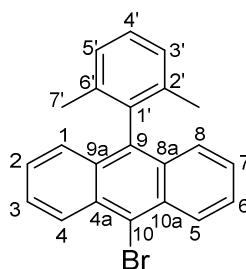
#### 6.4.1.5 9-Bromo((2-bromomethyl, 6-methyl)phenyl)anthracene (356)



$\nu_{\max}/\text{cm}^{-1}$ : 3030, 2970 (CH), 1550 (aromatic), 1438 ( $\text{CH}_2$  asym. deformations), 1380 ( $\text{CH}_3$  sym. deformations), 1333, 881 (aromatic ring) 757 (CBr); melting point: 165 - 167 °C;  $\delta_{\text{H}}$  (400 MHz,  $\text{CDCl}_3$ ): 8.64 (2H, d,  $J$  9.0, H-4, 5), 7.61 (2H, ddd,  $J$  9.0, 6.0,

1.5, H-3, 6), 7.58 (1H, d,  $J$  7.5, H-3'), 7.49 (1H, t, H-4'), 7.44 - 7.35 (5H, m, H-1, 2, 7, 8, 5'), 3.94 (2H, s, H-8'), 1.73 (3H, s, H-7');  $\delta_C$  (100 MHz, CDCl<sub>3</sub>): 138.4 (C<sub>quat</sub>), 137.2 (C-1'), 137.1 (C<sub>quat</sub>), 133.7 (C<sub>quat</sub>), 130.6 (C<sub>quat</sub>), 130.4 (C<sub>quat</sub>), 130.3 (C-5'), 128.8 (C-4'), 128.4 (C-3'), 128.1 (C-4, 5), 127.2 (C-3, 6), 126.5 (C-1, 8), 126.1 (C-2, 7), 123.4 (C-10), 31.8 (C-8'), 19.9 (C-7'); GCMS (EI):  $m/z$  C<sub>22</sub>H<sub>16</sub>Br<sub>2</sub> 440 [M]. This compound is previously unreported.

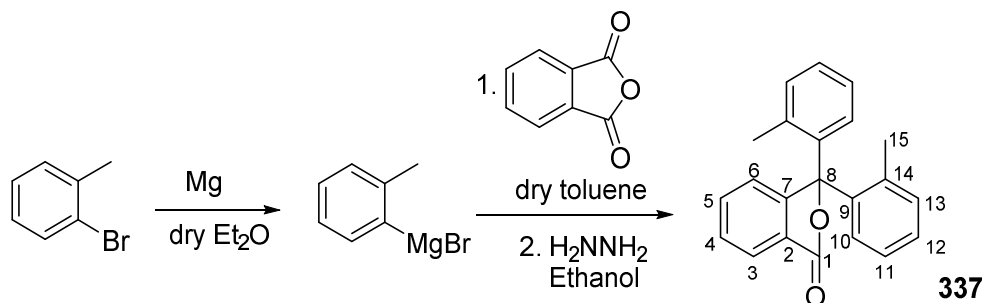
#### 6.4.1.6 9-Bromo(2,6-Dimethylphenyl)anthracene (357)



$\nu_{\max}/\text{cm}^{-1}$ : 2920, 2854 (CH), 1578 (aromatic), 1376 (CH<sub>3</sub> sym. deformations), 1333, 879 (aromatic ring) 754 (CBr); melting point: 159 - 162 °C;  $\delta_H$  (400 MHz, CDCl<sub>3</sub>): 8.63 (2H, d,  $J$  9.0, H-4, 5), 7.60 (2H, ddd,  $J$  9.0, 6.5, 1.0, H-3, 6), 7.47 (2H, br. d,  $J$  8.5, H-1, 8), 7.40 - 7.35 (3H, m, H-1', 2, 7), 7.27 (2H, d,  $J$  8.0, H-3', 5'), 1.74 (6H, s, H-7');  $\delta_C$  (100 MHz, CDCl<sub>3</sub>): 137.6 (C-2', 6'), 137.1 (C-1'), 136.3 (C-9), 130.5 (C-8a, 9a or 4a, 10a), 130.3 (C-8a, 9a or 4a, 10a), 128.1 (C-4, 5), 127.9 (C-4'), 127.5 (C-3', 5'), 127.1 (C-3, 6), 126.2 (C-1, 8), 125.9 (C-2, 7), 122.4 (C-10), 20.1 (C-7'); GCMS (EI):  $m/z$  C<sub>22</sub>H<sub>17</sub><sup>81</sup>Br 282 [M]. This compound is previously unreported.

## 6.4.2 Synthesis of 3,8-dihydro-3H,8H-dibenzo[cd,mn]pyrene

### 6.4.2.1 3,3-Di-*o*-tolyl-1,3-dihydro-2-benzofuran-1-one (337)



By the method of Allinson *et al.*<sup>388</sup>

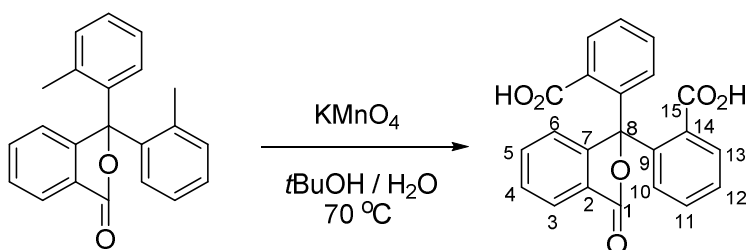
Dry diethyl ether (170 mL) was added to magnesium turnings (8.82 g, 0.36 mol) under a dinitrogen atmosphere *via* a cannula. The solution was heated to reflux and 2-bromotoluene (40.0 mL, 0.33 mol) was added drop-wise and the solution was left to reflux for a further 3 hours.

In a separate flask dry toluene (280 mL) was added *via* a cannula to solid phthalic anhydride (20.0 g, 0.13 mol) under a dinitrogen atmosphere. The *o*-tolylmagnesium bromide was then slowly added to the phthalic anhydride solution *via* a cannula and the reaction was left to reflux for one and a half days. The reaction was cooled and quenched with 2.00 M HCl (250 mL) on an ice bath. The organic layers were collected and washed with water (3 x 200 mL), dried over Na<sub>2</sub>SO<sub>4</sub> and the solvent was removed *in vacuo* to provide a crude viscous orange residue. The viscous orange residue was dissolved in ethanol (250 mL), followed by addition of hydrazine monohydrate (8.60 mL, 0.18 mol) and the reaction was heated to reflux for 24 hours. The ethanol was removed *in vacuo* and the solid was filtered and collected in a Büchner funnel which was then washed with cold ethanol (3 x 20 mL). The solid

was collected and left to dry in a desiccator to obtain a pure off-white powder (9.25 g, 22 %).

$\nu_{\max}/\text{cm}^{-1}$ : 1755 (C=O ester), 1597 (C=C), 1463 (CH deformations), 1118, 691 (aromatic ring); melting point: 171 - 174 °C (lit. 172 - 174 °C)<sup>388</sup>;  $\delta_{\text{H}}$  (500 MHz,  $\text{CDCl}_3$ ): 7.96 (1H, d,  $J$  7.5, H-3), 7.68 (1H, td,  $J$  7.5 1.0, H-5), 7.56 (1H, td,  $J$  7.5, 0.5, H-4), 7.39 (1H, d,  $J$  7.5, H-6), 7.23 (2H, td,  $J$  7.5, 1.0, H-12), 7.17 (2H, br. d,  $J$  7.0, H-13), 7.09 (2H, td,  $J$  7.5, 1.0, H-11), 7.02 (2H, dd,  $J$  8.0, 0.5, H-10), 2.14 (6H, s, H-15);  $\delta_{\text{C}}$  (125 MHz,  $\text{CDCl}_3$ ): 170.0 (C-1), 151.3 (C-7), 138.8 (C-9), 137.3 (C-14), 133.9 (C-5), 132.8 (C-13), 129.2 (C-4), 128.5 (C-12), 127.1 (C-10), 126.5 (C-2), 125.7 125.7 (C-3, 11), 125.2 (C-6), 94.1 (C-8), 21.5 (C-15); HRMS (ESI)  $m/z$  ( $\text{C}_{22}\text{H}_{18}\text{O}_2\text{Na}$   $[\text{M}+\text{Na}]^+$  requires 337.1199) found 337.1200. This compound is previously reported and data are consistent with these reports.<sup>388</sup>

#### 6.4.2.2 Di-(*o*-carboxyphenyl)-phthalide (338)



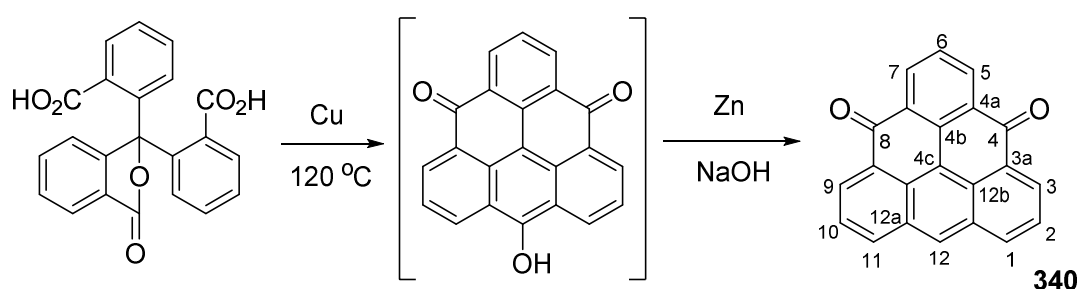
By the method modified from Clar *et al.* and Ye *et al.*<sup>316, 406</sup>

$\text{KMnO}_4$  (1.26 g, 7.97 mmol, 2.50 equiv.) was added portion-wise to a stirring solution of **337** (1.00 g, 3.18 mmol) in  $t\text{BuOH}/\text{H}_2\text{O}$  (1:1, 10.0 mL). The mixture was heated to  $70\text{ }^\circ\text{C}$  for 2 hours and then the reaction was cooled to room temperature and more  $\text{KMnO}_4$  (1.26 g, 7.97 mmol, 2.50 equiv.) was added portion-wise. The solution was then heated to  $70\text{ }^\circ\text{C}$  and left to react overnight. The hot reaction mixture was filtered through a pad of celite and washed through with hot water. The

water in the filtrate was removed *in vacuo* to approximately 10 % of its original volume. The residue was then acidified into an ice bath with concentrated HCl to pH 2 to form a precipitate. The precipitate was collected and dried in a desiccator to obtain a crystalline white solid (0.86 g, 72 %).

$\nu_{\max}/\text{cm}^{-1}$ : 3072 (OH), 1745 (C=O ester), 1712 (C=O acid) 1596 (C=C), 1115, 693 (aromatic); melting point: 255 - 261 °C;  $\delta_{\text{H}}$  (500 MHz,  $(\text{CH}_3)_2\text{SO}$ ): 12.72 (2H, br. s, OH), 7.85 (1H, br. d,  $J$  7.5, H-3), 7.80 (1H, br. d,  $J$  7.5, H-6), 7.77 (1H, td,  $J$  7.5, 1.0, H-5), 7.63 (1H, td,  $J$  7.5, 1.0, H-4), 7.48 - 7.45 (2H, m, H-13), 7.43 - 7.37 (4H, m, H-11, 12), 7.24 - 7.20 (2H, m, H-10);  $\delta_{\text{C}}$  (125 MHz,  $(\text{CH}_3)_2\text{SO}$ ): 169.5 (C-15), 168.9 (C-1), 151.3 (C-7), 137.9 (C-9), 133.9 (C-5), 132.9 (C-14), 129.6 (C-4), 129.5 (C-11 or 12), 129.1 (C-13), 128.2 (C-10 or 11 or 12), 128.1 (C-10 or 11 or 12), 125.7 (C-2), 125.2 (C-3 or 6), 125.1 (C-3 or 6), 90.5 (C-8); HRMS (ESI)  $m/z$  ( $\text{C}_{22}\text{H}_{14}\text{O}_6\text{Na}$   $[\text{M}+\text{Na}]^+$  requires 397.0683) found 397.0680. This compound is previously unreported.

#### 6.4.2.3 4,8-Dioxo-4H,8H-dibenzo[cd,mn]pyrene (340)



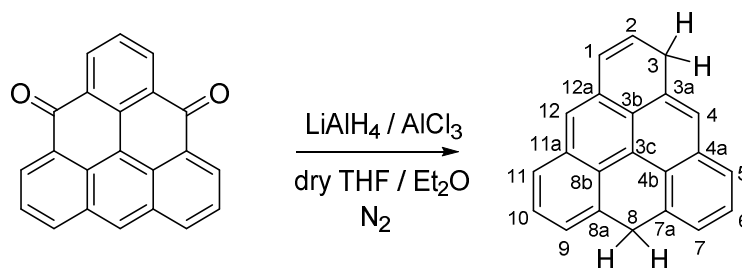
Method modified from literature.<sup>134, 316, 388</sup>

Copper powder (0.22 g, 3.50 mmol) and sulfuric acid (7.00 mL) were added to **338** (0.77 g, 2.06 mmol) and heated to 120 °C for 2 hours. The mixture was filtered hot through sintered glass. The solution was cooled and then cold water (5.00 mL) was

added, thereafter the dark blue precipitate was collected by filtration. The blue precipitate was then dissolved in minimum dilute 2.0 M NaOH (30 mL) with zinc dust added (1.5 g) and the mixture was left to react under a dinitrogen atmosphere. This was stirred (0.5 - 1 hour) until on exposure to air, the solution did not go back to a dark blue colour when left for about 5 minutes. The solution was then filtered and air was bubbled through it for approximately 15 minutes where a precipitate was observed. Concentrated HCl was added and the red solution was partitioned with dichloromethane (3 x 40 mL), the organic layers were collected and dried over Na<sub>2</sub>SO<sub>4</sub>. The dark red crude solid was purified by column chromatography using chloroform : ethyl acetate (9:1), to obtain a pure bright red solid (22 mg, 35 %).

$\nu_{\max}/\text{cm}^{-1}$ : 2918, 2848 (CH), 1644 (C=O), 1576 (C=C), 1220, 948, 750 (aromatic ring); melting point: >300 °C (lit. >300 °C)<sup>316</sup>;  $\delta_{\text{H}}$  (500 MHz, CDCl<sub>3</sub>): 8.96 (2H, dd, *J* 7.0, 1.0, H-3), 8.84 - 8.82 (3H, m, H-5, 12), 8.49 (2H, br. d, *J* 8.0, H-1), 7.89 (2H, dd, *J* 8.0, 7.0, H-2), 7.81 (1H, t, *J* 7.5, H-6);  $\delta_{\text{C}}$  (125 MHz, CDCl<sub>3</sub>): 182.9 (C-4), 136.3 (C-1), 135.5 (C-4b), 133.3 (C-3 or 5), 133.0 (C-3 or 5), 132.4 (C-12), 130.9 (C-3a or -12a), 130.7 (C-4a), 128.7 (C-3a or -12a), 128.2 (C-6), 126.7 (C-2), 126.7 (C-12b), 116.7 (C-4c); HRMS (ESI) *m/z* (C<sub>22</sub>H<sub>10</sub>O<sub>2</sub>Na [M+Na]<sup>+</sup> requires 329.0573) found 329.0575. This compound is previously reported and data are consistent with these reports.<sup>134</sup>

#### 6.4.2.4 3,8-Dihydro-3H,8H-dibenzo[cd,mn]pyrene (12a)



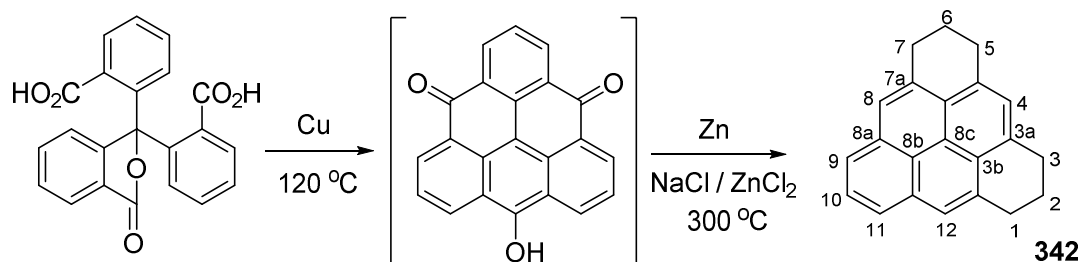
By the method of Hara *et al.*<sup>26</sup>

To a stirring solution of LiAlH<sub>4</sub> (9.90 mg, 0.26 mmol, 4.00 equiv.) and AlCl<sub>3</sub> (69.0 mg, 522 μmol, 8.00 equiv.) in dry diethyl ether (5.00 mL), **240** (20.0 mg, 65.0 μmol) in dry THF (5.00 mL) was added drop-wise in an ice bath under a dinitrogen atmosphere. The reaction was then left at room temperature for 1.5 hours to react. The solvent was removed *in vacuo*, dichloromethane was added (5.00 mL) to the reaction, followed by the sequential addition of water and aqueous HCl (1:3) under a dinitrogen atmosphere. The organic layers were collected and dried over Na<sub>2</sub>SO<sub>4</sub>, this was then filtered through a silica plug and the solvent was removed *in vacuo* to produce a red solid (17.0 mg, 93 %).

$\nu_{\text{max}}/\text{cm}^{-1}$ : 2953, 2919, 2849 (CH), 1585 (C=C), 1231, 930, 751 (aromatic ring) 710 (CH<sub>2</sub> rocking); melting point: 182 - 185 °C (lit. 178 - 181 °C)<sup>26</sup>;  $\delta_{\text{H}}$  (500 MHz, CDCl<sub>3</sub>): 7.94 (1H, d, *J* 8.0, H-5), 7.58 (1H, d, *J* 8.0, H-11), 7.53 - 7.49 (1H, m, H-6), 7.47 (1H, s, H-4 or 12), 7.41 (1H, dd, *J* 7.0, 1.0, H-7), 7.40 - 7.36 (1H, m, H-10), 7.35 (1H, s, H-4 or 12), 7.32 (1H, dd, *J* 7.0, 1.0, H-9), 6.74 (1H, dt, *J* 10.0, 2.0, H-1), 6.18 (1H, dt, *J* 10.0, 4.0, H-2), 4.87 (2H, br. s, H-8), 3.90 (2H, br. s, H-3);  $\delta_{\text{C}}$  (125 MHz, CDCl<sub>3</sub>): 146.2 (C-3c), 134.3 (C-7a), 133.0 (C-8a), 131.1 (C-11a), 129.4 (C-12a), 128.1 (C-8b), 127.9 (C-1), 127.6 (C-4b), 126.2 (C-6), 125.8 (C-2 or 10), 125.7 (C-2 or 10), 125.3 (C-11), 125.1 (C-7), 124.8 (C-9), 124.6 (C-3b), 123.9 (C-

4a), 123.7 (C-4 or 12), 118.0 (C-5), 111.7 (C-3a), 34.2 (C-8), 26.6 (C-3), \*one  $^{13}\text{C}$  peak missing due to overlapping peaks; HRMS (ESI)  $m/z$  ( $\text{C}_{22}\text{H}_{15}$   $[\text{M}+\text{H}]^+$  requires 279.1168) found 279.1168. This compound is previously reported and data are consistent with these reports.<sup>26</sup>

#### 6.4.2.5 1,2,3,5,6,7-Hexahydro-dibenzo[cd,mn]pyrene (342)



This method was modified from literature.<sup>134, 316, 388</sup>

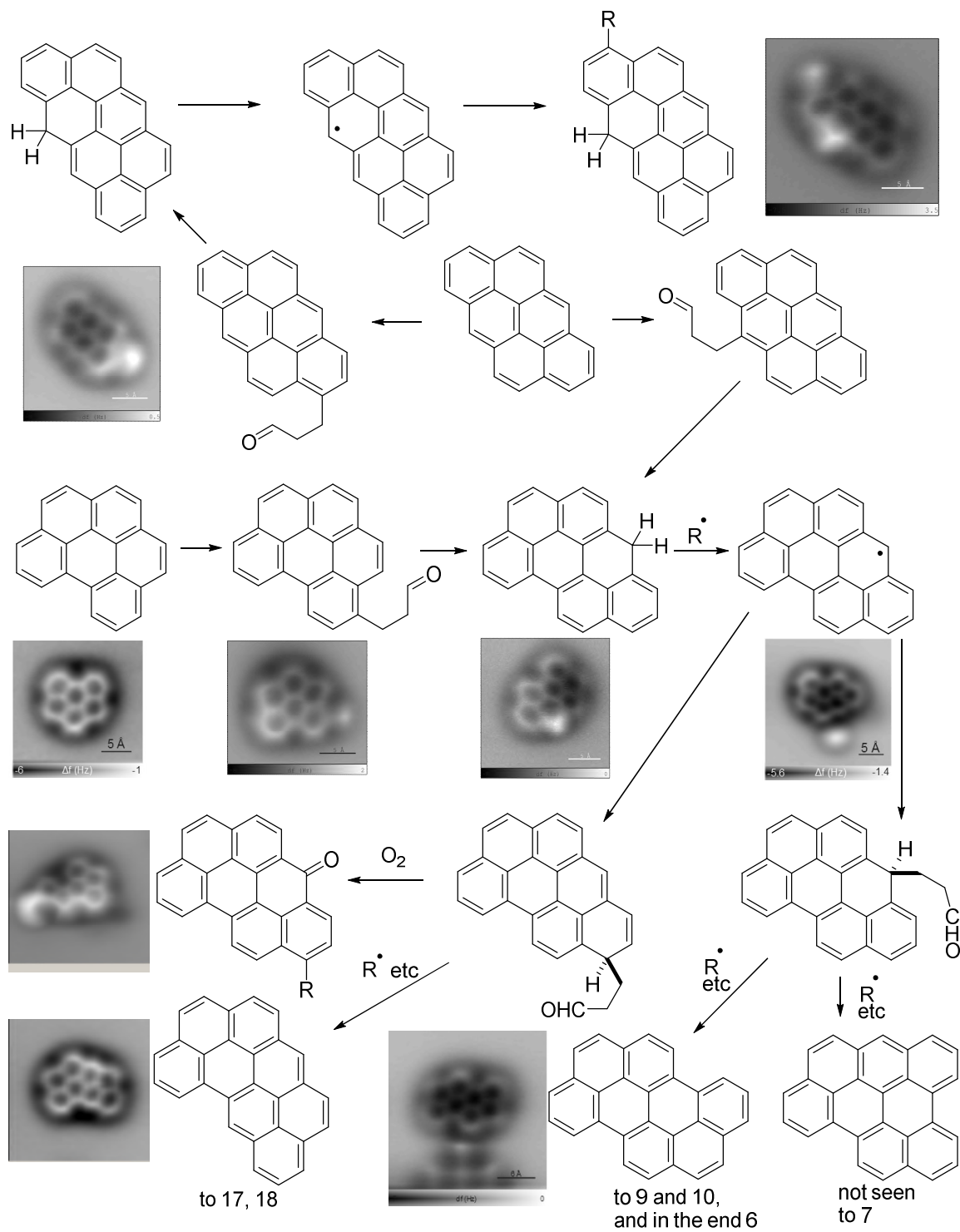
Copper powder (0.07 g, 1.10 mmol) and sulfuric acid (2.00 mL) were added to **338** and heated to 120 °C for 2 hours. The mixture was filtered hot through sintered glass. The solution was cooled and then cold water (10.0 mL) added, thereafter the dark blue precipitate was collected by filtration. The blue precipitate was added to a mixture of zinc dust (264 mg, 4.04 mmol, 6.00 equiv.), sodium chloride (274 mg, 4.70 mmol, 7.00 equiv.) and zinc chloride (1.47 g, 10.8 mmol, 16.0 equiv.) and was heated to 300 °C for 1 hour. The reaction was cooled and dilute acetic acid was added, which was then partitioned with dichloromethane (3 x 10 mL). The organics were collected, dried over  $\text{Na}_2\text{SO}_4$  and the solvent was removed *in vacuo* to give an orange residue. This was purified by silica column chromatography using petroleum ether 40 - 60 °C : chloroform (9:1), to yield an off white solid (30.0 mg, 16 %).

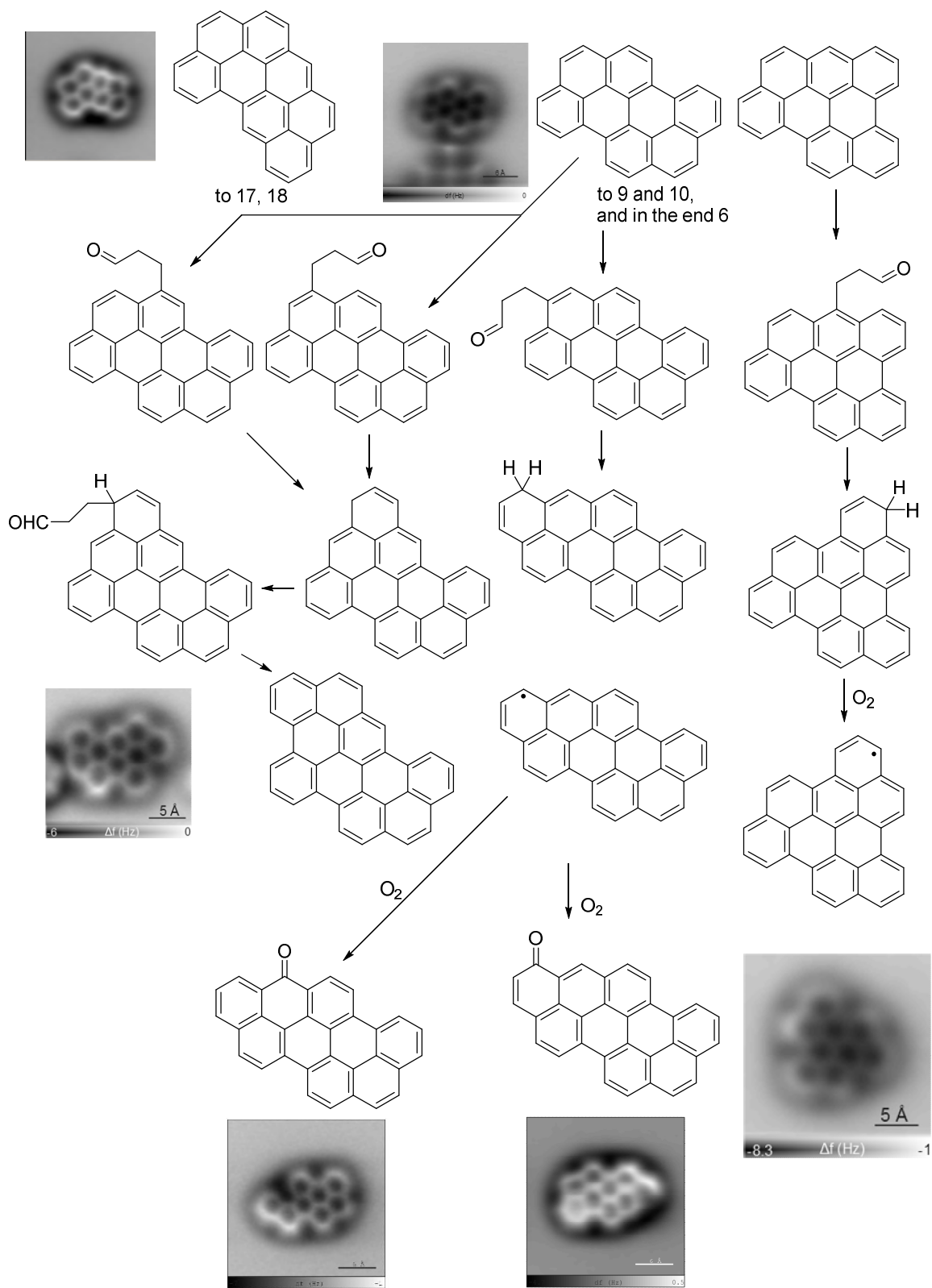
$\nu_{\text{max}}/\text{cm}^{-1}$ : 2917, 2851 (CH), 1579 (C=C), 1452, 1437 (CH deformations), 1214, 933, 758 (aromatic ring) 739 ( $\text{CH}_2$  rocking); melting point: 168 - 170 °C (lit. 175 - 176 °C)<sup>316</sup>;  $\delta_{\text{H}}$  (500 MHz,  $\text{CDCl}_3$ ): 7.96 (2H, br. d,  $J$  7.5, H-9), 7.89 (1H, dd,  $J$  8.5,



6.5, H-10), 7.72 (2H, br. s, H-8), 7.60 (1H, br. s, H-4), 3.35 (4H, br. t,  $J$  6.0, H-5), 3.28 (4H, td,  $J$  6.0, 1.0, H-7), 2.23 (4H, quin.,  $J$  6.0, H-6);  $\delta_{\text{C}}$  (125 MHz,  $\text{CDCl}_3$ ): 135.2 (C-7a), 134.0 (C-3a), 131.5 (C-8a), 126.1 (C-3b), 125.9 (C-10), 125.6 (C-4), 124.9 (C-8c), 123.6 (C-8b), 122.7 (C-8), 122.4 (C-9), 31.8 (C-7), 31.6 (C-5), 23.5 (C-6); HRMS Orbitrap XL (APCI)  $m/z$  ( $\text{C}_{22}\text{H}_{19}$   $[\text{M}+\text{H}]^+$  requires 283.1481) found 283.1483. This compound is previously reported and data (without NMR) are consistent with these reports.<sup>316</sup>







**Scheme 79: Possible explanation into AFM images observed of compounds from the pyrene black powder mixture. Images by IBM Zürich.<sup>321</sup>**

## 6.6 DFT calculation of the dihydro-triangulene isomers **12** & **12a**.

The energies (including zero-point energy) of the symmetrical **12** and non-symmetrical (**12a**) isomers of dihydro-triangulene were calculated using the B3LYP-D3(BJ) functional and the TZVP basis set. The asymmetrical isomer **12a** is 4.5 kJ/mol more stable.

**12** -847.2237083 0.288035

**12a** -847.2254338 0.287947

\*The same parameters were used for the DFT calculations for the HOMO of phenalene **182**, and SOMO of the phenalenyl radical **7** in section 3.7, and also the SOMO of radical **310** in section 3.9.9.

## 7 References

1. A. Ishizaki, K. Saito, N. Hanioka, S. Narimatsu and H. Kataoka, *J. Chromatogr. A*, 2010, **1217**, 5555-5563.
2. S. J. Cyvin and I. Gutman, *Comput. Maths. Appl.*, 1986, **12**, 859-876.
3. A. Kekulé, *Bull. Soc. Chim. Fr.*, 1865, **3**, 98-110.
4. A. S. Couper, *Ann. Chim. Phys.*, 1858, **53**, 469-489.
5. J. Loschmidt, *Chemische Studien*, Carl Gerold's Sohn, Vienna, Austria-Hungary, 1861.
6. W. J. Wiswesser, *Aldrichimica Acta.*, 1989, **22**, 17-19.
7. A. T. Balaban, P. v. R. Schleyer and H. S. Rzepa, *Chem. Rev.*, 2005, **105**, 3436-3447.
8. W. S. Fleischhacker, T., *Pioneering Ideas dor the Physical and Chemical Sciences: Loschmidt's Graphic Formulae of 1861*, Springer US, Vienna, Austria, 1997.
9. A. Kekulé, *Justus Liebigs Ann. Chem.*, 1866, **137**, 129-196.
10. M. Randic, *J. Am. Chem. Soc.*, 1977, **99**, 444-450.
11. E. Clar, *The Aromatic Sextet*, J. Wiley, New York, 1972.
12. E. Clar, I. A. Macpherson and H. Schulz-Kiesow, *Justus Liebigs Ann. Chem.*, 1963, **669**, 44-52.
13. M. Rule, A. R. Matlin, D. E. Seeger, E. F. Hilinski, D. A. Dougherty and J. A. Berson, *Tetrahedron*, 1982, **38**, 787-798.
14. T. Michinobu, J. Inui and H. Nishide, *Polyhedron*, 2003, **22**, 1945-1949.
15. G. J. Snyder and D. A. Dougherty, *J. Am. Chem. Soc.*, 1986, **108**, 299-300.
16. W. Schlenk and M. Brauns, *Ber. Dtsch. Chem. Ges.*, 1915, **48**, 661-669.
17. E. Müller and W. Bunge, *Ber. Dtsch. Chem. Ges.*, 1936, **69**, 2164-2172.
18. A. Rajca and S. Rajca, *J. Chem. Soc., Perkin Trans. 2*, 1998, 1077-1082.
19. A. Rajca, S. Rajca, S. R. Desai and V. W. Day, *J. Org. Chem.*, 1997, **62**, 6524-6528.
20. O. Stark and O. Garben, *Ber. Dtsch. Chem. Ges.*, 1913, **46**, 2252-2259.
21. O. Stark and O. Garben, *Ber. Dtsch. Chem. Ges.*, 1913, **46**, 659-666.
22. O. Stark, O. Garben and L. Klebahn, *Ber. Dtsch. Chem. Ges.*, 1913, **46**, 2542-2544.
23. O. Stark and L. Klebahn, *Ber. Dtsch. Chem. Ges.*, 1914, **47**, 125-130.
24. E. Clar, C. T. Ironside and M. Zander, *Tetrahedron*, 1959, **6**, 358-363.
25. K. Fukui, J. Inoue, T. Kubo, S. Nakazawa, T. Aoki, Y. Morita, K. Yamamoto, K. Sato, D. Shiomi, K. Nakasuji and T. Takui, *Synth. Met.*, 2001, **121**, 1824-1825.
26. O. Hara, K. Tanaka, K. Yamamoto, T. Nakazawa and I. Murata, *Tetrahedron Lett.*, 1977, **18**, 2435-2436.
27. O. Hara, K. Yamamoto and I. Murata, *Tetrahedron Lett.*, 1977, **18**, 2431-2434.
28. K. Yamamoto, Y. Matsue, O. Hara and I. Murata, *Tetrahedron Lett.*, 1982, **23**, 877-880.
29. J. Inoue, K. Fukui, T. Kubo, S. Nakazawa, K. Sato, D. Shiomi, Y. Morita, K. Yamamoto, T. Takui and K. Nakasuji, *J. Am. Chem. Soc.*, 2001, **123**, 12702-12703.
30. C. Jiao and J. Wu, *Nanosized Graphene: Chemical Synthesis and Applications in Material Science*, CRC Press USA, 2012.
31. T. Rengarajan, P. Rajendran, N. Nandakumar, B. Lokeshkumar, P. Rajendran and I. Nishigaki, *Asian Pac. J. Trop. Biomed.*, 2015, **5**, 182-189.
32. E. Clar, *Polycyclic hydrocarbons 1*, New York: Academic press, USA, 1964, **1**.
33. E. Clar, *Polycyclic hydrocarbons 2*, New York: Academic press, USA, 1964, **2**.
34. R. Scholl and J. Mansfeld, *Ber. Dtsch. Chem. Ges.*, 1910, **43**, 1734-1746.
35. R. Scholl, C. Seer and R. Weitzenböck, *Ber. Dtsch. Chem. Ges.*, 1910, **43**, 2202-2209.
36. J. Wu and K. Müllen, in *Carbon-Rich Compounds*, Wiley-VCH Verlag GmbH & Co. KGaA, 2006, pp. 90-139.
37. M. Solà, *Front. Chem.*, 2013, **1**, 22.
38. M. Randić, *Chem. Phys. Lett.*, 2014, **601**, 1-5.

39. J. W. Armit and R. Robinson, *J. Chem. Soc., Trans.*, 1925, **127**, 1604-1618.
40. Armstrong H. E., *Proc. Chem. Soc., London*, 1890, **6**, 95-106.
41. E. C. Crocker, *J. Am. Chem. Soc.*, 1922, **44**, 1618-1630.
42. C. H. Suresh and S. R. Gadre, *J. Org. Chem.*, 1999, **64**, 2505-2512.
43. L. Altschuler and E. Berliner, *J. Am. Chem. Soc.*, 1966, **88**, 5837-5845.
44. S. Behrens, A. M. Koester and K. Jug, *J. Org. Chem.*, 1994, **59**, 2546-2551.
45. R. Dabestani and I. N. Ivanov, *Photochem. Photobiol.*, 1999, **70**, 10-34.
46. T. Kato, K. Yoshizawa and K. Hirao, *J. Chem. Phys.*, 2002, **116**, 3420-3429.
47. C. F. Matta, J. Hernández-Trujillo, T.-H. Tang and R. F. W. Bader, *Chem. Eur. J.*, 2003, **9**, 1940-1951.
48. L. Pauling and J. Sherman, *J. Chem. Phys.*, 1933, **1**, 606-617.
49. J. Poater, R. Visser, M. Solà and F. M. Bickelhaupt, *J. Org. Chem.*, 2007, **72**, 1134-1142.
50. S. H. Chien, M. F. Cheng, K. C. Lau and W. K. Li, *J. Phys. Chem. A*, 2005, **109**, 7509-7518.
51. E. Clar and M. Zander, *J. Chem. Soc.*, 1958, 1861-1865.
52. E. Clar, *Tetrahedron*, 1960, **9**, 202-209.
53. E. Clar, B. A. McAndrew and J. F. Stephen, *Tetrahedron*, 1970, **26**, 5465-5478.
54. D. Moran, F. Stahl, H. F. Bettinger, H. F. Schaefer and P. v. R. Schleyer, *J. Am. Chem. Soc.*, 2003, **125**, 6746-6752.
55. E. Clar and W. Schmidt, *Tetrahedron*, 1975, **31**, 2263-2271.
56. E. Clar, C. T. Ironside and M. Zander, *J. Chem. Soc.*, 1959, 142-147.
57. E. Clar, G. S. Fell and M. H. Richmond, *Tetrahedron*, 1960, **9**, 96-105.
58. E. Clar, *Spectrochim. Acta*, 1950, **4**, 116-121.
59. E. Clar and W. Schmidt, *Tetrahedron*, 1977, **33**, 2093-2097.
60. E. Clar, *Tetrahedron*, 1959, **6**, 355-357.
61. E. G. Cox, D. W. J. Cruickshank and J. A. S. Smith, *P. Roy. Soc. Lond. A Mat.*, 1958, **247**, 1-21.
62. L. Pauling and L. O. Brockway, *J. Chem. Phys.*, 1934, **2**, 867-881.
63. V. Schomaker and L. Pauling, *J. Am. Chem. Soc.*, 1939, **61**, 1769-1780.
64. R. Wierl, *Ann. Phys. (Berlin)*, 1931, **400**, 521-564.
65. R. Wierl, *Ann. Phys. (Berlin)*, 1932, **405**, 453-482.
66. E. Clar, *Tetrahedron*, 1959, **5**, 98.
67. D. Cruickshank, *Acta Crystallogr.*, 1957, **10**, 504-508.
68. A. B. Almenningen, O.; Trætteberg, M., *Acta. Chem. Scand.*, 1958, **12**, 1221.
69. D. Cruickshank, *Acta Crystallogr.*, 1956, **9**, 915-923.
70. D. Cruickshank, *Acta Crystallogr.*, 1957, **10**, 470.
71. A. McL Mathieson, J. M. Robertson and V. C. Sinclair, *Acta Crystallogr.*, 1950, **3**, 245-250.
72. R. B. Campbell, J. M. Robertson and J. Trotter, *Acta Crystallogr.*, 1961, **14**, 705-711.
73. R. B. Campbell, J. M. Robertson and J. Trotter, *Acta Crystallogr.*, 1962, **15**, 289-290.
74. D. M. Donaldson, J. M. Robertson and J. G. White, *P. Roy. Soc. Lond. A Mat.*, 1953, **220**, 311-321.
75. M. I. Kay, Y. Okaya and D. E. Cox, *Acta Crystallogr. Sect. B-Struct. Sci.*, 1971, **27**, 26-33.
76. J. Trotter, *Acta Crystallogr.*, 1963, **16**, 605-608.
77. S. S. Shaik and P. C. Hiberty, *J. Am. Chem. Soc.*, 1985, **107**, 3089-3095.
78. Z. Zhou and R. G. Parr, *J. Am. Chem. Soc.*, 1989, **111**, 7371-7379.
79. Y. Ruiz-Morales, *J. Phys. Chem. A*, 2004, **108**, 10873-10896.
80. L. Pauling, *The Nature of the Chemical Bond and the Structure of Molecules and Crystals*, Cornell University Press, USA, 1939.
81. A. T. Balaban, M. Pompe and M. Randić, *J. Phys. Chem. A*, 2008, **112**, 4148-4157.
82. T. M. Ivan Gutman, and Susumu Naritac, *Z. Naturforsch.*, 2004, **59a**, 295 – 298.

83. D. P. Milan Randić, *Acta. Chim. Slov.*, 2011, **58**, 448-457.
84. M. Randić, *J. Chem. Inform. Comput. Sci.*, 2004, **44**, 365-372.
85. M. Randić and A. T. Balaban, *J. Chem. Inf. Model.*, 2006, **46**, 57-64.
86. B. Boggiano and E. Clar, *J. Chem. Soc.*, 1957, 2681-2689.
87. E. Clar, *Ber. Dtsch. Chem. Ges.*, 1939, **72**, 2137-2139.
88. I. Agranat and Y.-S. Shih, *J. Chem. Educ.*, 1976, **53**, 488.
89. R. D. Haworth, *J. Chem. Soc.*, 1932, 1125-1133.
90. R. D. Haworth, *J. Chem. Soc.*, 1932, 2717-2720.
91. C. A. Johnson and M. M. Haley, in *Carbon-Rich Compounds*, Wiley-VCH Verlag GmbH & Co. KGaA, 2006, pp. 1-25.
92. H. Limpricht, *Justus Liebigs Ann. Chem.*, 1866, **139**, 303-327.
93. A. Baeyer, *Justus Liebigs Ann. Chem.*, 1866, **140**, 295-296.
94. C. Graebe and C. Liebermann, *Ber. Dtsch. Chem. Ges.*, 1868, **1**, 49-51.
95. E. Clar, *Ber. Dtsch. Chem. Ges.*, 1939, **72**, 1645-1649.
96. C. Graebe and C. Liebermann, *Ber. Dtsch. Chem. Ges.*, 1969, **2**, 14.
97. A. H. Church and W. H. Perkin, *Q. J. Chem. Soc.*, 1857, **9**, 1-8.
98. K. Elbs, *J. Prakt. Chem.*, 1886, **33**, 180-188.
99. E. Clar and F. John, *Ber. Dtsch. Chem. Ges.*, 1930, **63**, 2967-2977.
100. C. Pramanik and G. P. Miller, *Molecules*, 2012, **17**, 4625.
101. E. Clar and F. John, *Ber. Dtsch. Chem. Ges.*, 1929, **62**, 3021-3029.
102. W. J. Bailey and M. Madoff, *J. Am. Chem. Soc.*, 1953, **75**, 5603-5604.
103. E. P. Goodings, D. A. Mitchard and G. Owen, *J. Chem. Soc., Perkin Trans. 1*, 1972, 1310-1314.
104. E. Clar, *Ber. Dtsch. Chem. Ges.*, 1939, **72**, 1817-1821.
105. E. Clar, *Ber. Dtsch. Chem. Ges.*, 1942, **75**, 1283-1287.
106. C. Marschalk, *Bull. Soc. Chim. Fr.*, 1939, **6**, 1112-1121.
107. C. Marschalk, *Bull. Soc. Chim. Fr.*, 1950, **16**, 311.
108. C. Tönshoff and H. F. Bettinger, *Angew. Chem. Int. Ed.*, 2010, **49**, 4125-4128.
109. J. Meisenheimer and K. Witte, *Ber. Dtsch. Chem. Ges.*, 1903, **36**, 4153-4164.
110. C. S. Wood and F. B. Mallory, *J. Org. Chem.*, 1964, **29**, 3373-3377.
111. M. Flammang-Barbieux, J. Nasielski and R. H. Martin, *Tetrahedron Lett.*, 1967, **8**, 743-744.
112. R. H. Martin, M. Flammang-Barbieux, J. P. Cosyn and M. Gelbcke, *Tetrahedron Lett.*, 1968, **9**, 3507-3510.
113. K. Mori, T. Murase and M. Fujita, *Angew. Chem. Int. Ed.*, 2015, **54**, 6847-6851.
114. C. Glaser, *Ber. Dtsch. Chem. Ges.*, 1872, **5**, 982-982.
115. E. Ostermayer and R. Fittig, *Ber. Dtsch. Chem. Ges.*, 1872, **5**, 933-937.
116. R. Pschorr, *Ber. Dtsch. Chem. Ges.*, 1896, **29**, 496-501.
117. C. Graebe, *Ber. Dtsch. Chem. Ges.*, 1874, **7**, 48-49.
118. E. Clar and W. Kelly, *J. Am. Chem. Soc.*, 1954, **76**, 3502-3504.
119. H. Brockmann and H. Laatsch, *Chem. Ber.*, 1973, **106**, 2058-2069.
120. E. Clar and A. Mullen, *Tetrahedron*, 1968, **24**, 6719-6724.
121. A. Bohnen, K.-H. Koch, W. Lüttke and K. Müllen, *Angew. Chem. Int. Ed. Engl.*, 1990, **29**, 525-527.
122. Y. Avlasevich, C. Kohl and K. Mullen, *J. Mater. Chem.*, 2006, **16**, 1053-1057.
123. F. O. Holtrup, G. R. J. Müller, H. Quante, S. De Feyter, F. C. De Schryver and K. Müllen, *Chem. Eur. J.*, 1997, **3**, 219-225.
124. H. Langhals and S. Poxleitner, *Eur. J. Org. Chem.*, 2008, **2008**, 797-800.
125. N. G. Pschirer, C. Kohl, F. Nolde, J. Qu and K. Müllen, *Angew. Chem. Int. Ed.*, 2006, **45**, 1401-1404.
126. J. Qu, N. G. Pschirer, M. Koenemann, K. Muellen and Y. Avlasevic, *Journal*, 2008.
127. Z. Yuan, S.-L. Lee, L. Chen, C. Li, K. S. Mali, S. De Feyter and K. Müllen, *Chem. Eur. J.*, 2013, **19**, 11842-11846.
128. E. Clar, K. F. Lang and H. Schulz-Kiesow, *Chem. Ber.*, 1955, **88**, 1520-1527.
129. R. H. Mitchell and F. Sondheimer, *J. Am. Chem. Soc.*, 1968, **90**, 530-531.



130. R. H. Mitchell and F. Sondheimer, *Tetrahedron*, 1970, **26**, 2141-2150.
131. H. A. Staab, A. Nissen and J. Ipaktschi, *Angew. Chem. Int. Ed. Engl.*, 1968, **7**, 226-226.
132. E. Clar and I. A. Macpherson, *Tetrahedron*, 1962, **18**, 1411-1416.
133. R. Kemalettin Erünlü, *Justus Liebigs Ann. Chem.*, 1969, **721**, 43-47.
134. G. Allinson, R. J. Bushby, M. V. Jesudason, J.-L. Paillaud and N. Taylor, *J. Chem. Soc., Perkin Trans. 2*, 1997, 147-156.
135. E. Clar and C. T. Ironside, *Proc. Chem. Soc.*, 1958, 150.
136. A. Halleux, R. H. Martin and G. S. D. King, *Helv. Chim. Acta*, 1958, **41**, 1177-1183.
137. W. Hendel, Z. H. Khan and W. Schmidt, *Tetrahedron*, 1986, **42**, 1127-1134.
138. C. Kubel, K. Eckhardt, V. Enkelmann, G. Wegner and K. Mullen, *J. Mater. Chem.*, 2000, **10**, 879-886.
139. R. Scholl and K. Meyer, *Ber. Dtsch. Chem. Ges.*, 1934, **67**, 1236-1238.
140. S. M. Arabei and T. A. Pavich, *J. Appl. Spectrosc.*, **67**, 236-244.
141. E. Clar, *Chem. Ber.*, 1948, **81**, 52-63.
142. E. Clar, *Chem. Ber.*, 1949, **82**, 46-60.
143. K. Zhang, K.-W. Huang, J. Li, J. Luo, C. Chi and J. Wu, *Org. Lett.*, 2009, **11**, 4854-4857.
144. A. Konishi, Y. Hirao, M. Nakano, A. Shimizu, E. Botek, B. Champagne, D. Shiomi, K. Sato, T. Takui, K. Matsumoto, H. Kurata and T. Kubo, *J. Am. Chem. Soc.*, 2010, **132**, 11021-11023.
145. J. Aihara, *J. Am. Chem. Soc.*, 1992, **114**, 865-868.
146. F. Diederich and H. A. Staab, *Angew. Chem. Int. Ed. Engl.*, 1978, **17**, 372-374.
147. B. Kumar, R. L. Viboh, M. C. Bonifacio, W. B. Thompson, J. C. Buttrick, B. C. Westlake, M.-S. Kim, R. W. Zoellner, S. A. Varganov, P. Mörschel, J. Teteruk, M. U. Schmidt and B. T. King, *Angew. Chem. Int. Ed.*, 2012, **51**, 12795-12800.
148. E. Clar and M. Zander, *J. Chem. Soc.*, 1957, 4616-4619.
149. R. Scholl and K. Meyer, *Ber. Dtsch. Chem. Ges.*, 1932, **65**, 902-915.
150. E. Clar, Ü. Sanigök and M. Zander, *Tetrahedron*, 1968, **24**, 2817-2823.
151. P. M. Donovan and L. T. Scott, *J. Am. Chem. Soc.*, 2004, **126**, 3108-3112.
152. H.-C. Shen, J.-M. Tang, H.-K. Chang, C.-W. Yang and R.-S. Liu, *J. Org. Chem.*, 2005, **70**, 10113-10116.
153. E. Clar, *Nature*, 1948, **161**, 238-239.
154. S. Saïdi-Besbes, É. Grelet and H. Bock, *Angew. Chem.*, 2006, **118**, 1815-1818.
155. E. Clar, W. Kelly, J. M. Robertson and M. G. Rossmann, *J. Chem. Soc.*, 1956, 3878-3881.
156. E. Clar, J. M. Robertson, R. Schloegl and W. Schmidt, *J. Am. Chem. Soc.*, 1981, **103**, 1320-1328.
157. R. D. Broene and F. Diederich, *Tetrahedron Lett.*, 1991, **32**, 5227-5230.
158. J. W. Cook and C. L. Hewett, *J. Chem. Soc.*, 1933, 1098-1112.
159. V. Boekelheide, W. E. Langeland and C.-T. Liu, *J. Am. Chem. Soc.*, 1951, **73**, 2432-2435.
160. V. Boekelheide and G. K. Vick, *J. Am. Chem. Soc.*, 1956, **78**, 653-658.
161. C. T. Blood and R. P. Linstead, *J. Chem. Soc.*, 1952, 2263-2268.
162. K. Amsharov and M. Jansen, *Chem. Commun.*, 2009, 2691-2693.
163. R. Diercks and K. P. C. Vollhardt, *J. Am. Chem. Soc.*, 1986, **108**, 3150-3152.
164. C. Dosche, M. U. Kumke, H. G. Lohmannsroben, F. Ariese, A. N. Bader, C. Gooijer, O. S. Miljanic, M. Iwamoto, K. P. C. Vollhardt, R. Puchta and N. J. R. van Eikema Hommes, *PCCP*, 2004, **6**, 5476-5483.
165. C. Liebermann and O. Bergami, *Ber. Dtsch. Chem. Ges.*, 1890, **23**, 317-322.
166. Y. N. Oded and I. Agranat, *Tetrahedron Lett.*, 2014, **55**, 636-638.
167. H. W. Kroto, J. R. Heath, S. C. O'Brien, R. F. Curl and R. E. Smalley, *Nature*, 1985, **318**, 162-163.
168. L. T. Scott, M. M. Boorum, B. J. McMahon, S. Hagen, J. Mack, J. Blank, H. Wegner and A. de Meijere, *Science*, 2002, **295**, 1500-1503.

169. C. D. Simpson, J. D. Brand, A. J. Berresheim, L. Przybilla, H. J. Räder and K. Müllen, *Chem. Eur. J.*, 2002, **8**, 1424-1429.
170. J. L. Durant, W. F. Busby Jr, A. L. Lafleur, B. W. Penman and C. L. Crespi, *Mutat. Res.-Genet. Toxicol.*, 1996, **371**, 123-157.
171. M. P. Fraser, G. R. Cass and B. R. T. Simoneit, *Environ. Sci. Technol.*, 1998, **32**, 2051-2060.
172. C. Moeckel, D. T. Monteith, N. R. Llewellyn, P. A. Henrys and M. G. Pereira, *Environ. Sci. Technol.*, 2014, **48**, 130-138.
173. A. Salamova, M. Venier and R. A. Hites, *Environ. Sci. Technol. Lett.*, 2015, **2**, 20-25.
174. C. D. Zeigler and A. Robbat, *Environ. Sci. Technol.*, 2012, **46**, 3935-3942.
175. E. B. Ledesma, M. A. Kalish, M. J. Wornat, P. F. Nelson and J. C. Mackie, *Energy Fuels*, 1999, **13**, 1167-1172.
176. R. Wang, G. Liu and J. Zhang, *Sci. Total Environ.*, 2015, **538**, 180-190.
177. N. Song, J. Ma, Y. Yu, Z. Yang and Y. Li, *Environ. Pollut.*, 2015, **205**, 415-423.
178. S. B. Hawthorne, D. G. Poppendieck, C. B. Grabanski and R. C. Loehr, *Environ. Sci. Technol.*, 2002, **36**, 4795-4803.
179. A. C. Eriksson, E. Z. Nordin, R. Nyström, E. Pettersson, E. Swietlicki, C. Bergvall, R. Westerholm, C. Boman and J. H. Pagels, *Environ. Sci. Technol.*, 2014, **48**, 7143-7150.
180. B. M. Jenkins, A. D. Jones, S. Q. Turn and R. B. Williams, *Environ. Sci. Technol.*, 1996, **30**, 2462-2469.
181. N. T. Kim Oanh, A. Tipayarom, T. L. Bich, D. Tipayarom, C. D. Simpson, D. Hardie and L. J. Sally Liu, *Atmos. Environ.*, 2015, **119**, 182-191.
182. C. Vieira de Souza and S. M. Corrêa, *Atmos. Environ.*, 2015, **103**, 222-230.
183. B. R. T. Simoneit, P. M. Medeiros and B. M. Didyk, *Environ. Sci. Technol.*, 2005, **39**, 6961-6970.
184. J. L. Durant, A. L. Lafleur, E. F. Plummer, K. Taghizadeh, W. F. Busby and W. G. Thilly, *Environ. Sci. Technol.*, 1998, **32**, 1894-1906.
185. L. Chibwe, M. C. Geier, J. Nakamura, R. L. Tanguay, M. D. Aitken and S. L. M. Simonich, *Environ. Sci. Technol.*, 2015, **49**, 13889-13898.
186. S. Suman, A. Sinha and A. Tarafdar, *Sci. Total Environ.*, 2016, **545-546**, 353-360.
187. J. W. Short, K. A. Kvenvolden, P. R. Carlson, F. D. Hostettler, R. J. Rosenbauer and B. A. Wright, *Environ. Sci. Technol.*, 1999, **33**, 34-42.
188. L. G. Tidwell, S. E. Allan, S. G. O'Connell, K. A. Hobbie, B. W. Smith and K. A. Anderson, *Environ. Sci. Technol.*, 2015, **49**, 141-149.
189. P. Šimko, *J. Chromatogr. B*, 2002, **770**, 3-18.
190. H. Alomirah, S. Al-Zenki, S. Al-Hooti, S. Zaghloul, W. Sawaya, N. Ahmed and K. Kannan, *Food Control*, 2011, **22**, 2028-2035.
191. B. Donn, *Astrophys. J.*, 1968, **152**, L129-L133.
192. G. P. v. d. Zwet and L. J. Allamandola, *Astron. Astrophys.*, 1985, **146**, 76-80.
193. D. A. García-Hernández, A. Manchado, P. García-Lario, L. Stanghellini, E. Villaver, R. A. Shaw, R. Szczerba and J. V. Perea-Calderón, *Astrophys. J. Lett.*, 2010, **724**, L39.
194. W. Hong, C. Chen, H. Cai-Na, L. Feng-Shan, W. Jian-Ling, X. Xiao-Yang, D. Zu-Gan and C. K.-S. Young, *Astrophys. J. Lett.*, 2005, **632**, L79.
195. G. C. Sloan, J. D. Bregman, T. R. Geballe, L. J. Allamandola and E. Woodward, *Astrophys. J.*, 1997, **474**, 735.
196. H. I. Teplitz, V. Desai, L. Armus, R. Chary, J. A. Marshall, J. W. Colbert, D. T. Frayer, A. Pope, A. Blain, H. W. W. Spoon, V. Charmandaris and D. Scott, *Astrophys. J.*, 2007, **659**, 941.
197. A. G. G. M. Tielens, *Annu. Rev. Astron. Astrophys.*, 2008, **46**, 289-337.
198. NASA, <http://www.astrochem.org/pahdb/>, (accessed 06/2015).
199. M. P. Bernstein, J. P. Dworkin, S. A. Sandford and L. J. Allamandola, *Meteorit. Planet. Sci.*, 2001, **36**, 351-358.

200. D. L. Poster, M. M. Schantz, L. C. Sander and S. A. Wise, *Anal. Bioanal. Chem.*, 2006, **386**, 859-881.
201. N. T. Crosby, D. C. Hunt, L. A. Philp and I. Patel, *Analyst*, 1981, **106**, 135-145.
202. G. N. M. Reddy and S. Caldarelli, *Analyst*, 2012, **137**, 741-746.
203. E. N. Ayyakkannu P., Palanivelu S., Panchanadham S, *J Biochem Tech*, 2014, **5**, 801-807.
204. J. Wei, G. Xie, S. Ge, Y. Qiu, W. Liu, A. Lu, T. Chen, H. Li, Z. Zhou and W. Jia, *J. Proteome Res.*, 2012, **11**, 1302-1316.
205. S. Badal and R. Delgoda, *J. Appl. Toxicol.*, 2014, **34**, 743-753.
206. M. Miyata, M. Furukawa, K. Takahashi, F. J. Gonzalez and Y. Yamazoe, *Jpn. J. Pharmacol.*, 2001, **86**, 302-309.
207. H. K. Bojes and P. G. Pope, *Regul. Toxicol. Pharm.*, 2007, **47**, 288-295.
208. ISO,  
[http://www.iso.org/iso/iso\\_catalogue/catalogue\\_tc/catalogue\\_detail.htm?csnumber=31666](http://www.iso.org/iso/iso_catalogue/catalogue_tc/catalogue_detail.htm?csnumber=31666), (accessed 02/2016).
209. EPA, <http://www3.epa.gov/ttn/atw/pollsour.html>, (accessed 02/2016).
210. M. Mas-Torrent, N. Crivillers, V. Mugnaini, I. Ratera, C. Rovira and J. Veciana, *J. Mater. Chem.*, 2009, **19**, 1691-1695.
211. Y. Yamashita, *Sci. Tech. Adv. Mater.*, 2009, **10**, 024313.
212. S. R. Forrest, *Nature*, 2004, **428**, 911-918.
213. C. M. Bernanose A., Voouaux P., *J. Chim. Phys*, 1953, **50**, 64.
214. M. Pope, H. P. Kallmann and P. Magnante, *J. Chem. Phys.*, 1963, **38**, 2042-2043.
215. C. W. Lee, O. Y. Kim and J. Y. Lee, *J. Ind. Eng. Chem.*, 2014, **20**, 1198-1208.
216. C. W. Tang, *Appl. Phys. Lett.*, 1986, **48**, 183-185.
217. A. Goel, M. Dixit, S. Chaurasia, A. Kumar, R. Raghunandan, P. R. Maulik and R. S. Anand, *Org. Lett.*, 2008, **10**, 2553-2556.
218. H. Sasabe and J. Kido, *Chem. Mater.*, 2011, **23**, 621-630.
219. Y. Sato, S. Ichinosawa and H. Kanai, *IEEE J. Sel. Top. Quantum Electron.*, 1998, **4**, 40-48.
220. H. Yuji, S. Takeshi, S. Kenichi and K. Kazuhiko, *Jpn. J. Appl. Phys.*, 1995, **34**, L824.
221. C. Liu, Y. Tang and S. Nie, *Cent. Eur. J. Chem.*, 2006, **4**, 723-731.
222. M. Gross, D. C. Muller, H.-G. Nothofer, U. Scherf, D. Neher, C. Brauchle and K. Meerholz, *Nature*, 2000, **405**, 661-665.
223. N. Koch, *ChemPhysChem*, 2007, **8**, 1438-1455.
224. C. D. Dimitrakopoulos and P. R. L. Malenfant, *Adv. Mater.*, 2002, **14**, 99-117.
225. T. W. Kelley, P. F. Baude, C. Gerlach, D. E. Ender, D. Muires, M. A. Haase, D. E. Vogel and S. D. Theiss, *Chem. Mater.*, 2004, **16**, 4413-4422.
226. Y. Sun, Y. Liu and D. Zhu, *J. Mater. Chem.*, 2005, **15**, 53-65.
227. C. R. Newman, C. D. Frisbie, D. A. da Silva Filho, J.-L. Brédas, P. C. Ewbank and K. R. Mann, *Chem. Mater.*, 2004, **16**, 4436-4451.
228. H. Koezuka, A. Tsumura and T. Ando, *Synth. Met.*, 1987, **18**, 699-704.
229. T. D. Anthopoulos, C. Tanase, S. Setayesh, E. J. Meijer, J. C. Hummelen, P. W. M. Blom and D. M. de Leeuw, *Adv. Mater.*, 2004, **16**, 2174-2179.
230. J. H. Schön, C. Kloc and B. Batlogg, *Org. Electron.*, 2000, **1**, 57-64.
231. M. M. Ling, P. Erk, M. Gomez, M. Koenemann, J. Locklin and Z. Bao, *Adv. Mater.*, 2007, **19**, 1123-1127.
232. D. A. da Silva Filho, E. G. Kim and J. L. Brédas, *Adv. Mater.*, 2005, **17**, 1072-1076.
233. J. J. M. Halls, K. Pichler, R. H. Friend, S. C. Moratti and A. B. Holmes, *Appl. Phys. Lett.*, 1996, **68**, 3120-3122.
234. D. Kotowski, S. Luzzati, G. Scavia, M. Cavazzini, A. Bossi, M. Catellani and E. Kozma, *Dyes Pigm.*, 2015, **120**, 57-64.
235. D. Fujishima, H. Kanno, T. Kinoshita, E. Maruyama, M. Tanaka, M. Shirakawa and K. Shibata, *Sol. Energy Mater. Sol. Cells*, 2009, **93**, 1029-1032.
236. W. Shockley and H. J. Queisser, *J. Appl. Phys.*, 1961, **32**, 510-519.

237. A. M. Bagher, *IRESR*, 2014, **3**, 53-58.
238. J. A. Gaj and *et al.*, *C. R. Physique*, 2007, **8**, 243-252.
239. S. A. Wolf, *et al.*, *Science*, 2001, **294**, 1488-1495.
240. F. Grillo, H. Fruchtl, S. M. Francis, V. Mugnaini, M. Oliveros, J. Veciana and N. V. Richardson, *Nanoscale*, 2012, **4**, 6718-6721.
241. Z. V. Vardeny, A. J. Heeger and A. Dodabalapur, *Synth. Met.*, 2005, **148**, 1-3.
242. F. J. Wang, Z. H. Xiong, D. Wu, J. Shi and Z. V. Vardeny, *Synth. Met.*, 2005, **155**, 172-175.
243. Z. Sun and J. Wu, *J. Mater. Chem.*, 2012, **22**, 4151-4160.
244. Y. Morita, S. Suzuki, K. Sato and T. Takui, *Nat. Chem.*, 2011, **3**, 197-204.
245. Z. Sun, Z. Zeng and J. Wu, *Acc. Chem. Res.*, 2014, **47**, 2582-2591.
246. M. Bieri, M. Treier, J. Cai, K. Ait-Mansour, P. Ruffieux, O. Groning, P. Groning, M. Kastler, R. Rieger, X. Feng, K. Mullen and R. Fasel, *Chem. Commun.*, 2009, 6919-6921.
247. J. Cai, P. Ruffieux, R. Jaafar, M. Bieri, T. Braun, S. Blankenburg, M. Muoth, A. P. Seitsonen, M. Saleh, X. Feng, K. Mullen and R. Fasel, *Nature*, 2010, **466**, 470-473.
248. A. Soncini, E. Steiner, P. W. Fowler, R. W. A. Havenith and L. W. Jenneskens, *Chem. Eur. J.*, 2003, **9**, 2974-2981.
249. M. Treier, C. A. Pignedoli, T. Laino, R. Rieger, K. Müllen, D. Passerone and R. Fasel, *Nat. Chem.*, 2010, **3**, 61-67.
250. J. V. Barth, G. Costantini and K. Kern, *Nature*, 2005, **437**, 671-679.
251. J. Shi, X. Zhang and D. C. Neckers, *J. Org. Chem.*, 1992, **57**, 4418-4421.
252. T. Weil, T. Vosch, J. Hofkens, K. Peneva and K. Müllen, *Angew. Chem. Int. Ed.*, 2010, **49**, 9068-9093.
253. J. H. Yao, C. Chi, J. Wu and K.-P. Loh, *Chem. Eur. J.*, 2009, **15**, 9299-9302.
254. C. Chotimarkorn, R. Nagasaka, H. Ushio, T. Ohshima and S. Matsunaga, *Biochem. Biophys. Res. Commun.*, 2005, **338**, 1222-1228.
255. R. D. Cadena-Nava, A. Cosultchi and J. Ruiz-Garcia, *Energy Fuels*, 2007, **21**, 2129-2137.
256. T. Weil, M. A. Abdalla, C. Jatzke, J. Hengstler and K. Müllen, *Biomacromolecules*, 2005, **6**, 68-79.
257. E. I. Altman, M. Z. Baykara and U. D. Schwarz, *Acc. Chem. Res.*, 2015, **48**, 2640-2648.
258. L. Gross, F. Mohn, N. Moll, P. Liljeroth and G. Meyer, *Science*, 2009, **325**, 1110-1114.
259. F. Albrecht, N. Pavliček, C. Herranz-Lancho, M. Ruben and J. Repp, *J. Am. Chem. Soc.*, 2015, **137**, 7424-7428.
260. J. Mendez, M. F. Lopez and J. A. Martin-Gago, *Chem. Soc. Rev.*, 2011, **40**, 4578-4590.
261. J. Lagoute, K. Kanisawa and S. Fölsch, *Phys. Rev. B*, 2004, **70**, 245415.
262. J. Repp, G. Meyer, S. Paavilainen, F. E. Olsson and M. Persson, *Science*, 2006, **312**, 1196-1199.
263. J. Repp, G. Meyer, S. M. Stojković, A. Gourdon and C. Joachim, *Phys. Rev. Lett.*, 2005, **94**, 026803.
264. D. G. de Oteyza, P. Gorman, Y.-C. Chen, S. Wickenburg, A. Riss, D. J. Mowbray, G. Etkin, Z. Pedramrazi, H.-Z. Tsai, A. Rubio, M. F. Crommie and F. R. Fischer, *Science*, 2013, **340**, 1434-1437.
265. J. Frommer, *Angew. Chem. Int. Ed. Engl.*, 1992, **31**, 1298-1328.
266. J. K. Gimzewski and C. Joachim, *Science*, 1999, **283**, 1683-1688.
267. W. Ho, *J. Chem. Phys.*, 2002, **117**, 11033-11061.
268. T. A. Jung, R. R. Schlittler and J. K. Gimzewski, *Nature*, 1997, **386**, 696-698.
269. N. Pavliček, B. Fleury, M. Neu, J. Niedenführ, C. Herranz-Lancho, M. Ruben and J. Repp, *Phys. Rev. Lett.*, 2012, **108**, 086101.
270. R. Pawlak, S. Kawai, S. Fremy, T. Glatzel and E. Meyer, *ACS Nano*, 2011, **5**, 6349-6354.

271. A. M. Sweetman, S. P. Jarvis, H. Sang, I. Lekkas, P. Rahe, Y. Wang, J. Wang, N. R. Champness, L. Kantorovich and P. Moriarty, *Nat. Commun.*, 2014, **5**.
272. J. Zhang, P. Chen, B. Yuan, W. Ji, Z. Cheng and X. Qiu, *Science*, 2013, **342**, 611-614.
273. F. Albrecht, M. Neu, C. Quest, I. Swart and J. Repp, *J. Am. Chem. Soc.*, 2013, **135**, 9200-9203.
274. K. Ø. Hanssen, B. Schuler, A. J. Williams, T. B. Demissie, E. Hansen, J. H. Andersen, J. Svenson, K. Blinov, M. Repisky, F. Mohn, G. Meyer, J.-S. Svendsen, K. Ruud, M. Elyashberg, L. Gross, M. Jaspars and J. Isaksson, *Angew. Chem. Int. Ed.*, 2012, **51**, 12238-12241.
275. L. Gross, F. Mohn, N. Moll, B. Schuler, A. Criado, E. Guitián, D. Peña, A. Gourdon and G. Meyer, *Science*, 2012, **337**, 1326-1329.
276. L. Gross, F. Mohn, N. Moll, G. Meyer, R. Ebel, W. M. Abdel-Mageed and M. Jaspars, *Nat Chem*, 2010, **2**, 821-825.
277. B. Schuler, S. Collazos, L. Gross, G. Meyer, D. Pérez, E. Guitián and D. Peña, *Angew. Chem. Int. Ed.*, 2014, **53**, 9004-9006.
278. B. Moreton, Z. Fang, M. Wills and G. Costantini, *Chem. Commun.*, 2013, **49**, 6477-6479.
279. M. Alemani, M. V. Peters, S. Hecht, K.-H. Rieder, F. Moresco and L. Grill, *J. Am. Chem. Soc.*, 2006, **128**, 14446-14447.
280. R. Fasel, M. Parschau and K.-H. Ernst, *Nature*, 2006, **439**, 449-452.
281. A. Kuhnle, T. R. Linderoth, B. Hammer and F. Besenbacher, *Nature*, 2002, **415**, 891-893.
282. M. Lingenfelder, G. Tomba, G. Costantini, L. Colombi Ciacchi, A. De Vita and K. Kern, *Angew. Chem. Int. Ed.*, 2007, **46**, 4492-4495.
283. G. P. Lopinski, D. J. Moffatt, D. D. M. Wayner and R. A. Wolkow, *Nature*, 1998, **392**, 909-911.
284. N. Pavliček, C. Herranz-Lancho, B. Fleury, M. Neu, J. Niedenführ, M. Ruben and J. Repp, *Phys. Status Solidi B*, 2013, **250**, 2424-2430.
285. J. R. Hahn and W. Ho, *Phys. Rev. Lett.*, 2001, **87**, 166102.
286. J. Henzl, M. Mehlhorn, H. Gawronski, K.-H. Rieder and K. Morgenstern, *Angew. Chem. Int. Ed.*, 2006, **45**, 603-606.
287. S.-W. Hla, L. Bartels, G. Meyer and K.-H. Rieder, *Phys. Rev. Lett.*, 2000, **85**, 2777-2780.
288. P. Liljeroth, J. Repp and G. Meyer, *Science*, 2007, **317**, 1203-1206.
289. G. Otero, G. Biddau, C. Sanchez-Sanchez, R. Caillard, M. F. Lopez, C. Rogero, F. J. Palomares, N. Cabello, M. A. Basanta, J. Ortega, J. Mendez, A. M. Echavarren, R. Perez, B. Gomez-Lor and J. A. Martin-Gago, *Nature*, 2008, **454**, 865-868.
290. A. Wiengarten, J. A. Lloyd, K. Seufert, J. Reichert, W. Auwärter, R. Han, D. A. Duncan, F. Allegretti, S. Fischer, S. C. Oh, Ö. Sağlam, L. Jiang, S. Vijayaraghavan, D. Écija, A. C. Papageorgiou and J. V. Barth, *Chem. Eur. J.*, 2015, **21**, 12285-12290.
291. R. R. Jones and R. G. Bergman, *J. Am. Chem. Soc.*, 1972, **94**, 660-661.
292. B. Schuler, S. Fatayer, F. Mohn, N. Moll, N. Pavliček, G. Meyer, D. Peña and L. Gross, *Nat. Chem.*, 2016, **8**, 220-224.
293. M. P. Boneschanscher, J. van der Lit, Z. Sun, I. Swart, P. Liljeroth and D. Vanmaekelbergh, *ACS Nano*, 2012, **6**, 10216-10221.
294. B. Schuler, G. Meyer, D. Peña, O. C. Mullins and L. Gross, *J. Am. Chem. Soc.*, 2015, **137**, 9870-9876.
295. J. van der Lit, M. P. Boneschanscher, D. Vanmaekelbergh, M. Ijäs, A. Uppstu, M. Ervasti, A. Harju, P. Liljeroth and I. Swart, *Nat. Commun.*, 2013, **4**, 2023.
296. A. Riss, S. Wickenburg, P. Gorman, L. Z. Tan, H.-Z. Tsai, D. G. de Oteyza, Y.-C. Chen, A. J. Bradley, M. M. Ugeda, G. Etkin, S. G. Louie, F. R. Fischer and M. F. Crommie, *Nano Lett.*, 2014, **14**, 2251-2255.
297. R. Scholl and H. K. Meyer, *Ber. Dtsch. Chem. Ges. B*, 1936, **69B**, 152-158.

298. H. Vollmann, H. Becker, M. Corell, H. Streeck and G. Langbein, *Justus Liebigs Ann. Chem.*, 1937, **531**, 1-159.
299. E. Clar and C. C. Mackay, *Tetrahedron*, 1972, **28**, 6041-6047.
300. E. Clar and D. G. Stewart, *J. Am. Chem. Soc.*, 1952, **74**, 6235-6238.
301. J. Morgenthaler and C. Rüchardt, *Eur. J. Org. Chem.*, 1999, 2219-2230.
302. D. H. Reid and W. Bonthron, *J. Chem. Soc.*, 1965, 5920-5926.
303. A. W. Johnson, *J. Org. Chem.*, 1959, **24**, 833-836.
304. K. W. Bair, R. L. Tuttle, V. C. Knick, M. Cory and D. D. McKee, *J. Med. Chem.*, 1990, **33**, 2385-2393.
305. T.-H. Chuang, S.-J. Lee, C.-W. Yang and P.-L. Wu, *Org. Biomol. Chem.*, 2006, **4**, 860-867.
306. L. J. Drummond and A. Sutherland, *Tetrahedron*, 2010, **66**, 5349-5356.
307. C. O. Kangani and B. W. Day, *Org. Lett.*, 2008, **10**, 2645-2648.
308. A. Srikrishna, G. Satyanarayana and U. V. Desai, *Synth. Commun.*, 2007, **37**, 965-976.
309. T. Voelker, H. Xia, K. Fandrick, R. Johnson, A. Janowsky and J. R. Cashman, *Biorg. Med. Chem.*, 2009, **17**, 2047-2068.
310. G. Weeratunga, M. Austrup and R. Rodrigo, *J. Chem. Soc., Perkin Trans. 1*, 1988, 3169-3173.
311. N. M. Yoon and H. C. Brown, *J. Am. Chem. Soc.*, 1968, **90**, 2927-2938.
312. T. Mizushima, A. Yoshida, A. Harada, Y. Yoneda, T. Minatani and S. Murata, *Org. Biomol. Chem.*, 2006, **4**, 4336-4344.
313. J. Arnbjerg, M. J. Paterson, C. B. Nielsen, M. Jørgensen, O. Christiansen and P. R. Ogilby, *J. Phys. Chem. A*, 2007, **111**, 5756-5767.
314. C. Tintel, M. Vanderbrugge, J. Lugtenburg and J. Cornelisse, *Recl. Trav. Chim. Pays-Bas*, 1983, **102**, 220-223.
315. Akanksha and D. Maiti, *Green Chem.*, 2012, **14**, 2314-2320.
316. E. Clar and D. G. Stewart, *J. Am. Chem. Soc.*, 1953, **75**, 2667-2672.
317. H. Lee and R. G. Harvey, *J. Org. Chem.*, 1982, **47**, 4364-4367.
318. S. Pogodin and I. Agranat, *Org. Lett.*, 1999, **1**, 1387-1390.
319. S. E. Stein and R. L. Brown, *J. Am. Chem. Soc.*, 1991, **113**, 787-793.
320. H. Friebohn, R. Roers, J. Ebenhoch, M. Gerst and C. Rüchardt, *Justus Liebigs Ann. Chem.*, 1997, **1997**, 385-389.
321. L. Gross and *et al.*, *Zürich, Switzerland*, 2012-2016.
322. A. J. S. Valentine and D. A. Mazziotti, *J. Phys. Chem. A*, 2013, **117**, 9746-9752.
323. M. Bonfanti, S. Casolo, G. F. Tantardini, A. Ponti and R. Martinazzo, *J. Chem. Phys.*, 2011, **135**, 164701-164710.
324. A. Mistry, B. Moreton, B. Schuler, F. Mohn, G. Meyer, L. Gross, A. Williams, P. Scott, G. Costantini and D. J. Fox, *Chem. Eur. J.*, 2015, **21**, 2011-2018.
325. B.A.S.F., *Dtsch. Reichs-Pat*, 1904.
326. B.A.S.F., *Dtsch. Reichs-Pat*, 1919.
327. R. Bai, H. Zhang, F. Mei, T. Li, S. Wang, Y. Gu and G. Li, *Green Chem.*, 2013.
328. S. M. Gade, M. K. Munshi, B. M. Chherawalla, V. H. Rane and A. A. Kelkar, *Catal. Commun.*, 2012, **27**, 184-188.
329. O. Gómez-Jiménez-Aberasturi, J. R. Ochoa-Gómez, A. Pesquera-Rodríguez, C. Ramírez-López, A. Alonso-Vicario and J. Torrecilla-Soria, *J. Chem. Technol. Biotechnol.*, 2012, **85**, 1663-1670.
330. P. Cremonesi, B. Hietbrink, E. G. Rogan and E. L. Cavalieri, *J. Org. Chem.*, 1992, **57**, 3309-3312.
331. S. I. G. Didenko, Yu. E., *Russ. J. Org. Chem. (English Translation)*, 1984, **20**, 193 – 194.
332. M. Gerst, J. Morgenthaler and C. Rüchardt, *Chem. Ber.*, 1994, **127**, 691-696.
333. M. Suenaga, Y. Miyahara and T. Inazu, *J. Org. Chem.*, 1993, **58**, 5846-5848.
334. V. S. Thirunavukkarasu and C.-H. Cheng, *Chem. Eur. J.*, 2011, **17**, 14723-14726.

335. C. Tintel, J. Lugtenburg, G. A. J. van Amsterdam, C. Erkelens and J. Cornelisse, *Recl. Trav. Chim. Pays-Bas*, 1983, **102**, 228-231.
336. D. W. Cameron, D. G. I. Kingston and P. E. Schutz, *J. Chem. Soc.*, 1967, 2113-2118.
337. E. Clar, *Ber. Dtsch. Chem. Ges.*, 1935, **68**, 2066-2070.
338. S. Pogodin and I. Agranat, *J. Am. Chem. Soc.*, 2003, **125**, 12829-12835.
339. Z. H. Skraup, *Monatsh. Chem. Verw. Tl.*, 1880, **1**, 316-318.
340. Z. H. Skraup, *Monatsh. Chem. Verw. Tl.*, 1881, **2**, 139-170.
341. A. S. Amarasekara and M. A. Hasan, *Tetrahedron Lett.*, 2014, **55**, 3319-3321.
342. S. E. Denmark and S. Venkatraman, *J. Org. Chem.*, 2006, **71**, 1668-1676.
343. J. J. Eisch and T. Dluzniewski, *J. Org. Chem.*, 1989, **54**, 1269-1274.
344. C. A. Knueppel, *Dtsch. Reichs-Pat*, 1894, **4**, 1135.
345. C. A. Knueppel, *Ber. Dtsch. Chem. Ges.*, 1896, **29**, 703-709.
346. W. Koenigs, *Ber. Dtsch. Chem. Ges.*, 1880, **13**, 911-913.
347. B. M. Margosches, *J. Prakt. Chem.*, 1904, **70**, 129-136.
348. H. Saggadi, D. Luart, N. Thiebault, I. Polaert, L. Estel and C. Len, *Catal. Commun.*, 2014, **44**, 15-18.
349. W. Bühler, E. Dinjus, H. J. Ederer, A. Kruse and C. Mas, *J. Supercrit. Fluids*, 2002, **22**, 37-53.
350. J. L. Dubois, C. Duquenne and W. Holderich, 2008.
351. B. Katryniok, S. Paul, V. Belliere-Baca, P. Rey and F. Dumeignil, *Green Chem.*, 2010, **12**, 2079-2098.
352. A. Talebian-Kiakalaieh, N. A. S. Amin and H. Hezaveh, *Renew. Sustainable Energy Rev.*, 2014, **40**, 28-59.
353. M. Watanabe, T. Iida, Y. Aizawa, T. M. Aida and H. Inomata, *Bioresour. Technol.*, 2007, **98**, 1285-1290.
354. G. D. Yadav, R. V. Sharma and S. O. Katole, *Ind. Eng. Chem. Res.*, 2013, **52**, 10133-10144.
355. K. Fukui, T. Yonezawa and H. Shingu, *J. Chem. Phys.*, 1952, **20**, 722-725.
356. M. J. Rossi, D. F. McMillen and D. M. Golden, *J. Phys. Chem. A*, 1984, **88**, 5031-5039.
357. J. W. McClaine and M. J. Wornat, *J. Phys. Chem. C*, 2007, **111**, 86-95.
358. M. Gerst and C. Rüchardt, *Chem. Ber.*, 1993, **126**, 1039-1045.
359. S. Zheng, J. Lan, S. I. Khan and Y. Rubin, *J. Am. Chem. Soc.*, 2003, **125**, 5786-5791.
360. P. Devin, L. Fensterbank and M. Malacria, *Tetrahedron Lett.*, 1998, **39**, 833-836.
361. P. Devin, L. Fensterbank and M. Malacria, *Tetrahedron Lett.*, 1999, **40**, 5511-5514.
362. K. Maruyama, M. Taniuchi and S. Oka, *Bull. Chem. Soc. Jpn.*, 1974, **47**, 712-714.
363. T. Horaguchi, E. Hasegawa, T. Shimizu, K. Tanemura and T. Suzuki, *J. Heterocycl. Chem.*, 1989, **26**, 365-369.
364. M. Lafrance, M. Roggen and E. M. Carreira, *Angew. Chem. Int. Ed.*, 2012, **51**, 3470-3473.
365. G. Sabitha, C. Srinivas, T. R. Reddy, K. Yadagiri and J. S. Yadav, *Tetrahedron: Asymmetry*, 2011, **22**, 2124-2133.
366. O. Bally and R. Scholl, *Ber. Dtsch. Chem. Ges.*, 1911, **44**, 1656-1670.
367. W. S. Calcott, J. M. Tinker and V. Weinmayr, *J. Am. Chem. Soc.*, 1939, **61**, 949-951.
368. V. Weinmayr, 1939.
369. B.A.S.F., *Dtsch. Reichs-Pat*, 1913.
370. S.-H. Chung and A. Violi, *P. Combust. Inst.*, 2011, **33**, 693-700.
371. L. D. A. IG Farbenindustrie AG, Kacer Dr Filyi, *Dtsch. Reichs-Pat*, 1926, **16**, 525.
372. J. O. Oña-Ruales and Y. Ruiz-Morales, *J. Phys. Chem. A*, 2014, **118**, 12262-12273.
373. N. P. Buu-Hoi and D. Lavit, *Recl. Trav. Chim. Pays-Bas*, 1957, **76**, 200-204.
374. M. Zander and W. H. Franke, *Chem. Ber.*, 1966, **99**, 1275-1278.
375. P. E. Hansen, O. K. Poulsen and A. Berg, *Org. Magn. Resonance*, 1975, **7**, 23-25.

376. P. E. Hansen, O. K. Poulsen and A. Berg, *Org. Magn. Resonance*, 1975, **7**, 475-477.
377. P. E. Hansen, O. K. Poulsen and A. Berg, *Org. Magn. Resonance*, 1977, **9**, 649-658.
378. K. N. Kudin, B. Ozbas, H. C. Schniepp, R. K. Prud'homme, I. A. Aksay and R. Car, *Nano Lett.*, 2008, **8**, 36-41.
379. D. C. Marcano, D. V. Kosynkin, J. M. Berlin, A. Sinitskii, Z. Sun, A. Slesarev, L. B. Alemany, W. Lu and J. M. Tour, *ACS Nano*, 2010, **4**, 4806-4814.
380. S. Some, Y. Kim, Y. Yoon, H. Yoo, S. Lee, Y. Park and H. Lee, *Scientific Reports*, 2013, **3**, 1929.
381. H. R. Thomas, S. P. Day, W. E. Woodruff, C. Vallés, R. J. Young, I. A. Kinloch, G. W. Morley, J. V. Hanna, N. R. Wilson and J. P. Rourke, *Chem. Mater.*, 2013, **25**, 3580-3588.
382. H. R. Thomas, C. Valles, R. J. Young, I. A. Kinloch, N. R. Wilson and J. P. Rourke, *J. Mater. Chem. C*, 2013, **1**, 338-342.
383. A. C. Ferrari, *Solid State Commun.*, 2007, **143**, 47-57.
384. H. Shinohara, Y. Yamakita and K. Ohno, *J. Mol. Struct.*, 1998, **442**, 221-234.
385. H.-K. Jeong, Y. P. Lee, M. H. Jin, E. S. Kim, J. J. Bae and Y. H. Lee, *Chem. Phys. Lett.*, 2009, **470**, 255-258.
386. J. P. Rourke, P. A. Pandey, J. J. Moore, M. Bates, I. A. Kinloch, R. J. Young and N. R. Wilson, *Angew. Chem. Int. Ed.*, 2011, **50**, 3173-3177.
387. E. Clar, *Springer-Verlag*, 1941, 311.
388. G. Allinson, R. J. Bushby, J.-L. Paillaud and M. Thornton-Pett, *J. Chem. Soc., Perkin Trans. 1*, 1995, **0**, 385-390.
389. Y. Li, K.-W. Huang, Z. Sun, R. D. Webster, Z. Zeng, W. Zeng, C. Chi, K. Furukawa and J. Wu, *Chem. Sci.*, 2014, **5**, 1908-1914.
390. O. A. Gapurenko, A. G. Starikov, R. M. Minyaev and V. I. Minkin, *Russ. Chem. Bull.*, 2011, **60**, 1517-1524.
391. E. Clar and D. G. Stewart, *J. Chem. Soc.*, 1951, 3215-3218.
392. E. Clar, W. Kemp and D. G. Stewart, *Tetrahedron*, 1958, **3**, 325-333.
393. E. Clar and D. G. Stewart, *J. Am. Chem. Soc.*, 1954, **76**, 3504-3507.
394. G. Allinson, R. J. Bushby and J. L. Paillaud, *J. Mater. Sci. Mater. Electron.*, 1994, **5**, 67-74.
395. G. Allinson, R. J. Bushby, J. L. Paillaud, D. Oduwole and K. Sales, *J. Am. Chem. Soc.*, 1993, **115**, 2062-2064.
396. Q. Zhao, C. Li, C. H. Senanayake and W. Tang, *Chem. Eur. J.*, 2013, **19**, 2261-2265.
397. G. Altenhoff, R. Goddard, C. W. Lehmann and F. Glorius, *J. Am. Chem. Soc.*, 2004, **126**, 15195-15201.
398. Y. Y. Gao-Qiang Li, Norio Miyaura, *Synlett*, 2011, **12**, 1769-1773.
399. T. Hoshi, T. Nakazawa, I. Saitoh, A. Mori, T. Suzuki, J.-i. Sakai and H. Hagiwara, *Org. Lett.*, 2008, **10**, 2063-2066.
400. M. G. Organ, S. Çalimsiz, M. Sayah, K. H. Hoi and A. J. Lough, *Angew. Chem. Int. Ed.*, 2009, **48**, 2383-2387.
401. C. M. So, W. K. Chow, P. Y. Choy, C. P. Lau and F. Y. Kwong, *Chem. Eur. J.*, 2010, **16**, 7996-8001.
402. L. Wu, E. Drinkel, F. Gaggia, S. Capolicchio, A. Linden, L. Falivene, L. Cavallo and R. Dorta, *Chem. Eur. J.*, 2011, **17**, 12886-12890.
403. J. Yin, M. P. Rainka, X.-X. Zhang and S. L. Buchwald, *J. Am. Chem. Soc.*, 2002, **124**, 1162-1163.
404. S. M. Raders, J. N. Moore, J. K. Parks, A. D. Miller, T. M. Leißing, S. P. Kelley, R. D. Rogers and K. H. Shaughnessy, *J. Org. Chem.*, 2013, **78**, 4649-4664.
405. O. J. Gelling and B. L. Feringa, *J. Am. Chem. Soc.*, 1990, **112**, 7599-7604.
406. L. Ye, D. Ding, Y. Feng, D. Xie, P. Wu, H. Guo, Q. Meng and H. Zhou, *Tetrahedron*, 2009, **65**, 8738-8744.
407. A. Mistry, N. Pavliček and *et al.*, *In preparation*, 2016.
408. K. Popaj and M. Hesse, *Helv. Chim. Acta*, 2001, **84**, 180-186.



409. S. Sadhukhan, Y. Han, G.-F. Zhang, H. Brunengraber and G. P. Tochtrop, *J. Am. Chem. Soc.*, 2010, **132**, 6309-6311.
410. J. Wu, D. Zhang and S. Wei, *Synth. Commun.*, 2005, **35**, 1213-1222.
411. B. Hermans, F. C. De Schryver, N. Boens, M. Ameloot, R. Jerome, P. Teyssie, E. Goethals and E. Schacht, *J. Phys. Chem. A*, 1994, **98**, 13583-13593.
412. S. Noël, C. Luo, C. Pinel and L. Djakovitch, *Adv. Synth. Catal.*, 2007, **349**, 1128-1140.
413. J. T. M. van Dijk, A. Hartwijk, A. C. Bleeker, J. Lugtenburg and J. Cornelisse, *J. Org. Chem.*, 1996, **61**, 1136-1139.
414. A. Späth, C. Leibl, F. Cieplik, K. Lehner, J. Regensburger, K.-A. Hiller, W. Bäumler, G. Schmalz and T. Maisch, *J. Med. Chem.*, 2014, **57**, 5157-5168.
415. R. S. Atkinson, D. R. G. Brimage, R. S. Davidson and E. Gray, *J. Chem. Soc., Perkin Trans. 1*, 1973, 960-964.
416. M. J. R. Reddy, U. Srinivas, K. Srinivas, V. V. Reddy and V. J. Rao, *Bull. Chem. Soc. Jpn.*, 2002, **75**, 2487-2495.
417. Cinzia D. Pietro, S. Campagna, V. Ricevuto, M. Giannetto, A. Manfredi, G. Pozzi and S. Quici, *Eur. J. Org. Chem.*, 2001, **2001**, 587-594.
418. H. J. Williams and R. L. Harlow, *J. Chem. Soc., Perkin Trans. 1*, 1975, 1537-1539.
419. N.-c. C. Yang, D. W. Minsek, D. G. Johnson, J. R. Larson, J. W. Petrich, R. Gerald and M. R. Wasielewski, *Tetrahedron*, 1989, **45**, 4669-4681.
420. J. Oh and J.-I. Hong, *Org. Lett.*, 2013, **15**, 1210-1213.
421. V. H. Pham, T. V. Cuong, S. H. Hur, E. Oh, E. J. Kim, E. W. Shin and J. S. Chung, *J. Mater. Chem.*, 2011, **21**, 3371-3377.
422. P. Natarajan and M. Schmittel, *J. Org. Chem.*, 2013, **78**, 10383-10394.
423. Y.-H. Lai and A. H.-T. Yap, *J. Chem. Soc., Perkin Trans. 2*, 1993, 703-708.
424. K. D. Stewart, M. Miesch, C. B. Knobler, E. F. Maverick and D. J. Cram, *J. Org. Chem.*, 1986, **51**, 4327-4337.